
THE UNIVERSITY
*of* EDINBURGH

# Chemical and biological properties of a wall-enzyme activating factor from plants

**CAM-TU NGUYEN-PHAN**


Doctor of Philosophy – Cell and Molecular Biology

The University of Edinburgh

2015

## DECLARATION

This thesis and the work of which it is a record was composed by myself. Where substantial input has been made by third parties, acknowledgement is made on the following page. This work has not been submitted for any degree or professional qualification other than that specified.

CAM-TU NGUYEN-PHAN

## ACKNOWLEDGEMENTS

First and foremost, I would like to express my special appreciation and thanks to my supervisor Professor Dr. Stephen C. Fry. Thank him for giving me a chance to come to the UK, study in the University of Edinburgh and take part in a challenging but very interesting project. He has been a tremendous mentor for me. He has helped me to develop and improve not only my cell wall knowledge but also my biochemistry techniques. I have learnt from him how to interpret experimental data, organise my work and also speak and write proper English. I am so lucky to have an opportunity to work with an excellent example of both a successful scientist and a good teacher.

I would especially like to thank to my second supervisor, Dr. Steven H. Spoel for kindly teaching me plant molecular and genetic techniques. All the work on choosing *Arabidopsis* mutants, growing *Arabidopsis* plants, DNA extraction, RNA extraction, PCR have been done in his laboratory. I appreciate all his contributions of time and ideas to not only my PhD, but also my scientific career.

I am also highly appreciative and thankful to my boss, Dr. Naomi Nakayama from the BF+F group for financial helping me in my fourth year. Thank her for being understanding and supportive during my writing up. I also thank her for tutoring me molecular plant biology.

Many thanks to Dr. Karen Halliday for being one of my committee members and giving me many suggestions during my PhD project. I would like to thank my examination panel for giving me an enjoyable viva, and for their brilliant comments and suggestions.

I would also like to give my official thanks to people who I have collaborated with: Professor Dr. Paul J. Knox, the University of Leeds who kindly provided all AGPs antibodies for my project and advised me on the ELISA results; Dr. Thierry le Bihan and Ms. Lisa Imrie from KPF SynthSys, the University of Edinburgh who conducted mass-spectrometry analysis; Professor Dr. Marcia J. Kieliszewski and Mick Held, the University of Ohio who carried out the HF-treatment; and Mr. Tim Gregson, a former lab technician who helped me with all HPLC work.

I would especially like to thank Mrs. Janice G. Miller, Dr. Lenka Franková and all the old and new members of the Edinburgh Cell Wall Group, members in Spoel's lab and

members in BF+F group. Thank you for looking after me and being supportive throughout the years since I first came to Edinburgh, during my pregnancy, to my motherhood and writing up time. I also want to say thank you to people from the Institute of Molecular Plant Sciences for being friendly and helpful during my PhD project, especially Mr. Mario, Andreas MSc., Dr. Claire Holland, Dr. Christina O'Rourke and Ms. Rebecca Dewhirst for helping with the last corrections.

I would also like to thank to the Vietnamese government and the School of Biological Sciences, the University of Edinburgh for the financial support.

Last but not least, a special thanks to my family. Words cannot express how grateful I am to my mother, my father and my two younger sisters for all their love and encouragement. Special thanks to my mother, who has travelled a long distance and stayed far away from her home for almost six months to help me look after my daughter, thus I have more time to finish my writing up. Many thanks to my mother-in law and father-in-law for being understanding and helpful.

Finally, special thanks to my husband Minh Nguyen Quy for all his love, patience, care and support, from the beginning till the end of this tough time. Without him none of this would have been possible. And all my love to my nine-month old daughter Caroline Ha-Mi Nguyen. Her smile has cheered me up during my writing up time.

Thank you all!

*For the hard-working years in Edinburgh,*

*And for my family, with all my love!*

## ABSTRACT

Xyloglucan endotransglucosylase activity (XET), one of the two main activities of wall xyloglucan endotransglucosylase/hydrolase proteins (XTHs), is of interest because it is responsible for cutting and re-joining xyloglucan of the hemicellulose-cellulose microfibril network in the plant cell wall. XET activity causes transient matrix cleavage without hydrolysis, thus providing a molecular mechanism for controlled, turgor-driven wall expansion. XET activity can be involved in both wall-loosening, thus facilitating cell expansion, and wall-tightening, thus suppressing cell expansion depending on the molecular size, location and age of the participating xyloglucan chains.

I have studied the existence of an 'XET activating factor' (XAF) in the cold-water-extractable polymers of cauliflower florets. Remaining water-soluble on boiling but losing activity upon proteinase K- and trypsin-digestions implied a heavily glycosylated glycoprotein. XAF was extracted from a wide range of plants and organs. XAF solubilised *Arabidopsis* cell-wall XTHs, increasing their XET activity on soluble xyloglucan up to 120-fold, tested by a novel method developed in my project. XAF had effects similar to those of 15 mM $Ca^{2+}$ and 100 mM $Na^{+}$ in this respect, although it was only weakly ionic. Interestingly, XAF had the unique ability to solubilise XET activity but no other tested wall enzymes from *Arabidopsis* cell walls, suggesting a specific interaction of XAF to XTH proteins.

XAF was successfully purified by the use of several methods, developed in this project. These included cation-exchange column chromatography followed by anion-exchange column chromatography, resulting in two main XAF-activity fractions; or a native-PAGE electro-elution, resulting in three main fractions. Purified XAF contained a major amount of glucose, arabinose, galactose and uronic acid residues. Both boiled cauliflower preparation (BCP) and partially purified XAF were positive with AGP antibodies but the purification of AGP from BCP by the use of Yariv reagent did not enrich XAF activity.

Mass-spectrometry analyses of the purified XAF fractions showed some candidates for XAF, including fasciclin-like arabinogalactan-protein 7 (FLA7), stress-responsive protein (LTI65, LTI140) and early nodulin-like protein 14 (ENODL14). Homozygous

*Arabidopsis* mutants (confirmed by genotyping) defective in these genes were used to determine XAF as well as its biological role on plant cell growth. Although there was no phenotype observed, several organs of the mutant plants had significant increases or decreases in XAF activity compared to that of wild type plants. This is the first work that suggests a role of *fla7*, *enodl14* and *lti65* in the solubilisation, and thus activation, of *Arabidopsis* XET.

## ABBREVIATIONS

**AG** = Arabinogalactan

**AGA** = Apiogalacturonan

**AGP** = Arabinogalactan-protein

**ATAF** = *Arabidopsis thaliana* transcription activation factor

**AX** = Arabinoxylan

**Ara** = Arabinose

**BAW** = Butanol/ acetic acid/ $dH_2O$

**BAP** = Boiled *Arabidopsis* preparation

**BCP** = Boiled cauliflower preparation

**BPP** = Boiled plant preparation

**CSLC** = Cellulose synthase-like C

**CPM** = Counts per minute

**CUC** = Cup-shaped cotyledon

**$dH_2O$** = Distilled water

**$ddH_2O$** = Distilled de-ionised water

**DP** = Degree of polymerisation

**DTT** = Dithiothreitol

**EGase** = Endo-glucanase

**EXP** = Expansin

**EXPL** = Expansin-like proteins

**EXPR** = Expansin-related protein

**EPyAW** = Ethyl acetate/ pyridine/ acetic acid/ dH2O

**Fru** = Fructose

**Fuc** = Fucose

**Gal** = Galactose

**GalA** = Galacturonic acid

**GAX** = Glucuronoarabinoxylan

**GGM** = Galactoglucomannan

**GH** = Glycoside Hydrolase

**GlcA** = Glucuronic acid

**Glm** = Glucomannan

**GM** = Galactomannan

**GRPs** = Glycine-rich proteins

**GX** = Glucuronoxylan

**HEC** = Hydroxyethyl cellulose

**HG** = Homogalacturonan

**IP** = Isoprimeverose

**Kdo** = 2-keto-3-deoxy-D-*manno*-octulosonic acid

**KOR** = Korrigan

**Man** = Mannose

**$Man_6$** = β-(1→4)-Mannose hexasaccharide

**MeOH** = Methanol

**MET** = Mannan *endo*transglycosylase

**MLG** = Mixed linkage β-(1→3), (1→4)-glucan

**MLGO** = MLG oligosaccharide

**MXE** = MLG: xyloglucan *endo*transglucosylase

**NAC** = NAM/ ATAF / CUC

**NAM** = No Apical Meristem

**NST** = NAC secondary wall thickening promoting factor

**PCW** = Primary cell wall

**PRPs =** Proline-rich proteins

**PyAW** = Pyridine/ acetic acid/ dH2O

**RG-I/ -II** = Rhamnogalacturonan-I/ -II

**Rha** = Rhamnose

**Rib** = Ribose

**SCW** = Secondary cell wall

**TC** = Terminal complex

**TLC** = Thin-layer Chromatograpy

**TFA** = Trifluoroacetic acid

**XAF** = XET activating factor

**XEH** = Xyloglucan *endo*hydrolase

**XET** = Xyloglucan *endo*transglucosylase

**XGA** = Xylogalacturonan

**XGO** = Xyloglucan oligosaccharide

**XTH** = Xyloglucan *endo*transglycosylase/ hydrolase

**XXT** = Xyloglucan α-1,6-xylosyltransferase

**XXXG** = Xyloglucan-derived heptasaccharide

**[$^3$H]XXXGol =** Reductively tritiated XXXGol

**XyG** = Xyloglucan

**Xyl** = Xylose

**$Xyl_{\underline{p}6}$** = β-(1→4)-Xylose hexasaccharide

**CONTENTS**

## Table of Figures

## List of Tables

# 1 INTRODUCTION

## 1.1 The plant cell wall

### 1.1.1 The plant cell wall and its role in plants

The plant cell wall is an elaborate extraprotoplasmic structure that encompasses each plant cell. It was the thick cell walls of cork, visible through a primitive microscope, which allowed Robert Hooke to distinguish and name these cells for the first time in 1663 (Alberts et al., 2002). The plant cell wall, which surrounds and adheres to the plasma membrane of each plant cell (Zhu et al., 1993), is one of the unique features that makes plant cells differ from cells of other organisms. It is a dynamic network, extremely complex and highly diverse in structure (Keegstra et al., 1973; Darvill et al., 1978; McCann et al., 1990; Carpita and Gibeaut, 1993; Pennell, 1998; Caffall and Mohnen, 2009) and functions (Cosgrove, 1986; McCann et al., 2001; Bellincampi et al., 2014) between different plant species, organs, cell types, and cells in different stages of the cell cycle (Pennell, 1998; Dolan et al., 1997; Ito et al., 1998).

The plant cell wall is the outermost part of a plant cell that connects it to the external environment. It acts as a gate-keeper by controlling which molecules can enter and exit the cell. Whereas water-soluble molecules and ions such as $O_2$, $CO_2$, nitrate, phosphate, sugars and amino acids diffuse freely through cell walls, large molecules including proteins, polysaccharides; bacteria and viruses cannot permeate the wall, (Fry, 2001). Thus, the cell wall protects the plant from environmental stresses and pathogen attacks (Braam, 1992; Brownlee, 2002; Vorwerk et al., 2004). The wall is an important defence system of the plant cell with both constitutive and inducible defence mechanisms (Glazebrook, 2005; Jones and Dang, 2006).

The cell wall plays an important role in helping the plant to stand upright on the earth The homozygous double knockout mutant *Arabidopsis* (*nst1 nst3*) is characterized by mutations in the *NST* (NAC (NAM (no apical meristem)/ ATAF (*Arabidopsis thaliana* transcription activation factor)/ CUC (Cup-shaped cotyledon)) secondary wall thickening promoting factor) genes, which code for plant-specific transcription factors. The *NST* double mutation results in a complete loss of the plant's lignified material in the regions where interfascicular fibres would be formed in wild-type plants. Under

short-day conditions, *nst1 nst3* plants are unable to remain upright after gaining more than 15 cm in height because they are unable to synthesise effective secondary walls in their stem cells. Neither cellulose nor lignin was produced in inflorescence stems (Mitsuda et al., 2007).

The plant cell wall contributes not only to the shape of the plant but also to the biomechanical properties of its organs, such as their rigidity or viscoelastic properties. The cell walls strengthen plant organs through internal vascular and fibre cells, which have thickened cell walls. Cell walls also mediate cell-to-cell adhesion, which is integral to the organ integrity and robustness that are required to withstand and respond to mechanical impacts (Verhertbruggen et al., 2013).

The cell wall is sufficiently structured to resist the build-up turgor pressure, which is the pressure of the cell contents against the wall (Lockhart, 1965; Westgate and Boyer, 1985; Taylor and Davies, 1986; Cosgrove, 1986). This pressure is vital for plants as it is the main driving force for cell expansion during growth while also providing much of the mechanical rigidity found in living plant tissues (Boyer et al., 1985; Volkenburgh and Cleland, 1986; Cosgrove, 1985; Cosgrove, 1987; Alberts et al., 2002). The cytoplasm of a plant cell contains numerous compounds that are dissolved at high concentrations. As a result, water enters the cells under normal conditions and makes the cell's central vacuole swell and press against the cell wall. However, in an intact cell, the stiff exoskeleton - the cell wall has a back-pressure opposed this, prevents the cell from bursting (Fry, 2001). In growing plant cells, cell wall synthesis and remodelling causes the matrix to yield to the turgor pressure, thus allowing the cell to grow (Hamant and Traas, 2010).

The plant cell wall also controls the rate and direction of growth. For example, cellulose microfibril orientation controls the direction of cell elongation (Saxena and Brown, 2005). In addition, the ripening of fruits and the change in shelf life of vegetables are associated with changes in the cell wall structure and composition (Rose and Bennett, 1999; Harrison et al., 2001, Wagstaff et al., 2010). Therefore, the structure and function of the plant cell wall is of great interest to plant scientists.

### 1.1.2 Structure of a plant cell wall

All plant cell types possess a primary cell wall (PCW) and many specialised cells, including tracheary elements, fibres and other slerenchymatous cells, also produce a secondary cell wall (SCW) (Fig. 1) (Zhong and Ye, 2014). PCW and SCW are parts of the apoplast and differ in many aspects, including structure, arrangement and mobility of matrix polymers; rheological and mechanical properties; and their roles in a plant life (Cosgrove and Jarvis, 2012).

The PCW is a wall layer whose microfibrils were laid down while it was still capable of growing in area (Fry, 2001). The PCW provides the young cell with mechanical strength to withstand the tensile forces arising from turgor pressure (Cosgrove, 1985; Volkenburgh and Cleland, 1986) but is also dynamic, allowing the cell to grow and divide (Thompson, 2005; Hamant and Traas, 2010).

The SCW is a wall layer whose microfibrils were deposited once the cell growth had ceased (Fry, 2001), making the cell more thickened and strengthened (Caffall and Mohnen, 2009). This type of wall accounts for most of the plant's biomass. The SCW is often extremely rigid, provides compression strength due to a high content of rather uniformly oriented cellulose microfibrils that are normally lignified, and is often layered (Cosgrove and Jarvis, 2012). The SCW is less hydrated than PCW, containing only 30% water at saturation (Cosgrove and Jarvis, 2012).

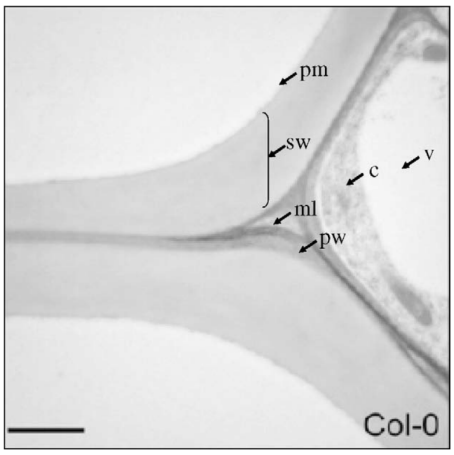


Figure 1. Cell walls from the metaxylem region of *Arabidopsis thaliana.*

Primary wall (pm), secondary wall (sw), middle lamella (ml), plasma membrane (pm), cytosol (c) and vacuole (v) in a transverse root section of wildtype *Arabidopsis thaliana* Col-0 under transmission electron micrograph (Persson et al., 2007) Bar = 2 µm.

PCWs are composed of cellulose microfibrils, pectin and hemicelluloses (Carpita and Gibeaut, 1993; Cosgrove, 2005) while the SCWs are composed of cellulose microfibrils, lignin and hemicelluloses (Mellerowicz and Sundberg, 2008; Persson et al., 2007; Popper, 2008). While the amounts of pectin and hemicellulose are relatively equal in dicot PCWs, hemicelluloses exceed pectins in grass PCWs (Carpita et al., 2001a; Gibeaut et al., 2005). The hemicelluloses are more abundant in SCWs than in the PCWs of both dicots and poalean monocot species. Cellulose is abundant, contributing between 35 and 50% of the polymers in wood SCWs. By contrast, the hemicellulose content of the SCWs is around 20-35% while lignin is between 0 and 25%. The major hemicellulose component of the PCW is xyloglucan (Carpita and Gibeaut, 1993), except that mixed-linkage (1→3),(1→4)-β-D-glucan (MLG) is dominant in Poaceae (grasses and cereals) and some related families of the order Poales (Labavitch and Ray, 1978; Popper and Fry, 2004; Fry et al., 2008). On the other hand, xylans (including glucuronoxylans in dicots and arabinoxylans and glucuronoarabinoxylans in grasses) and glucomannans in gymnosperms are the main hemicelluloses in the SCWs (York and O'Neill, 2008; Popper, 2008).

### 1.1.3 Synthesis of the plant cell wall

All plant cell walls are created during cell division after the formation of a cell plate during cytokinesis, which makes a new boundary between the two daughter nuclei. New cells are usually produced in the meristems and are generally small compared with their final size (Alberts et al., 2002; Popper, 2008). Therefore, although the PCWs are tough, they are flexible and extensible enough to allow the cell to enlarge to its mature volume (Cosgrove, 2005). After the cessation of cell growth, the wall no longer needs to be extensible. In some cases, the PCW is retained without any major modifications but, in most cases, a rigid SCW is added via the deposition of new layers inside the PCW (Alberts et al., 2002; Popper, 2008). As the SCW is produced after the completion of the PCW, it is the PCW that plays the key role in the control of cell expansion. The extensibility of the PCW is essential for the control of irreversible expansion of the plant cell (Boyer et al., 1985; Cosgrove, 1987; Cosgrove, 1993; Cosgrove, 2005).

## 1.2 The primary cell wall and its role in the control of plant cell expansion

### 1.2.1 The primary cell wall

A PCW is about 0.1- 10 µm thick (Fry, 2000; Popper, 2008). Growing primary walls are approximately 65% water, almost all of which is in the matrix. The "matrix" (in a cell-wall context) is all the glycoproteins and polysaccharides that are traditionally divided into pectins and hemicelluloses except cellulose (Cosgrove, 2005). Water is an important structural component in the PCW as it is necessary for the formation of pectic gels in the matrix (Fry, 2000). Although the cell walls of higher plants vary in both composition and organization, the PCW is a complex of polysaccharides with multiple functions consisting of three major components (Carpita and Gibeaut, 1993; Somerville, 2006; Mohnen, 2008; Scheller and Ulvskov, 2010); some structural glycoproteins (Jamet et al., 2006); and other materials such as two phenolic compounds — feruloylated disaccharides of D-galactose and L-arabinose (Fry, 1982). Sometimes additional components such as lignin, cutin, suberin and extensin are infiltrated between the microfibrils of a PCW (Fry, 2001) (Fig. 2).

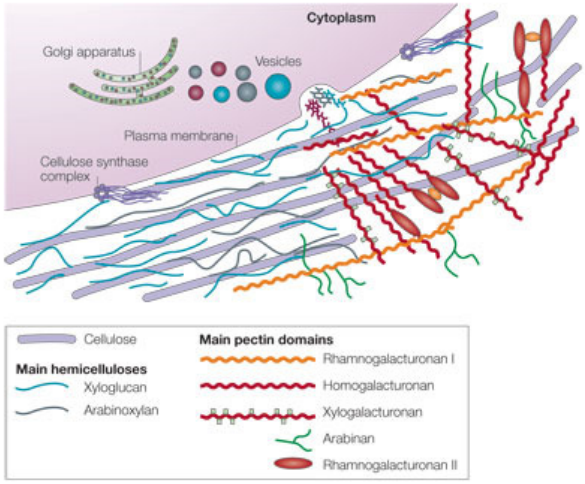


Figure 2. Structure of the primary cell wall (Cosgrove, 2015).

The cellulose–hemicellulose scaffold constitutes the main load-bearing network of the PCW in dicots. This scaffold is formed by cellulose microfibrils, which create the skeleton of the cell wall, and hemicelluloses, which tether adjacent cellulose microfibrils via hydrogen-bonding (Fry, 1989; Hayashi et al., 1994). The pectin is

composed of polyuronide molecules including neutral monosaccharide residues glycosidically linked to uronic acid residues to form complex acidic polymers which gell into a network by calcium cross-bridging. The structural protein network is covalently linked by oxidative phenolic cross-bridges and perhaps other linkages. These three networks are probably intertwined and may be covalently linked with each other (Cosgrove, 1993).

#### 1.2.1.1 Cellulose

Cellulose, which is the most abundant organic molecule on earth (Alberts et al., 2002), usually contributes 30% of the dry weight of the unlignified PCW in both grasses and other higher plants (Fry, 2000). Cellulose is composed of unbranched polymer chains of at least five hundred D-glucopyranose residues joined by β-(1→4) linkages to form a ribbon-like structure, which dictates the shape and strength of the cell wall (Fry, 2000; Saxena and Brown, 2005). A cellulose microfibril is formed from several dozen linear cellulose chains by intermolecular hydrogen bonds between them in overlapping parallel arrays (Alberts et al., 2002; Cosgrove, 2005).

Microfibrils are highly ordered crystalline aggregates with a tensile strength comparable to steel (Alberts et al., 2002). Microfibrils are 3–5 nm wide and sufficiently long to wind around the circumference of a cell many times (Cosgrove, 2005). Cellulose microfibrils are arranged in layers, called lamellae, in which each microfibril is positioned 20–40 nm from its neighbours (McCann et al., 1990), and are connected to each other by long hemicellulose molecules that are bound by hydrogen bonds to the cellulose microfibril's surface (Alberts et al., 2002).

A large number of glucan chains are synthesised simultaneously by a cellulose synthase (CESA) complex that localises in the plasma membrane and extrudes a microfibril from the cell surface (Cosgrove, 2005; Saxena and Brown, 2005). The CESA complexes comprise multiple subunits that form a rosette structure of six globular CESA-containing complexes (Mueller and Brown, 1980; Kimura et al., 1999). Using freeze-fractured plasma membranes from corn seedling tissue, Mueller and Brown (1980) found that rosettes and terminal complexes (TCs) were associated with the ends of microfibril impressions, and Kimura et al. (1999) confirmed that the catalytic unit for cellulose synthase was located in the rosette TC of vascular plant

cells by using immunocytochemical labelling. In vascular plants, this complex appears as a 'rosette' with a six-fold symmetry and a diameter of 25–30 nm (Mueller and Brown, 1980).

There are 10 genes in the CESA family in *Arabidopsis thaliana* (Cosgrove, 2005). Three different *CESA* genes are normally required to make a functional cellulose-synthesising complex. *CESA1*, *CESA3* and *CESA6* are responsible for biosynthesis of PCWs, whereas *CESA4*, *CESA7* and *CESA8* are required to make SCWs. The CESA uses sitosterol-β-glucoside, which is commonly synthesised in the plant plasma membrane, and uridine 5'-diphosphate-glucose to form short sterol-linked glucans. Then a membrane-bound endoglucanase (Korrigan) trims sterol residues from nascent glucan primers or trims out-of-register glucans to aid crystallization of the microfibril (Peng et al., 2002). However, the protein is not specifically associated with CESA complexes and *kor* mutants have normal amounts of sterol glucoside, so its action on microfibril formation might be indirect (Cosgrove, 2005).

#### 1.2.1.2 Hemicelluloses

Hemicelluloses are one of the three major polysaccharide classes constructing the PCWs, together with celluloses and pectin. Hemicelluloses are GalA-free, neutral or slightly acidic polysaccharides that are extractable from the wall with aqueous NaOH (optimally 6 M at 37°C) (Edelmann and Fry, 1992) and can be adsorbed from neutralized aqueous solutions by hydrogen-bonding to cellulose (e.g. filter paper) (Fry, 2004). Hemicelluloses are a class of heterogeneous polysaccharides that have β-1,4-linked backbones with an equatorial configuration at C1 and C4, thus the backbones have structural similarity (Scheller and Ulvskov, 2010). The structural similarity between hemicelluloses and cellulose most likely results from a conformational homology that can lead to a strong, non-covalent association of hemicelluloses with cellulose microfibrils (Rose, 2003).

Hemicelluloses include a variety of different polysaccharides. Some of the principal hemicelluloses are xyloglucans, xylans, mannans and MLG. Xyloglucan (including fucogalactoxyloglucan, arabinoxyloglucan and arabinoxyloglucan) is the most abundant hemicellulose in the PCW in most vascular land plants that have been analysed (except for poalean). It has a backbone of (1→4)-linked β-D-Glc*p* residues

(Carpita and Gibeaut, 1993; Fry, 1989a; Hayashi, 1989). Xylan, the second most abundant hemicellulose in the PCW of dicots and non-poalean monocots, has a backbone of (1→4)-linked β-D-Xyl*p* residues and may be found as arabinoxylan (AX), glucuronoarabinoxylan (GAX) and glucuronoxylan (GX) (Correia et al., 2011). Mannans include galactomannan (GM) and galactoglucomannan (GGM), which are structurally important components of the cell wall as well as an important source of storage polysaccharides, having a backbone of (1→4)-linked β-mannose or mannose and glucose residues.

The proportion of each hemicellulose in the PCW varies between different families. For example, in grasses, arabinoxylan and MLG are the main PCW hemicelluloses and together they contribute around 30% of the dry weight of the unlignified PCW (Carpita et al., 2011; Labavitch and Ray, 1978; Popper and Fry, 2004). By contrast, xyloglucan is the most abundant hemicellulose in other higher plants, where it contributes approximately 25% of the total dry weight of the unlignified PCW (Fry, 2000).

The most important biological role of hemicelluloses is thought to be their contribution to the strengthening of the cell wall via interactions with cellulose and, in some walls, lignin (Scheller and Ulvskov, 2010). Hemicelluloses are synthesized by glycosyltransferases (including glycan synthases), located in the Golgi membranes (plasma membrane in the case of MLG), and are deposited at the cell periphery through exocytosis in Golgi-derived vesicles (Scheller and Ulvskov, 2010; Fry, 2000; Cosgrove, 2005). Many of the glycosyltransferases needed for the biosynthesis of xyloglucans, mannans and MLG are already known. By contrast, the biosynthetic system of xylans remain more elusive as recent studies have led to more questions than answers (Scheller and Ulvskov, 2010).

#### 1.2.1.3 Pectin

Pectin, which is the most abundant class of polysaccharides in the dicot PCW and the middle lamella, contributes to up to 35% of the dry weight of the unlignified PCW of dicots and non-poalean monocots (Fry, 2000). Pectin is a heterogeneous group of branched polysaccharides that contains many negatively charged galacturonic acid units (Caffall and Mohnen, 2009). Pectins are “block” polymers, composed of several domains such as homogalacturonan (HG), xylogalacturonan

(XGA), apiogalacturonan (AGA), and rhamnogalacturonans (RG-I and RG-II) (Caffall and Mohnen, 2009).

Homogalacturonans contain a backbone of unbranched α-D-Gal*p*A residues connected by (1→4) linkages (Ridley et al., 2001). The backbone of HG is covalently linked to RG-I and RG-II (Nakamura et al., 2002; Coenen et al., 2007) and may be covalently associated with xyloglucan (Keegstra et al., 1973; Popper and Fry, 2007).

RG-II is one of the most complex polysaccharide domains as it comprises 12 different sugar residues, including some rare sugars such as 2-*O*-methylxylose, 2-*O*-methylfucose (Darvill et al., 1987) and 2-keto-3-deoxy-D-*manno*-octulosonic acid (Kdo) (York et al., 1985).

RG-I, which has a DP of about 1000, consists of a backbone with the repeating disaccharide unit [–α-D-Gal*p*A-(1→2)-α-L-Rha*p*-(1→4)–], where approximately half of the repeats bear an Ara- and/or Gal-rich side-chain at the 4-position of the Rha residue (Fry, 2000).

Pectic polysaccharides are involved in many of a plant's biological functions, including complex physiological processes such as cell growth and cell differentiation, determination of the integrity and rigidity of the plant tissue, defence against plant pathogens and wounding, regulation of ion transport (especially $Ca^{2+}$), control of the permeability of the walls for enzymes, and determination of the water holding capacity of the cell (Voragen et al., 2009). The abundance and composition of pectic polysaccharides in fruits, vegetables and other plant products determines the quality parameters of fresh and processed food products (Voragen et al., 2009).

In contrast to cellulose, the matrix polysaccharides, except MLG, are synthesised intraprotoplasmically in the Golgi apparatus and exported to the wall in membrane-bounded vesicles (Zhang and Staehelin, 1992; Cosgrove, 2005). The movement of these vesicles, which contain the polymers, is presumably along actin microfilaments that have myosin motors (Nebenführ et al., 1999). Possible modifications of pectic sugar residues include methyltransferase-catalysed methylesterification or *O*-methylation, acetyltransferase-catalysed *O*-acetylation and in some Amaranthaceae species, feruloylation by feruloyltransferases (Mohnen, 2008).

#### 1.2.1.4 Proteins

Unlike the extracellular matrix of animal cells, which is rich in proteins and other nitrogen-containing polymers, the plant PCW usually contains only a small amount of proteins (Keller, 1993) which are different in abundance dependent on the cell type. Cell wall proteins include insoluble structural proteins, soluble mucilage, enzymes and lectins. The most abundant, well-studied and widely documented plant cell wall proteins are the extensins, the glycine-rich proteins (GRPs), the proline-rich proteins (PRPs), the solanaceous lectins, and the arabinogalactan-proteins (AGPs) (Showalter, 1993). Most cell wall proteins are encoded by multigene families (Jamet et al., 2006).

The nature of the cell wall proteins is as varied as the numerous functions of plant cell walls (Cassab, 1998). Many PCW proteins are glycosylated – polypeptides with carbohydrate side-chains, which can be a mono-, oligo-, or polysaccharide (Fry, 2001). There are two types of glycosidic bond between the carbohydrate side-chain and the polypeptide backbone of a glycoprotein: *O*-glycosidic bonds, where the reducing terminus of the carbohydrate is attached to an –OH group on the polypeptide, and *N*-glycosidic bonds, which form between a sugar residue (usually *N*-acetylglucosamine) and the side-chain N atom of L-asparagine (Fry, 2000).

Although the sequence for the polypeptide backbone is encoded by a gene, and therefore has a predefined initial size, post-translational proteolysis and modifications can introduce variation. The number and size of the carbohydrate side-chains, and the shape of the wall glycoproteins also vary. For example, extensins have a rod-like shape, arabinogalactan-proteins adopt a much more globular 'wattle blossom' shape, and wall enzymes adopt a more common globular shape. The charge (or isoelectric point) also differs between PCW (glyco)proteins, spanning between the two extremes. For example, while extensins are highly basic (e.g. pI 11, rich in lysine and histidine), AGPs are often highly acidic (e.g. pI 1.5, rich in uronic acid residues), and cell wall enzymes present a wide range of different pI values (Fry, 2000), one of the most acidic (pI ≈ 4.1) being the recently discovered hetero-trans-β-glucanase of *Equisetum* (Simmons et al., 2015).

Researchers on cell wall proteomes have proposed classification into functional classes: proteins acting on polysaccharides (PAC, such as glycoside hydrolases, XTH,

carbohydrate esterases and lyases), oxido-reductases (OR, such as peroxidases and multicopper oxidases), proteases (P, such as Asp proteases, Cys proteases, Ser carboxypeptidases), proteins having interacting domains (ID) with polysaccharides (such as lectins) or proteins (such as enzyme inhibitors, leucine-rich repeats proteins), proteins possibly involved in lipid metabolism (LM, such as lipid transfer proteins), proteins possibly involved in signalling (S, such as AGPs), structural proteins (SP, such as expansins, leucine-rich repeat extensins, GRPs) and protein of yet unknown function (UF) (Albenne et al., 2014).

It has been estimated that approximately 10–15% of about 27000 protein-coding genes in the *Arabidopsis* genome are dedicated to cell wall development; however, only about 121 *Arabidopsis* genes thus far have experimental evidence validating cell wall function (Carpita et al., 2001; Mewalal et al., 2014). For example, several cell wall proteins have been demonstrated to provide a structural contribution, by cross-linking into the wall such as extensins, PRP2 (Keller, 1993; Lamport et al., 2011). Some structural and catalytic proteins have been proposed that are necessary for expansion during cell differentiation such as expansins, extensins and XTHs (Fry, 1992; Pennell, 1998). Moreover, AGPs are readily soluble and play a major role in cell-cell interactions during development (Cassab, 1998).

Little is known about how different proteins interact with each other and with other components of the cell wall. The precise localisation and developmental expression pattern of PCW proteins are also unclear (Keller, 1993).

### 1.2.2 Plant cell growth control

Physically, the irreversible enlargement of plant cells results from two interdependent physical processes: water absorption and cell wall yielding (Westgate and Boyer, 1985; Volkenburgh and Cleland, 1986; Cosgrove, 2005). Growth originates from the yielding of the load-bearing network in the wall, inducing "relaxation" of the tensile wall elements and thus a reduction in the wall stress, which simultaneously decreases the turgor pressure (Cosgrove, 1985). The relaxation of the wall reduces the cell water potential and results in a passive water influx, which in turn increases the cell volume and extends the cell wall (Cosgrove, 1986, 1993). A young cell may grow to more than 1000 times its original volume such as a hair cell on the surface of a young cotton seed

(Cosgrove, 2005). As the cell wall has a high tensile strength, for expansion to be possible, it must be modified and loosened (Tomos and Pritchard, 1994). Therefore, the susceptibility of the PCW to turgor-driven expansion is the principal factor that controls plant cell growth (Cosgrove, 1993; Fenwick et al., 1999).

The tensile skeleton of the PCW is established through the interlinking of cellulose microfibrils and non-cellulosic polysaccharide matrices (Carpita and Gibeaut, 1993).The breakage of this network is integral to cell expansion (Passioura and Fry, 1992). As cellulose microfibrils cannot be stretched longitudinally, they move relative to each other during cell expansion or elongation. The microfibrils align in transverse or helical orientations to the elongation axis (Carpita and Gibeaut, 1993). For expansion to occur, the hemicellulose tethers between cellulose microfibrils must be selectively loosened and rearranged. The integrity of tethers can be affected by numerous agents, including expansin, β-glucanase, xyloglucan endotransglucosylase/ hydrolase (XTH) protein and hydroxyl radicals. These agents weaken the cellulose–hemicellulose framework of the cell, thus allowing expansion.

#### 1.2.2.1 Expansin

Expansins are a large multigene family of proteins that bind tightly to the cell wall and have the ability to promote cell wall loosening *in vitro* and catalyse pH-dependent wall extension and stress relaxation during acid growth (Fry, 2001; Cosgrove, 2002; Sampedro and Cosgrove, 2005). All expansins contain two domains: domain 1 is homologous to the catalytic domain of proteins in the glycoside hydrolase family 45 (GH45) and domain 2 is homologous to group-2 grass pollen allergens without known biological functions (Sampedro and Cosgrove, 2005).

Expansins were first extracted in a crude salt-solubilised fraction of wall fragments, which were isolated from the growing hypocotyls of dark-grown cucumber seedlings (McQueen-Mason et al., 1992). This cucumber wall extract had the ability to induce the extension of heat-inactivated walls. The active material – expansins – appeared to be restricted to the growing region of the cucumber hypocotyl. It was found that this extract was active not only on the cucumber wall but also on the cell walls of various dicot seedlings (pea, radish, tomato) and monocots of the family Amaryllidaceae (onion and zephyr lily).

McQueen-Mason et al. (1992) separated two proteins from the cucumber wall extract with relative molecular masses of 29 kDa and 30 kDa. The two proteins were separated via ammonium sulphate precipitation and sequential HPLC, first using a hydrophobic interaction column and then a cation-exchange column. Each protein was able to induce rapid extension of the heat-inactivated walls but there was no detectable release of monosaccharides or oligosaccharides, suggesting that they had little or no exoglycanase or typical endoglycanase activities. Therefore, the induction of extension was thought to be the result of a novel biochemical mechanism (McQueen-Mason et al., 1992)

Further study by this group indicated that expansins were instead bound to the surface of cellulose microfibrils at non-crystalline regions, which form the junction between the cellulose surface and matrix hemicelluloses, disrupting the hydrogen bonds formed between microfibrils and allowing the wall to yield to the tensile stresses created by the turgor pressure, leading to extension (McQueen-Mason and Cosgrove, 1995).

Currently, two large families of expansin genes have been discovered in plants, encoding α-expansins (EXPA) and β-expansins (EXPB) (Fry, 2001; Cosgrove, 2002). They are similar to each other in size (~25–28 kDa for the mature protein) and have distant but significant sequence similarity to each other throughout the length of the protein backbone (Cosgrove et al., 2002). Both families have been identified in a wide range of land plants, from angiosperms and gymnosperms to ferns and mosses (Li et al., 2002). Their members show diverse organ-, tissue- and cell-specific expression patterns (Cosgrove et al., 2002).

The model plant, *Arabidopsis thaliana*, contains around 26 different α-expansin genes; and 10 β-expansin genes which can be further divided into 3 subgroups, designated as β1 through β3 (Li et al., 2002). There are also expansin-like proteins (EXPLA and B) and a single, more distant protein expansin-related protein (EXPR) whose sequences fall outside the two existing expansin families and characteristic expansin activities have not been tested (Cosgrove et al., 2002; Sampedro and Cosgrove, 2005).

#### 1.2.2.2 β-Glucanase

The β-glucanases (EGases, EC 3.2.1.4) are enzymes that hydrolyse 1,4-β-D-glucans and play a role in various physiological processes (Yu et al., 2013). They are encoded by a large gene family, which belongs to the glycosyl hydrolase gene family 9 (GH9) (Henrissat, 1991), and can be divided into α, β, and γ subfamilies based on phylogenetic analysis (Libertini et al., 2004). The α- and β-subfamily contains proteins involved in a number of physiological roles such as elongation, ripening and abscission. The γ-subfamily is composed of proteins that are predicted to have a membrane-spanning domain and to be localised at the plasma membrane; they may have a role in cellulose biosynthesis such as Korrigan (KOR) (Libertini et al., 2004; Maloney et al., 2012).

Alternatively, this glycosyl hydrolase (GH) multigene family can be grouped into three subclasses: A subclass (GH9A) including membrane-anchored GH proteins, B subclass (GH9B) including secreted GH protein, and C subclass (GH9C) including secreted proteins with a carbohydrate binding module according to their sequence domain (Urbanowicz et al., 2007). In *Arabidopsis*, the α-subfamily mainly consists of GH9B and GH9C proteins, except for one GH9A protein; the γ-subfamily proteins belongs to GH9A subclass; and the subclass of proteins in the β-subfamily remain uncertain because of a lack of experimental data and clear typical domain prediction (Yu et al., 2013). There are about 25 genes encoding endoglucanases that belong to glycosyl hydrolase family 9 (GH9) proteins in *Arabidopsis* (Maloney et al., 2012).

The α-subfamily contains the majority of the secreted glucanases currently identified. A large number of studies have implicated this subfamily in cell wall disassembly, e.g. during the fruit ripening process, as well as in wall reconstruction, which allows wall loosening during cell expansion (Brummell et al., 1997b; Llop-Tous et al., 1999; Yu et al., 2013).

Brummell et al. (1997a) found that the expression of an endo-1,4-β-glucanase cDNA clone, *Cel4*, isolated from tomato positively correlated with rapid cell expansion in the pistils, the growing zone of etiolated hypocotyls, and in the young expanding leaves of tomato.

Matsumoto et al. (1997) isolated a 70-kDa protein from the apoplast fraction of auxin-treated pea (*Pisum sativum*) stems, in which both the rate of stem elongation and the amount of xyloglucan solubilised were high, by gel-permeation chromatography on Superdex 200. This enzyme specifically cleaved the 1,4-glucosyl linkages within the xyloglucan backbone to yield mainly nona- and heptasaccharides. It did not hydrolyse carboxymethylcellulose, or (1→3,1→4)-β-glucan. It also did not have a transglycosylase activity on xyloglucan, thus differentiating itself from cellulase and xyloglucan endotransglucosylase activities. This xyloglucan-specific endo-1,4-β-glucanase enzyme hydrolysed both non-fucosylated and fucosylated xyloglucan at random, promoting cell wall expansion and stem elongation (Matsumoto et al., 1997).

In *Arabidopsis thaliana*, a strong transcript signal of an α-type EGase gene (*Cel1*), encoding a 54-kD protein, was detected in the elongation zone of the flowering stems of normal plants but not in the fully expanded leaves or the basal internode of the flowering stem. This locality suggests a role for this enzyme in cell wall expansion (Shani et al., 1997).

A membrane-bound endoglucanase called Korrigan (KOR) has been shown to be required for synthesis of the ordered, load-bearing cellulose–hemicellulose network (Nicol et al., 1998). Mutation in *KOR* caused cellulose deficiency and growth defects (Molhoj et al., 2002). *KOR* was originally found in a short hypocotyl mutant in *Arabidopsis thaliana* plant. In *kor1-1* mutant which had a reduction in the amount of KOR, seedlings and adult plants were dwarfed and all cell types showed reduced cell elongation, except for tip-growing cells. Under dark-grown conditions, the growth defect in hypocotyls was associated with pronounced changes in the cellulose–xyloglucan network within the primary wall (Nicol et al., 1998). In *kor1-2*- a stronger mutant allele, no KOR was produced and the plant was extremely dwarfed and showed abnormal cell plates and incomplete cell walls, causing cytokinesis defects (Zuo et al., 2000). In addition, *KOR* has been shown to be partially functionally conserved between gymnosperms and angiosperms (Maloney et al., 2012).

#### 1.2.2.3 XET activity

Xyloglucan endotransglucosylase activity (XET) can cleave and re-join xyloglucan chains, allowing expansion of the cellulose–hemicellulose network. XET activity is

the main focus of this thesis and therefore further information can be found related to this enzyme activity in section 1.4.2.

#### 1.2.2.4 Non-enzymic scission

The last cell wall loosening agent pertinent to plant cell wall expansion is the non-enzymic scission that has been demonstrated in a number of studies. The breakdown of several cell wall polysaccharides, including cellulose, sodium carboxymethylcellulose, pectin, polygalacturonic acid, xylan and arabinogalactan, was observed following their incubation with 0.1-10 mM hydrogen peroxide. These incubations resulted in a reduction in solution viscosity or an increase in reducing groups (Miller, 1986). This was the first observation that suggested a role for hydrogen peroxide in cell wall degradation and, consequently, cell wall expansion in plants.

The hydroxyl radical, $^{\bullet}OH$, was another compound that has been shown to cause non-enzymic cell wall loosening *in vitro* and probably also *in vivo*, thus enabling cell expansion, fruit ripening and organ abscission (Fry et al., 1998). The hydroxyl radical is significantly more reactive than hydrogen peroxide and can be produced by a Fenton reaction: $Cu^{+} + H_2O_2 \rightarrow {}^{\bullet}OH + OH^{-} + Cu^{2+}$ (Fry, 1998). It is thought that $^{\bullet}OH$ reacts with cellobiose by abstracting hydrogen from the C-1, C-4, or C-5 of a sugar residue in a (1→4)-linkage, leading to the scission of a glycosidic bond (Schuchmann and von Sonntag, 1978). Fry (1998) showed that a combination of 5 mM $H_2O_2$ and 5 mM L-ascorbate caused a very rapid scission in all of the polysaccharides tested, including xyloglucan, carboxymethylcellulose, pectin, dextran, alginate and methylcellulose *in vitro*. Addition of ascorbate to a xyloglucan solution that already contained 1 mM $H_2O_2$ was observed to cause a sudden burst of scission *in vitro* (Fry, 1998).

It was experimentally confirmed that, *in vivo*, $^{\bullet}OH$ radicals could be produced by a mixture of naturally occurring compounds in the cell wall of the living plant cell, including $O_2$, Cu and ascorbate. Oxygen is ubiquitous in healthy plants. Plant tissues typically have Cu contents of about 3-30 mg/kg dry weight and much of the Cu is located in the cell walls (Fry, 1998). The last requirement, ascorbate, which could reduce apoplastic $Cu^{2+}$ to $Cu^{+}$ and $O_2$ to $H_2O_2$, has been reported to present in the apoplast of several species' organs, for example in barley (Vanacker et al., 1998) and *Betula pendula* leaves (Kollist et al., 2008). In fact, reactive oxygen intermediates

including superoxide radicals, hydrogen peroxide, and $^{\bullet}OH$ was reported to be generated in the apoplastic space of germinating radish seeds (Schopfer et al., 2001). $^{\bullet}OH$ *in vivo* could be scavenged by solutes present in the apoplast, high concentrations of scavengers, such as 50 mM cysteine or > 30 mM salicylate were demonstrated to be efficient to block xyloglucan scission completely. This suggested that any apoplastic $^{\bullet}OH$ formed was likely to cause the oxidative scission of polysaccharide chains in the cell wall, thus playing a useful role in the loosening of the cell wall (Fry, 1998).

Schopfer (2001) pre-impregnated isolated cell walls of coleoptiles or hypocotyls from maize, cucumber, soybean, sunflower or Scots pine seedlings with Fe or Cu ions and then incubated them in solutions containing $H_2O_2$ and ascorbate to generate $^{\bullet}OH$ in the cell wall. This treatment induced irreversible wall extension (creep) in walls stretched in an extensiometer. The reaction could be promoted by acid pH and inhibited by several $^{\bullet}OH$ scavengers including thiourea, histidine and adenine. Generation of $^{\bullet}OH$ by the same reaction in living coleoptile or hypocotyl segments also caused elongation growth. This results suggested that $^{\bullet}OH$ may be an essential component of the biochemical mechanism engaged in wall loosening during auxin-induced extension growth (Schopfer, 2001).

## 1.3 Xyloglucan and its role in plant cell growth control

### 1.3.1 Structure of xyloglucan

Xyloglucan is a neutral hemicellulose that comprises a linear backbone of (1→4)-linked β-D-glucose residues, of which approximately 60-75% have a side-chain substitution of α-D-xylose at position 6. Xyloglucan's cellulose-like backbone, which is between 0.15 and 1.5 μm long, consists of between 300 and 3000 β-(1→4)-linked D-glucopyranose residues (Fry, 1989a). Typically, every fourth glucose residue is non-xylosylated and is, therefore, susceptible to cleavage by certain cellulases (Fry, 1989a; Hayashi, 1989).

Table 1*:* Nomenclature of xyloglucan oligosaccharides.

The following code letters are used for describing concisely the sequence of side-chains and unbranched glucose residues along the (1→4)-β-D-glucan backbone of xyloglucan. Oligosaccharides are named by listing these building blocks in sequence from non-reducing to reducing end. All residues are pyranose except arabinose which may be pyranose (Arap) or furanose (Araf). Square brackets indicate branching. For example, in 'C' an α-Xyl residue is linked to the 6-position of the Glc* and an α-Ara-(1→3)-β-Xyl group is linked to the 2-position of the same Glc*; thus 'C' could be represented as α-Xyl→β-Glc*←β-Xyl←α-Ara. Likewise, in 'N' an $Ara_p$ residue is linked to the 2-position of the Xyl and a β-Gal-(1→6)-β-Gal group is linked to the 4-position of the same Xyl (Franková and Fry, 2012; Peña et al., 2012).

| Code | Structure |
|---|---|
| A | α-D-Xyl-(1→6)-[α-L-Araf-(1→2)]-β-D-Glc* |
| B | α-D-Xyl-(1→6)-[β-D-Xyl-(1→2)]-β-D-Glc* |
| C | α-D-Xyl-(1→6)-[α-L-Araf-(1→3)-β-D-Xyl-(1→2)]-β-D-Glc* |
| D | α-L-Arap-(1→2)-α-D-Xyl-(1→6)-β-D-Glc* |
| E | α-L-Fuc-(1→2)-α-L-Arap-(1→2)-α-D-Xyl-(1→6)-β-D-Glc* |
| F | α-L-Fuc-(1→2)-β-D-Gal-(1→2)-α-D-Xyl-(1→6)-β-D-Glc* |
| G | β-D-Glc* with no side-chain attached |
| Gol | Glucitol (the former reducing terminus after reduction with NaBH4) |
| J | α-L-Gal-(1→2)-β-D-Gal-(1→2)-α-D-Xyl-(1→6)-β-D-Glc* |
| L | β-D-Gal-(1→2)-α-D-Xyl-(1→6)-β-D-Glc* |
| M | α-L-Arap-(1→2)-[β-D-Gal-(1→4)]-α-D-Xyl-(1→6)-β-D-Glc* |
| N | α-L-Arap-(1→2)-[β-D-Gal-(1→6)-β-D-Gal-(1→4)]-α-D-Xyl-(1→6)-β-D-Glc* |
| P | β-D-GalA-(1→2)-[β-D-Gal-(1→4)]-α-D-Xyl-(1→6)-β-D-Glc* |
| Q | β-D-Gal-(1→4)-β-D-GalA-(1→2)-[β-D-Gal-(1→4)]-α-D-Xyl-(1→6)-β-D-Glc* |
| S | α-L-Araf-(1→2)-α-D-Xyl-(1→6)-β-D-Glc* |
| T | β-L-Araf-(1→3)-α-L-Araf-(1→2)-α-D-Xyl-(1→6)-β-D-Glc* |
| U | β-D-Xyl-(1→2)-α-D-Xyl-(1→6)-β-D-Glc* |
| V | α-D-Xyl-(1→4)-α-D-Xyl-(1→6)-β-D-Glc* |
| X | α-D-Xyl-(1→6)-β-D-Glc* (=isoprimeverose) |
| Y | β-D-GalpA-(1→2)-α-D-Xylp-(1→6)-β-D-Glc* |
| Z | α-L-Fucp-(1→2)-β-D-GalpA-(1→2)-α-D-Xylp-(1→6)-β-D-Glc* |

* The β-D-Glc in each structure is part of the (1→4)-β-glucan backbone of the xyloglucan

Franková and Fry (2012) discovered a new xyloglucan building block in which an α-D-xylosyl bond is formed to the 4-position of the xylose residue of an existing isoprimeverose unit by trans-α-xylosidase activity in *Asparagus*, forming the structure α-D-xylosyl-(1→4)-α-D-xylosyl-(1→6)-β-D-glucosyl, coded as V (Franková and Fry, 2012).

A single-letter nomenclature is used to simplify the identification of xyloglucan side-chain structures, as illustrated in *Table 1*. According to this system, a backbone glucose residue without any further substitution is depicted by the letter G while a backbone glucose residue with an additional xylosyl unit at the *O*-6 position is denoted by X (Fry et al., 1993). Backbone residues can carry further side-chain substitutions at position *O*-2 of either the xylose or glucose residues which have different structures and names. To date, there have been eighteen known xyloglucan repeat-units besides G and X have been identified, each with a unique code listed in Table 1 (Franková and Fry, 2012; Peña et al., 2012).

If the reducing glucose moiety has been converted to an alditol moiety, it is indicated by the code "Gol". Acetylated sidechains are depicted with an underline, such as in S and L. To date, only three distinct XyG glycosyl units have been found to be acetylated (Schultink et al., 2014). These include unsubstituted glucosyl backbone residues (G) (Jia et al, 2005; Gibeaut et al., 2005), the arabinofuranosyl-residue of S groups (Jia et al., 2005), and the D-galactosyl-residue of L, F and J groups (Kiefer et al., 1989; Scheller and Ulvskov, 2010; Gille et al., 2011).

Peña et al. (2012) showed that *Arabidopsis thaliana* root hair walls consist of a specific xyloglucan that is composed of both neutral and GalA-containing subunits, the latter containing β-D-galactosyluronic acid-(1→2)-α-D-xylosyl-(1→ assigned as Y and/or α-L-fucosyl-(1→2)-β-D-galactosyluronic acid-(1→2)-α-D-xylosyl-(1→) assigned as Z (Peña et al., 2012).

Xyloglucan sidechains are not randomly positioned but are organized into xyloglucan oligosaccharide motifs that can be released for identification by digestion of xyloglucan with endoglucanases, which cleave xyloglucan at unsubstituted glucose residues (Pauly et al., 1999; Rose et al., 2002; Hoffman et al., 2005). *Arabidopsis* and many other dicots share the common xylosylation motif of XXXG in which three consecutive (1→4)-linked β-D-glucopyranosyl backbone residues are substituted at *O*-6 with a glycosyl side chain (including XXFG, XXLG, XLLG, XLFG) (Scheller and Ulvskov, 2010). Motif $XXGG_n$ (with n is from 1 to 3) with a reduced degree of xylosylation was observed in the Poaceae, including barley and rice (Hoffman et al., 2005; Schultink et al., 2014). In this motif, alternatively, an *O*-acetylation of the glucan

backbone occurred at some positions (Schultink et al., 2014). In Solanaceae, such as in tomato and tobacco, less xylosylation was also found with the dominant xyloglucan motif being XXGG (Hoffman et al., 2005; Jia et al., 2005). In contrast, some additional xylosylation motifs have also been identified including XXXXG and XXXXXG, e.g. as part of seed storage xyloglucan (Buckeridge, 2010).

While the majority of xyloglucan oligosaccharides released from a particular species and tissue follow the dominant xylosylation pattern, there are exceptions. Besides the dominant xyloglucan oligosaccharide pattern, there have been some exceptions such as a small amount of XXG being found in xyloglucan digestion in both monocot and dicot species (Schultink et al., 2014).

### 1.3.2 Synthesis of xyloglucan

As with other hemicelluloses, xyloglucan is synthesised in the Golgi membrane by numerous proteins that have been identified in recent years.

The xyloglucan glucan backbone may be synthesized by CSLC4, a member of the cellulose synthase-like C (CSLC) family that belong to CAZy family GT2. Cocuron et al. (2007) found *CSLC4* overrepresented in the cDNA library produced from mRNA isolated during the deposition of xyloglucan at the last stages of nasturtium (*Tropaeolum majus*) seed maturation. Heterologous expression of *TmCSLC4* in *Pichia pastoris* resulted in the production of β-(1,4) glucan *in vitro* and the expression of its orthologue in *Arabidopsis*, *AtCSLC4*, was coordinated with that of other genes involved in xyloglucan biosynthesis (Cocuron et al., 2007).

Cavalier et al. (2008) isolated and characterized *Arabidopsis* mutants on xyloglucan α-1,6-xylosyltransferase including *xxt1*, *xxt2*, and *xxt1 xxt2*. The *xxt1* and *xxt2* mutants had a slight decrease in xyloglucan content and showed slightly altered distribution patterns for xyloglucan epitopes. The *xxt1 xxt2* double mutant had short root hairs with bulging bases and lacked detectable xyloglucan resulting in significant changes in the mechanical properties of the plant including reduced stiffness and ultimate stress. These results indicated the role of xylosyltransferases in xyloglucan biosynthesis (Cavalier et al., 2008)

Recently, Vuttipongchaikij et al. (2012) studied seven genes of the glycosyltransferase GT34 family and revealed that five genes encoding xyloglucan α-1,6-xylosyltransferase (XXT1-5). The truncated proteins (lacking the N-terminal transmembrane domain) of XXT1, XXT2 and XXT4 expressed in *E. coli* as GST fusion proteins showed the xylosyltransferase activity. The *xxt2* and *xxt5* mutants had a reduced level of xyloglucan in the cell walls of a range of tissues, with the most dramatic reductions in stems, embryos and seedlings (Vuttipongchaikij et al, 2012).

Use of LM15 antibody which binds to the xyloglucan backbone suggested that the double mutants *xxt1 xxt5* and *xxt2 xxt5* showed a further reduction in xyloglucan epitopes in both stem and embryo sections and no detectable labelling in the primary xylem as well as in the cell wall of the mutant embryos compared to the reduced level seen in the *xxt2* and *xxt5* single mutants (Vuttipongchaikij et al., 2012).

Moreover, the extractable xyloglucan content was significantly reduced in the *xxt2, xxt5, xxt1 xxt*5 and *xxt2 xxt5* mutants. XXXG was found to be reduced while XXFG and XLXG were increased in *xxt2, xxt4* and *xxt2 xxt4* mutants proving that *XXT4* had a role in xyloglucan biosynthesis. In contrast, XXXG was increased and all galactosylated and fucosylated oligosaccharides were lowered in the cell wall of *xxt2 xxt5*. The molecular mass distribution of xyloglucans in the stem cell walls of these mutants was also changed compared to wild type. *XXT1* or *XXT3* overexpression demonstrated a strong complementation in *xxt2, xxt5* and *xxt2 xxt5* mutant backgrounds indicated that *XXT3* also encoded an active protein for xyloglucan biosynthesis (Vuttipongchaikij et al., 2012).

There have been several genes in the GT47 family identified as being responsible for adding β-glycosyl groups to the *O*-2 position of a xylosyl group of xyloglucan, including *MUR3* and *XLT2* with galactosyltransferase activity, *XST1* and *XST2* with arabinosyltransferase activity and *XUT1* for xyloglucan-specific galacturonosyltransferase activity (Madson et al., 2003; Schultink et al., 2013; Peña et al., 2012).

Madson et al. (2003) studied on a *mur3* mutation in *Arabidopsis* resulting in a reduction of cell wall fucose and galactose content in both 1 M KOH and 4 M KOH extractable fractions and a failure of attachment of the Gal residue on the third xylosyl

unit in the XXXG core structure. In this mutant, the α-L-Fuc-(1→2)-β-D-Gal-(1→2) side group, which was considered important for xyloglucan binding to cellulose (Levy et al., 1997), was completely absent and the galactosylation at the second xylose residue was enhanced, suggesting that *MUR3* represented the structural gene for xyloglucan galactosyltransferase (Madson et al., 2003).

Schultink et al. (2013) overexpressed either *XST1* or *XST2* in an *Arabidopsis* double-mutant lacking xyloglucan galactosylation (*mur3.1 xlt2*). These glycosyltransferases were identified from tomato by comparative genomics with known xyloglucan galactosyltransferases gene from *Arabidopsis*. The result showed a production of arabinosylated xyloglucan indicating that XST1 and XST2 had arabinosyltransferase activity (Schultink et al., 2013).

Peña et al. (2012) found that a loss-of-function mutation in *At1g63450*, a root hair-specific gene, encoding a CAZy family GT47 glycosyltransferase that forms the β-D-galactosyluronic acid-(1→2)-α-D-xylosyl linkage, resulting in the synthesis of xyloglucan lacking galacturonic acid. In addition, the root hairs of this mutant were shorter than those of the wild type and these phenotypes could be complemented by *At1g63450*. Moreover, the overexpression of *At1g63450* in tissues that contained no acidic xyloglucan such as the leaf and stem cell walls led to the synthesis of galacturonic acid-containing xyloglucan in proposing the activity for this gene as a xyloglucan-specific galacturonosyltransferase (XUT1). This activity was responsible for catalysing the formation of the β-D-galactosyluronic acid-(1→2)-α-D-xylopyranosyl linkage in the root hair cell walls (Peña et al., 2012).

One gene in the GT37 family, *MUR2/FUT1,* was found in *Arabidopsis* to be responsible for fucosyltransferase activity. Genetic disruption of the gene encoding FUT1 in the *mur2* mutant resulted in non-fucosylated xyloglucan (Vanzin et al., 2002).

A gene responsible for acetyltransferase activity has been identified in *Arabidopsis* as Altered Xyloglucan 4 (*AXY4)*. The *axy4-1* and *axy4-2* mutant in *Arabidopsis thaliana* had a 20 to 35% reduction in xyloglucan *O*-acetylation. Loss of *AXY4* transcript resulted in a complete lack of *O*-acetyl substituents on xyloglucan in several tissues, except seeds which was instead *O*-acetylated by paralogue AXY4like (*AXY4L*). Wall fractionation analysis of *axy4* knockout mutants indicated that only a fraction

containing xyloglucan was non-*O*-acetylated suggesting that *AXY4/AXY4L* was responsible for xyloglucan-specific *O*-acetyltransferase activity (Gille et al., 2011).

### 1.3.3 The role of xyloglucan in controlling cell expansion

#### 1.3.3.1 Why is xyloglucan important for cell expansion?

Two thirds of the dry primary cell wall mass is the cellulose–hemicellulose network. About five different xyloglucan domains have been defined in the cell wall: entrapped xyloglucan in the cellulose microfibrils, xyloglucan on the surface of the microfibrils, xyloglucan tethers between microfibrils, newly secreted xyloglucan that do not attach to microfibrils and the non-reducing and the reducing terminal loose ends of xyloglucan (Smith and Fry, 1991; Pauly et al., 1999a; Thompson and Fry, 2001). In the primary cell wall of all dicotyledonous and non-poalean monocotyledonous plants, xyloglucan is the most quantitatively abundant hemicellulosic polysaccharide (Pauly et al., 1999a). Thus, the major tension-bearing structure in the dicot primary wall is normally thought to be the xyloglucan–cellulose complex (Hayashi, 1989; McCann et al., 1990).

Xyloglucan has a central role in contemporary plant cell wall models in which it serves as key a cross-linking molecule, responsible for coating and tethering the load-bearing cellulose microfibrils (Carpita and Gibeaut, 1993). Like all other hemicelluloses, xyloglucans connect to cellulose microfibrils by hydrogen-bonding and this bond is strongly affected by the DP of the xyloglucan (e.g. small (DP 7-9) xyloglucan oligosaccharides (XGOs) almost lack this ability) (Hayashi et al., 1994).

Xyloglucan is important for the structural function of land plants, involving in the evolution of organisms from water to drier habitats (Popper and Fry, 2008) as well as for the providing hexose and pentose sources for developing seedlings. In a special sub-set of dicotyledonous plants including nasturtium (*Tropaeolum majus*), tamarind (*Tamarindus indica*), *Impatiens* and *Annona*, the seed wall reserve polysaccharide is xyloglucan. A *Tropaeolum* seed weighing about 120 mg can contain about 30 mg of xyloglucan, making its cotyledon a really thick cell wall and this cell wall become remarkably thin after germination because the xyloglucan was cleaved to monosaccharides. (Reid, 1985; Buckeridge et al., 2000; Buckeridge, 2010).

#### 1.3.3.2 Xyloglucan plays two very different roles in the control of cell growth

At a high concentration of about 10% (w/v) in the wall *in vivo*, xyloglucan is a major building material of the wall, responsible for wall extensibility and the rate of cell expansion (Fry, 1989).

In cell elongation caused by auxin stimulation, cell wall loosening caused by degradation of xyloglucan was evidenced (Labavitch and Ray, 1974; Gilkes and Hall, 1977; Hoson et al., 1991). A small proportion of the xyloglucan initially present in the tissue (and labelled by brief feeding of [$^{14}$C]Glc followed by a cold chase) disappeared upon subsequent treatment with auxin, presumably because of being hydrolysed to mono- and oligo-saccharides (Gilkes and Hall, 1977). A further proportion of the remaining xyloglucan which was previously insoluble became soluble in water upon auxin treatment, indicating a highly selective pattern of xyloglucan turnover process with the influence of auxin (Labavitch and Ray, 1974). Using polyclonal antibodies against XGOs (including isoprimeverose, XXXG and XXLG), Hoson et al. (1991) showed that the antibodies suppressed auxin-induced elongation of epicotyl segments of azuki bean (*Vigna angularis*). The antibodies also caused a decrease in the minimum stress-relaxation time and the relaxation rate of the cell walls of azuki segments, suggesting that they inhibited auxin-induced cell wall loosening. In addition, the decrease in molecular mass of xyloglucan caused by treatment of azuki bean epicotyl segments with IAA was completely inhibited in the presence of the XXXG and XXLG antibodies. These antibodies also inhibited the autolytic release of xylose-containing products from the cell wall preparation of azuki epicotyls (Hoson et al., 1991).

Park et al. (2003) overexpressed poplar cellulase in *Arabidopsis thaliana*, resulting in a 1.6-fold increase in diameter of rosettes of transgenic plants compared to the wild type. Both epidermal and parenchyma cells in the hypocotyl and leaves were larger in the transgenic plants than in the wild type plants. Assays of the mechanical properties of the leaf cell wall showed a higher total extensibility at breaking point and larger elongation values in the transgenic plants compared to the wild type. The transgenic plants had less hemicellulose than the wild type plant. The transgenic plants contained less 4%-KOH-insoluble xyloglucan. NMR spectra showed a small but substantial

difference between the transgenic and wild type plants: the higher field resonance (which are thought to originate from more mobile chains than that in crystal-core) of C4 and C6 became less prominent in the transgenic plants, indicating a decrease in the mobile chains of 1,4-β-glucans. These results indicate that the expressed cellulase decreases the disordered 1,4-β-glucan chains on cellulose microfibrils in the wall, thus solubilises some xyloglucans that are intercalated there to form paracrystalline microfibrils which in turn accelerates growth in the transgenic plants (Park et al., 2003).

Another study by the same group, on the overexpression of *Aspergillus* xyloglucanase in *Populus alba* resulted in a greater elongation of the internode in transgenic plants. Leaf epidermal cells were expanded in the transgenic plant and its leaf dry weight was also greater than that of the wide type. Cell wall analysis showed that xyloglucan amount was decreased by 80% in the primary cell wall of transgenic. Moreover, the Young's modulus in the elongating regions of the transgenic plants was also decreased consistent with a decrease in xyloglucan amount tethering between cellulose microfibrils. These results suggested that the expressed xyloglucanase cleaved the xyloglucans tethering cellulose microfibrils, thus promoted stem elongation by loosening the wall (Park et al., 2004).

Recently, xyloglucan were documented to form a complex with Al, thus may be a key factor affecting Al sensitive in *Arabidopsis* roots. Adding xyloglucan into Col0 culture medium significantly alleviated Al-induced root inhibition by decreasing Al accumulation in roots and cell wall. *xxt1 xxt2*, a double mutant in *Arabidopsis* which have no detectable xyloglucans contains lower levels of Al in the root and accumulates and adsorbs less Al in the root cell wall (Zhu et al., 2012).

At a tiny concentration of ≈ 0.73 nM a fucose-containing oligosaccharide XXFG which is released from xyloglucan has a hormone-like anti-auxin effect on growth. Hydrolysis of xyloglucan results in oligosaccharides with regulatory effects on living plant tissue. For example, at 1 nM, XXFG antagonizes 2,4-dichlorophenoxyacetic acid (2,4-D)-stimulated growth while at 100 nM, it gains a growth promoting effect. XFFG and FG also have the growth inhibitory effect at 1 nM but FG retains its growth-inhibitory effect at 100 nM (Fry, 1994). At approximately 1 μM, four different

cellotetraose-based XGOs (including XXXG, XXLG, XXFG and XLLG) mimic auxin in that they induce growth (Fry, 1994).

Enzymes of xyloglucan metabolism are of interest because of their important role in controlling wall strength and extensibility. No fewer than six GH families from microorganisms include endo-hydrolytic activities towards xyloglucan chains: GH 5, 7, 12, 16, 44 and 74 (Gilbert et al., 2008). In contrast, the only plant enzyme responsible for the cleavage and/or rearrangement of xyloglucan backbones has so far been identified is in GH16 named xyloglucan endotransglucosylase/hydrolase (XTH) (Rose et al., 2002). XTH proteins with their XET and XEH activity have been implicated in many aspects of cell wall biosynthesis (Zhu et al., 2012). XTHs either cut and rejoin xyloglucan chains through xyloglucan endotransglucosylase (XET) activity (Fry et al., 1992; Nishitani and Tominaga, 1992; Thompson and Fry, 2001) or catalyse the hydrolysis of xyloglucan through xyloglucan endohydrolase (XEH) activity (Van Sandt et al., 2007). In this study, I am focusing on XTHs and their XET activity which will be discuss more in details in the below section.

## 1.4 XTH proteins and their XET activity

### 1.4.1 XTH proteins

According to the Enzyme Commission, XET-active XTHs are referred to EC.2.4.1.207. The first transglycosylation was documented in 1989 when Baydoun and Fry fed 10 nM $^{3}$H-labelled XXFG and its naturally-occurring acetylated derivatives (XXFG·Ac) to rapidly-growing *Spinacia* cell cultures, and found that they became attached to soluble extracellular xyloglucan (Baydoun and Fry, 1989). Two year later, the first XET activity was demonstrated *in vivo* (Smith and Fry, 1991) and *in vitro* (Fry et al., 1992). In 1992, the first purification of the protein with same activity from apoplastic fluid of epicotyls of *Vigna* seedlings was done by Nishitani and Tominaga, who termed the protein endoxyloglucan transferase (EXT, later re-designated EXGT) (Rose et al., 2002). In the same year, Farkaš et al. (1992) showed that xyloglucan-specific endo-β-1,4-glucanase from nasturtium seeds exhibits XET activity *in vitro* which incorporated [$^{14}$C]XXFG to xyloglucan, thus reducing xyloglucan $M_r$ without hydrolysis. Later experiments on gene cloning proved that a protein from five different plant species including *V. angularis*, *Triticum aestivum*, *Arabidopsis thaliana*, *Lycopersicon*

*esculentum*, and *Glycine max* with XET activity belongs to the same class as the xyloglucanase from nasturtium (Okazawa et al., 1993).

The names XET and EXGT existed for a long time until scientists agreed to use a new name at the Ninth Cell Wall Meeting in 2001. In a review, Rose et al. (2002) gave a new unifying nomenclature for that family of enzymes, now known as XTH proteins which have one or both of two different activities: xyloglucan endotransglucosylase (XET) activity and xyloglucan endohydrolase (XEH) activity.

XTH proteins are encoded by xyloglucan endo-transglucosylase/hydrolase *(XTH*) genes. These form a large multi-gene family (33 genes in *Arabidopsis*, 41 in poplar, 29 in rice, 25 in tomato, at least 22 in barley, more than 58 in wheat, and at least 9 in the early-diverging spore-plant *Selaginella* (Maris et al., 2009)). Many XTHs share three common features: (i) a conserved DEIDFEFLG or DEIDLEFLG sequence (in *Selaginella kraussiana*) and some close alternatives such as DEIDIELLG, DELDFEFLG, DELDIEFLG, DEVDFEFLG, and DEVDIEFLG in some of the 33 *Arabidopsis* XTHs (Van Sandt et al., 2006, Eklöf and Brumer, 2010) which is related to the active site of *Bacillus* β-glucanases, functioning as the catalytic site both for hydrolase and transferase activity; (ii) a beginning sequence of the first exon signalling for direct secretion into the apoplast; (iii) four highly conserved Cys residues in the C-terminal portion of the protein that could form disulphide bridges, which help to stabilise the C-terminal extension, although the position of the second Cys residue varies slightly (Xu et al., 1995; Eklöf and Brumer, 2010).

XTHs have traditionally been divided into three major phylogenetic groups on the basic of sequences similarity: group I has four, group II has two or three and group III has four or five exons. Phylogenetic grouping has not been definitely shown to reflect any particular biochemical characteristics or mechanism of action. However, a comparison of XTH genes in the *Arabidopsis thaliana* and rice (*Oryza sativa*) genomes has indicated that there is no longer a clear division between the previously distinct groups I and II (Yokoyama et al., 2004). Baumann et al. (2007) performed a new bioinformatic analysis of the GH16 subfamily and provided an updated phylogenetic framework for XTHs. According to this, XTHs are divided into two predominant clusters. The largest cluster is merging of group I and II, referred at group I/II and it

can be subdivided into a number of smaller, statistically significant clades of protein sequences. The other cluster encompasses fewer sequences and coincides with the historical group III which can be further subdivided into two predominant clades: III-A and III-B (Baumann et al., 2007).

Heterologously expressed *XTH* genes from groups I/II have all exhibited exclusively XET activity, although in most cases donor and acceptor substrate specificities have not been extensively analysed (Eklöf and Brumer, 2010). All members of group III-B and the putative ancestral group may be strict, or at least predominant, XETs, while mixed-function XEHs/XETs are found only in group III-A (Baumann et al., 2007). The archetypal XEH-active XTHs, including TmNXG1 from nasturtium (Ibatullin et al., 2009), VaXGH from azuki bean (Tabuchi et al., 2001) and XTH31 from *Arabidopsis* (Zhu et al., 2012) belong to group III-A are among the *XTH* gene products with demonstrable hydrolytic (XEH) activity (Zhu et al., 2012). In contrast, heterologously expressed *XTH* genes in group III-B (*AtXTH27*, *SlXTH5*, and *HvXTH8*) show predominantly or exclusively XET activity, thus validating a functional distinction between the III-A and III-B clades (Eklöf and Brumer, 2010).

Using real-time PCR to quantify mRNA levels accurately, Yokoyama and Nishitani (2001) revealed that some XTHs exhibit distinct organ or tissue specific expression profiles. Individual *XTH* genes responded differently to plant hormones and environmental stimuli. Each *XTH* gene was likely to have a unique "fingerprint" of expression and regulation reflecting a unique physiological function (Rose et al., 2002).

A key feature of the canonical "retaining" catalytic mechanism employed by all members of GH16 is the formation of a covalent glycosyl–enzyme intermediate, which can be broken down by water, yielding hydrolysis (XEH activity), or an incoming saccharide substrate, yielding transglycosylation (XET activity) (Gilbert et al., 2008). XET activity cleaves the backbone of a xyloglucan molecule (donor substrate) and joins the newly formed, potentially reducing terminus on to the non-reducing end of an acceptor substrate, which can be another xyloglucan chain or a xyloglucan-derived oligosaccharide (Smith and Fry, 1991). One of its roles is integrating newly secreted xyloglucan chains into an existing wall-bound xyloglucan and the other role is restructuring existing cell wall material by catalysing transglycosylation between

previously wall bound xyloglucan molecules (Thompson and Fry, 2001). XEH activity has the same effect as cellulase on one xyloglucan chain: hydrolyses the backbone at any of the non-xylosylated Glc residues (Fanutti et al., 1993). Some proteins have only XET activity; some have only XEH activity (Fanutti et al., 1993) and the others have both. XEH activity may have developed as a gain of function in an ancestral XET-active XTH and also that an "ancestral group" of XTH sequences clustered closest to a bacterial β-(1→3, 1→4)-glucanase (Baumann et al., 2007; Eklöf and Brumer, 2010). The only known donor substrates for XTHs are xyloglucans and, in one case, $Glc_8$-based XGOs while $Glc_4$-based XGOs and xyloglucan polysaccharides are acceptors with an essential Xyl/Glc rich backbone. XTHs are principally apoplastic proteins with pH optima for this location between 5 to 6 (Campbell and Braam, 1999; Rose et al., 2002). XTHs can reversibly (XET) or irreversibly (XEH) loosen existing wall material, enabling cell expansion through the wall restructuring ability (Thompson and Fry, 2001; Van Sandt et al., 2007)

### 1.4.2 XET activity of XTHs

XET activity is responsible for cutting and re-joining of xyloglucan in the plant cell wall, causing transient matrix cleavage without hydrolysis, thus providing a molecular mechanism for controlled, turgor-driven wall expansion (Rose et al., 2002). XET activity was extractable from the growing parts of all plants tested including dicotyledons (pea, lupin, cow parsley, tomato, dandelion, nasturtium …), poalean monocotyledons (maize and Yorkshire fog grass), liliaceous monocotyledons (chives peduncle), a moss (gametophyte) and a liverwort (Fry et al., 1992; Stratilová et al., 2010). XET activity may participate in both wall-loosening, thus facilitating cell expansion, and wall-tightening, thus suppressing cell expansion, depending on the molecular size, location and age of the participating xyloglucan chains (Thompson and Fry, 2001; Maris et al., 2009).

XET activities are closely related to various physiological aspects of plant growth, such as seed germination (Farkaš et al., 1992; Fanutti et al., 1993), cell expansion (Fry et al., 1992), auxin-induced elongation (Nishitani and Matsuda, 1982), somatic embryogenesis (Hetherington and Fry, 1993) and fruit ripening (Redgwell and Fry, 1993). Extractable XET activity is positively correlated with growth rate in different

zones of the pea stem (Fry et al., 1992). Xyloglucan turnover is associated with rapid cell expansion, such as that which occurs during auxin-induced elongation (Nishitani and Masuda, 1982). XET activity is partially responsible for cell elongation because a slight decrease in *AtXTH18* mRNA abundance by RNAi resulted in a small but significant reduction in the epidermal cell length of the *Arabidopsis* primary root (Osato et al., 2006). In addition, higher expression of a *Brassica campestris* homologue of *AtXTH19* in *Arabidopsis* evoked a pronounced increase in cell expansion (Maris et al., 2009).

XTHs can also integrate newly synthesized xyloglucans into the cell wall through XET activity. Such integration is necessary for wall synthesis in meristems and also usually accompanies vacuolation since wall thickness is usually maintained during cell expansion. Thompson et al. (1998) demonstrated newly secreted xyloglucan chains undergo interpolymeric transglycosylation at the time of their binding to the cell wall.

XET is involved in the response of plants to hormonal and environmental stimuli. The expression of *XTH22*, formerly known as *TCH4*, a touch-inducible protein, was rapidly upregulated by hormones (10 and 50 μM IAA and 1 μM 24-epibrassinolide) and by touch, darkness, heat shock and cold shock. *XTH22* was found to be expressed in young expanding leaves, trichomes, lateral root primordia, vascular tissue, abscission zones and elongating hypocotyl grown under low light. This rapid upregulated expression of *XTH22* suggested its role in the adaptation of the plant to changing environmental conditions through the modification of the cell wall structure and properties. XET activity is well known for its ability to modify xyloglucan polymer length and arrangement, thus regulating cell wall extensibility and strength and controlling hormone-induced cell expansion. In response to mechanical stimulation, *XTH22* expression was increased in young expanding leaves, trichomes, and lateral root primordia but the plant became less elongated than untreated plants, indicating that the expansion promoted by XTH22 protein was limited to a radial direction or its XET activity was directed toward strengthening cell walls to make stronger and/or more flexible plants (Xu et al., 1995). Lee et al. (2005) used microarrays and quantitative RT-PCR to show that together with *XTH22*, *XTH17* and *XTH25* were also increasingly expressed in touched and darkness-treated aerial portion of *Arabidopsis*

*thaliana*. In contrast, *XTH31* and *XTH32* exhibited a greater than twofold reduction in expression in response to darkness in the same organ (Lee et al., 2005).

XET activity is also involved in the formation of secondary walls of xylem and/or phloem cells which was clearly demonstrated by Bourquin et al. (2002). Using an *in situ* assay for XET action and immunolocalisation of fucosylated xyloglucan with CCRC-M1 antibody, the presence of XET action as well as fucosylated xyloglucan in several types of secondary xylem and phloem cells during secondary wall deposition including xylem fibres, phloem fibres and xylem ray cells was documented. The immunological label especially increased during early secondary wall deposition of xylem fibres and accumulated at the primary/secondary (S1) layer. These results suggested a new role for XET in biogenesis of the secondary cell wall in which the newly produced xyloglucan was secreted and transported to the primary wall layer, where it was incorporated, thus creating reinforcing cross-links between microfibrils of the primary and secondary wall (S1), helping to bind these wall layers together. It was also found that *PttXET16*, a gene coding an enzyme in the GH16 family that was the closest relative of *XTH4* and *XTH5* of *Arabidopsis*, *NtXET1* of tobacco and *VaEXT* of adzuki bean, was highly upregulated in the mature stem where it was expressed in the phloem/cambium fraction as well as in the xylem fraction containing mainly secondary wall-forming cells. This enzyme was detected by immunolabelling in the wall of sieve tubes, in the innermost secondary wall layer of developing phloem fibres, in both fusiform and ray initials of the cambium. This indicated that this enzyme was the major isozyme with XET activity responsible for incorporation of xyloglucan in parts of the stem that exhibit secondary growth (Bourquin et al., 2002)**.**

### 1.4.3 *Arabidopsis* XTHs

There are 33 *XTH* genes in *Arabidopsis*, located in five chromosomes (I–V) with one-third of the genes occurring as a cluster of two to four members, probably resulting from genome duplication and gene reshuffling (Rose et al., 2002). Among these genes, only two (*XTH31* and *XTH32)* are in class III-A, are predicted to encode a protein with hydrolase activity (Baumann et al., 2007). XTH31 expression in yeast yields a protein with an demonstrated *in vitro* XEH:XET activity ratio of >5000:1 (Zhu et al., 2012).

All 33 members of *Arabidopsis XTHs* exhibit tissue specific expression. At least 10 genes were found to be predominantly expressed in roots including *AtXTH17, 18, 19*, and *20* while *AtXTH22* was predominantly expressed in siliques and *AtXTH24* was predominantly expressed in stems (Rose et al., 2002). Liu et al. (2007) found that *AtXTH21* is highly expressed in flowers and roots, and is up-regulated by treatment with gibberellin and cold shock.

Each *AtXTH* gene may have a different physiological and biological function (Maris et al, 2011). For example, *AtXTH21* plays a principal role in the growth of the primary roots by altering the deposition of cellulose and the elongation of the cell wall (Liu et al., 2007). Two loss-of-function mutants for the *AtXTH27* gene (Class III-B), *xth27-1* and *xth27-2* exhibited short-shaped tracheary elements in tertiary veins, and reduced the number of tertiary veins in the first leaf. In addition, the highest level of *AtXTH27* mRNA expression in the rosette leaves was observed during leaf expansion, when the tracheary elements were elongating indicating that *AtXTH27* plays an essential role during the generation of tracheary elements in the rosette leaves of *Arabidopsis* (Matsui et al., 2005). Maris et al. (2009) showed that *AtXTH14* and *AtXTH26* play a role in strengthening the side-walls of root-hairs and cell walls in the root differentiation zone after the completion of cell expansion. The incubation of growing *Arabidopsis* seedlings with purified AtXTH14 and AtXTH26 resulted in differences in root length. Also, the root hairs of the seedlings stacked very close together and were swollen at the base in the incubation with AtXTH14 whereas the seedlings showed very little or no elongation and root hair formation had ceased completely with swollen or irregularly appeared cortical cells in the incubation with AtXTH26. Moreover, the addition of purified AtXTH26 to the heat-inactivated onion epidermis caused a concentration-dependent decrease in the wall extension at pH 5.7, restoring the greater part of the wall tightness lost during heat-inactivation (Maris et al., 2009).

## 1.5 Arabinogalactan-proteins and their biological functions

### 1.5.1 Arabinogalactan-proteins

Arabinogalactan proteins (AGPs) are among the most complex macromolecules found in plants, belonging to the HRGPs family (Liu and Mehdy, 2007; Ellis et al., 2010). They are a class of highly glycosylated proteins and abundant in the plant cell wall and

plasma membrane. One of their distinguishing features is the ability to bind to a class of synthetic chemical dyes, Yariv reagents, especially β-glucosyl Yariv reagent (Yariv et al., 1967) although some AGPs do not exhibit Yariv reactivity (Kitazawa et al., 2013). AGPs belong to the Pro/Hyp-rich glycoprotein/ proteoglycan family, together with Pro-rich proteins and extensins (Showalter, 1993; Nothnagel, 1997). They are found in plasma membranes, cell walls and plant exudates (Seifert and Roberts, 2007). They are widely distributed in the plant kingdom, from bryophytes to angiosperms, and also charophytes (Popper and Fry, 2003; Popper and Tuohy, 2010).

#### 1.5.1.1 Structure of arabinogalactan-proteins

AGPs are composed of three major components: a protein backbone, polysaccharide chains and lipid. The diversity of the glycans decorating the protein backbone and the extent of this glycosylation as well as the diversity of protein backbones all contribute to the complexity of AGPs.

The carbohydrate moiety contributes from 90 to 98% while the protein contributes 1-10% of the weight of an AGP. The carbohydrate moiety of AGPs is rich in L-Ara*f* and D-Gal*p*, and in some cases D-GlcA, along with other less-abundant sugars L-Rha*p*, D-Man*p*, D-Xyl*p*, D-Glc*p*, L-Fuc, D-glucosamine, D-GalA, and 4-*O*-methyl derivatives (Clarke et al., 1979; Showalter, 2001). The carbohydrate component is usually a type II arabinogalactan (AG), which has (1→3)-β-D-linked Gal*p* residues that form a backbone substituted at O-6 by D-galactose side chains, usually terminating in L-Ara*f*, L-Rha*p* and D-Gal*p* residues (Ellis et al., 2010). Native AG chains can range in size from 5 to 25 kDa, with approximately 30-120 sugar residues (Ellis et al., 2010). This carbohydrate is linked to the protein backbone by an *O*-linkage to the noncontiguous Hyp residues of it. There are a few short arabino-oligosaccharides that attach to the contiguous Hyp residues (Showalter, 2001).

The protein backbone is rich in several amino acids including Hyp/ Pro, Ala, Ser and Thr, usually in dipeptide motifs Ala-Hyp, Ser-Hyp, Thr-Hyp, Val-Pro, Gly-Pro and Thr-Pro (Ellis et al., 2010). A hydrophobic C-terminal domain is found in most AGP protein backbones, predicting the presence of a glycosylphosphatidylinositol (GPI) membrane anchor (Schultz et al., 1998). Some major AGP backbone peptides are only 10 to 13 residues long and are termed AG peptides (Schultz et al., 2000).

#### 1.5.1.2 Classification of arabinogalactan-proteins

AGP used to be characterised, classified into classical AGPs and non-classical AGPs. The classical AGP contains a core protein with a short domain, rich in basic amino acids, that interrupts the central Pro/Hyp, Ala, Ser, Thr-rich domain (Gao et al., 1999). The amino acid sequence of all known and putative classical AGPs has a hydrophobic transmembrane domain at its C terminus which is absent or replaced by a GPI lipid anchor in mature AGP (Schultz et al., 1998). The non-classical AGPs have a core protein containing either a Cys-rich C-terminal domain or one or two Asn-rich domains that follow or enclose the Pro/ Hyp, Ala, Ser, Thr-rich domain (Schultz et al., 2002). They do not have the hydrophobic C-terminal domain or GPI modification.

However, this classification have been altered and AGPs are now classified into classical AGPs which have a P/Hyp rich peptide domain and C-terminus domain, AG peptides which have a short peptide backbone, fasciclin-like AGPs (FLA), Lys-rich AGPs, nonspecific lipid transfer protein (nsLTP)-like AGPs and early nodulin-like (ENDOL) AGPs. The term chimeric AGPs are used to describe classical AGPs that harbour an additional protein domain such as FLAs, Lys-rich, nsLTP-like AGPs and plastocyanin-like AGPs (Nguema-Ona et al., 2012).

Moreover, in *Arabidopsis*, the GPI-anchored AGPs can be divided into four subclasses including 13 classical AGPs, 3 AGPs with the core protein contains a short Lys-rich domain between the Pro-rich domain and the hydrophobic C terminus, 10 AG peptides, and 21 fasciclin-like AGPs (FLAs) (Schultz et al., 2002). Fasciclin-like AGPs are a large group of AGPs that contain one or two fasciclin domains though to be involved in protein–protein interactions that are variably GPI modified (Johnson et al., 2003). Fasciclin domains, which are 110 to 150 amino acids long, have been shown to work as adhesion molecules in many organisms. Although having low sequence similarity, all fasciclin domains contain two highly conserved regions (H1 and H2) of approximately 10 amino acids each (Johnson et al., 2003).

### 1.5.2 Roles of arabinogalactan-proteins in biological processes

AGPs have been implicated in various processes associated with plant growth and development, including embryogenesis and cell proliferation (Knox, 1995).

The cross-linking effect of β-glucosyl Yariv reagent with AGPs in the cell wall inhibited cell growth in "Paul's Scarlet" rose suspension culture and this growth inhibition effect was reversible. Yariv reagent did not affect cell viability and cell sizes in control and β-GlcY-treated cultures were similar, suggesting that the mechanism of growth inhibition by Yariv reagent involved suppression of cell division (Serpe and Nothnagel, 1994).

Seedlings of *Arabidopsis thaliana* that were germinated and grown in medium containing 30 μM β-GlcY Yariv reagent had a reduction on the overall growth of both the root and the shoot. Reduced root growth was a consequence of a reduction in cell elongation during the post-proliferation phase of elongation at the root apex and this was associated with extensive radial expansion of root epidermal cells. Moreover, when 30 μM β-GlcY Yariv reagent was added to carrot suspension-cultured cells that had been induced to elongate rather than proliferate, the cell elongation was inhibited. These results suggest that β-GlcY Yariv reagent interacts with AGPs and inhibits cell elongation (Willats and Knox, 1996).

Similarly, Ding and Zhu (1997) found an inhibition of root growth on treatment of *Arabidopsis thaliana* seedlings with β-GlcY Yariv reagent. The phenotype of these seedlings mimicked a *root epidermal bulger* (*reb1-1)* mutant which was identified from a root-swelling phenotype in *Arabidopsis*. *REB1* encodes an isoform of UDP-D-glucose 4-epimerase which functions in forming UDP-D-galactose. The *reb1* mutant lacks galactosylated xyloglucan and arabinosylated (1→6)-β-D-galactan (Seifert et al., 2002). Extracted AGPs from *reb1-1* showed an approximately 30% lower content of AGPs and smaller peaks upon crossed electrophoresis than the wild type. These results indicates that defective or missing root AGPs affect the control of root epidermal cell expansion (Ding and Zhu, 1997).

## 1.6 Mechanisms of enzyme regulations

The activity of an enzyme can be regulated by different means including pH, feedback inhibition, concentration of substrates, coenzymes, cofactors, covalent modifications, and activators and inhibitors. Some of these regulations are reversible while others are not.

### 1.6.1 Regulation of enzymes by pH

Many enzymes are pH sensitive, for example, fructose-1,6-bisphosphatase and sedoheptulose-1,7-bisphosphatase of the Calvin cycle are activated when the pH of the stroma changes from 7.2 to 8- the optimum pH for them, during the dark/light transition (Heldt et al., 2011). The catalytic sites of the β-subunits of a membrane-bound H+-ATP synthase are instantly switched off when the pH gradient across the thylakoid membrane is lower than a threshold value, and they are switched on again when the pH gradient is restored under the light (Berg et al., 2002).

### 1.6.2 Regulation of enzymes by feedback inhibition

Feedback inhibition is one common type of enzyme regulation, occurring when an enzyme has a high affinity to its product. In this regulation, the accumulation of a product of a metabolic pathway inhibits the activity of an enzyme involved in its synthesis by binding to the allosteric site of the enzyme and closing its active site (Cooper, 2000). For example, the chloroplast fructose-1,6-bisphosphatase and sedoheptulose-1,7-bisphosphatase are inhibited by their corresponding products, fructose-6-phosphate and sedoheptulose-7-phosphate, respectively. Likewise, the activity of Rubisco is inhibited by its product 3-phosphoglycerate (Heldt et al., 2011). The first step in the isoleucine synthesis pathway is catalysed by threonine deaminase which is inhibited by an adequate amount of the end product, isoleucine. When the concentration of isoleucine reduces, feedback inhibition is relieved, threonine deaminase is no longer inhibited, and additional isoleucine is synthesised (Cooper, 2000).

### 1.6.3 Regulation of enzymes by their substrate concentration

When the concentration of a substrate is low, the enzyme reaction rate is low because there are too few substrate molecules to make use of all the active sites. The reaction rate is increased when the substrate concentration is increased because more active sites of the enzyme become involved. At the point all the active sites are occupied, the enzyme reaction has reached its maximum and any further increase in substrate concentration fails to increase the rate of reaction. The inhibition by access of substrate was found for photosynthetic NADP-ME, an enzyme that catalyses the oxidative

decarboxylation of L-malate in maize. β-Hexosaminidase from *Penicillium oxalicum* was also inhibited by access of substrate p-nitrophenyl-N-acetyl-D-glucosamine (Doubnerova and Ryslava, 2013).

### 1.6.4 Regulation of enzymes by coenzymes

A coenzyme is an organic molecule that is necessary for an enzyme to function. When a coenzyme molecule binds to an enzyme, temporarily by ionic- or hydrogen-bonding or permanently by covalent bonding, the optimal conformation of the enzyme is obtained and the enzyme functions for its respective activity. Coenzymes are usually recycled and can participate in multiple enzyme reactions. Coenzymes are not irreversibly altered by the reactions in which they are involved (Cooper, 2000). Dietary vitamins are among the most common coenzymes in the human body, for example, vitamin C is a coenzyme for multiple enzymes that take part in building collagen. Nicotinamide adenine dinucleotide (NAD) is a prominent example of a coenzyme. NAD functions as a carrier of electrons in oxidation-reduction reactions and is used by hundreds of enzymes.

### 1.6.5 Regulation of enzyme by cofactors

A cofactor is an inorganic molecule that is necessary for an enzyme to function. For example, DNA polymerase requires $Zn^{2+}$ to build DNA molecules. The activity of NADP-ME from *Nicotiana tabacum* L. is regulated by the following divalent metal ions: $Mg^{2+}$ (100% of activity), $Mn^{2+}$ (140%), $Co^{2+}$ (59%), $Ni^{2+}$ (54%), and $Zn^{2+}$ (20% activity compared to $Mg^{2+}$ ions). The active conformation of ribulose-1,5-bisphosphate carboxylase/oxygenase (Rubisco) is activated by a complex formation with $Mg^{2+}$ (Lorimer et al., 1976).

### 1.6.6 Covalent modifications

In this modification, a donor molecule provides a functional moiety that covalently attaches, thus changing the properties of an enzyme. Some examples are phosphorylation, de-phosphorylation, acetylation, and de-acetylation (Berg et al., 2002).

#### 1.6.6.1 Phosphorylation and de-phosphorylation

Phosphorylation is one of the most effective reversible modification of enzyme activity. The terminal (γ) phosphoryl group of ATP as a donor substrate is transferred to an acceptor substrate which is one of three amino acids with a hydroxyl group as a side chain including serine, threonine, and tyrosine. Phosphorylation is catalysed by protein kinase which belongs to one of the largest protein families known. This family includes about 100 homologous in yeast and 500 in humans. The protein kinase that transfers to serine and threonine is different from the one that transfers to tyrosine. Phosphorylation adds more negative charges to the modified proteins, thus altering substrate binding and catalytic activity. The added phosphate group can form more than three hydrogen bonds and its tetrahedral geometry makes these hydrogen bonds highly directional, allowing for specific interactions with hydrogen-bond donors. Phosphorylation can take place in less than a second or over hours and its kinetics can be adjusted to meet the timing needs of a physiological process. A single activated kinase can phosphorylate hundreds of target proteins in a short interval.

De-phosphorylation is catalysed by protein phosphatase. This enzyme removes the phosphoryl group attached to a protein by hydrolysis. The products of this reaction include a free hydroxyl side-chain of an amino acid and an orthophosphate ($P_i$).

Phosphorylation and de-phosphorylation are not the reverse of each other. The rate of cycling between the phosphorylated and the dephosphorylated states depends on the relative activities of kinases and phosphatases, which is highly related to the hydrolysis of ATP to ADP and $P_i$. One of the most important phosphorylases is the glycogen phosphorylation which is responsible for the interconversion of glycogen and glucose-1-phosphate. Glucose-1-phosphate is then converted to glucose-6-phosphate which can act as fuel for glycolysis and the pentose phosphate pathway. Regulation of proteins by reversible phosphorylation is only for intracellular proteins, XTH, a typical apoplastic protein cannot be activated by this modification.

#### 1.6.6.2 Acetylation and de-acetylation

One of the major regulatory mechanisms of an enzyme is reversible lysine acetylation. There are a large number of acetylated cellular proteins, approximately 2000 in mammalian cells, in which many are metabolic enzymes. Acetylation is involved in controlling enzyme activity in three ways: the amount of enzyme, the catalytic activity, and the accessibility of substrates (Xiong and Guan, 2012). Acetylation regulates the amount of a metabolic enzyme by promoting the degradation of the enzyme through either ubiquitin-proteasomal system in the case of phophoenolpyruvate carboxykinase (PCK1) (Jiang et al., 2011) or chaperone-mediated autophagy (CMA) in the case of pyruvate kinase (PK) M2 isoform (Lv et al., 2011; Xiong and Guan, 2012). Acetylation also affects enzyme catalytic activity by directly neutralising residues in the active site of the enzyme, for example, ornithine transcarbamylase (OTC) (Shi et al., 2001). Acetylation can also modify the conserved Lys residues located on the hydrophilic surface of a succinate dehydrogenase subunit A (SDHA), thus controlling the entry of the substrate into its active site (Cimen et al., 2010).

### 1.6.7 Regulation of enzymes by inhibitors and activators

An inhibitor or activator is a specific molecule that can inhibit or promote, respectively, an enzyme reaction. There are two kinds of inhibitors: competitive and non-competitive. The competitive inhibitor molecule is so structurally similar to an enzyme substrate that it can bind to the active site, thus blocking the substrate from binding to the enzyme. The non-competitive inhibitor binds to the enzyme at an allosteric site and changes its conformation. Therefore, the enzyme is no longer in the optimal condition to catalyse a reaction although the substrate can still bind to it. An allosteric activator binds to an enzyme at its allosteric site, inducing a conformational change that increases the affinity of the enzyme's active site for its substrate, thus promoting enzyme activity. For example, fructose-1,6-biphosphatase is inhibited by Pi, fructose-6-phosphate, adenosine 5'-monophosphate (AMP) and fructose-2,6-biphosphate. $CO_2$, separate from the substrate $CO_2$, is an activator for Rubisco (Lorimer et al., 1976).

## 1.7 XET activating factor (XAF) and its ability to promote XET activity

Takeda and Fry (2004) discovered the presence of an endogenous factor in boiled extract of cauliflower florets that can promote XET activity of de-salted cauliflower enzyme as well as *Arabidopsis* XTH24. The authors found that crude enzyme extracts of cauliflower florets and many other plants lost a high proportion of their XET activity during the dialysis process and this loss was not prevented by anti-oxidants or BSA, suggesting that the high XET activity of crude extracts was dependent on the presence of low-$M_r$ substances that were lost during dialysis. The activity could be restored by addition of salts, both organic and inorganic, and the valency of the cation but not the anion strongly modulated the effect. XET activity of de-salted cauliflower enzyme, tested without NaCl, could also be restored by addition of hypochlorite-oxidised (thus anionic) xyloglucan (Ox-TXyG) while the XET activity of XTH24, a protein produced by expression of *AtXTH24* in baculovirus-infected insect cells, could be restored by another polyanion, carboxymethylcellulose (CMC). In the presence of 100 mM NaCl, the XET activity of de-salted cauliflower extracts which had already been partially activated by the NaCl was further enhanced by pectin as well as gum arabic, but was inhibited by alginate, γ-carrageenan, HG and methylglucuronoxylan suggesting that acidic wall polysaccharides may contribute to the regulation of XET action *in vivo* (Takeda and Fry, 2004).

Moreover, 1.38% (w/v) BCP (a cold-water extractable, heat-stable preparation from cauliflower florets) completely restored the high XET activity that had been lost during de-salting, but it was not able to enhance any further the high XET activity present in a crude enzyme extract. This result suggests that the crude enzyme was extracted with its highest XET activity due to the natural occurrence of substances that may act as its endogenous regulator. The high-$M_r$ fractions of BCP, obtained by precipitation with ethanol or acetone and re-dissolving in water, also partially restored XET activity to de-salted enzyme from cauliflower. After chromatographic fractionation of BCP, the major active principle was found to be negatively charged and of relatively low $M_r$. These results suggest the presence in cauliflower florets of small (approximately $M_r <$ 5000) heat-stable, water-soluble, acidic polymers that may act as endogenous regulators of the action of XTHs *in vivo* (Takeda and Fry, 2004).

Following this research, Takeda et al. (2008) found that the Ox-TXyG and CMC were not suitable donor substrates for XET activity. When Ox-TXyG or CMC was the only polysaccharide present in a transglycanase assay as the potential donor substrate, negligible activity was found. However, when non-oxidised xyloglucan was present as donor substrate, Ox-TXyG, CMC, and Ox-CMC caused a dose-dependent (up to fourfold, twofold and fourfold, respectively) increase in XET activity of XTH24. These results suggested that although anionic polysaccharides did not act as donor substrates for XET activity, they promoted XET activity, as did pectin, gum arabic and BCP. It is possible that they act as mimics of endogenous anionic wall polymers, such as arabinogalactan-proteins, that possess GlcA and/or GalA residues. These naturally occurring polyanions may be responsible for controlling the XET activity of wall-localised XTHs (Takeda et al., 2008). However, what kinds of anionic polymers in BCP are responsible for promoting XET activity? How are they related to naturally occurring plant cell wall polymers? How do they work? These questions need to be answered to know whether/ how endogenous regulators control the action of XTHs *in vivo*.

Unpublished work by Sandra C. Sharples and Stephen C. Fry at the Edinburgh Cell Wall Group, the University of Edinburgh, has shown that BCP can increase XET action *in vitro* and *in vivo* by either preventing XTHs from binding to natural (cell walls) and artificial solid surfaces (cellulose, plastic, and glass) or releasing XTHs adsorbed on the cell wall into the reaction mixture solution. BCP did not modify the measured enzymological parameters e.g. $K_m$, but acted principally by controlling adsorption/desorption of the enzyme. After acid hydrolysis, the cauliflower polyanions yielded much Ara, Gal and Glc and smaller amount of GalA and GlcA; amino acids were also present and the polymer was Yariv-positive, suggesting that the polymers contained AGPs. However, the XAF-active substances were unusually low in molecular weight compared with classical AGPs (Takeda and Fry, 2004). Moreover, unlike BCP, AGP-enriched preparations from gum arabic could not release XTH24 that had bound to the glass surfaces of borosilicate tubes; thus, XAF-active substances in BCP did differ from known AGPs. BCP did not affect the behaviour of XTHs on gel-permeation chromatography. BCP did not desorb [$^3$H]xyloglucan from paper nor prevent [$^3$H]xyloglucan binding to paper, suggesting that it did not affect xyloglucan–

cellulose hydrogen-bonding as well as bind to xyloglucan. The remaining questions from this study are: Are the presences of AGPs in BCP contribute to XAF activity? If yes, what kinds of AGPs in BCP have XAF activity? How do the XAF-active substances interact with XTHs to promote XET activity?

In order to answer those remaining questions from the previous studies, I carried out this project. My project was designed to test effects of BCP and XAF-active substances on the XET activity of XTHs in *Arabidopsis* cells (suspension culture) by using a novel method. I wished to determine the chemical properties of the XAF-active substances in BCP by applying a wide range of purification and analysis methods. I also wanted to investigate if the XAF-active substances that I have characterised in this study play any functional role on the growth of plant by using *Arabidopsis* mutants. Further, I aimed to look for an endogenous XAF in the growing parts of diverse plants as a contribution elucidating the mechanisms of plant cell growth control.

# 2 MATERIALS AND METHODS

## 2.1 MATERIALS

### 2.1.1 Mutant *Arabidopsis* lines

From the mass-spectrometry analysis (see section 3.6) I chose several proteins that could potentially work as XET activating factors (XAFs), including three fasciclin-like arabinogalactan proteins (FLAs), two stress-responsive proteins (low temperature induced, LTI) and an early nodulin-like protein (ENODL). Mutants of these genes in *Arabidopsis* were studied for the biological activity of XAF *in vitro*. Mutant *Arabidopsis* were chosen from the SALK Institute Genomic Analysis Laboratory and bought from the European *Arabidopsis* Stock Centre (Table 2).

Table 2. *Arabidopsis* mutants used in this study.

| Protein Name | Gene | NASC ID | Line Name | Description |
|---|---|---|---|---|
| Fasciclin-like arabinogalactan protein 7 (FLA7) | AT2G04780 | N613729 | SALK_113729 (BS) | Segregating as single insertion, confirmed with flanking sequence, T3-generation T-DNA line generated by vacuum infiltration of Columbia (Col) plants with *Agrobacterium tumefaciens* vector pROK2 |
| | | N27280 | GT1414 | Transposon insertion line which carries a unique insertion of a genetrap (GT) transposable Ds element, which may disrupt gene function and/or serve as a reporter for gene expression |
| | | N506728 | SALK_006728 | Segregating as single insertion, confirmed with flanking sequence, T3-generation T-DNA line generated by vacuum infiltration of Col plants with *Agrobacterium tumefaciens* vector pROK2 |
| Fasciclin-like arabinogalactan protein 6 (FLA6) | AT2G20520 | N564179 | SALK_064179 (AP) | Segregating as single insertion, confirmed with flanking sequence, T3-generation T-DNA line generated by vacuum infiltration of Col plants with *Agrobacterium tumefaciens* vector pROK2 |

| | | | | |
|---|---|---|---|---|
| Fasciclin-like arabinogalactan protein 11 (FLA11) | AT5G03170 | N859641 | SALK_015044 (E) (R) | Genotyping confirmed SALK homozygous line isolated from original SALK line SALK_015044 |
| Stress-responsive protein (LTI140) | AT5G52310 | N859786 | SALK_080395_237 | Kanamycin resistant, genotyping confirmed line isolated from original SALK line, homozygous for the insertion |
| Stress-responsive protein LTI65 | AT5G52300 | N552958 | SALK_052958 (AI) | Insertion in exon, segregating as single insertion, confirmed with flanking sequence, T3-generation T-DNA line generated by vacuum infiltration of Col plants with *Agrobacterium tumefaciens* vector pROK2 |
| Early nodulin-like protein 14 (ENODL14) | AT2G25060 | N519896 | SALK_019896 (W) (CD) | Segregating as single insertion, confirmed with flanking sequence, T3-generation T-DNA line generated by vacuum infiltration of Col plants with *Agrobacterium tumefaciens* vector pROK2 |

### 2.1.2 Primers for genotyping

Primers used in the PCR for testing the genotype of Col0 and mutants were bought from Sigma-Aldrich (Table 3).

Table 3. Primers for genotyping

| Name | Sequence (5'-3') | Length | Tm (°C) | BP+RP product size |
|---|---|---|---|---|
| FLA7(1)_LP | TTATAATGGTTGCCATTTGCC | 21 | 59.69 | 441-741 |
| FLA7(1)_RP | AATCTCCATGGTTATTTCCGG | 21 | 60.03 | |
| FLA7(2)_LP | GCTTATCGTCTGCTCTGCATC | 21 | 60.14 | 471-771 |
| FLA7(2)_RP | TTAGGGTTCGGGTATTATGCC | 21 | 60.05 | |
| Ds3-1 | ACCCGACCGGATCGTATCGGT | 21 | 72.4 | - |
| FLA7(3)_LP | CGGTTAGACACGAATTTTTCG | 21 | 59.63 | 601-901 |
| FLA7(3)_RP | TCGGTGAGATTCACATTTTCC | 21 | 59.92 | |
| FLA6_LP | AACTTCTTTTGCAAGTCACGC | 21 | 59.55 | 606-906 |
| FLA6_RP | TGCAAAGGCTCTAAACTTCTTG | 22 | 58.83 | |
| FLA11_LP | TAATGGCTTAACCGTGTTTGC | 21 | 60.01 | 517-817 |
| FLA11_RP | GAAATCGCTGCAGCTTATGAG | 21 | 60.13 | |

| | | | | |
|---|---|---|---|---|
| LTI140_LP | TTTAATCCTCCCAACCATTCC | 21 | 60.01 | 463-763 |
| LTI140_RP | TTCCAGGTGAATCAGGAGTTG | 21 | 60.10 | |
| LTI65_LP | AACAACACACAGTGCATTTGC | 21 | 59.68 | 545-845 |
| LTI65_RP | GAGCCTCTCTGCTCTCTCCTC | 21 | 59.99 | |
| ENODL14_LP | CTATTTTCTTTGGGCCAGGAG | 21 | 60.08 | 513-813 |
| ENODL14_RP | TGGTTCCAAATCAGAACCAAG | 21 | 59.96 | |
| LBb1.3 | ATTTTGCCGATTTCGGAAC | 19 | 63.6 | - |

Tm: melting point

LP, RP: left, right genomic primer

BP: T-DNA border primer LB: the left T-DNA border primer

### 2.1.3 Primers for RT-PCR

Primers used in the RT-PCR for testing RNA products expressed from specific genes in Col0 and mutants were bought from Sigma-Aldrich (Table 4).

Table 4. Primers for RT-PCR

| Name | Sequence (5'-3') | Length | Tm (°C) |
|---|---|---|---|
| FLA7FSEQ | TCTTTATCGCTGTCGTTGCG | 20 | 66.2 |
| FLA7RSEQ | GTACCAAAGATTGCTTCGGG | 20 | 63.3 |
| FLA6FSEQ | CCCATACATTCAAAGCCAGC | 20 | 64.2 |
| FL6RSEQ | CCGGTGGAAACATTCACTTG | 20 | 65.2 |
| FLA11FSEQ | AGCCACTACTTATGGTCAGG | 20 | 58.3 |
| FLA11RSEQ | GATCAACCTGATAAACGGCC | 20 | 63.2 |
| LTI140Fseq | ATGCACCGGCTCATTCTGTAAGG | 23 | 70.0 |
| LTI140Rseq | TTCCGGCGAATACTCGTTTCTTCC | 24 | 71.4 |
| LTI140_2Fseq | GAAGTTACCTATCTCCGGAG | 20 | 56.9 |
| lti140_2rseq | CTTAAAGCTCCTTCTGCACC | 20 | 60.6 |
| LTI65Fseq | GTGGTTCGGCCATATGTCATCG | 22 | 70.3 |
| LTI65Rseq | TTTCCGTCGTTCTTACAGGATCAGC | 25 | 69.9 |
| ENODL14Fseq | TCGCCGCTGCAAATGAAGTCAC | 22 | 73.4 |
| ENODL14Rseq | GGCTCAGCTTCTGACCTTTCTCACA | 25 | 70.7 |

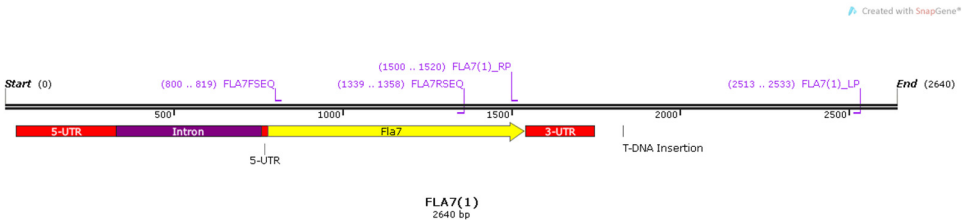


**FLA7(1)**
2640 bp

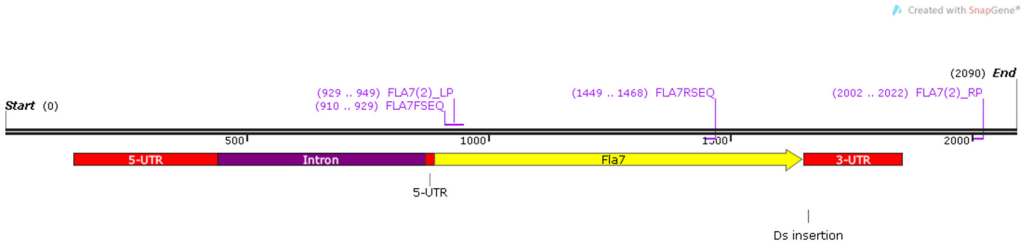


**FLA7(2)**
2090 bp

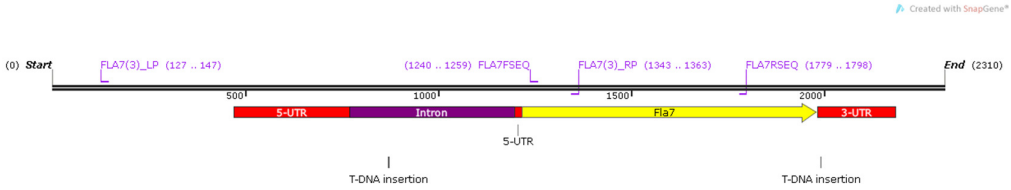


**FLA7(3)**
2310 bp

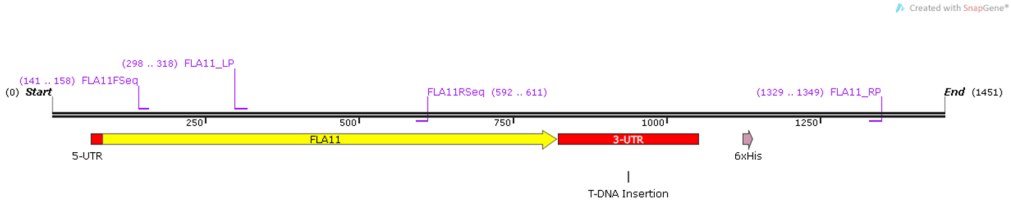


**FLA11**
1451 bp

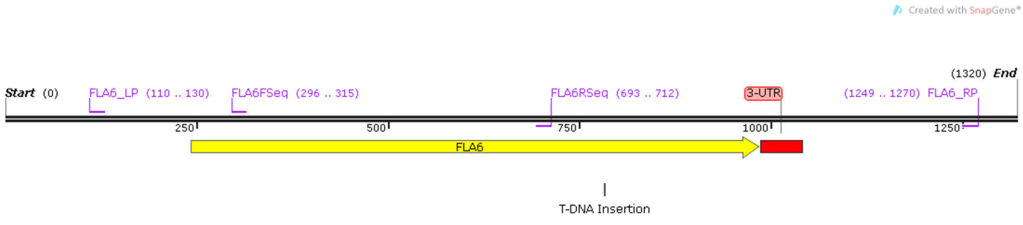


**FLA6**
1320 bp

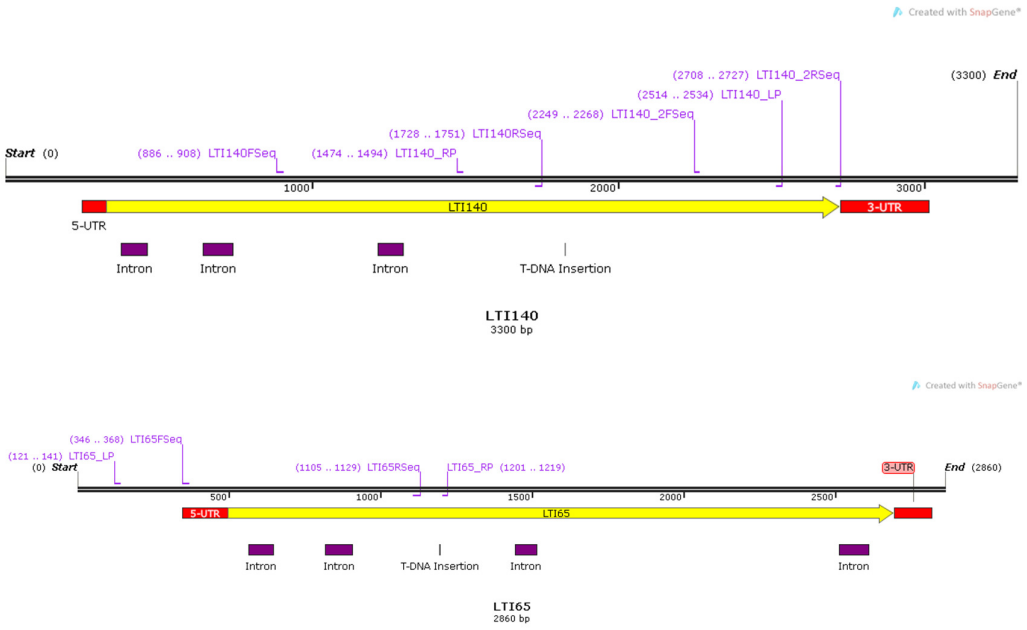


Figure 3. Diagram representing structure of genes used in this study

Each gene structure including the position of insertions, primers used to genotype, primers used for RT-PCR was generated with SnapGene.

### 2.1.4 Enzymes

Driselase was bought from Sigma and partially purified in the lab as described by Fry, (1982). Mannanase from *Bacillus* sp. was bought from Megazyme with specific activity 390 U/ml (Catalogue number: E-BMABS). Xyloglucan endoglucanase (XEG) was a generous gift from Novo Nordisk A/S. α-Glucosidase was bought from Megazyme with specific activity 680 U/ml (Catalogue number: E-MALTS). A cellulase which does not digest xyloglucan from *Aspergillus niger* was bought from Megazyme with specific activity 820 U/ml (Catalogue number: E-CELAN). α-Amylase type XII-A from *Bacillus licheniformis* was bought from Sigma Life Science with specific activity 853 U/mg (Lot number: 080M1664). Endo-polygalacturonase (EPG) was bought from Megazyme with specific activity 1800 U/ml (Catalogue number: E-PGALS). Exo-β-1,3-galactanase from *Clostridium thermocellum* was bought from Nzytech with specific activity 40 U/ml (Catalogue number: CR0029).Proteinase K from *Tritirachium album* was bought from Sigma Life Science with specific activity ≥ 30 U/mg (CAS: 39450-01-6). Trypsin from bovine pancreas type I was bought from Sigma Chemical Co. with specific activity 11000 U/mg solid

(CAS: 9002-07-7). Peroxidase from horseradish was bought from Sigma Life Science with specific activity 193 purpurogallin U/mg solid (CAS: 9003-99-0).

Crimson Taq DNA polymerase (including 5x Crimson Taq reaction buffer pack) was bought from Biolabs New England with the specific activity as 5000 U/ml. Lot number: M0324S.

Superscript II reverse transcriptase was bought from Invitrogen Life technologies with the concentration as 200 U/µl. Catalogue number: 18064-014.

### 2.1.5 Monosaccharides, oligosaccharides and polysaccharides

Glucose, galactose, mannose, arabinose, sucrose, ribose, rhamnose, glucuronic acid, galacturonic acid, xylose, maltohexaose were bought from Sigma-Aldrich.

$Cell_6$ and $Man_6$ was bought from Megazyme.

$Xyl_6$ and $Ara_8$ were prepared in the laboratory by Professor. Fry S C.

Starch ladder were prepared in the lab by Thomas Simmons.

*Tamarind* xyloglucan and *Nasturtium* xyloglucan were generous gifts of Mr. K. Yamatoya, Dainippon Pharmaceutical Co., Osaka, Japan.

Arabinogalactan (AG), gum arabic (GA), cellulose, carboxymethyl cellulose (CMC) pectin, galactan, xylan, polygalacturonic acid (PGA), blue dextran and starch were bought from Sigma-Aldrich.

XXXGol was bought from Megazyme. [$^3$H]XXXGol was prepared in the lab as described by Hetherington and Fry (1993) with the specific radioactivity as 100 MBq/µmol. It was routinely used as 0.5 or 1 kBq/µl in each assay.

### 2.1.6 Antibodies

All of the primary antibodies (JIM4, JIM13, JIM16, LM2, LM6, LM14) used in this projects were kindly provided by Professor. Paul Knox from the centre for plant sciences, faculty of Biological Sciences, University of Leeds.

**Monoclonal antibody to AGP/ LM2**

Specificity: Generated to rice arabinogalactan-proteins (AGPs). Recognises a carbohydrate epitope containing β-linked glucuronic acid. It can recognise AGPs in several species. In competitive inhibition ELISA antibody binding to gum arabic was

inhibited (50%) by 70 µmg/ml 1-*O*-methyl-β-D-GlcA. The binding of the antibody to AGPs can be fully inhibited by 10 mM 1-*O*-methyl-β-D-GlcA.

**Monoclonal antibody to AGP/ LM14**

Cat. No. LM14 (Rat IgM)

Specificity: Isolated from a HTP screen of antibodies generated subsequent to immunization with a pectic fraction. Recognizes arabinogalactan-proteins and will also bind to larch arabinogalactan. It can recognise AGPs in several species.

**Monoclonal antibody to AGP/ LM6 (Rat IgG)**

Specificity: Generated using a neoglycoprotein (arabinoheptaose-BSA). Recognises a linear pentasaccharide in (1-5)-α-L-arabinans. It can recognise pectic polysaccharides in several species. It has no cross-reactivity with gum arabic but it may recognize arabinogalactan-proteins (AGPs) in some species. In competitive inhibition ELISAs, antibody binding to (1→5)-α-L-arabinan was inhibited (50%) by 40 ng/ml (1→5)-α-L-arabinopentaose and 19 ng/ml (1→5)-α-L-arabinohexaose.

The secondary anti-rat IgG (whole molecule)-peroxidase antibody produced in goat was bought from Sigma-Aldrich.

96-well microplate with lid (flat bottom, tissue culture treated polystyrene) was bought from Iwaki, Japan.

### 2.1.7 General biochemicals

BSA (albumin, bovine) (96-99%) was bought from Sigma chemical Co.

40% acrylamide/ Bis solution, 29:1 was bought from Bio-Rad.

Q-Sepharose, Sepharose CL-6B, SP-Sephadex (Sigma stock no SP-C50-120, lot 53F-0092), Biogel-P2 were bought from Sigma.

Ultrapure Tris was bought from Invitrogen. Trizma base was bought from Sigma chemical.

Merck silica-gel 20 x 20 cm TLC plates were bought from VWR.

Solvents and scintillant were bought from Fisher Scientific. Other general chemicals were bought from Sigma.

SYBR® Safe DNA gel stain was bought from Invitrogen Life technologies. Catalogue number: S33102.

100 mM dNTP Set (dNTPs) consisting of four deoxynucleotides (dATP, dCTP, dGTP, dTTP), each at a concentration of 100 mM dNTPs was bought from Invitrogen Life technologies. Catalogue number: 10297-018.

Oligo(dT)$_{20}$ primer (15µg) was bought from Invitrogen Life technologies. Catalogue number: 18418-020.

## 2.2 METHODS

### 2.2.1 Thin-layer chromatography (TLC)

Sugars were determined by TLC on 20 cm x 20 cm silica-gel plates. Sugars were loaded 1 cm from one edge and 2 cm from bottom. The plate was placed in a closed tank with appropriate solvent (Fry, 2000). For separation of monosaccharides, 110 ml ethyl acetate/pyridine/acetic acid/water (6:3:1:1) (EPAW 6:3:1:1) or 100 ml butanol/acetic acid:/water (4:1:1) (BAW 4:1:1) was used. For separation of oligosaccharides, 100 ml butanol/acetic acid/water (2:1:1) (BAW 2:1:1) was used. For staining, the plate was dipped in thymol (2.5 g thymol in 485 ml ethanol and 25 ml $H_2SO_4$), air-dried and heated at 105ºC for 10 minutes until the coloured spots appeared (Fry, 2000). The monosaccharide and polysaccharide markers were normally loaded as 2 µg on the TLC.

### 2.2.2 Paper chromatography

Amino acid components of proteins and glycoproteins were determined by paper chromatography. A sheet of Whatman no. 1 (stationary phase) was hung from a glass trough containing solvent (mobile phase). The whole assembly was housed in a large glass tank and closed with a greased, well-fitting, glass lid. The sheet of paper was normally 46 x 57 cm and was hung (long edge vertical) with the samples dried on to the paper 9 cm from a short edge. Samples were dried and re-dissolved in water, loaded onto the paper as 1-1.5 cm spots and spaced at least 2.5 cm apart, centre-to-centre (Fry, 2000). BAW 12:3:5 was normally used as the solvent and the chromatography was done for 20 h. After chromatography, the paper was hung up to dry in a fume cupboard and the paper was stained by dipping in 0.5% ninhydrin in acetone quickly, drying 5 min and heating at 105ºC for 5 min until the coloured spots appeared. For determination of hydroxyproline, the paper was quickly dipped in isatin and ninhydrin

(270 mg ninhydrin, 130 mg isatin and 2 ml triethylamine in 100 ml acetone), dried 5 min and heated at 80ºC, and examined at 1-min intervals until the coloured spots appeared. For quantification, the paper was washed in water to de-colourise background and dried, and the spots were eluted in acetone/ethanol (1:2) and measured for absorbance at 515 nm (Fry, 2000).

### 2.2.3 High-voltage paper electrophoresis

The samples were mixed with 5 µl 0.5% DNP-Lys in water, dried on to Whatman no. 1 paper as spots (1-1.5 cm diameter) near to the cathode. The top of the paper was held in a trough containing about 250 ml of the buffer and a platinum cathode; the bottom dipped into another layer of buffer (about 500 ml) containing a platinum anode. Coils with running tap-water kept an immiscible coolant (in this case: white spirit) below 30ºC (Fry, 2000). The electrophoresis was done with a buffer of formic acid/acetic acid/water (1:4:45), pH 2 at 3 kV for 60 min. The paper was taken out and dried in the fume cupboard, then stained with ninhydrin or isatin and ninhydrin.

### 2.2.4 Dialysis

Boiled cauliflower preparation (BCP) in water or 0.2 M MES were measured for conductivity (with a Jenway 4060 conductivity meter) and split into 2-ml aliquots, which were dialysed against 3 l de-ionised water in dialysis tubings with MWCO 3500 and 12000-14000 for 1 h or 24 h at room temperature. After dialysis, all samples were adjusted to the same volume by addition of water and the conductivity was measured again. Salt concentration before and after dialysis was calculated based on a standard curve of conductivity of NaCl.

### 2.2.5 Column chromatography

#### 2.2.5.1 Gel-permeation column chromatography

Bio-Gel P-2 and Sepharose CL-6B columns with bed volume 100 ml were used. These were washed with approximately 2 column volumes of pyridine/acetic acid/water (1:1:98) (PyAW 1:1:98) in 0.5% chlorobutanol. A mixture of 3.8 ml BCP in water, 0.1 ml 0.1% blue dextran, and 0.1 ml 0.5% glucose in PyAW 1:1:98 was applied onto the column and 50 fractions of 2 ml were collected with PyAW 1:1:98 as the eluent. In

some experiments, [$^{14}$C]Glc (0.3 kBq) was used as an internal marker. Absorbance at 280 nm and 620 nm of each fraction were measured and fractions were then dried in the SpeedVac and re-dried from 100 µl of de-ionised water (twice).

#### 2.2.5.2 Cation-exchange column chromatography

To prepare for a 36-ml bed-volume column, 15 g SP-Sephadex gel was soaked in 4% pyridine adjusted to pH 3 with formic acid. The gel was washed three times with 50 ml 20 mM pyridine adjusted to pH 3 with formic acid and stored in a fridge until use. The column was packed, carefully rinsed with 20 ml 20 mM pH 3 buffer and left to settle overnight.

Dried BCP (10 ml, 2 mg/ml) was dissolved in 20 mM pyridine adjusted to pH 3 with formic acid and applied onto the column. Fractions (6 ml each) were eluted (0.2 ml/min) with sequentially:

20 mM pyridine adjusted to pH 3 with formic acid [care was taken not to lose any solutes that came straight off the column]
30 mM pyridine adjusted to pH 5.3 with acetic acid
70 mM pyridine adjusted to pH 5.3 with acetic acid
200 mM pyridine adjusted to pH 5.3 with acetic acid
700 mM pyridine adjusted to pH 5.3 with acetic acid
2000 mM pyridine adjusted to pH 5.3 with acetic acid
Water

#### 2.2.5.3 Anion-exchange column chromatography

Q-Sepharose was soaked in 2 M acetic acid adjusted to pH 7 with NaOH and left overnight in a fridge. The gel was then poured into a 10-ml Poly-Prep column and left to settle to 5 ml. The column was equilibrated with 20 mM acetic acid adjusted to pH 4.7 with pyridine. BCP in water (5 ml, 2 mg/ml) was loaded onto the column and 1-ml fractions were collected with sequential eluents as below:

20 mM acetic acid adjusted to pH 4.7 with pyridine
100 mM acetic acid adjusted to pH 4.7 with pyridine
500 mM acetic acid adjusted to pH 4.7 with pyridine

1 M acetic acid adjusted to pH 4.7 with pyridine

2 M acetic acid adjusted to pH 4.7 with pyridine

The anion-exchange column was also used to further purify peak fractions from a cation-exchange column. For this purpose, a 2-ml bed volume column was used and 1 ml of the peak fraction from the cation column was loaded onto the column and eluted with 6 ml of each eluent. Fractions (1 ml each) were collected, dried in the SpeedVac and re-dissolved in 1 ml water.

### 2.2.6 Phenol-sulfuric acid carbohydrate assay

For measurement of the carbohydrate content in samples, 400 µl (dilute if necessary) of each sample was mixed well with 1 ml $H_2SO_4$ and 10 µl phenol. The reaction solution was left at room temperature for 20 min before reading the absorbance at 485 nm. The concentration of carbohydrate in each sample was calculated based on a standard curve of known dextran concentrations. To make the standard curve, 400 µl of different concentrations of dextran (0, 1, 2, 3, 4, 5, 7.5, 10, 12.5, 15, 17.5, 20, 50, 100 µg/ml) were used.

### 2.2.7 Bradford protein assay

For measurement of the protein concentration in samples (BCP or fractions from chromatography columns), 300 µl of each sample (dilute if necessary) was incubated with 100 µl Bradford and 800 µl water for 5 min at room temperature and measured for absorbance at 595 nm. The protein concentration in each sample was calculated based on a standard curve of known BSA concentrations. To make the standard curve, 300 µl of different concentrations of BSA solution in water (0, 50 10, 12.5, 15, 20 µg/ml) were used.

### 2.2.8 Polyacrylamide gel electrophoresis

#### 2.2.8.1 18% Acrylamide SDS gels

I prepared 18% acrylamide SDS gels with ingredients as below:

5% acrylamide stacking gel (1.5 ml):

40% acrylamide: 187.5 µl

1 M Tris (adjusted to pH 6.8 with HCl): 187.5 µl

Water: 1.1 ml

10% ammonium persulphate: 15 µl

10% SDS: 15 µl

TEMED: 1.5 µl

18% acrylamide separating gel (5 ml):

40% acrylamide: 2.25 ml

1.5 M Tris (pH 8.8): 1.25 ml

Water: 1.4 ml

10% ammonium persulphate: 50 µl

10% SDS: 50 µl

TEMED: 2 µl

SDS sample buffer (1x) was prepared by Mohler K in the laboratory with the final concentration as below:

50 mM Tris-HCl pH 6.8

2% SDS

10% glycerol

1% β-mercaptoethanol

12.5 mM EDTA

0.02% bromophenol blue

Sample in water was mixed with 10x SDS sample buffer and 5-10 µl of that was applied into each well of the SDS gel. The gel was run in the running buffer (1.5 g Tris, 7.2 g glycine and 0.8 g SDS in 500 ml water) at 75 volts for 15-20 min until all bands aligned at the beginning of the separating gel and then at 200 volts for 1.5 h.

The gel was taken out of the tank and stained with Coomassie blue or silver nitrate as described in 2.2.8.3.

#### 2.2.8.2 10% acrylamide native gels

I prepared 10% acrylamide native gels with ingredients as below:

4% acrylamide stacking gel (1 ml):

40% acrylamide: 0.1 ml

1 M Tris (adjusted to pH 6.8 with HCl): 252 µl

Water: 646 µl

10% ammonium persulphate: 5 µl

TEMED: 1 µl

10% acrylamide separating gel (4 ml):

40% acrylamide: 1 ml

1.5 M Tris (pH 8.8): 1 ml

Water: 1.98 ml

10% ammonium persulphate: 20 µl

TEMED: 2 µl

10x native sample buffer (5 ml)

0.5% bromophenol blue: 0. 5 ml

1 M Tris (base) pH 6.8: 2 ml

Glycerol: 2.5 ml

Sample in water was mixed with 10x native sample buffer and 5-10 µl of that was applied into each well of the gel. The gel was run at 100 volts for 3 h with a running buffer at pH 8.5 (0.125 M Tris (base) and 0.96 M glycine). The gel was taken out of the tank and stained with Coomassie blue or silver nitrate as described in 2.2.8.3.

### 2.2.8.3 Staining the acrylamide SDS or native gels

For silver nitrate staining, the gel was soaked in fixing solution (50% ethanol, 12% acetic acid, 0.05% formaldehyde) for 30 min. The gel was carefully washed 3 times with 50% ethanol, soaked in 0.01% sodium thiosulphate for 60 s and carefully washed 3 times with water. The gel was soaked in staining solution (0.1% $AgNO_3$, 0.075% formaldehyde) for 20 min on a shaker and then carefully washed 3 times with water. The gel was then soaked in developing solution (3% $Na_2CO_3$, 0.5% formaldehyde, $10^{-4}$% sodium thiosulphate) until bands appeared. After that, I quickly poured stopping solution (40 g/l Tris in 2% acetic acid) into the gel.

For Coomassie blue staining, the gel was soaked in Coomassie blue R in 40% methanol and 10% acetic acid on the shaker for 30 min and de-stained by washing several times with 20% methanol and 10% acetic acid.

### 2.2.9 Purification of XAF from native gels by electro-elution

I thawed 2 ml frozen BCP, dried it in the SpeedVac, re-dissolved it in 90 µl of water and mixed it with 10 µl of native sample buffer, then loaded it onto a 10% acrylamide native gel. After running, 2 edges of the gel were cut to be stained with Coomassie blue. The rest of gel was cut into 1-cm slices, including the stacking gel, and each slice was put into a 12000-14000 MWCO dialysis tubing with 5 ml native gel running buffer (Tris-glycine) (making sure that there were no bubbles inside the sacs). The dialysis sacs were placed into an electrophoresis tank which was fully filled with native running buffer and run at 200 volts for 15 min. I took the sacs out of the tank and put them into a 5-l beaker full of 0.2% chlorobutanol to be dialysed overnight. The sacs were then put into another 5-l beaker to be dialysed against 4 l of water for 5 h. Each sac was carefully rinsed with water and the solution inside it was transferred to a tube and adjusted to 6 ml with water. Of that, I took 2 ml solution, dried in the SpeedVac, re-dissolved in 75 µl 0.075 M NaCl/ 0.2 M MES for XAF assay. Another 2 ml was dried in the SpeedVac, re-dissolved in 9 µl water, mixed with 1 µl loading sample buffer, electrophoresed on a 10% acrylamide native gel, and stained with silver nitrate. For a control, 53 µl BCP was used for XAF assay and gel electrophoresis.

For this purpose, 2 ml of fraction F.15 from a cation-exchange column was used and the elution was carried out as described above to yield 6 ml dialysed solution. Of that, I took 3 ml, dried it in the SpeedVac, and re-dissolved it in 75 µl 0.075 M NaCl/ 0.2 M MES for XAF assay. A further 80 µl of fraction F.15 was dried, re-dissolved in 75 µl 0.075 M NaCl/ 0.2 M MES for XAF assay as a control. I also took 1 ml of fraction F.15, dried, re-dissolved in 9 µl of water, mixed with 1 µl loading sample buffer for native gel electrophoresis, and stained with silver nitrate. As controls for gel, 9 µl BCP and 27 µl of F.15 were used.

Similarly, 1.8 ml fraction F.30 from the same cation-exchange column was used for electrode-elution with some modification: running and cutting the gel, electrode-elution, and dialysis were carried out in the cold room. For dialysis, 3500 MWCO dialysis tubing was used in place of 12000-14000. After dialysis, the solution inside each sac was adjusted to 6.5 ml; of that, 1 ml was used for testing on an analytical gel and 3.5 ml was used for XAF assay.

### 2.2.10 Preparation of XET activating factor (XAF) from cauliflower, *Arabidopsis* and other plants

Cauliflower florets; *Arabidopsis* leaves, flowers and seeds, stems; snowdrop leaves, flower, stems; crocus leaves, flowers; carrot root, leaves and stems; spinach leaves; whole asparagus; celery petioles, very young petioles and leaves; whole watercress; lettuce leaves; parsley leaves; spring onion basal leaves and stems, leaves; and tobacco leaves, flowers and stems were vigorously homogenised in a blender (300 g in approximately 100 ml de-ionised $H_2O$).

For rose, spinach, and *Arabidopsis* culture, I used 200 ml of each cell suspension culture (7–9 days old).

For mutant *Arabidopsis*, I collected leaves, stems, flowers and seeds from 12 plants separately in 50-ml tubes and froze them at –80ºC, then ground them in a mortar with liquid nitrogen to a fine powder. After that, I homogenized them with 30 ml water.

The homogenate was filtered through three layers of Miracloth and the filtrate was poured into 50-ml tubes. The tubes were placed in a boiling water bath for 1 h and filtered through Miracloth again. The filtrate (crude extract) was stored frozen (–20ºC).

Each tube of crude extract was thawed, mixed well, and centrifuged at 4000 rpm for 30 min. Ethanol (35 ml) was added to 15 ml of clear supernatant with thorough mixing; the mixture was incubated in the cold room overnight and centrifuged at 3500 rpm for 30 min. The supernatant was discarded and the pellet was carefully washed twice with 50 ml 96% ethanol and once with 40 ml 80% ethanol. The pellet was air-dried and re-dissolved in 5 ml de-ionised water then freeze-dried. The dried pellet was weighed and dissolved in water or 0.2 M MES ($Na^+$), pH 5.5, at a concentration of 2 mg/ml. The solution was stored at –20ºC until use.

### 2.2.11 Preparation of frozen, washed *Arabidopsis* cells

*Arabidopsis* suspension-culture was grown in the culture medium as described by May and Lever (1993) with the modification of 2% (w/v) glucose. Cells were grown under continuous low intensity light (about 25 µmol/$m^2$/s) with constant shaking at 150 rpm. Sub-culturing was performed after seven days by transfer of approximately 20 ml of suspension culture to 180 ml of fresh medium in a 500-ml conical flask.

*Arabidopsis* cell-suspension culture (~200 ml, 7–9-day-old cells) was homogenised for 2 min by hand food mixer then passed through Miracloth. The cells on the Miracloth were washed with 1 l of ice-cold water, squeezed to semi-dry and frozen overnight at –20ºC. The cells were thawed and re-washed on Miracloth with another 1 l of ice-cold water. The cells were squeezed and then re-suspended in 100 ml de-ionised water in a 250-ml beaker. The cell suspension was kept stirring when 1.5-ml-cell-suspension aliquots were made and the aliquots were stored frozen at –20ºC for further use. Six aliquots were dried in the freeze-drier to measure dried cell weight.

Before a new batch of *Arabidopsis* cells was used, I tested the effect of the cell concentration on the solubilisation of XET activity from the cells by BCP to determine the amount of cells used for each XAF assay. I thawed one cell aliquot, washed three times with water and re-suspended in 1.5 ml of water. While the tube was kept stirring, I took different volume of cells (3 µl to 66 µl) into a well in a 96-well plate and centrifuged at 4000 rpm for 10 min. Water was discarded and the cells were incubated with 66 µl 0.075 M NaCl/ 0.2 M MES with or without BCP and the extract was then assayed for XAF activity.

### 2.2.12 Testing XAF activity through radioactive XET assay

Thawed and water-washed *Arabidopsis* cells were dispensed into wells of a 96-well plate at 66 µl per well. The plate was centrifuged at 4000 rpm for 10 min and the supernatant was carefully discarded by use of tissue paper. The pellet in each well was incubated in 66 µl of a putative XAF solution (appropriately buffered), depending on the purpose of each experiment. After 30 min on the shaker at room temperature, the cell suspension was centrifuged and 20 µl of supernatant was transferred into a well in a new 96-well plate. The XET assay was performed based on that of Fry et al. (1992): 20 µl of radioactive XET reaction mixture (dried [$^3$H]XXXGol (1 kBq) in 0.4% (w/v) tamarind xyloglucan in 0.5% (w/v) chlorobutanol) was added into each well and incubated for 16 h at room temperature. After that, 50 µl 45% formic acid was used to stop the reaction and the whole solution was loaded and dried on a 4 x 4 cm piece of Whatman no. 3 paper (marked in pencil on a large sheet) and washed in running tap-water overnight.

In order to understand the relationship between XAF activity and BCP concentration, a standard curve was made. BCP (2 mg/ml) in water was thawed and adjusted to different concentrations, from 0.13 to 16 mg/ml in 0.075 M NaCl/ 0.2 M MES, and 66 µl of each concentration was used for each XAF assay.

### 2.2.13 Solubilisation of other cell-wall enzymes by XAF and assays of their activities

#### 2.2.13.1 Solubilisation of other cell-wall enzymes

A 1.5-ml aliquot of frozen *Arabidopsis* cells was thawed, washed 3 times with water and re-suspended in 7.5 ml 0.075 M NaCl/ 0.2 M MES, pH 5.5 for 30 min on a shaker. The tube was centrifuged at 4000 rpm for 10 min and the solution was taken into a new tube (solution 1), and stored frozen until use. The cell pellet was re-suspended in 7.5 ml BCP (2 mg/ml) in 0.075 M NaCl/ 0.2 M MES, pH 5.5 for 30 min on the same shaker. The tube was centrifuged at 4000 rpm for 10 min and the solution was taken into a new tube (solution 2), and stored frozen until use. The cell pellet was finally re-suspended in 7.5 ml 1 M NaCl/ 0.2 M MES, pH 5.5, for 30 min on the same shaker. The tube was centrifuged again and the solution was taken into a new tube (solution 3).

#### 2.2.13.2 Assays of cell-wall enzymes

##### 2.2.13.2.1 β-Glucosidase

Each enzyme solution (0.5 ml) was added into a tube containing 0.5 ml of 5 mM p-nitrophenyl-β-D-glucopyranoside (pNP-Glc) prepared in 0.2 M MES, pH 5.5, and each tube was incubated for a different time, from 30 to 240 min, duplicated. The reaction was stopped by addition of 1 ml 1 M $Na_2CO_3$ and the tube was left 2 min at room temperature before measurement of absorbance at 400 nm. For 0 min, 1 M $Na_2CO_3$ was added before the addition of 0.5 ml enzyme (Fry, 2000).

##### 2.2.13.2.2 Phosphatase

Each enzyme solution (0.5 ml) was added into a tube containing 0.5 ml of 5 mM p-nitrophenylphosphate ($Na^+$) prepared in 0.2 M MES, pH 5.5, and each tube was

incubated for a different time, from 30 to 180 min, duplicated. The reaction was stopped by addition of 1 ml 1 M $Na_2CO_3$ and the tube was left 2 min at room temperature before measurement of absorbance at 400 nm. For 0 min, 1 M $Na_2CO_3$ was added before the addition of 0.5 ml enzyme (Fry, 2000).

#### 2.2.13.2.3 Invertase

For making 25 ml 3,5-dinitrosalicylic acid (DNS) solution , 0.25 g DNS was dissolved in 5 ml 2 M NaOH and mixed for 1 h at 90ºC (suspension A). Making solution B by dissolving 7.5 g potassium sodium tartrate in 12.5 ml water. I mixed suspension A and solution B and stirred the mixture at 90ºC till dissolved and adjusted to 25 ml with water.

Each enzyme solution (400 µl) was added into a tube containing 50 µl 0.4 M sucrose and 50 µl 0.2 M MES, pH 5.5. The tube was incubated for 30 min at 30ºC in a water bath. After that, 200 µl DNS solution was added and the solution was heated for exactly 10 min in a boiling water bath. The tube was then cooled in water for 5 min and 2 ml of water was added and mixed well, and the absorbance of the solution at 540 nm was measured. For a blank, 400 µl water was used in place of enzyme solution. The amount of glucose and fructose was interpreted by the use of a standard curve of known glucose concentrations. To make this standard curve, 500 µl solution containing different amounts of glucose was used (0-250 µg) in the reaction under the same conditions as described above.

#### 2.2.13.2.4 Peroxidase

Peroxidase activity was conducted as described by Fry S C (2000) with some modifications. Each enzyme solution (100 µl) was added into a plastic cuvette containing 2 ml 0.1 M $NaH_2PO_4$ in 0.2 M MES adjusted to pH 5.5 by 10 M NaOH, 0.5 ml 0.8 mM *o*-dianisidine and 0.5 ml 0.8 mM $H_2O_2$ at room temperature for 30 min. Continuous colorimeter readings at 420 nm were taken every 30 s. 0.01 µg/ml peroxidase horseradish was used as a positive control.

#### 2.2.13.2.5 Xyloglucan endo-transglucosylase

Each enzyme solution (20 µl) was added into a well of a 96-well plate containing [$^3$H]XXXGol (0.5 kBq) in 20 µl 0.4% (w/v) tamarind xyloglucan containing 0.5% (w/v) chlorobutanol and incubated for 0, 4, 8, 16 and 24 h. The reaction was stopped by addition of 50 µl 45% formic acid and the reaction solution was loaded onto paper and washed in running tap-water overnight. $^3$H-labelled products were measured as described in 2.2.23.

### 2.2.14 Hydrolysis of BCP and XAF

#### 2.2.14.1 Acid hydrolysis

##### 2.2.14.1.1 2 M TFA hydrolysis

For testing monosaccharide components, sample was incubated with 2 M TFA in a tightly capped Sarstedt tube in the oven at 120ºC for 1 h. After that, the samples were cooled on ice and dried in the SpeedVac (Fry, 2000).

##### 2.2.14.1.2 0.1 M TFA hydrolysis

Samples were incubated with 0.1 M TFA on a hot plot at 85ºC for different time periods, cooled on ice, dried in the SpeedVac (Fry, 2000).

#### 2.2.14.2 Alkaline hydrolysis

Samples were incubated with 0.45 M NaOH (final concentration) at room temperature for different times and the reaction was stopped by the addition of acetic acid to pH 1 (Fry, 2000). Polymers in the samples were precipitated with ethanol and assayed for XAF activity.

#### 2.2.14.3 Enzyme hydrolysis

Samples were incubated with different enzymes at different conditions (details below). The reactions were stopped by different method, depending on the used enzyme. The reaction solutions were cooled on ice, centrifuged and the supernatants were divided into two new tubes. Solution in both tubes were dried in the Speedvac, re-dried twice from water. Pellet in tube 1 was re-dissolved in water and loaded onto a TLC for testing

sugar components. Pellet in tube 2 was re-dissolved in 0.075 M NaCl/ 0.2 M MES for XAF assay.

#### 2.2.14.3.1 Driselase

Samples were incubated with 0.167% or 0.0003% Driselase (final concentration) in PyAW 1:1:98, pH 4.7 in tightly capped Sarstedt tubes at room temperature for 24 h. The reaction was stopped by heating to 105ºC in the oven for 70 min. For the controls, PyAW 1:1:98 was used in place of driselase for non-treated sample and water was used in place of sample for enzyme only.

#### 2.2.14.3.2 Xyloglucan endo-glucanase (XEG)

To determine the appropriate concentration of XEG for digestion of XAF, XEG at different final concentrations (5.2, 20.8, 83.3, 333 µg/ml) in PyAW 1:1:98 was incubated with different substrates including xyloglucan oligosaccharides, tamarind xyloglucan, maltohexaose, cellohexaose, polygalacturonic acid, and dialysed gum arabic (all 0.67 mg/ml in water) in a tightly capped Sarstedt tube. The mixture was incubated at room temperature for 0, 0.37, 1.5, 6, or 24 h. The reaction was stopped by heating to 120ºC in the oven for 70 min. For a control, 40 µl water was used in place of sample for enzyme only.

From the above experiment, 5.2 µg/ml XEG and 1.5 h were determined as the optimum conditions for XEG activity and were used to hydrolyse BCP. For the controls, 100 µl PyAW 1:1:98 was used in place of XEG for non-treated BCP and 200 µl water was used in place of BCP for enzyme only.

#### 2.2.14.3.3 β-Galactanase

BCP was incubated with 0.0013 U/µl β-galactanase (final concentration) in pyridine and acetic acid, pH 5.6 in a tightly capped Sarstedt tube at 55ºC for 4 h. The reaction was stopped by heating to 120ºC for 70 min. For the controls, pyridine and acetic acid, pH 5.6 was used in place of enzyme for non-treated BCP and water was used in place of BCP for enzyme only.

#### 2.2.14.3.4 α-Glucosidase

BCP was incubated with 0.0167 U/µl (final concentration) α-glucosidase in 1% lutidine and 0.3% acetic acid, pH 6.6 in a tightly capped Sarstedt tube at room temperature for 48 h. The reaction was stopped by addition of 100 µl formic acid. For controls, 100 µl lutidine and acetic acid buffer or 100 µl water was used in place of enzyme and 200 µl water was used in place of BCP for enzyme only.

Also, 50 µl 1 mg/ml maltohexaose or maltose were incubated with 25 µl α-glucosidase or lutidin/acetate buffer at the same condition, dried, re-dried from water, re-dissolved in 2 µl water and loaded onto a TLC plate for the α-glucosidase specific substrate control.

#### 2.2.14.3.5 Mannanase

BCP was incubated with 0.0167 U/µl (final concentration) mannanase in 0.05 M ammonium acetate, pH 8.8 at room temperature for 24 h. The reaction was stopped by addition of 100 µl formic acid. For the controls, 200 µl water was used in place of BCP for enzyme only and 100 µl 0.05 M ammonium acetate, pH 8.8 was used in place of mannanase for non-treated BCP.

Also, 50 µl 1 mg/ml mannohexaose was incubated with 25 µl mannanase or ammonium acetate buffer under the same conditions, dried, re-dried from water, re-dissolved in 2 µl water and loaded onto a TLC plate for the mannanase specific substrate control.

#### 2.2.14.3.6 Cellulase, endo-polygalacturonase (EPG), α-amylase

BCP was incubated with 0.0167 U/µl (final concentration) cellulase, EPG or α-amylase in PyAW 1:1:98, pH 4.7 in a tightly capped Sarstedt tube at room temperature for 24 h. The reaction was stopped by heating to 105ºC for 70 min in the oven. A sample with 200 µl water in place of BCP was used as enzyme only control.

#### 2.2.14.3.7 Proteinase K

BCP was incubated with 100 µg/ml (final concentration) proteinase K in 50 mM ammonium acetate, pH 8.8 in a tightly capped Sarstedt tube at 37ºC at two different

time-courses 0.5 to 72 h and 0 to 30 min. The reaction was stopped by heating to 105ºC on a hot plate for 10 min and the solution was cooled on ice and centrifuged. A portion of the supernatant was dried in the SpeedVac and re-dissolved in 150 µl 0.075 M NaCl/ 0.2 M MES for XAF assay. A further portion was dried in the SpeedVac, re-dissolved in 12 µl water and mixed with 3 µl loading sample buffer. Of that, 10 µl was subjected to SDS gel electrophoresis and stained with Coomassie blue, and another 5 µl to SDS gel electrophoresis and stained with silver nitrate. For a sample at 0 h, the enzyme was boiled for 10 min before the addition of BCP.

#### 2.2.14.3.8 Trypsin

For determination of the optimum concentration of trypsin for digestion of BCP, BCP was incubated with different final concentrations of trypsin (0 to 5 mg/ml) in 50 mM ammonium acetate, pH 8.8, in 0.1 % chlorobutanol in a tightly capped at 37ºC for 24 h. The reaction was stopped by heating to 105ºC for 30 min and centrifuged. For XAF assay, 150 µl supernatant was dried in the SpeedVac and re-dissolved in 75 µl 0.075 M NaCl/ 0.2 M MES. The rest was stored in a freezer for later use.

For testing the effect of fresh and boiled trypsin on destroying XAF activity of BCP, I prepared 2.5 µg/ml trypsin in ammonium acetate buffer and divided it into 2 tightly capped Sarstedt tubes. One tube was heat to 110ºC for 30 min to obtain boiled trypsin and the other tube was kept on ice. BCP was incubated with fresh or boiled trypsin under the same conditions as mentioned above. After stopping the reaction and centrifuging the solution, 300 µl supernatant was dried and re-dissolved in 150 µl 0.075 M NaCl/ 0.2 M MES for XAF assay. For the controls, 300 µl ammonium acetate was used in place of trypsin for non-treated BCP and 300 µl water was used in place of BCP for enzyme only.

### 2.2.15 Arabinogalactan-protein antibody-captured ELISA

Dried BCP was dissolved in 50 mM $Na_2CO_3$, pH 9.6, to a concentration of 50 µg/ml and 100 µl of that was added to appropriate wells of an Iwaki microplate 96 well and incubated overnight at 4ºC. The last row of wells contained $Na_2CO_3$ in place of BCP as a blank. The next day, I removed the solution from each well and blocked all remaining binding sites with 200 µl 3% BSA in PBS for 2 h at room temperature. The

plate was then carefully washed 9 times with water (this was most readily done by repeated submerging of the plate in a tray full of running tap water, shaking and forcibly throwing water out). I mixed 20 µl of primary antibody (JIM4, JIM13, JIM16, LM2, LM6, or LM14) with 80 µl BSA in PBS and added 100 µl of this into wells of the first row of the plate. A series of 5-fold dilution was made by mixing 20 µl of the solution in the above well with 80 µl new BSA in PBS into the below well and incubated for at least 1.5 h. The plate was washed 15 times again with water as described above.

I prepared secondary antibody solution by adding 10 µl of commercial secondary antibody (anti-rat IgG coupled to horseradish peroxidase (HRP)) to 10 ml 3% BSA. I added 100 µl of this solution into each well and incubated for at least 1.5 h. The plate was washed again with water as described before and the antibody binding to the plate was determined by addition of 150 µl HRP substrate prepared immediately before use to each well (18 ml de-ionised water, 2 ml 1 M sodium acetate, pH 6.0, 200 µl tetramethylbenzidine, 20 µl 6% (v/v) hydrogen peroxide). Colour development was stopped by the addition of 35 µl 2 N $H_2SO_4$ into each well. Absorbance was determined at 450 nm in a microplate reader.

### 2.2.16 Purification of AGP from BCP by the use of Yariv reagent

AGP was purified from BCP based on a method developed by Liu and Mehdy (2007). I mixed 10 ml 2 mg/ml BCP with 20 mg Yariv reagent (Yariv et. al., 1967) in 200 ml 1% NaCl and incubated for 24 h in the cold room. The solution was centrifuged at 4000 rpm for 15 min and the pellet was collected. The supernatant was re-precipitated with an additional 10 mg Yariv reagent overnight in the cold room and centrifuged the next day to obtain a second pellet. The pellets were pooled and washed 3 times with 50 ml 1% NaCl and 50 ml methanol and left to dry at room temperature. The pellet was re-dissolved in 5 ml DMSO and minimal $Na_2S_2O_4$ with water until pale yellow. The whole solution was dialysed in 12000-14000 MWCO dialysis tubing against 5 l of water overnight. The solution inside the dialysis sac was freeze-dried, weighed and re-dissolved in water as a concentration of 2 mg/ml. The solution outside the dialysis sac was also freeze-dried but was too light to be weighed, thus was re-dissolved in 2.5

ml water. For XAF assay, 150 µl of each solution was dried and re-dissolved in 150 µl 0.075 M NaCl/ 0.2 M MES.

### 2.2.17 96-well format DNA extraction with CTAB

This method was from Weigel and Glazebrook (2002) with some modifications. I put a single ball-bearing into each 1.2-ml tube in a 96-place box. The tissue (3–4 *Arabidopsis* leaves) was collected and put into each tube and stored at –80ºC until use. The box was put into liquid nitrogen and the tissue was disrupted by shaking with a paint shaker for 2 min at 25 frequency/s (repeated if clumps of tissue remained). The box was briefly centrifuged to bring down tissue dust and 300 µl CTAB solution (100 mM Tris-Cl, pH 8.0, 20 mM EDTA, pH 8.0, 1.4 M NaCl, 2% (w/v) cetyl trimethyl ammonium bromide (CTAB), 1% PVP 40000) was added into each tube. The tube was tightly capped and heated at 65ºC in a water bath for 30 min and left to cool to room temperature. The box was centrifuged briefly at 1500 rpm for 2 min and 300 µl chloroform was added into each tube. The tube was tightly capped and inverted by hand for 10–20 s. The box was centrifuged at 3250 rpm for 15 min. During centrifugation, I prepared 96-well deep well plates by adding 200 µl propan-2-ol to each well. I transferred 200 µl of the chloroform-extracted supernatant into the new plates (avoiding any of the material from the interface, or any of the organic layer). The plate was incubated at room temperature for 10 min and centrifuged at 3250 rpm for 15 min. The supernatant was poured off into the sink and the pellet was washed with 200 µl of 70% ethanol. The plate was re-covered and centrifuged for 7-10 min at 3250 rpm. The supernatant was removed again and the remaining solution was dried on paper towels and then the plate was left to air-dry for more than 3 h in a fume cupboard. The pellet was re-dissolved in 100 µl sterile water and left overnight at 4ºC. For a 10-µl PCR reaction, 0.5 µl of this DNA was used.

### 2.2.18 PCR reaction for testing genomic DNA

#### 2.2.18.1 PCR mixture (for 1 sample)

The following mixture was added into each tube:

Water: 13 µl

Crimson Taq reaction buffer: 4 µl

dNTPs: 0.4 µl

Primer 1 (10 µM): 0.5 µl

Primer 2 (10 µM): 0.5 µl

Primer 3 (10 µM): 0.5 µl

DNA solution: 1 µl

Crimson Taq DNA polymerase: 0.1 µl

#### 2.2.18.2 PCR reaction

The PCR reaction was conducted in a PCR machine with the below time scale:

95ºC: 3 min

95ºC: 30 s
55ºC: 30 s
68ºC: 1 min 30 s } 30 cycles

68ºC: 5 min

10ºC: ∞

For *fla7(2)*, I used 35 cycles in place of 30 cycles and for *enodl14(1)*, I used 52ºC in place of 55ºC.

### 2.2.19 Total RNA extraction

*Arabidopsis* tissue was collected into 2-ml tubes containing a single ball-bearing and immediately frozen in liquid $N_2$. The tissue was ground very finely in liquid nitrogen and 0.5 ml RNA extraction (100 mM Tris-HCl, pH 8.0, 100 mM LiCl, 10 mM EDTA, 1% SDS; autoclaved, then warmed to 80ºC in a microwave) and 0.5 ml phenol/chloroform/3-methyl-1-butanol (25:24:1) was added into each sample and the sample was vigorously vortexed to extract RNA. The tube was centrifuged at 4000 rpm for 5 min at 4ºC and the aqueous phase (upper phase) was transferred to a new tube in which 0.5 ml cold chloroform/3-methyl-1-butanol (24:1) was added and the tube was vortexed vigorously. The tube was again centrifuged at 4000 rpm for 5 min at 4ºC and the aqueous phase (upper phase) was transferred to a new tube to which 0.5 ml cold chloroform/3-methyl-1-butanol (24:1) was added and vigorously vortexed for one more time. The tube was centrifuged and the aqueous phase was transferred to a

new tube in which 1/3 volume of 8 M LiCl was added and the tube was incubated overnight at 4ºC. (Optional: if the protocol was started with small amounts of tissue, 25 µg glycogen (5 µl of 5 mg/ml stock) was also added to visualize RNA pellet in the next step).

The next day, the tube was centrifuged for 15 min at 4ºC and a small clear pellet of total RNA was visible at this time. From now on, I kept the tube on ice at all time. Without disturbing the pellet, I carefully removed the supernatant with a pipette. The RNA pellet was gently washed with 0.5 ml of 70% ethanol (–20ºC) without re-suspending the pellet. The tube was centrifuged for 1 min at 4ºC to make sure the RNA pellet stayed in place and the supernatant was discarded. I repeated the centrifugation to remove any remaining 70% ethanol. The RNA pellet was dried in the SpeedVac for 1 min without heating and 400 µl doubled distilled de-ionised water ($ddH_2O$) was added into it and the tube was kept on ice for 30 min to re-hydrate the RNA pellet. The RNA pellet was dissolved by vigorously pipetting the solution up and down. To this tube, 40 µl of 3 M sodium acetate, pH 5.2 and 1 ml of 96% ethanol (–20ºC) were added and the tube was inverted to mix. The tube was incubated at least 60 min at –20ºC. The tube was centrifuged for 15 min at 4ºC and a gel-like pellet of pure RNA was now visible. Without disturbing the pellet, I removed the supernatant very carefully with a pipette and the RNA pellet was gently washed with 0.5 ml of 70% ethanol (–20ºC). The tube was centrifuged for 1 min at 4ºC to make sure the RNA pellet stayed in place. The supernatant was discarded without disturbing the pellet and the tube was centrifuged again to remove any remaining 70% ethanol. The RNA pellet was dried in the SpeedVac for 1 min at 4ºC without heating and 25 µl $ddH_2O$ (autoclaved) was added into it and the tube was left on ice for 30 min to re-hydrate the RNA pellet. Finally, the RNA pellet was re-suspended by pipetting up and down. The RNA amount was measured from $A_{260/280}$ and $A_{260/230}$ and stored at –80ºC until use.

#### 2.2.19.1 RT-PCR to make cDNA from mRNA

First-strand cDNA synthesis:

The following 20-µl reaction volume was used for 10 pg-5 µg of total RNA or 10 pg-500 ng mRNA. The following components were added to a nuclease-free PCR tube:

1 µl of oligo(dT)20 (50 µM)

10 pg- 5 µg total RNA (ideally 2 µg) or 10 pg- 500 ng mRNA

1 µl of 10 mM dNTPs

Sterile ddH2O to 14 µl

The mixture was heated to 65ºC for 5 min in a PCR machine, followed by incubation on ice for at least 1 min.

The contents of the tube were collected in the bottom of the tube by brief centrifugation and the following mixture was added to each tube:

4 µl of 5x first-strand buffer

1 µl of 0.1 M DTT

1 µl Superscript II reverse transcriptase (200 U/µl)

The solution in the tube was gently mixed and incubated at 50ºC for 60 min in a PCR machine. The reaction was stopped by heating at 70ºC for 15 min in a PCR machine. For a standard PCR, 1 µl of this solution was used.

### 2.2.20 PCR for testing the cDNA products made from mRNA

#### 2.2.20.1 PCR mixture (for 1 sample)

The following mixture was added into each tube:

Water: 12.5 µl

dNTPs: 0.4 µl

→ Primer: 1 µl (10 µM)

← Primer: 1 µl (10 µM)

Crimson Taq reaction buffer: 4 µl

Crimson Taq polymerase: 0.1 µl

cDNA: 1 µl

For UBQ, I used 1 µl of each UBQ10 primer

#### 2.2.20.2 PCR reaction

The PCR reaction was conducted in a PCR machine with the below time scale:

95ºC: 5 min

95ºC: 30 s
55ºC: 30 s } 25-30 cycles
68ºC: 30 s
68ºC: 10 min

### 2.2.21 Testing products of PCR on agarose gel

To make 5x Tris/Borate/EDTA electrophoresis buffer (TBE) (Sambrook and Russell, 2001):

54 g Tris base
27.5 boric acid
20 ml 0.5 EDTA (pH 8.0)

PCR products (10 µl) were loaded onto agarose gels for electrophoresis (1% agarose in 100 µl TBE with 4 µl SYBR and 6 µl 1-kB DNA ladder. The gel was run at 100 volts for 30 min and the picture was captured under UV light.

### 2.2.22 Growing *Arabidopsis* mutants and testing their XAF activity

Seeds were soaked in water for 30 min. The water was removed and the seeds were soaked in 96% ethanol for exactly 5 min. The ethanol was removed and the seeds were soaked in 10% bleach for exactly 5 min. The seeds were washed carefully with water several times until there was no ethanol and bleach smell. The seeds were soaked in water and left in the dark in a fridge for at least 2 days before being sown into a small pot. After 10 days, the seedlings were transplanted into a tray (72 plants/tray). Green leaves were collected after 5 weeks for genotyping and mRNA extraction. After 7 weeks, leaves; flowers and seeds; and stems from 48 plants of a single tray were collected separately, extracted XAF as described in 2.2.10. XAF activity was only performed on homozygous mutant plants (confirmed by genotyping).

### 2.2.23 Assay of radioactivity

For assaying [$^{14}$C]Glc, 50 µl of each fraction from the Sepharose CL-6B or Biogel-P2 column was mixed with 150 µl de-ionised water and 2 ml OptiScint scintillant and counted in a scintillation counter.

For assaying $^{3}H$-labelled products, the paper was re-dried, cut in pieces, put in vials, and counted in the scintillation counter (with 2 ml OptiScint scintillant/paper rectangle).

# 3 RESULTS

## 3.1 Boiled cauliflower preparation (BCP) and other plant extracts contain a cold-water-soluble, heat-stable XAF

### 3.1.1 XAF activity of BCP, salts and other compounds

#### 3.1.1.1 XAF activity of BCP in comparison to NaCl

In a previous experiment, Sandra C. Sharples and Stephen C. Fry, the Edinburgh cell wall group, the University of Edinburgh (unpublished work) proved that a factor from a cauliflower extract had the ability to release XET activity from *Arabidopsis* cells and 240 mM NaCl more lastingly solubilised XET activity from *Arabidopsis* cells. They also found that the factor and NaCl together strongly and lastingly solubilised XET, suggesting that factor solubilises XET from walls, then NaCl stops it re-binding to an ionic site.

Therefore, in this first experiment of my study, I wanted to test the XET activity solubilised from *Arabidopsis* cells by BCP (extracted in cold water, boiled to denature proteins and precipitated in ethanol to eliminate low $M_r$ compounds; thus, freed of low $M_r$ salts) and NaCl in various combinations (Figure 4A, B). This experiment also aimed to set up the method for testing the action of the factor from BCP on XET activity from *Arabidopsis* cells.

Without BCP and NaCl (0 mg/ml BCP and 0 M NaCl), there was negligible soluble XET activity, proving that the *Arabidopsis* cells had been carefully washed and there was almost no water-soluble XET activity in the cells before treatment with BCP and NaCl (Figure 4A, B). In the presence of BCP or NaCl, XET activity was solubilised dependent on their concentration. NaCl itself increased extractable XET activity by up to 1400-fold when its concentration was increased to 0.338 M. Similarly, BCP itself caused an increment in XAF activity of up to 120-fold when its concentration was increased to 1.82 mg/ml (Table 5).

There was a synergistic effect of NaCl and BCP on the solubilisation of XET activity. The higher the concentration of NaCl, the lower fold-promotion caused by BCP was obtained and vice versa (Table 5). The fold-promotion effect caused by NaCl was emphasised in the absence of BCP and vice versa. It was clear that BCP had a greater

fold effect at solubilising XET activity in the presence of less than 0.1 M NaCl (Figure 4A, B; Table 5).

A

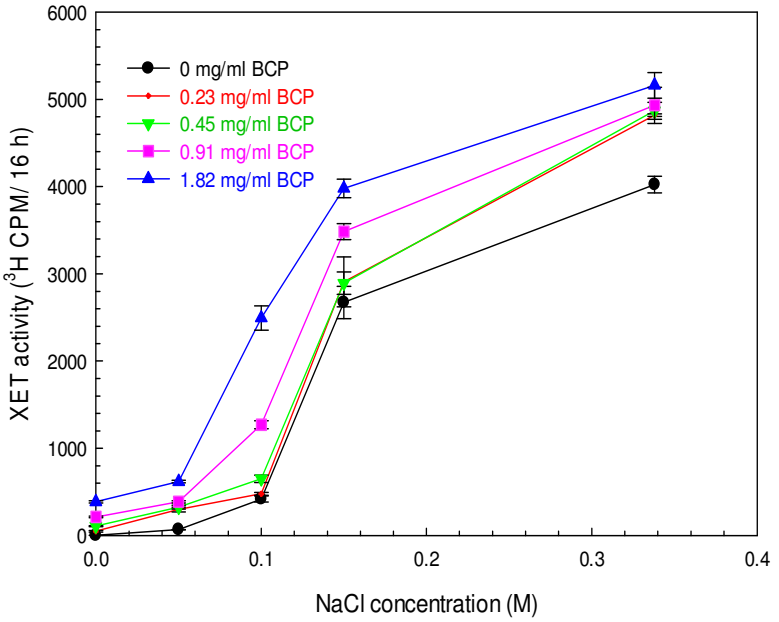


B

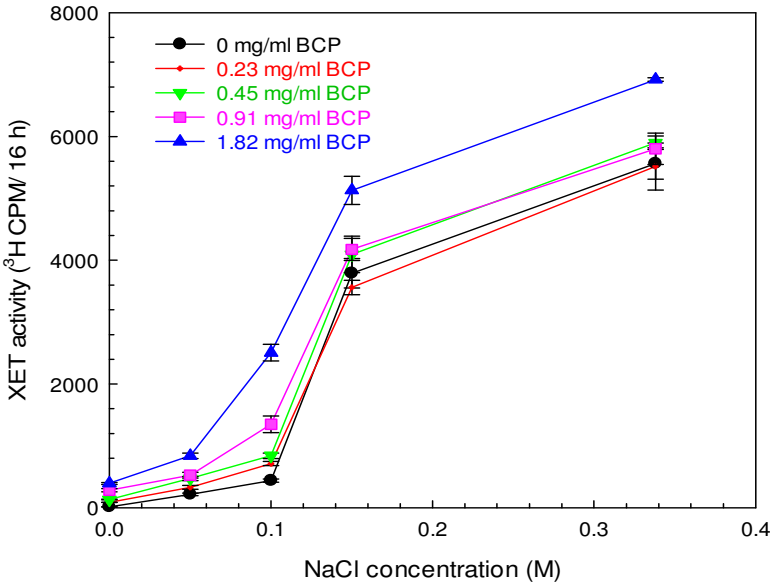


Figure 4. XET activity solubilised from *Arabidopsis* cells by BCP and/or NaCl.

Thawed and washed *Arabidopsis* cells were incubated in 66 µl of different mixtures (all containing 183 mM MES, pH 5.5) for 1 h. After centrifugation, 20 µl of supernatant was assayed for XET activity for 16 h. Data show the mean of four determinations ± SE. The experiment was carried out 5 times with similar results; two of them are presented here (A and B).

Table 5. Fold effect of NaCl and BCP on solubilisation of XET activity from *Arabidopsis* cells*

| BCP (mg/ml) | NaCl concentration (M) | Ionic strength (mM) | XET activity ($^3$H CPM per 16 h) | Fold promotion by NaCl | Fold promotion by BCP |
|---|---|---|---|---|---|
| 0 | 0 | 0 | 3 ± 2 | - | - |
| | 0.05 | 50 | 68 ± 2 | 24.8 | - |
| | 0.1 | 100 | 438 ± 11 | 159.4 | - |
| | 0.15 | 150 | 2673 ± 186 | 971.8 | - |
| | 0.338 | 338 | 4024 ± 95 | 1463.4 | - |
| 0.23 | 0 | 0 | 52 ± 5 | - | 17.3 |
| | 0.05 | 50 | 299 ± 27 | 6.1 | 4.4 |
| | 0.1 | 100 | 479 ± 17 | 9.7 | 1.1 |
| | 0.15 | 150 | 2908 ± 287 | 59.0 | 1.1 |
| | 0.338 | 338 | 4819 ± 16 | 97.9 | 1.2 |
| 0.45 | 0 | 0 | 109 ± 6 | - | 36.3 |
| | 0.05 | 50 | 326 ± 23 | 3.0 | 4.8 |
| | 0.1 | 100 | 651 ± 41 | 6.0 | 1.6 |
| | 0.15 | 150 | 2894 ± 128 | 26.7 | 1.1 |
| | 0.338 | 338 | 4870 ± 97 | 44.9 | 1.2 |
| 0.91 | 0 | 0 | 214 ± 9 | - | 71.3 |
| | 0.05 | 50 | 387 ± 13 | 1.8 | 5.7 |
| | 0.1 | 100 | 1271 ± 48 | 5.9 | 3.0 |
| | 0.15 | 150 | 3485 ± 90 | 16.3 | 1.3 |
| | 0.338 | 338 | 4933 ± 206 | 23.1 | 1.2 |
| 1.82 | 0 | 0 | 387 ± 12 | - | 129.0 |
| | 0.05 | 50 | 619 ± 16 | 1.6 | 9.1 |
| | 0.1 | 100 | 2495 ± 138 | 6.5 | 6.0 |
| | 0.15 | 150 | 3980 ± 108 | 10.3 | 1.5 |
| | 0.338 | 338 | 5162 ± 147 | 13.3 | 1.3 |

"-": not applicable

* Data are from the experiment shown in Figure 4A.

Ionic strength: $\mu=\frac{1}{2}\sum_{i=1}^{n} c_i z_i^2$ where $c_i$ is the molar concentration of ion I (mol/L), $z_i$ is the charge number of that ion, and the sum is taken over all ions in the solution.

### 3.1.1.2 XAF activity of BCP in comparison to $Ca^{2+}$

Recently, Lamport and Varnai (2013) demonstrated that paired glucuronic carboxyl groups of AGP were the sites for binding $Ca^{2+}$ on the plasma membrane and the release of $Ca^{2+}$ at low pH was the principle of a global $Ca^{2+}$ signalling pathway in land plants.

Thus, an experiment was carried out to study any $Ca^{2+}$ effect on solubilisation of XET activity from *Arabidopsis* cells.

In the first experiment (Figure 2A), testing XET activity solubilised by 0 to 0.1 M $CaCl_2$, the solubilised XET activity reached a plateau at 0.03 M $CaCl_2$ (ionic strength 75 mM). Therefore, in the later experiment (Figure 2B; Table 2), I used lower concentrations of $CaCl_2$, from 0 to 0.015 M (ionic strength: 0 to 37.5 mM). The BCP (2 mg/ml) itself has an ionic strength of 9.9 mM (based on its NaCl-equivalent concentration). As with BCP and NaCl, $CaCl_2$ also had a concentration-dependent effect on solubilisation of XET-active XTHs from *Arabidopsis* cells (Table 5, Table 6). The effect of BCP and $CaCl_2$ on solubilising XET activity was not synergistic: when the concentration of $CaCl_2$ was increased, the fold promotion by BCP was not always decreased (Table 6). BCP at the concentration of 1.82 mg/ml accompanied by 15 mM $CaCl_2$ caused an obvious increment in solubilised XET activity, 4-fold higher than 15 mM $CaCl_2$ without BCP (Figure 2B). It was also the largest XET promotion for any BCP + $CaCl_2$ combination obtained in this experiment. BCP at all concentrations had its highest XAF activity in the presence of 15 mM $CaCl_2$. However, the strongest relative effect of BCP, which was 5–30-fold, was obtained in the samples without $CaCl_2$ (Table 6).

This result was consistent with the previous experiment, showing that the largest-fold XET activity solubilisation fold effect of 1.82 mg/ml BCP was obtained in the absence of inorganic salts. However, in all plant extracts, there are always some salts naturally present. Therefore, in future experiments to document BCP action, I decided to use a small amount of NaCl (as 75 mM in 200 mM MES, pH 5.5; (referred as NaCl/MES buffer) as the buffer for testing XAF activity from now on.

A

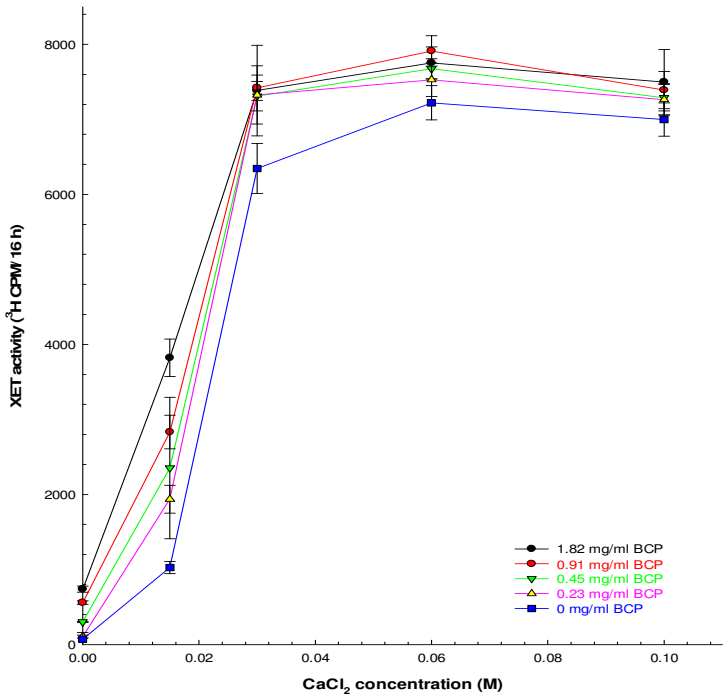


B

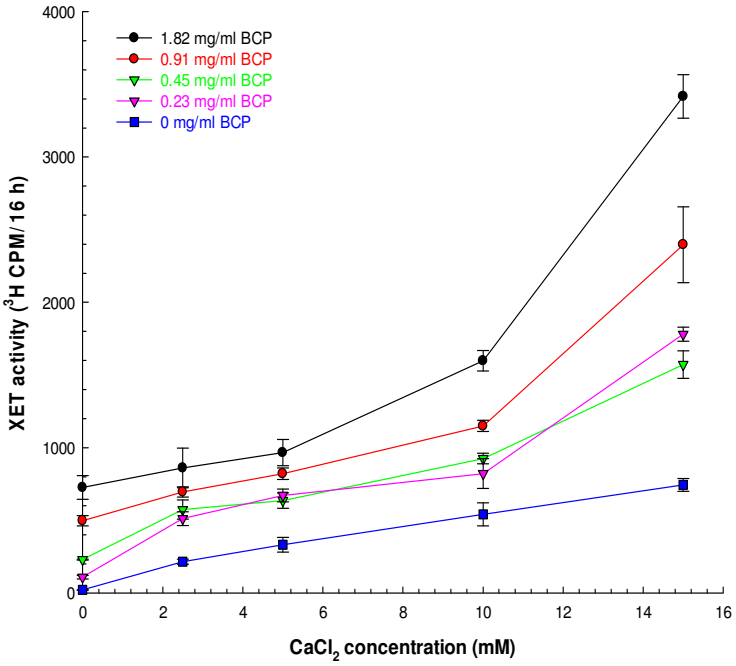


Figure 5. XET activity solubilised from *Arabidopsis* cells by BCP and $CaCl_2$ in the presence of BSA.

A, higher $CaCl_2$ concentration; B, lower $CaCl_2$ concentration. Frozen washed *Arabidopsis* cells were incubated for 1 h in 0.183 M MES ($Na^+$), pH 5.5, containing 0 to 1.82 mg/ml BCP and 0 to 15 mM $CaCl_2$ then 19 µl of supernatant was assayed for solubilised XET activity for 16 h in the presence of 0.25% BSA. Data show the mean of four determinations ± SE.

Table 6. Effect of $CaCl_2$ and BCP on solubilisation of XET activity from *Arabidopsis* cells in the presence of 0.25% BSA*

| BCP (mg/ml) | Ionic strength due to BCP (mM) (Based on NaCl-equivalent) | $CaCl_2$ concentration (mM) | Ionic strength due to $CaCl_2$ (mM) | XET activity ($^3H$ CPM per 16 h) | Fold promotion by $CaCl_2$ | Fold promotion by BCP |
|---|---|---|---|---|---|---|
| 0 | 0 | 0 | 0 | 21 ± 1 | - | - |
| | 0 | 2.5 | 6.25 | 216 ± 18 | 10.2 | - |
| | 0 | 5 | 12.5 | 331 ± 51 | 15.6 | - |
| | 0 | 10 | 25 | 541 ± 79 | 25.5 | - |
| | 0 | 15 | 37.5 | 744 ± 45 | 35.0 | - |
| 0.23 | 1.14 | 0 | 0 | 109 ± 12 | - | 5.1 |
| | 1.14 | 2.5 | 6.25 | 512 ± 48 | 4.7 | 2.4 |
| | 1.14 | 5 | 12.5 | 671 ± 43 | 6.1 | 2.0 |
| | 1.14 | 10 | 25 | 822 ± 102 | 7.5 | 1.5 |
| | 1.14 | 15 | 37.5 | 1780 ± 49 | 16.3 | 2.4 |
| 0.45 | 2.23 | 0 | 0 | 230 ± 4 | - | 10.8 |
| | 2.23 | 2.5 | 6.25 | 574 ± 65 | 2.5 | 2.7 |
| | 2.23 | 5 | 12.5 | 637 ± 53 | 2.8 | 1.9 |
| | 2.23 | 10 | 25 | 925 ± 36 | 4.0 | 1.7 |
| | 2.23 | 15 | 37.5 | 1572 ± 94 | 6.8 | 2.1 |
| 0.91 | 4.50 | 0 | 0 | 498 ± 35 | - | 23.4 |
| | 4.50 | 2.5 | 6.25 | 696 ± 35 | 1.4 | 3.2 |
| | 4.50 | 5 | 12.5 | 821 ± 40 | 1.7 | 2.5 |
| | 4.50 | 10 | 25 | 1149 ± 39 | 2.3 | 2.1 |
| | 4.50 | 15 | 37.5 | 2396 ± 260 | 4.8 | 3.2 |
| 1.82 | 9.01 | 0 | 0 | 726 ± 81 | - | 34.2 |
| | 9.01 | 2.5 | 6.25 | 861 ± 136 | 1.2 | 4.0 |
| | 9.01 | 5 | 12.5 | 966 ± 90 | 1.3 | 2.9 |
| | 9.01 | 10 | 25 | 1598 ± 70 | 2.2 | 3.0 |
| | 9.01 | 15 | 37.5 | 3416 ± 149 | 4.7 | 4.6 |

*: Data are from the experiment shown in Figure 5B.

"-": not applicable.

### 3.1.1.3 Abilities of various agents to prevent solubilised XTHs from binding to tube walls

In their previous study, Sharples and Fry (unpublished work) showed that insect-expressed XTH24 was able to bind to the surfaces of borosilicate glass tubes, thus reducing XET activity, and that this binding could be prevented by the use of tubes pre-treated with 0.5% poly-lysine. However, in my experiment, after 5 h incubation in tubes pre-coated with different concentrations of poly-lysine (0 to 1% (w/v)), the XET activity of 15% (v/v) NaCl-solubilised *Arabidopsis* XTHs was negligible at any poly-lysine concentration (Figure 6). This result suggested that poly-lysine did not prevent solubilised *Arabidopsis* XTHs from binding to the tubes. Therefore, I carried out an experiment to look for an agent with the ability to prevent solubilised XTHs from binding to several surfaces to use in further experiments.

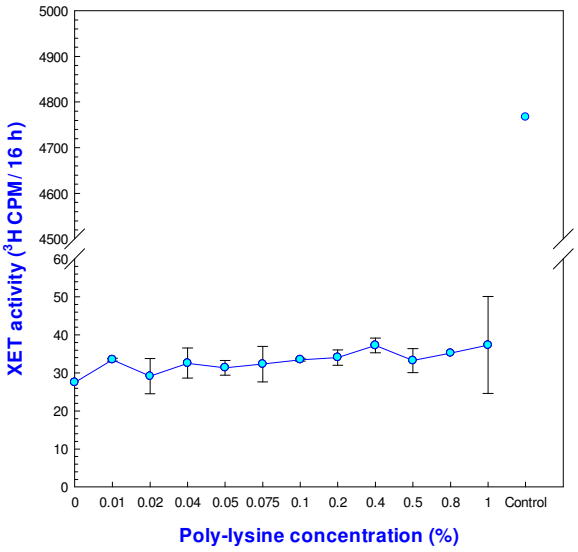


Figure 6. XET activity of solubilised *Arabidopsis* XTHs in poly-lysine pre-coated tubes

Each PCR tube was fully filled with different concentration of poly-lysine in chlorobutanol overnight, rinsed well with water and air-dried. XTHs were solubilised from *Arabidopsis* cells by 0.338 M NaCl/ 0.183 M MES for 1 h, tested for XET activity (control). Into each poly-lysine pre-coated tube, 85% (v/v) 0.2 M MES and 15% (v/v) NaCl-solubilised *Arabidopsis* XTHs was added, incubated for 5 h (time for the XTHs to bind to the tubes) and then assayed for XET activity. Data show the mean of three determinations ± SE. The experiment was done twice, one with 96-well plate and one with PCR tubes, with the same result. The result of the PCR tubes is presented here.

Solubilised XTHs were prepared by incubation of *Arabidopsis* cells with 0.338 M NaCl in 0.183 M MES for 1 h. The enzyme solution, at a final concentration of 15%

or 50% (v/v), was incubated in wells or tubes in the presence of different agents including a surfactant (0.1% Triton X-100), a protein (0.5% BSA), a salt at high concentration (0.338 M NaCl), and a homopolymer of an amino acid (poly-lysine; in this case the tubes were incubated with 0.5% poly-lysine overnight, then the poly-lysine was poured off and the tubes were rinsed in water and dried at room temperature). The final MES concentration in all incubations was kept at approximately 0.19 M. All solutions containing enzyme and agents were left at room temperature for 5.5 h (giving time for the enzyme to bind to the tubes or wells), and then 20 µl of radioactive XET reaction mixture was added and the XET activity was assayed as routine.

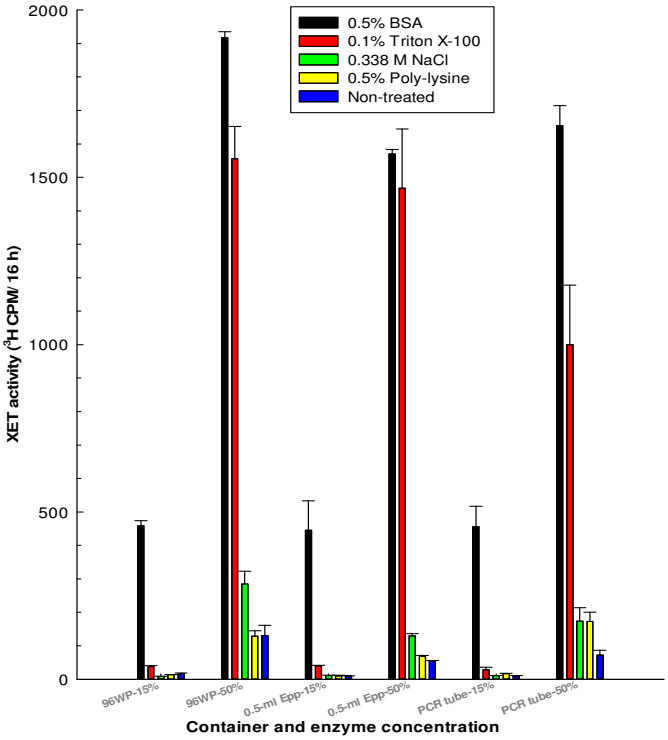


Figure 7. Abilities of various agents to prevent solubilised XTHs from binding to the tube walls.

Solubilised XTHs were prepared by incubating *Arabidopsis* cells in 0.338 M NaCl with 0.183 M MES, pH 5.5 for 1 h. Then 15% (v/v) or 50% (v/v) enzyme extract, always in final concentration of ~0.19 M MES (pH 5.5) and 0.05 M or 0.169 M NaCl, with various agents as indicated on the graph legend, were incubated in a well of 96-well plate (96WP), a 0.5-ml Eppendorf tube (0.5-ml Epp), or a PCR tube. In case of 0.338 M NaCl, in addition to the NaCl already present in the enzyme extract, NaCl was added to the final concentration. To make a poly-lysine pre-coated well, Eppendorf tube and PCR tube, 200 µl, 700 µl, and 300 µl 0.5% poly-lysine in 0.5% chlorobutanol was added, respectively. Non-treated: XTHs incubated in 0.183 M MES in non-poly-lysine coated wells or tubes. After 5.5 h of incubation, 20 µl radioactive substrate mixture was added and the XET activity was assayed after 16 h incubation. Data show the mean of two determinations ± SE.

Of these agents, BSA had the strongest ability to retain XET activity, presumably by preventing solubilised XTHs from binding to the tube walls, followed by 0.1% Triton X-100 (Figure 7). The type of tube did not affect to the ability of agents to prevent solubilised XTHs from binding to the tube walls. Remarkably, BSA was far more effective than other agents in the presence of low XTH concentration (Figure 7) in preventing either denaturation or binding to the tube walls of the enzyme. In conclusion, BSA at a final concentration of 0.25% in 0.2 M MES was the best one in all agents tested to keep the solubilised enzyme at its high activity, and will be used in all future experiments. I used 96-well plates for XAF assays because of their convenience to deal with a large number of samples.

#### 3.1.1.4 The ability of BSA to prevent BCP/NaCl-solubilised *Arabidopsis* from binding to the tube walls

In the previous experiment, I found that 0.25% BSA in MES buffer retained XET activity of XTHs previously solubilised by 0.338 M NaCl in 0.183 M MES ($Na^+$), pH 5.5. In the following experiments, I further tested whether I should use BSA as a routine agent in XAF assays.

In the first experiment, BSA was added to the cells at the same time as NaCl and BCP (Figure 8) during the solubilisation step, and in the second experiment, BSA was added to the reaction after XTHs had been solubilised from *Arabidopsis* cells by BCP and/ or NaCl and the cells had been removed (Figure 9). The results revealed that BSA itself did not have XET activity (Figure 9) or XAF activity (first experiment) (Figure 8). After using 0.075 M NaCl accompanied by 0 or 1.82 mg/ml BCP to solubilise XTHs from the cells, the addition of 0.25% BSA promoted XET activity up to 1.9- or 1.2-fold compared with the BSA-free control, respectively (Table 7). This suggested that BSA acts to prevent XTHs solubilised by BCP and/ or NaCl from binding to the tube walls or being denatured.

BCP had a remarkable stimulatory effect on solubilisation of XET activity throughout this experiment. Consistent with the result in 3.1.1.1, the highest-fold promotion effect of BCP was obtained in the absence of NaCl. Interestingly, BSA helped to retain this high effect, which was 80-fold with BSA compared to 60-fold without BSA (Figure 9). Without BCP, BSA also helped to retain a high promotion effect caused by 0.338

M and 0.075 M NaCl, 800-fold with BSA compared to 600-fold without BSA and 20-fold with BSA compared to 10-fold without BSA, respectively (Table 7). In the presence of both NaCl and BCP, an effect of BSA was not observed (Table 7), suggesting that NaCl or/ plus BCP may also have the ability to prevent solubilised XTHs from binding to the tube walls or being denatured.

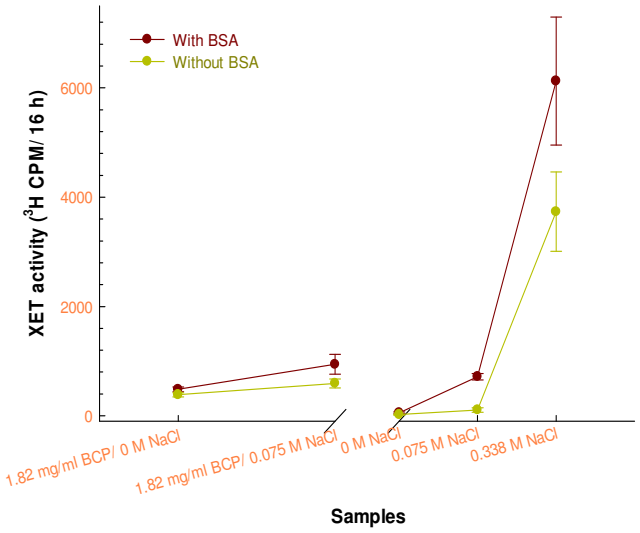


Figure 8. XET activity solubilised from *Arabidopsis* cells by various combinations of BCP, NaCl and BSA.

Thawed washed *Arabidopsis* cells were incubated with 66 µl of 0 or 1.82 mg/ml BCP accompanied by 0 M, 0.075 M or 0.338 M NaCl, all in 0.2 M MES, with or without 0.5% BSA for 1 h. The mixture was then spun down and 20 µl supernatant was transferred to a new well of a 96 well-plate to assay XET activity with 20 µl [$^3$H]XXXGol and Tm XyG. Data show the mean of six determinations ± SE.

In conclusion, 0.25% BSA in some cases helped to stabilise the XET activity previously solubilised by NaCl or BCP, presumably by preventing its binding to the cells and the tube surfaces or being denatured. Again, NaCl had a concentration-dependent effect on XET solubilisation. BCP had the strongest XET solubilisation effect, up to 80-fold without NaCl and this fold-effect became smaller in the presence of high concentration of NaCl (Table 7). Therefore, 0.075 M NaCl in 0.2 M MES with 0.25% BSA was used as a standard buffer during XET assays to prevent solubilised XTHs from binding to tube walls or being denatured from now on. For technical convenience, 0.5% BSA was mixed with [$^3$H]XXXGol (25 kBq/ml) in 0.4% (w/v) tamarind xyloglucan in 0.5% (w/v) chlorobutanol and added into the BCP/XAF-solubilised enzyme solution for XET assay from now on.

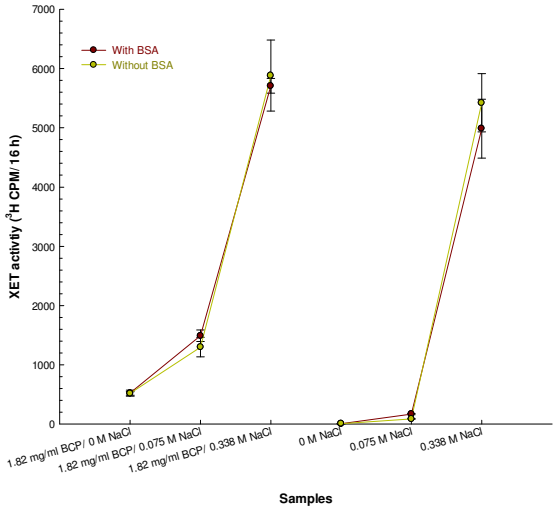


Figure 9. XET activity solubilised from *Arabidopsis* cells by BCP and/ or NaCl, followed by addition of 0.25% BSA into the reaction mixture after removing cells.

Thawed washed *Arabidopsis* cells were incubated in 66 µl of 0 or 1.82 mg/ml BCP in 0.2 M MES accompanied by 0 M, 0.075 M or 0.338 M NaCl for 1 h and 19 µl of supernatant was transferred into a new well which already contained 1 µl 10% (w/v) BSA in 0.2 M MES or 0.2 M MES alone to assay XET activity with 20 µl [$^3$H]XXXGol and Tm XyG. Data show the mean of three determinations ± SE.

Table 7. Effect of BSA on XET activity of XTHs previously solubilised by BCP and/ or NaCl from *Arabidopsis* cells*.

| BCP (mg/ ml) | NaCl concentration (M) | BSA concentration (%) | XET activity ($^3$H CPM) per 16 h | Fold "promotion" by BSA[!] | Fold "promotion" by NaCl[ı] | Fold "promotion" by BCP[ı] |
|---|---|---|---|---|---|---|
| 0 | 0 | 0 | 8 ± 1 | - | - | - |
| | 0.075 | | 88 ± 7 | - | 11.0 | - |
| | 0.338 | | 5422 ± 490 | - | 677.8 | - |
| | 0 | 0.5 | 6 ± 1 | 0.8 | - | - |
| | 0.075 | | 170 ± 11 | 1.9 | 28.3 | - |
| | 0.338 | | 4987 ± 496 | 1.1 | 831.2 | - |
| 1.82 | 0 | 0 | 519 ± 30 | - | - | 64.9 |
| | 0.075 | | 1301 ± 167 | - | 2.5 | 14.8 |
| | 0.338 | | 5882 ± 598 | - | 11.3 | 1.1 |
| | 0 | 0.5 | 522 ± 50 | 1.0 | - | 87.0 |
| | 0.075 | | 1492 ± 98 | 1.2 | 2.9 | 8.8 |
| | 0.338 | | 5708 ± 124 | 1.0 | 10.9 | 1.1 |

*: Data from Figure 8.

[!]: Added after solubilisation of XTHs from *Arabidopsis* cells

[ı]: Added during solubilisation of XTHs from *Arabidopsis* cells

Concentration approximately halved during XET assay

#### 3.1.1.5 XAF activity of several polysaccharides

To prepare BCP, I homogenised cauliflower florets in cold water and boiled the extract for 1 h, then centrifuged and took the supernatant. This supernatant was frozen and thawed, centrifuged and precipitated with ethanol. Thus, most of the proteins in the extract were denatured and discarded (except for any heat-stable proteins). All low molecular weight compounds such as monosaccharides, amino acids, oligosaccharides, peptides are soluble in ethanol and were therefore removed. The BCP was expected to contain high molecular weight substances that cannot be denatured by boiling, for example polysaccharides or glycosylated proteins. In order to characterise which compounds are responsible for the XAF activity of BCP, I assayed some possible natural polysaccharides for their XAF activities.

Of all polysaccharides tested, tamarind xyloglucan, gum arabic, carboxymethylcellulose (CMC), and pectin at 0.5% (w/v) had XAF activity, from the highest to the lowest (Figure 10). In contrast, BCP at a lower concentration (0.2% (w/v)), had a much higher activity. This indicated that BCP was not simply any of these polysaccharides. Surprisingly, tamarind xyloglucan had as high XAF activity as that of gum arabic while nasturtium xyloglucan did not have any XAF activity. In this case, Tm XyG used for solubilising XET from the cells added to the Tm XyG used as the donor substrate for XET activity, giving a final concentration of 0.45% in place of 0.2% as usual, thus could increase XET activity. However, Ns XyG did not have this ability suggesting that there may be some other substances rather than xyloglucan in the Tm XyG preparation but not in the Ns XyG preparation contributing for its XAF activity.

Yariv reagent is well-known for its ability to precipitate AGP and was used to test the presence of AGPs in all of these polysaccharides. The result showed that gum arabic and BCP contained AGP (Figure 11). The precipitation of AGP in gum arabic was greater than in BCP (Figure 11) but its XAF activity was smaller than that of BCP (Figure 10). Although tamarind xyloglucan did not contain AGP, its XAF activity was as high as that of gum arabic and this activity was not found in nasturtium xyloglucan (Figure 10). This result suggested that BCP may contain non-classical AGP.

From these results, I concluded that BCP contained both classical and non-classical AGPs, and these AGPs were contributing for its XAF activity.

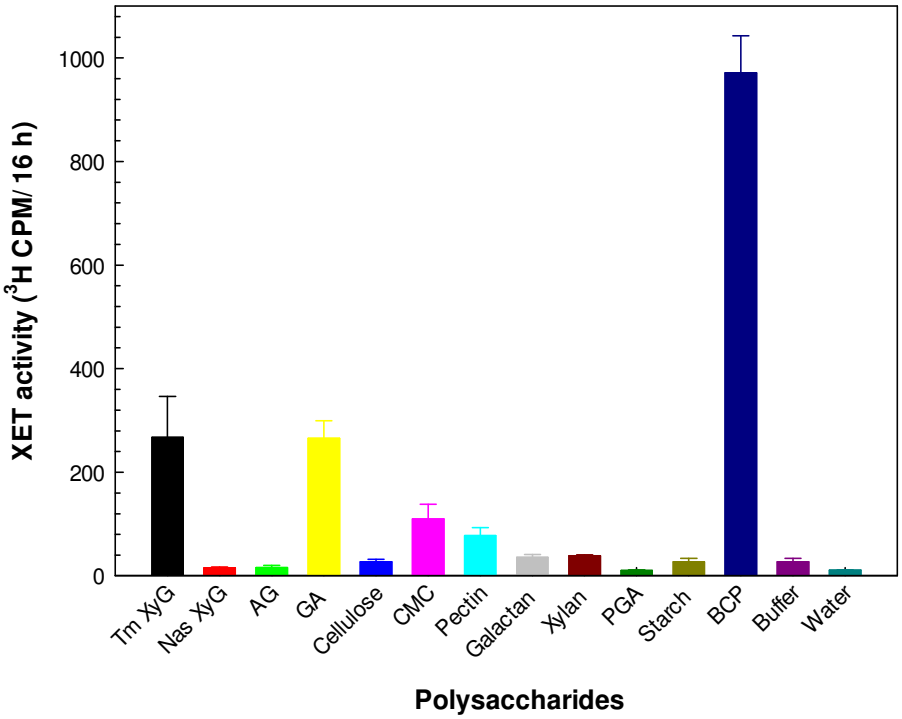


Figure 10. XET activity solubilised from *Arabidopsis* cells by several polysaccharides.

Tamarind xyloglucan (Tm XyG), Nasturtium xyloglucan (Nas XyG), larch wood arabinogalactan (AG), Acacia tree gum arabic (GA), CMC, esterified citrus fruit pectin, potato galactan, birch wood xylan, polygalacturonic acid (PGA), and soluble starch were dissolved at 5 mg/ml in NaCl/MES buffer for XAF assay, except for cellulose powder (5 mg/ml suspension). Each sample was assayed for XAF activity with the presence of 0.25 % BSA in triplicate. BCP (2 mg/ml) was used as a control. Data show the means of three determinations ± SE.

Figure 11. The presence of arabinogalactan-protein (AGP) in various polysaccharides, tested by Yariv reagent.

A mixture of 40 µl of 2 mg/ml Yariv reagent in 1% NaCl with 16 µl of 0.5% polysaccharide in 0.1% chlorobutanol or 40 µl 2 mg/ml BCP in water was made. The plate was photographed 0.5 h after mixing. 1, Tamarind XyG; 2, nasturtium XyG; 3, arabinogalactan; 4, gum arabic; 5, cellulose powder (suspension); 6, carboxymethyl cellulosic; 7, pectin; 8, galactan; 9, xylan; 10, polygalacturonic acid; 11, starch; XAF, BCP; W, water. Biological sources of the polysaccharides are as indicated in Figure 10.

### 3.1.2 The effect of the weight of *Arabidopsis* cells and the concentration of BCP on the solubilisation of XET activity

#### 3.1.2.1 Effect of weight of *Arabidopsis* cells

In this experiment, the initial suspension of washed *Arabidopsis* cells contained 2.8 mg (dry weight) per ml, and different amounts of cells were taken to be incubated with BCP.

The dry weight of *Arabidopsis* cells used in an assay had a strong effect on the solubilisation of XET activity by 2 mg/ml BCP. The "fold" promotion effect by BCP increased from 1- to 8-fold as the cell weight decreased from 182.8 µg to 18.3 µg (Figure 12A); then the effect was unchanged at ~8-fold while the cell weight decreased from 18.3 µg to 10.2 µg, and finally slightly decreased when the cell weight was 8.3 µg (Figure 12B). The buffer contained 0.075 M NaCl and 0.2 M MES and at this ionic strength it could solubilise some XTHs from the cells as correspondent with the results in section 3.1.1.1 and 3.1.1.4, then BSA added in the XET assay mixture helped to retain these enzymes in the reaction solution to cause some XET activity. When plenty of cells were present, so XTHs were abundantly present, the XET activity solubilised by buffer already reached a plateau; thus any further XET solubilisation by BCP was not detectable. The lower the weight of cells, the further from the plateau the XET activity was, and the higher the effect of XAF was (Table 8).

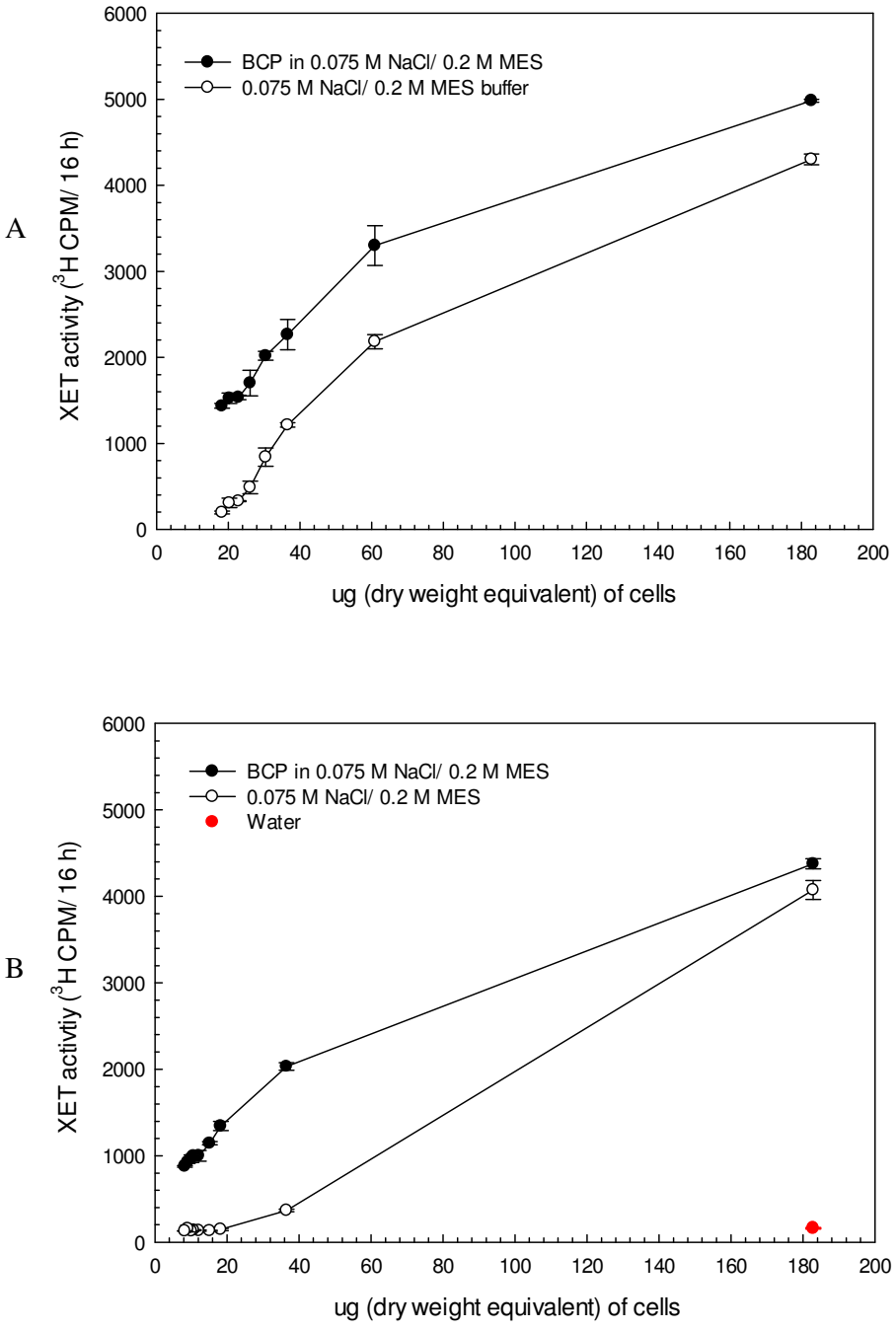


Figure 12. XET activity solubilised from different concentrations of *Arabidopsis* cells suspension by BCP.

*Arabidopsis* cell suspension (3 to 66 µl) was washed several times with water and the water was removed. The moist cell pellet (equivalent to 8.3 – 182.8 µg dry weight) was incubated with 66 µl of 2 mg/ml BCP in 0.075 M NaCl/ 0.2 M MES and the XAF activity was assayed as routine in the presence of 0.25% BSA. A, higher cell weight; B, lower cell weight. Red circle: water was used in place of BCP or buffer. Data show the means of four determinations ± SE.

Table 8. The effect of *Arabidopsis* dry cell weight on the solubilisation of XET activity by 2 mg/ml BCP*

| BCP in NaCl/MES buffer | The weight of *Arabidopsis* cells (µg) | XET activity ($^3$H CPM per 16 or 17 h) | Fold "promotion" by BCP |
|---|---|---|---|
| 0 mg/ml | 182.8 | 4302 ± 62<br>4074 ± 111 | - |
| | 60.9 | 2182 ± 84 | - |
| | 36.6 | 1213 ± 26 | - |
| | 30.5 | 840 ± 106 | - |
| | 26.1 | 489 ± 73 | - |
| | 22.9 | 329 ± 4 | - |
| | 20.3 | 308 ± 55 | - |
| | 18.3 | 197 ± 15<br>146 ± 14 | - |
| | 15.2 | 131 ± 7 | - |
| | 12.2 | 133 ± 7 | - |
| | 10.8 | 127 ± 1 | - |
| | 10.2 | 156 ± 37 | - |
| | 9.1 | 129 ± 1 | - |
| | 8.3 | 165 ± 3 | - |
| 2 mg/ml | 182.8 | 4983 ± 18<br>4377 ± 59 | 1.2<br>1.1 |
| | 60.9 | 3300 ± 230 | 1.5 |
| | 36.6 | 2264 ± 177 | 1.9 |
| | 30.5 | 2018 ± 52 | 2.4 |
| | 26.1 | 1702 ± 147 | 3.5 |
| | 22.9 | 1534 ± 26 | 4.7 |
| | 20.3 | 1525 ± 60 | 5.0 |
| | 18.3 | 1435 ± 28<br>1344 ± 18 | 7.3<br>9.2 |
| | 15.2 | 1144 ± 18 | 8.7 |
| | 12.2 | 1000 ± 62 | 7.5 |
| | 10.8 | 999 ± 3 | 7.5 |
| | 10.2 | 967 ± 45 | 7.6 |
| | 9.1 | 926 ± 13 | 7.2 |
| | 8.3 | 879 ± 9 | 5.3 |

"-": not applicable

*: Data from the experiment shown in Figure 12A and B.

In conclusion, the optimum dry cell weight of *Arabidopsis* for testing XAF activity of BCP was from 15.2 µg to 18.3 µg. This concentration is used throughout experiments in this study.

#### 3.1.2.2 Effect of BCP concentration

There was an increment in XAF activity dependent on the concentration of BCP. The higher the concentration of BCP was, the more XET activity was solubilised from *Arabidopsis* cells. However, the relationship between them was not linear (Figure 13 A, B). The XAF activity was almost reaching a plateau when the concentration of BCP was higher than 8 mg/ml. This plateau is not simply because the assay was running out of [$^3$H]XXXGol or tamarind xyloglucan because with the same amount of reaction mixture and reaction time, the yield of the product exceeded 2500 cpm/16 h when more enzyme was present as in Figure 12. Therefore, Figure 13 is used as a standard curve for calculating BCP-equivalent concentration of a potential XAF (purified XAF or XAF from other plants) from its known XET activity from now on.

Table 9. Effect of BCP concentration on its ability to solubilise XET activity from *Arabidopsis* cells

| BCP concentration (mg/ml) | XET activity ($^3$H CPM per 16 h) | Fold "promotion" by BCP |
|---|---|---|
| 0.00 | 22 ± 3 | - |
| 0.13 | 241 ± 19 | 11.0 |
| 0.25 | 365 ± 13 | 16.6 |
| 0.50 | 475 ± 16 | 21.6 |
| 1.00 | 555 ± 8 | 25.2 |
| 2.00 | 769 ± 16 | 35.0 |
| 4.00 | 1434 ± 21 | 65.2 |
| 8.00 | 2249 ± 20 | 102.2 |
| 16.00 | 2456 ± 166 | 111.6 |

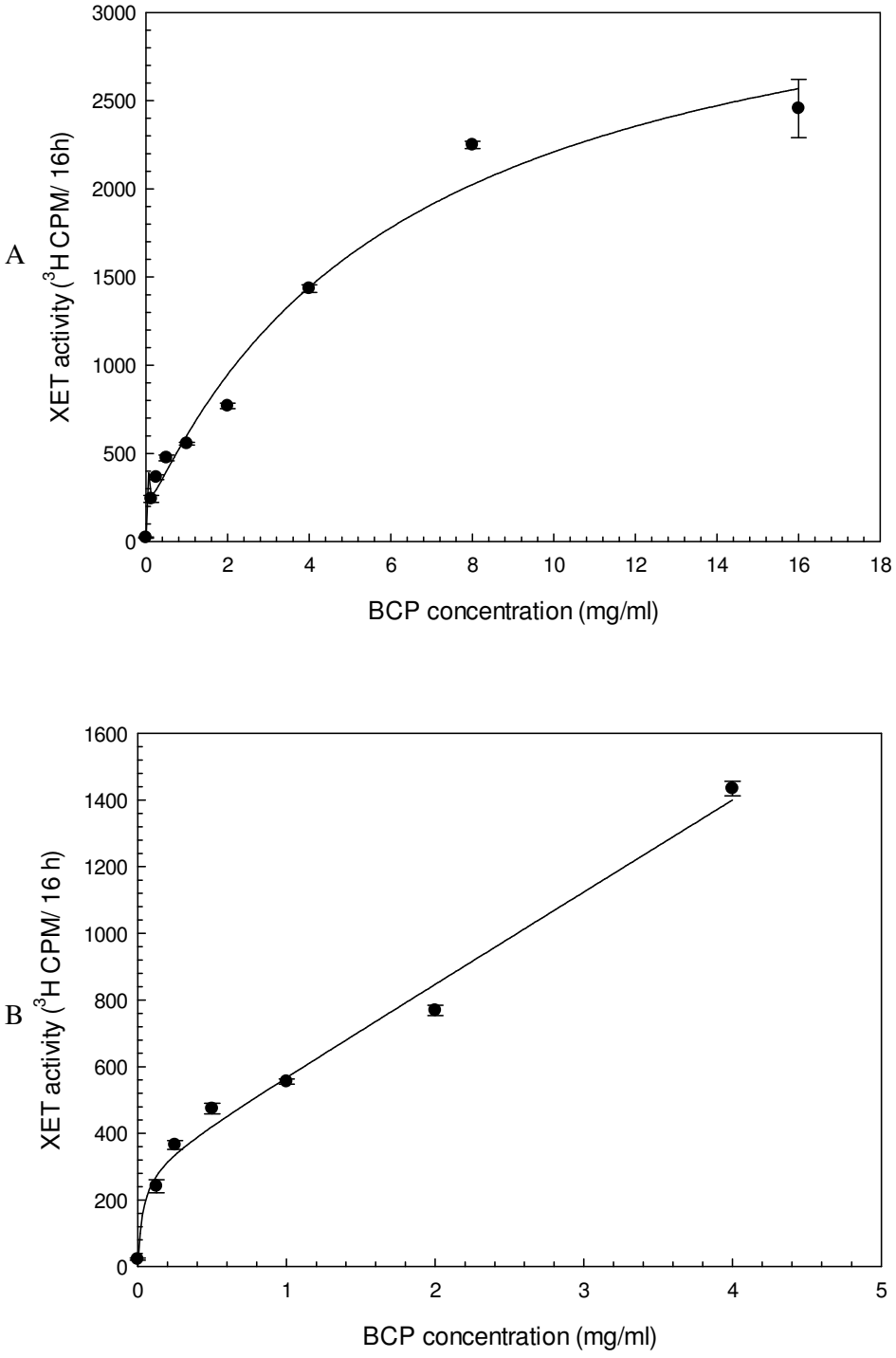


Figure 13. Standard curve of different BCP concentrations and their XAF activities.

Different concentrations of BCP was assayed for XAF in the presence of 0.25 % BSA. A, from 0 to 16 mg/ml BCP; B, zoom in from 0 to 4 mg/ml BCP. Data show the means of two determinations ± SE.

### 3.1.3 The presence of XAF in the plant kingdom

The above work showed that cauliflower florets had XAF activity. Was this activity unique to cauliflower? In other words, how widespread was XAF activity in the plant kingdom? I conducted the following experiment to answer this question.

Each boiled plant extract was precipitated with ethanol, freeze-dried, and weighed. Then it was re-dissolved in water for conductivity measurement and TFA hydrolysis or in NaCl/MES buffer for XAF assay.

XAF activity was widely present in all samples tested, monocots and dicots, from all organs (leaves, roots, stems, flowers and petiole), from cell-suspensions (rose, *Arabidopsis*) to mature plants (*Arabidopsis*, crocus, snowdrop, tobacco), from young (watercress, asparagus, and very young celery petiole) to old tissues (tobacco stem, carrot root), with two exceptions: maize culture and beansprout hypocotyl. *Arabidopsis* leaves, watercress and parsley leaves had the highest XAF activity (Figure 14). There were about nine species having a higher XAF activity than the cauliflower florets. Considering salts present in these BPPs may contribute an XTHs-solubilisation effect rather than the factor, I measured the conductivity of all these BPPs and their NaCl-equivalent concentrations were calculated based on the standard curve in Figure 15. Although I expected to remove salts by the careful wash BPPs with 96% and 80% ethanol, all BPPs contained a small amount of salts, from 1 to 13 mM equivalent NaCl. However, the XAF activities of BPPs were independent of their NaCl-equivalent concentrations (Figure 16). The XAF activities of the BPPs were also independent of the content of polymers obtained from 1 ml of each boiled plant extract (Figure 17).

TFA hydrolysis of the various BPPs revealed that all of them contained a major amount of Gal, Ara and uronic acids, as with BCP (Figure 18, Figure 19, Figure 20) suggesting the contribution of AGP to the XAF activity of the BPPs. Mannose was present in all BPPs with a smaller amount compared to other monosaccharides (Figure 18, Figure 22). Interestingly, the amount of mannose in the BPPs was very different: very high in asparagus- and spring onion leaves-BPP; quite high in snowdrop-, parsley leaves-, and cauliflower-BPP; and not detectable in spinach leaves-, and tobacco leaves-BPP. Rib or Fuc was not detectable in any BPP (Figure 18). There were big differences between the BPPs in certain monosaccharides such as Glc, Xyl, Rha (Figure 18). Many BPPs

contained a very high amount of Glc such as tobacco stem, *Arabidopsis*, BCP, rose culture, spinach culture, and carrot root whereas spinach leaves- and watercress-BPP contained almost no detectable Glc. While most of BPPs had a small amount of Xyl, some BPPs had a very high amount of it, including tobacco stem-, lettuce leaves-, celery petiole-BPP and some BPPs had no detectable Xyl, including *Arabidopsis* leaves, snowdrop leaves, spinach leaves and tobacco leaves. There was a trace amount of Rha in most of BPPs, excepted for *Arabidopsis* flower, rose culture, spinach culture, and tobacco stem where Rha was predominant. The BPPs from asparagus and spring onion leaves contained an unknown sugar which moved faster than Rha (Figure 18). However, there were no significant correlations (the $R^2$ values were very low) between any monosaccharide contents and the XAF activities (Figure 19, Figure 20, Figure 21, Figure 22, Figure 23, Figure 24).

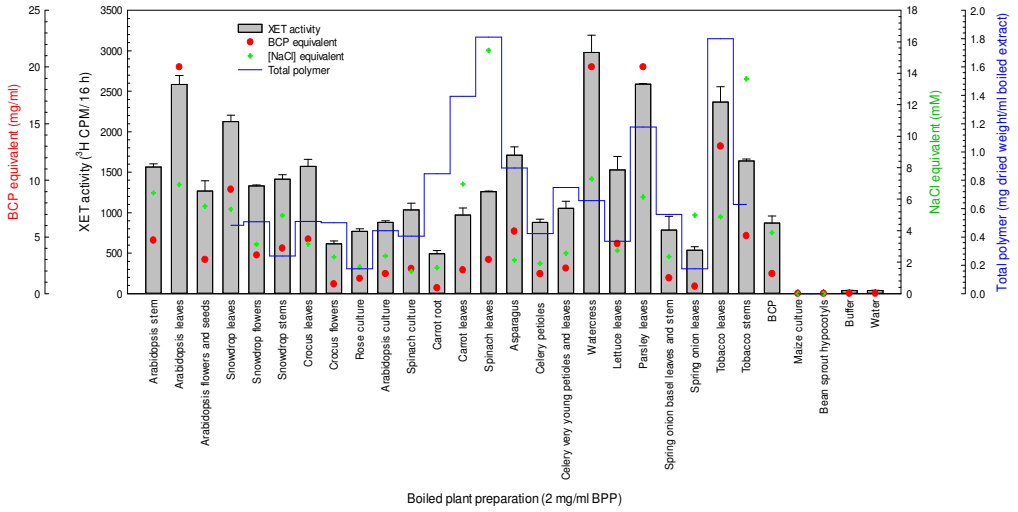


Figure 14. XAF activity in diverse boiled plant preparations (BPPs).

Each boiled plant extract (15 ml) was precipitated with 67.2% ethanol and the precipitate was carefully washed three times with 96% ethanol and one time with 80% ethanol to remove all low $M_r$ compounds and air-dried. The dry material was then freeze-dried and the total polymer was measured by weighing the dried BPP after freeze-drying from 1 ml boiled plant extract (did not measure in the cases of *Arabidopsis* stem, leaves, and flowers and seeds, BCP). In the cases of maize culture and bean sprout hypocotyl, there was no precipitation obtained after the treatment with ethanol. The dry material was re-dissolved in water at 2 mg/ml. Of that, 150 µl (= 300 µg) was dried in the SpeedVac and re-dissolved in 150 µl NaCl/MES buffer; 66 µl of it was used in an XAF assay. Data show the means of two determinations ± SE. BCP equivalent was interpreted from the standard curve in Figure 13. An additional 300 µg of the EtOH-washed BPP was re-dissolved in water and its conductivity was measured with a Jenway 4060 conductivity meter; the NaCl-equivalent salt concentration of each BPP was calculated from the standard curve in Figure 15.

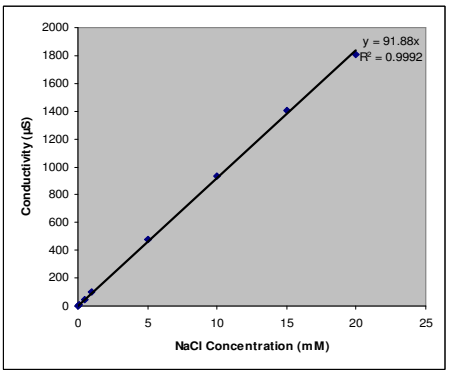


Figure 15. Standard curve for conductivity of NaCl.

Different concentrations of NaCl were measured for conductivity with a Jenway 4060 conductivity meter.

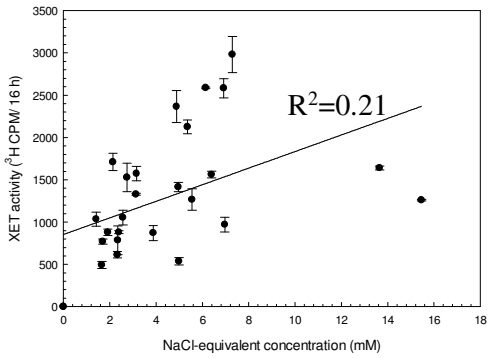


Figure 16. Scattergram showing the relationship between NaCl-equivalent concentration and XAF activity of BPPs.

Data are from Figure 14.

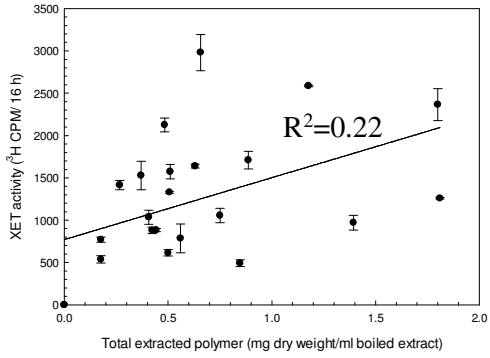


Figure 17. Scattergram showing the relationship between total extracted polymer and XET activity of BPPs.

Data are from Figure 14.

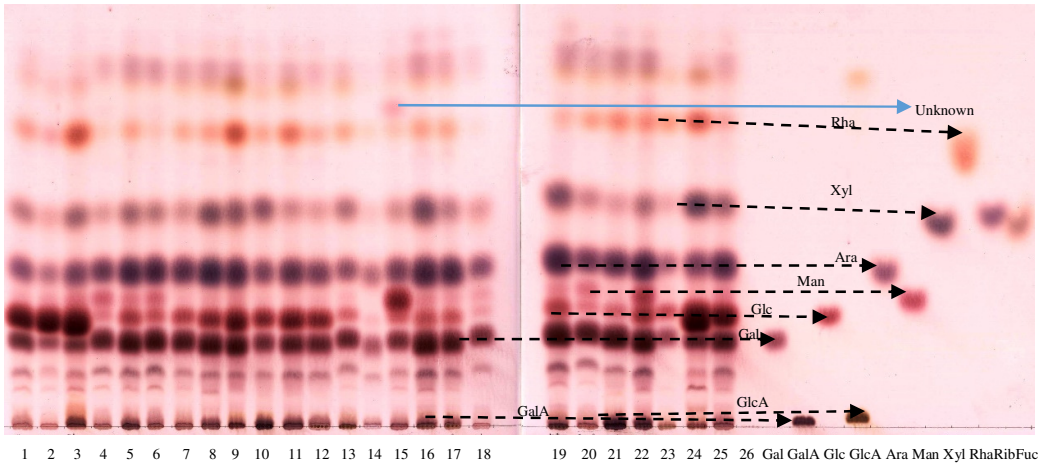


Figure 18. TLC profile of TFA hydrolysis products of BPPs.

BPP (100 µg) was hydrolysed with 2 M TFA, dried, re-dissolved in 2 µl water and loaded onto the TLC plate. Solvent: EPAW 6:3:1:1, thymol staining. 1, 2, 3/ *Arabidopsis* stems, leaves, flowers, 4, 5, 6/ snowdrop leaves, flowers, stems, 7, 8/ crocus leaves, flowers, 9/ rose culture, 10/ *Arabidopsis* culture, 11/ spinach culture, 12, 13/ carrot root, leaves, 14/ spinach leaves, 15/ asparagus, 16/ celery petiole, 17/ very young celery petiole and stem, 18/ watercress without roots, 19/ lettuce leaves, 20/ parsley leaves, 21/ spring onion basal stem and leave, 22/ spring onion leaves, 23, 24/ tobacco leaves, stem, 25/ BCP, 26/ TFA.

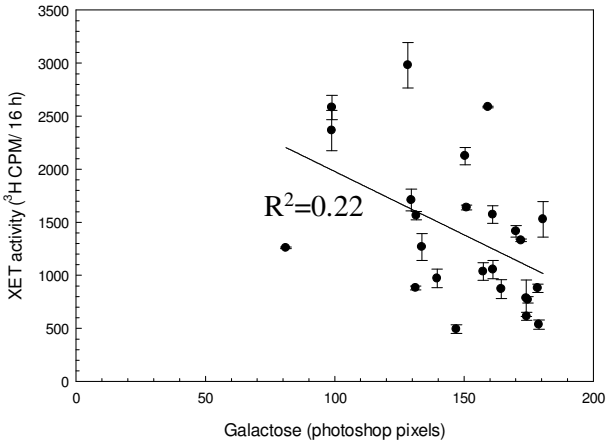


Figure 19. Scattergram showing the relationship between galactose and XAF activity.

The mean intensity of each Gal spot in each BPP on the TLC in Figure 18 was measured using Photoshop software. The ellipse tool (fixed size: 0.87 cm X 0.61 cm) was chosen to measure the mean intensity of each Gal spot. The measurement was done by choosing the tap image- histogram- channel-green (because it usually gave the lowest mean). That mean intensity was subtracted by a negative control (the mean pixel value of a blank track, containing no sugars in the Gal zone, which was 220 pixels in this case). The result was plotted on the x-axis as "photoshop pixels". The higher the "photoshop pixels" was, the more intensive the sugar spot on the TLC was. For examples, the most intense Gal spot was given by lettuce leaves-BPP, which produced a value of 181 on the pixel scale, whereas the least intense one was given by spinach leaves-BPP, which produced a value of 81. XAF activity is from Figure 14.

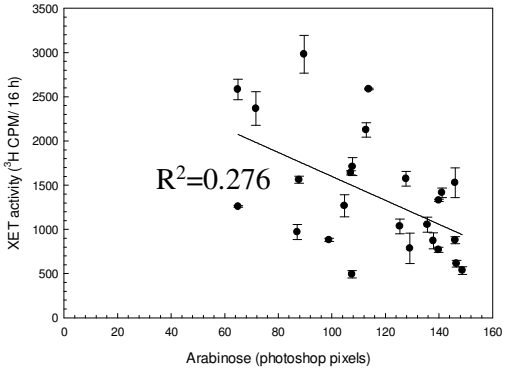


Figure 20. Scattergram showing the relationship between arabinose and XAF activity.

The mean intensity of each Ara spot in each BPP on the TLC in Figure 18 was measured. Other details as in Figure 19.

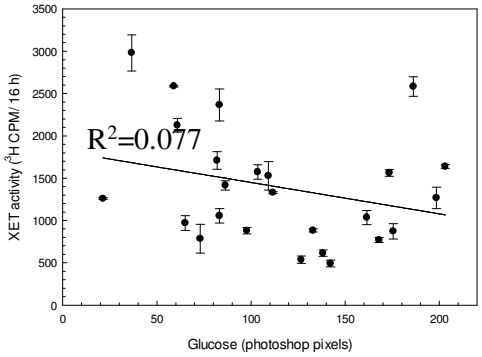


Figure 21. Scattergram showing the relationship between glucose and XAF activity.

The mean intensity of each Glc spot in each BPP on the TLC in Figure 18 was measured. Other details as in Figure 19.

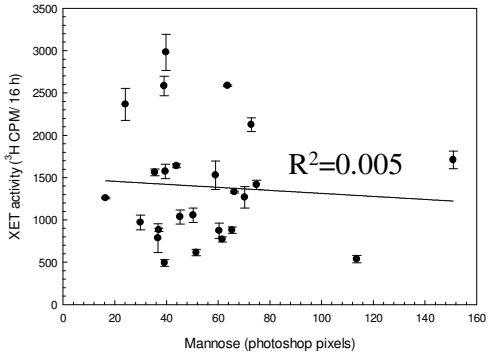


Figure 22. Scattergram showing the relationship between mannose and XAF activity.

The mean intensity of each Man spot in each BPP on the TLC in Figure 18 was measured. Other details as in Figure 19.

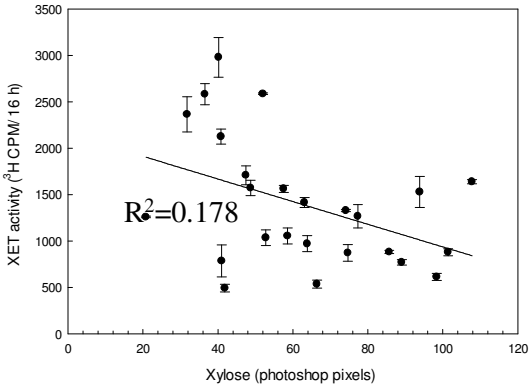


Figure 23. Scattergram showing the relationship between xylose and XAF activity.

The mean intensity of each Xyl spot in each BPP on the TLC in Figure 18 was measured. Other details as in Figure 19.

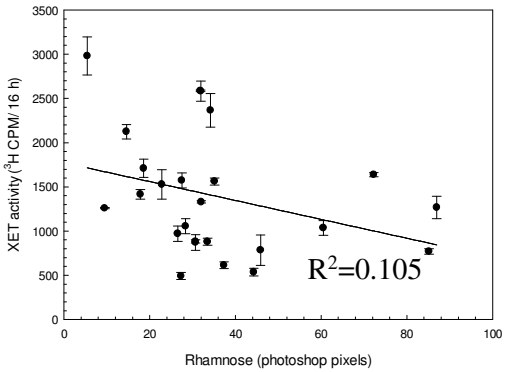


Figure 24. Scattergram showing the relationship between Rhamnose and XAF activity.

The mean intensity of each Rha spot in each BPP on the TLC in Figure 18 was measured. Other details as in Figure 19.

## 3.2 The specificity of XAF in solubilisation of cell wall enzyme activities

The aim of this experiment was to test whether XAF can solubilise other enzyme activities from the cell wall besides XET activity. I used NaCl/MES buffer, BCP in NaCl/MES buffer and a high concentration of salt (1 M NaCl in 0.2 M MES) to sequentially solubilise enzymes from *Arabidopsis* cell walls, then assayed the extracts for several enzyme activities including β-D-glucosidase, phosphatase, peroxidase, invertase and XET.

Both NaCl/MES buffer and BCP in NaCl/MES buffer were fairly ineffective while 1 M NaCl in 0.2 M MES effectively solubilised β-D-glucosidase and phosphatase from

the *Arabidopsis* cell walls. NaCl/MES buffer solubilised approximately 3% and BCP solubilised 15% while 1 M NaCl in 0.2 M MES solubilised 82% of β-D-glucosidase activity that can be solubilised from the cell walls (Figure 25) (some of the β-D-glucosidase activity may not be extractable at all (covalently wall-bound enzymes)). In case of phosphatase activity, BCP solubilised 9%, MES/NaCl buffer solubilised 24%, and 1 M NaCl in 0.2 M MES solubilised 67% of the total soluble activity (Figure 26). Again, some of the phosphatase activity may not be extractable at all.

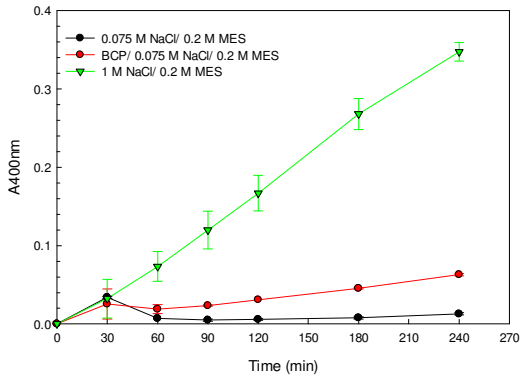


Figure 25. β-D-Glucosidase activity solubilised from *Arabidopsis* cell walls by different solutions.

*Arabidopsis* cells were incubated with NaCl/MES buffer, BCP in NaCl/MES buffer and 1 M NaCl/ 0.2 M MES for 30 min, sequentially. The supernatant obtained after centrifuging each incubation was assayed for β-D-glucosidase activity. The product of this enzyme reaction was p-nitrophenol which is yellow (in $Na_2CO_3$) and its absorbance was measured at 400 nm.

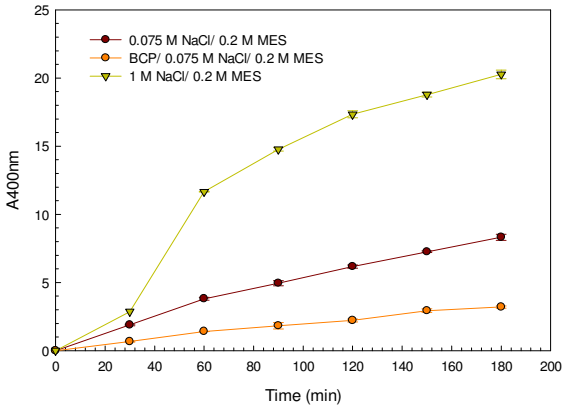


Figure 26. Phosphatase activity solubilised from *Arabidopsis* cell walls by different solutions.

*Arabidopsis* cells were incubated with NaCl/MES buffer, BCP in NaCl/MES buffer and 1 M NaCl/ 0.2 M MES for 30 min, sequentially. The supernatant obtained after centrifuging each incubation was assayed for phosphatase activity. The product of this enzyme reaction was p-nitrophenol which is yellow (in $Na_2CO_3$) and its absorbance was measured at 400 nm.

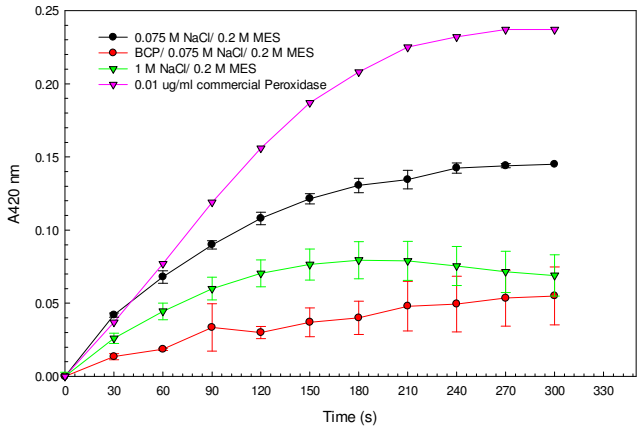


Figure 27. Peroxidase activity of a commercial peroxidase enzyme and the peroxidase activity solubilised from *Arabidopsis* cell walls by different solutions.

*Arabidopsis* cells were incubated with NaCl/MES buffer, BCP in NaCl/MES buffer and 1 M NaCl/ 0.2 M MES for 30 min, sequentially. The supernatant obtained after centrifuging each incubation was assayed for peroxidase activity. The product of this enzyme reaction is red and its absorbance was measured at 420 nm.

NaCl/MES buffer solubilised most of the peroxidase that can be extractable from *Arabidopsis* cell walls. Some of the peroxidase may not be extractable at all (covalently wall-bound enzymes). Although BCP was used before the use of 1 M NaCl in 0.2 M MES, it solubilised less peroxidase activity than the high salt solution (Figure 27). The addition of another dose of $H_2O_2$ did not help to recover activity suggesting that the loss of activity was not due to the lack of substrates. One possible explanation was that the enzyme bound to the tube walls, thus the use of surfactants during reaction such as 0.5% BSA or 0.5% Triton X-100 may be necessary.

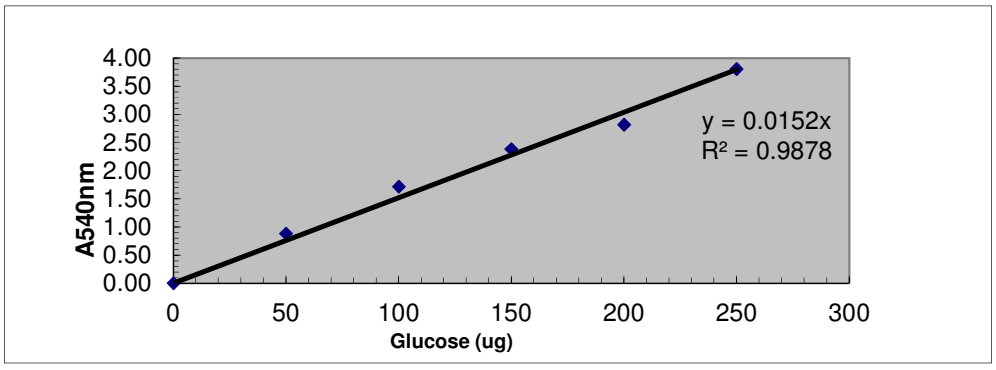


Figure 28. Standard curve of different glucose concentrations.

Different concentrations of glucose were mixed with DNS and the solution was heated for exactly 10 min in a boiling water bath, cooled and 2 ml of water was added and mixed well, then the absorbance of the solution at 540 nm was measured.

Table 10. Invertase activity solubilised from *Arabidopsis* cell walls by different solutions.

| Solution | Enzyme activity (µmol/min/ml)* |
|---|---|
| 0.075 M NaCl/ 0.2 M MES | 0.0 |
| BCP in 0.075 M NaCl/ 0.2 M MES | 0.0 |
| 1 M NaCl/ 0.2 M MES | 0.0 |

*: The solutions were assayed for invertase activity as described in 2.2.13.2.3, the absorbance at 540 nm was measured and the glucose concentration was interpreted from the standard curve in Figure 28. Then the invertase activity was calculated as the amount of enzyme which produced 1 micromole of reducing sugar (expressed as invert sugar) per minute per ml under the conditions specified in this assay.

None of the extracts tested showed any invertase activity (Table 10) suggesting that all solutions used were not sufficient to solubilise invertase activity firmly bound to the cell walls or that all the invertase activity had been solubilised and washed away by water in the previous washing step.

Interestingly, BCP was highly effective in solubilisation of XET activity from the cell walls while low and high salt concentration solutions were not (Figure 29).

These results showed that the XAF of BCP had the unique ability to solubilise XET activity but no other tested wall enzymes from *Arabidopsis* cell walls. This suggested that there was a specific interaction of XAF to XTH proteins that helped XAF to solubilise XTH from their firmly bound sites on the cell walls. This will be further investigated in the next experiments throughout my thesis.

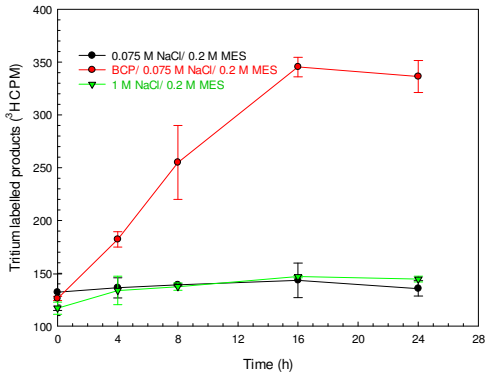


Figure 29. XET activity solubilised from *Arabidopsis* cell walls by different solutions.

*Arabidopsis* cells were incubated with NaCl/MES buffer, BCP in NaCl/MES buffer and 1 M NaCl/ 0.2 M MES for 30 min, sequentially. The supernatant obtained after centrifuging each incubation was assayed for XET activity.

## 3.3 XAF is a heavily-glycosylated protein

### 3.3.1 Investigation of molecular weight of XAF by dialysis

In this experiment, I aimed to test whether dialysis could eliminate salt contaminating a BCP without having any effect on its XTH-solubilisation activity, and to roughly estimate the molecular weight of XAF-active substances.

After 24 h of dialysis against water, salt concentrations in the samples were as low as water suggesting that salt was completely eliminated from samples (Table 11). BCP initially in water and in MES buffer had the same equivalent salt concentration after dialysis (Table 11) and produced the same XAF activity after 24 h dialysis against water in both kinds of dialysis tubing (Figure 30, Figure 31). These results indicated that MES was completely eliminated from the samples after 24 h dialysis.

Table 11. Salt concentration of BCP before and after dialysis against water

| Samples | Salt concentration (mM NaCl equivalent)* | | | | |
|---|---|---|---|---|---|
| | 12000-14000 MWCO tubing | | | 3500 MWCO tubing | |
| | BCP/ 0.2 M MES | BCP/ $H_2O$ | 0.2 M MES | BCP/ 0.2 M MES | 0.2 M MES |
| Before dialysis | 26.6 ± 1.7 | 9.9 ± 0.3 | 19.5 | 25.7 ± 0.6 | 19.5 |
| After dialysis for 1 h | 12.0 ± 0.2 | - | 3.4 | 7.5 ± 2.4 | 3.4 |
| After dialysis for 24 h | 1.0 ± 0.1 | 0.9 ± 0.1 | 0.4 ± 0.2 | 1.0 ± 0.1 | 0.4 ± 0.0 |

"-": Not tested

*: Each solution was measured for the conductivity before dialysis. The solution was split into 2-ml aliquots in a dialysis tubing and dialysed against water for 1 h or 24 h. The solution inside each tubing was measured again for conductivity. Then the NaCl-equivalent concentration of each solution was calculated from the standard curve in Figure 15. Some samples had more than one aliquots, so the mean and SE are both presented here; the others had only one aliquot and the only result is presented here.

BCP in MES buffer retained most of its XAF activity during the first hour but lost 63–65% after 24 h of dialysis against water in both kinds of dialysis tubing, with and without 0.25% BSA present at the XET assay stage (Figure 30, Figure 31). This suggested that there was a wide range of molecular weights of the XAF-active substances XAF: from less than 3500 to larger than 12000. However, more than 60% of the XAF activity was due to low molecular weight compounds (≤ 3500) which were lost during dialysis (Figure 31). Therefore, other techniques should be used to gain final conclusions about XAF's $M_r$.

The results also suggested that dialysis was not an ideal method to eliminate salt contaminating a BCP because it caused some loss of XAF activity.

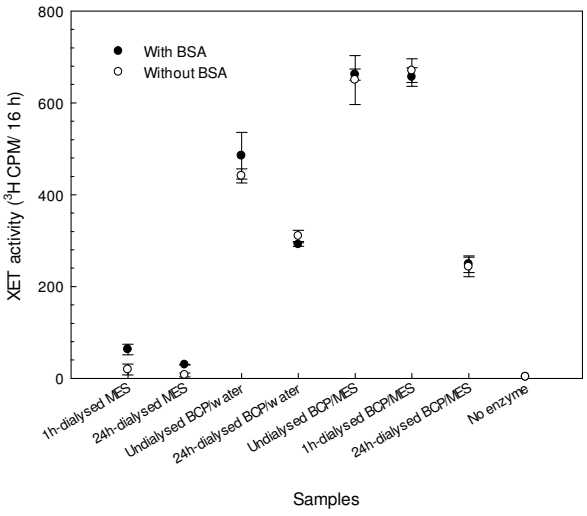


Figure 30. XAF activity of BCP after dialysis against water in 12000-14000 MWCO dialysis tubing.

BCP in MES or in water was split into 2-ml aliquots, and dialysed against 3 l water in dialysis tubing with MWCO 12000-14000 for 1 h or 24 h. After dialysis, all samples were adjusted to 3 ml with water, dried in the SpeedVac, re-dissolved in 3 ml NaCl/MES buffer and 66 µl of the resulting solution was used in an XAF assay. Black circles: With BSA (1 µl 10% BSA was added into the wells with 19 µl dialysed/ undialysed BCP-solubilised *Arabidopsis* XTHs), white circles: without BSA. Data show the mean of three determinations ± SE.

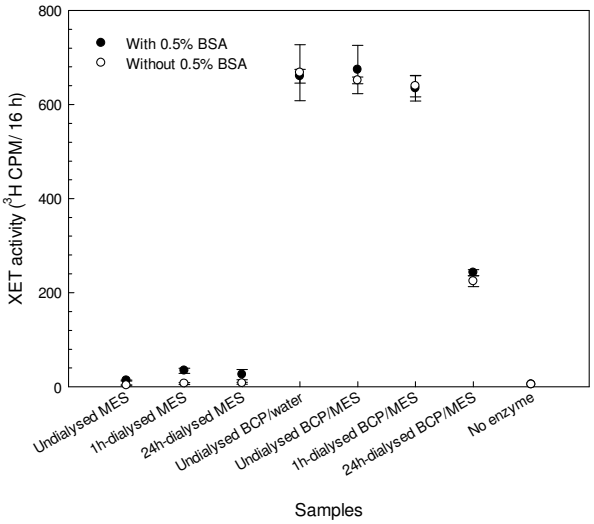


Figure 31. XAF activity of BCP after dialysis against water in 3500 MWCO dialysis tubing.

Other details as in Figure 30.

### 3.3.2 Partial purification and determination of the molecular weight of XAF by gel-permeation column chromatography

XAF could be partly purified from BCP for further analysis by the use of gel-permeation columns, either Bio-Gel P-2 or Sepharose CL-6B.

Through the Bio-Gel P-2 column, I obtained 2 peaks of $A_{280}$ (Figure 32). Most XAF activity was eluted at $V_0$, together with blue dextran (data not show) suggesting that the active XAF was a polymer with $M_r > 1800$.

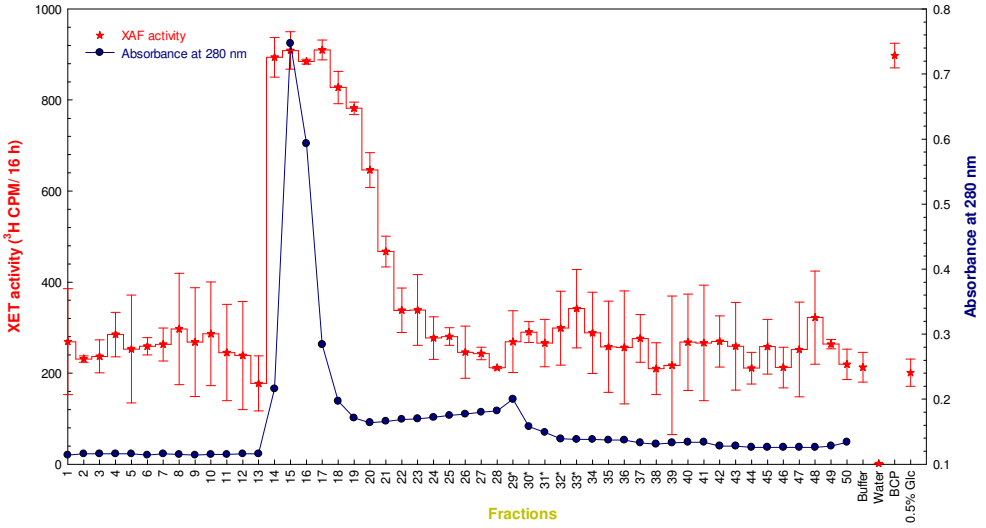


Figure 32. Absorbance at 280 nm and XAF activity of fractions of BCP after Bio-Gel P-2 column chromatography.

A mixture of 3.8 ml BCP in water, 0.1 ml 0.1% blue dextran, and 0.1 ml 0.5% glucose in PyAW 1:1:98 was applied onto a 100 ml bed-volume column and 50 fractions of 2 ml were collected with PyAW 1:1:98 as the eluent. Red line: XAF activity: each fraction was dried, washed with water and re-dissolved in NaCl/MES buffer for XAF assay, data show the mean of four determinations ± SE. Blue line: Absorbance at 280 nm. *: Fractions containing glucose, confirmed by Wilson's dip (data not show). The experiment was triplicated, with similar results (data not shown); one of them is presented here.

Through the Sepharose CL-6B column, I also obtained 2 peaks that absorbed at 280 nm; the first peak was exactly eluted together with blue dextran, the second peak was eluted just before the included volume (confirmed by glucose) (Figure 33). The main XAF activity was eluted from fraction 25 to 35 ($K_{av}$ 0.375-0.792) suggesting that the active XAF could be oligosaccharides or polysaccharides which had a wide range of molecular weight from 10000 to 100000. Because some of the last high XAF-activity fractions overlapped with the second peak of $A_{280}$, I pooled fractions 24 to 31 (Figure

33) as partially purified XAF-active fraction in the following analyses, including acid, alkaline and enzyme hydrolysis.

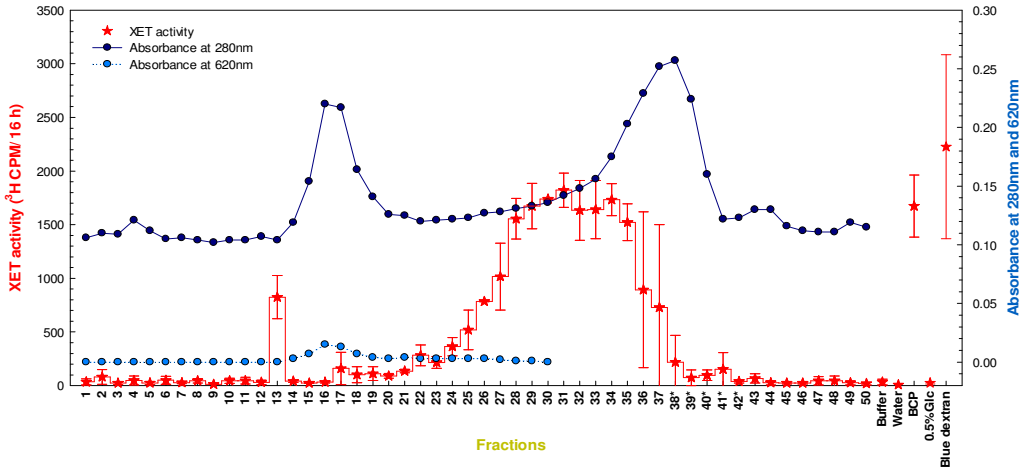


Figure 33. Absorbance at 280 nm and XAF activity of fractions of BCP after Sepharose CL-6B column chromatography.

$A_{620}$: Absorbance of blue dextran, other details as in Figure 32. Fractions 24 to 31 were pooled as partially purified XAF-active fraction for further analyses.

### 3.3.2.1 Acid hydrolysis of XAF-active fractions

#### 3.3.2.1.1 Hydrolysis with 2 M TFA at 100ºC

The XAF-active fractions from CL-6B column in Figure 33 were pooled, divided into 0.25-ml aliquots and incubated with 2 M TFA at 100ºC, over a time course. Theoretically, under this condition, neutral furanosyl bonds are completely hydrolysed while neutral pyranosyl bonds are gradually hydrolysed; thus, this method will give me an idea about the sidechain which is responsible for the XAF activity. For controls, 0.25 ml water was used in place of the TFA or the XAF-active pool. Half of each sample was dried in the SpeedVac, and half was precipitated by ethanol; both halves were assayed for XAF activity.

About half of the XAF activity was lost after 8 min in hot acid (Figure 34B). However, in case of using ethanol for precipitating TFA hydrolysis product, the acid-untreated

sample had no XAF activity suggesting that XAF could not be re-precipitated by ethanol; thus this method was not trusted (Figure 34A). Possibly a trace of salt was necessary for aiding ethanol-precipitation. I therefore used the SpeedVac method for obtaining XAF products after acid hydrolysis from now on. Nevertheless, the results showed that the XAF activity was susceptible to hot acid treatment. The XAF activity was gradually lost upon this treatment indicating that the pyranosyl bonds are responsible for the XAF activity.

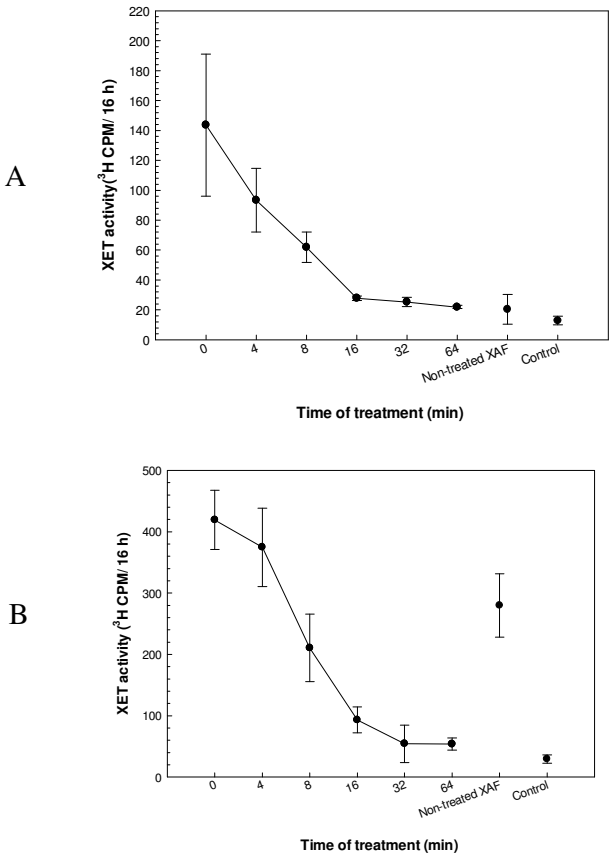


Figure 34. Loss of XAF after hot acid treatment

The partially purified XAF-active fractions were pooled from the Sepharose CL-6B column in *Figure 33*, divided into 0.25-ml aliquots and treated with 2 M TFA at 100ºC, over a time-course. After acid hydrolysis, half the sample (0.25 ml) was mixed with 1.25 ml 96% ethanol and 12.5 µl 10% ammonium formate and left in the cold room overnight, then centrifuged and the pellet was washed twice with 80% ethanol, re-dried and re-dissolved in NaCl/MES buffer for XAF assay (A). The other half was dried in the SpeedVac, re-dried from water and re-dissolved in NaCl/MES buffer for XAF assay (B). Non-treated XAF and control: water was used in place of TFA and the XAF-active fractions, respectively. Data show the mean of three determinations ± SE.

### 3.3.2.1.2 0.1 M TFA at 85°C

The XAF-active fractions from the Sepharose CL-6B column in Figure 33 were pooled, divided into 125-µl aliquots and incubated with 0.1 M TFA at 85ºC, over a time course. After 64 min of treatment, XAF activity still remained (Figure 35), suggesting that XAF was stable to mild acid treatment. Thin-layer chromatography of the XAF-active fractions after hydrolysis showed that Ara was released from it after 16 min of treatment by 0.1 M TFA at 85ºC and after 4 min of treatment by 2 M TFA at 100ºC. Gal and GalA were released from the XAF-active fractions after being treated by 2 M TFA at 100ºC for 32 min but not by 0.1 M TFA at 85ºC, even after 64 min (Figure 36). In order to look for more details on the glycosidic bonds of XAF, I demonstrated how a pyranosyl and furanosyl backbone was broken down under the conditions of acid hydrolysis used above. Furanose-linked arabino-octaose ($Ara_{\underline{f}8}$) and pyranose-linked xylo-hexaose ($Xyl_{\underline{p}6}$), both 0.2%, were treated with TFA under the same conditions as used for hydrolysis of XAF.

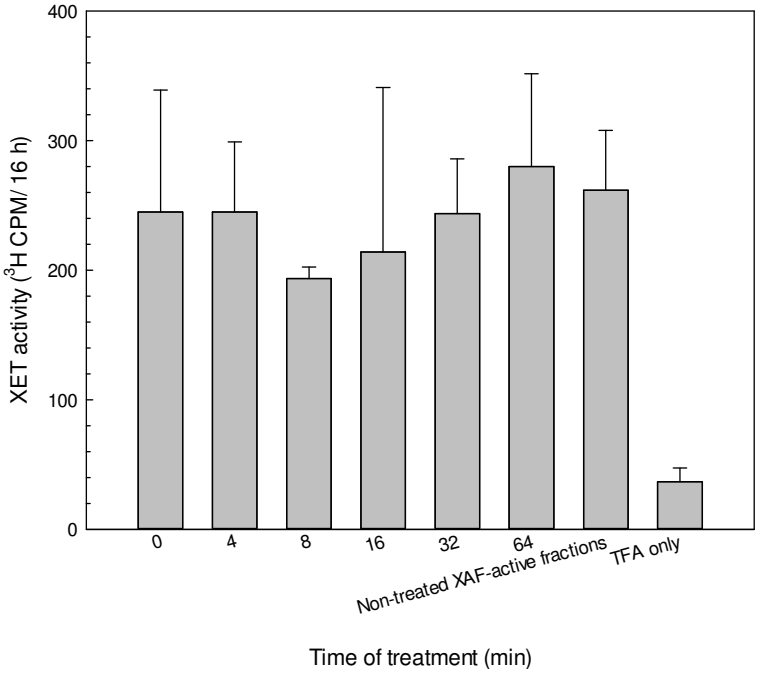


Figure 35. XAF activity of XAF-active fractions after the treatment with 0.1 M TFA at $85^0$C.

The XAF-active fractions from the Sepharose CL-6B column (Figure 33) were pooled, divided into 125-µl aliquots and incubated with 0.1 M TFA at 85ºC, over a time course. Water (125 µl) was used in place of acid (non-treated XAF-active fractions) and XAF-active fractions (T: TFA only) for controls. The tubes were cooled on ice, dried in the SpeedVac, re-dried twice from water and re-dissolved in 250 µl water. Of that, 200 µl was re-dried in the SpeedVac and re-dissolved in 200 µl NaCl/MES buffer and 66 µl of it was used for XAF assay. Data show the mean of three determinations ± SE.

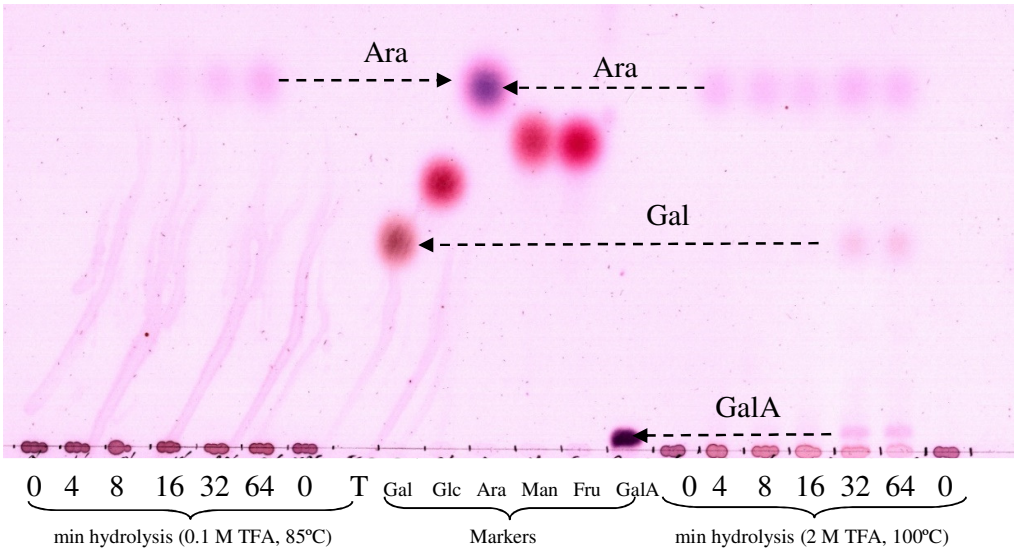


Figure 36. Thin-layer chromatography of TFA-hydrolysate of the XAF-active fractions.

The XAF-active fractions from the Sepharose CL-6B column (125 µl) in Figure 33 was hydrolysed by A, 0.1 M TFA at 85ºC; B, 2 M TFA at 100ºC, over a time course. Water (125 µl) was used in place of acid (0: non-treated XAF-active fractions) and XAF-active fractions (T: TFA only) for controls. After acid hydrolysis, TFA was removed in a SpeedVac, and 2.4% of the sample was loaded onto a TLC plate. Solvent: EPyAW 6:3:1:1, thymol staining. The experiment was repeated, with similar results and one of them is present.

On treatment with 2 M TFA at 100ºC, $Xyl_{\underline{p}6}$ was broken down to smaller oligosaccharides after 4, 8 and 16 min, and completely hydrolysed to Xyl after 32 min. In contrast, $Ara_{\underline{f}8}$ was completely broken down to Ara after 4 min of treatment (Figure 37). Treatment with 0.1 M TFA, 85ºC, $Xyl_{\underline{p}6}$ was gradually slowly broken down to $Xyl_4$, $Xyl_3$, $Xyl_2$, and Xyl after 8, 16, 32, and 64 min, respectively. At min 64 of treatment, hydrolysis products of $Xyl_{\underline{p}6}$ included all the four xylose oligosaccharides ($Xyl_2$ to $Xyl_5$) and Xyl and some remaining $Xyl_{\underline{p}6}$ showing that this hydrolysis reaction was not complete (Figure 38). In a contrast, $Ara_{\underline{f}8}$ was quickly digested to seven arabinose oligosaccharides within 4 min and was completely broken down Ara by 64 min of treatment (Figure 38).

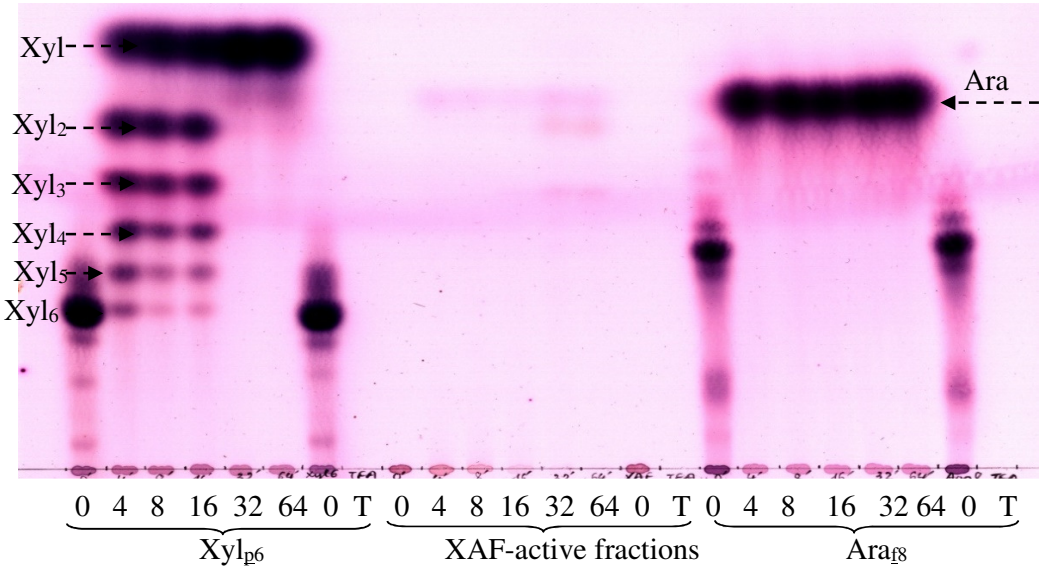


Figure 37. Thin-layer chromatography of 2 M TFA-hydrolysate of XAF-active fractions, $Xyl_{p6}$, and $Ara_{f8}$.

The XAF-active fractions from the Sepharose CL-6B column in Figure 33 (125 µl), $Xyl_{p6}$ (25 µl), $Ara_{f8}$ (25 µl) was hydrolysed by 2 M TFA at 100ºC, over a time course. Water was used in place acid (0: non-treated XAF-active fractions) and XAF-active fractions, $Xyl_{p6}$, or $Ara_{f8}$ (T: TFA only) for controls. After acid hydrolysis, TFA was removed in a SpeedVac; and 2.4% of the hydrolysates of XAF-active fractions, 20% of hydrolysates of $Xyl_{p6}$ or $Ara_{f8}$ was loaded onto a TLC plate. Solvent: BAW: 2:1:1, thymol staining.

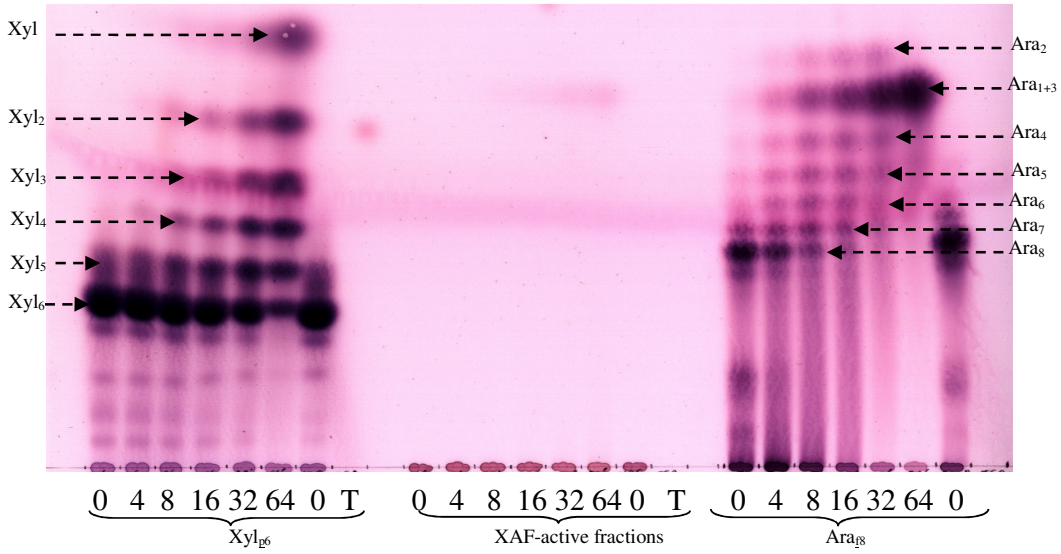


Figure 38. Thin-layer chromatography of 0.1 M TFA-hydrolysate of XAF-active fractions, $Xyl_{p6}$, and $Ara_{f8}$.

The XAF-active fractions from the Sepharose CL-6B column in Figure 33 (125 µl), $Xyl_{p6}$ (25 µl), $Ara_{f8}$ (25 µl) was hydrolysed by 0.1 M TFA at 85ºC, over a time course. Other details as in Figure 37.

From this demonstration, I confirmed that furanosyl bonds were more susceptible to acid hydrolysis than pyranosyl. Also, the treatment of the XAF-active fractions with 0.1 M TFA at 85ºC resulted in Ara from min 16 (Figure 36, Figure 38) but the XAF activity did not reduce even after 64 min (Figure 35) indicating that furanosyl sidechains were not essential for XAF activity. In contrast, Gal was released after 32 min on the treatment of XAF-active fractions with 2 M TFA at 100ºC (Figure 36, Figure 37) and resulted in the loss of most XAF activity (Figure 34A), suggesting that XAF may have a pyranosyl backbone which was essential for its activity.

#### 3.3.2.1.3 Complete acid hydrolysis of fractions of BCP after Sepharose CL-6B column chromatography

In order to discover the main monosaccharide and amino acid components of XAF that are responsible for its activity, I treated fractions of BCP after CL-6B column chromatography (Figure 39) under severe acid hydrolysis conditions.

Acid hydrolysis released many monosaccharides from fractions 21 to 42 (corresponding to the peak in XAF activity), including Xyl, Ara, Man, Glc, Gal, GlcA, GalA and probably an aldobiouronic acid (for example GlcA-Gal and GlcA-Xyl) (Figure 40). This suggested the presence of some potential polysaccharides in XAF, for example arabinogalactan, xyloglucan and mannan. BCP also released many amino acids, including Asp, Gly, Glu, Ala, Tyr and Leu (Figure 40) in the same peak of XAF activity, together with those monosaccharides, suggesting the presence of glycoproteins or proteins that were responsible for XAF activity.

There were some free sugars (Figure 42) and amino acids (Figure 43) in the late fractions that were eluted in the included volume, indicating that the BCP still contained some low molecular weight compounds (Glc, Fru, Suc and traces of some amino acids) that were not completely precipitated by ethanol. This suggested that I needed a better washing procedure to remove all low molecular compounds from BCP.

Therefore, I prepared a better ethanol-washed BCP (tested by TLC to confirm that no low molecular weight compounds were left; data not shown) and passed it through another CL-6B column (Figure 44). The fractions were collected and paired, and treated with 2 M TFA at 120ºC for 60 min. This TFA treatment completely destroyed

XAF activity of the XAF peak after 60 min treatment (Figure 45). An HPLC profile showed an abundance of Ara, Gal, Glc and Xyl residues in the peak of XAF activity after acid hydrolysis (Figure 46). This result agreed with the TLC profile (Figure 40).

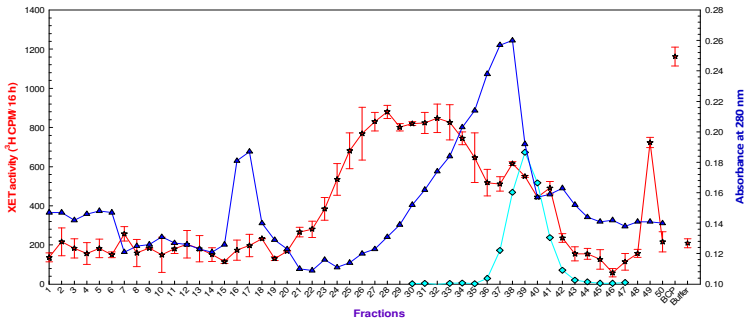


Figure 39. UV-Absorbance and XAF activity of fractions of BCP after Sepharose CL-6B column chromatography.

A mixture of 4 ml BCP and 40.5 µl [$^{14}$C]Glc (0.3 kBq) as an internal marker in PyAW 1:1:98 was applied onto a 100-ml-bed-volume CL-6B column and 50 fractions of 1.8 ml were collected with PyAW 1:1:98 as the eluent, measured the absorbance at 280 nm (blue line). Each fraction was dried of solvent in the SpeedVac, washed with water, and re-dissolved in 760 µl water. Of that, 132 µl was dried and re-dissolved in 132 µl NaCl/MES buffer for XAF assay, data show the mean of two determinations ± SE (red line). An additional 50 µl of each fraction in water was counted for [$^{14}$C]Glc (cyan line). The experiment was repeated, with similar results (data not shown).

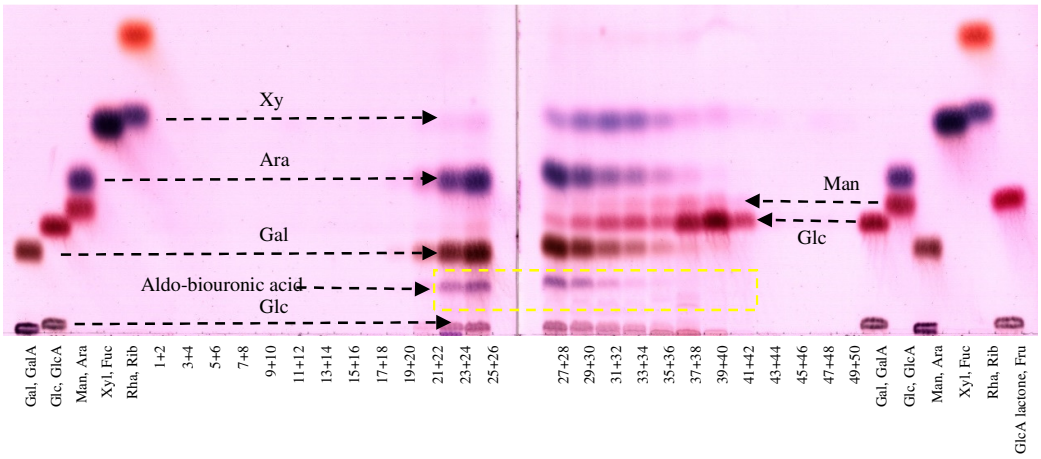


Figure 40. Thin-layer chromatography of TFA-hydrolysates of fractions of BCP after Sepharose CL-6B column chromatography.

After CL-6B column chromatography (Figure 39), dried fractions were re-dissolved in 760 µl of water. Pairs of fractions (250 µl each) were pooled and hydrolysed with 2 M TFA, 120ºC for 60 min, dried in the SpeedVac and re-dissolved in 30 µl of water. Of that, 3 µl was loaded onto the TLC plate. Solvent: EPyAW: 6:3:3:1, thymol staining. 1+2: pool of fraction 1 and 2, 3+4: pool of fraction 3 and 4..., 49+50: pool of fraction 49 and 50.

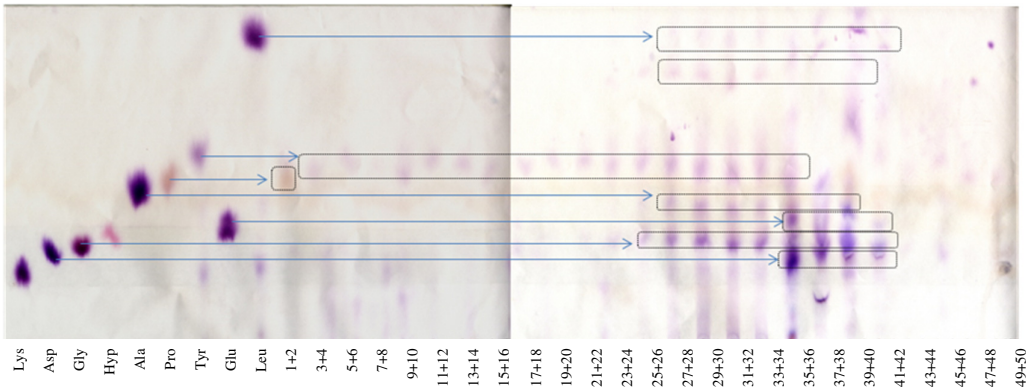


Figure 41. Paper chromatography of TFA-hydrolysates of fractions of BCP after Sepharose CL-6B column chromatography.

After CL-6B column chromatography (Figure 39), dried fractions were re-dissolved in 760 µl of water. Pairs of fraction (250 ml each) were pooled and hydrolysed with 2 M TFA, 120ºC for 60 min, dried in the SpeedVac and re-dissolved in 30 µl of water; and 5 µl of that was loaded for paper chromatograph. Solvent: BAW: 12:3:5, ninhydrin staining. Other details as in Figure 40.

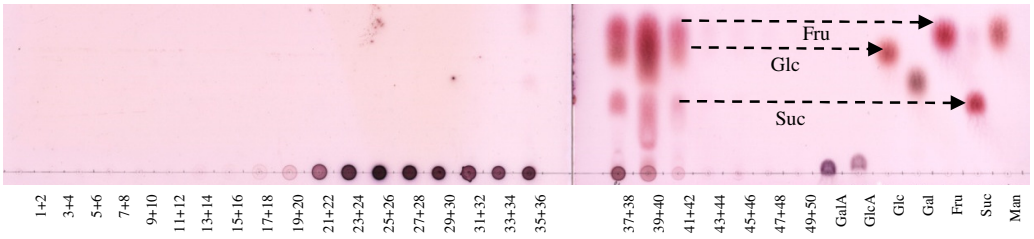


Figure 42. Thin-layer chromatography of fractions of BCP after Sepharose CL-6B column chromatography.

After CL-6B column chromatography (Figure 39), 84 µl of each fraction was paired, dried of solvent in the SpeedVac, and re-dissolved in 10 µl water. Of that, 3 µl was loaded onto the TLC plate. Solvent: EPyAW: 6:3:3:1, thymol staining. Other details as in Figure 40.

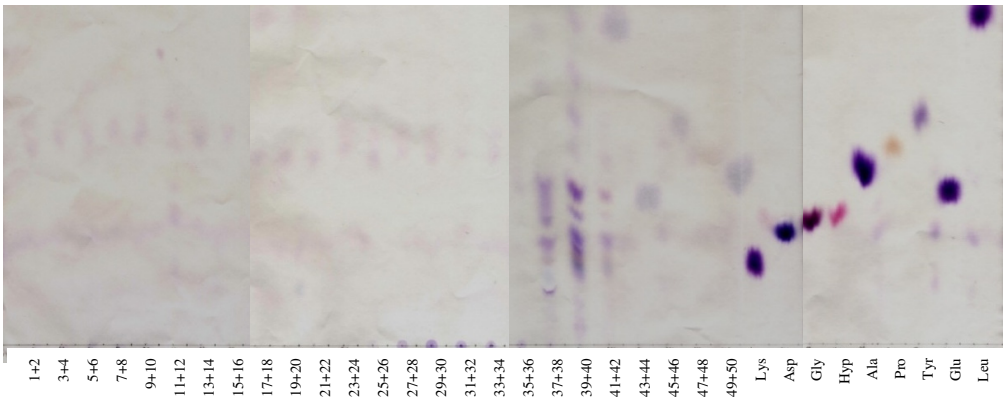


Figure 43. Paper chromatography of fractions of BCP after Sepharose CL-6B column chromatography.

After CL-6B column chromatography (Figure 39), 84 µl of each fraction was paired, dried of solvent in the SpeedVac, re-dissolved in 10 µl water and 5 µl of that was loaded for paper chromatography. Solvent: BAW: 12:3:5, ninhydrin staining. Other details as in Figure 40.

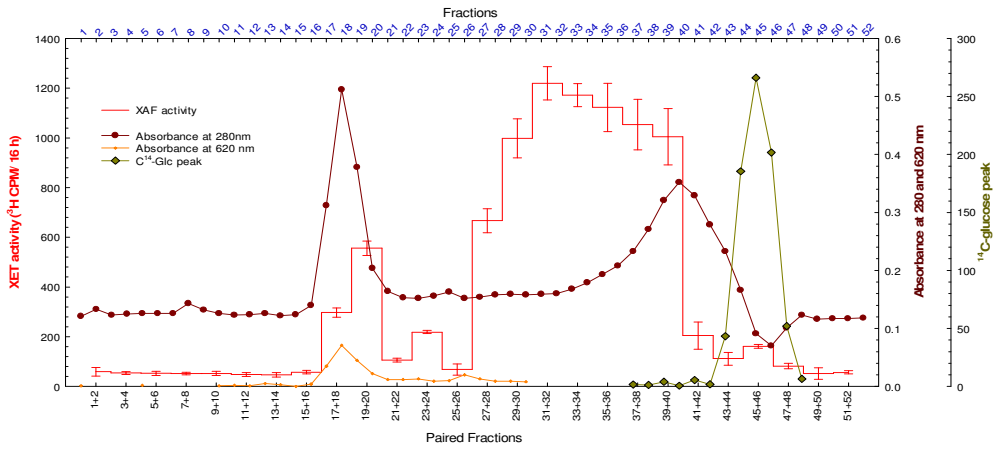


Figure 44. Absorbance and XAF activity of fractions of the better ethanol-washed BCP after Sepharose CL-6B column chromatography.

BCP was prepared as routine and the ethanol-precipitated pellet was carefully washed (7 times) with 96% ethanol, dried until no ethanol smell remained and re-dissolved in water. A portion of each fraction was loaded onto a TLC plate to confirm that there were no free sugars left (data not shown). A mixture of 10 ml of this BCP (2 mg/ml), 1 ml blue dextran, and 100 µl [$^{14}$C]Glc was applied onto a 220-ml-bed volume CL-6B column and 6-ml fractions were collected with PyAW 1:1:98 as the eluent. The fractions were measured for the absorbance at 280 nm (for the phenolic compounds) and 620 nm (for peak of blue dextran) (brown and orange line, respectively). Each fraction was dried of solvent in the SpeedVac, re-dried from water, and re-dissolved in 2 ml water; and 50 µl of that was counted for [$^{14}$C]Glc peak (green line). Pairs of fractions (75 µl each) were pooled, dried, and re-dissolved in 150 µl NaCl/MES buffer for XAF assay, data show the mean of two determinations ± SE (red line). The experiment was repeated, with similar results (data not shown).

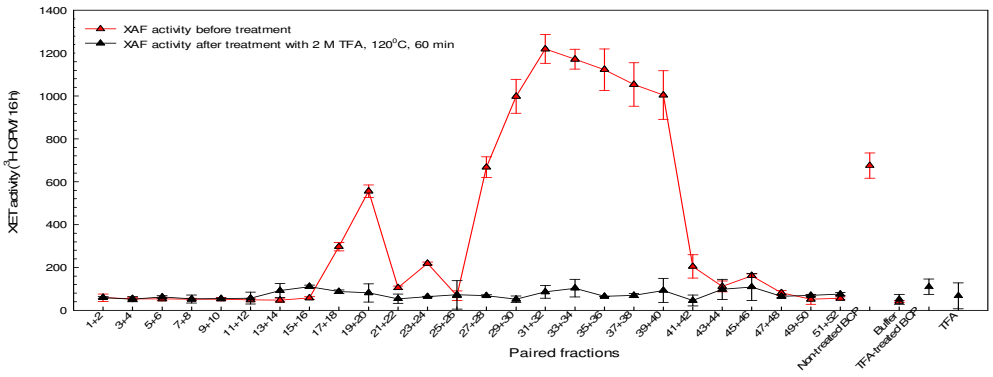


Figure 45. XAF activity of paired fractions of BCP after Sepharose CL-6B column chromatography before and after TFA hydrolysis.

Pairs of fractions (250 µl each) in Figure 44 were pooled and treated with 2 M TFA, 120ºC for 60 min. After the treatment, TFA was removed by drying in the SpeedVac and the sample was re-dissolved in 1ml water. Of that, 150 µl was dried in the SpeedVac and re-dissolved in 150 µl NaCl/MES buffer for XAF assay (black line). At the same time, pairs of fractions (75 µl each) was also dried in the SpeedVac and re-dissolved in NaCl/MES buffer for XAF assay (black line). Data show the mean of two determinations ± SE. Other details as in Figure 44.

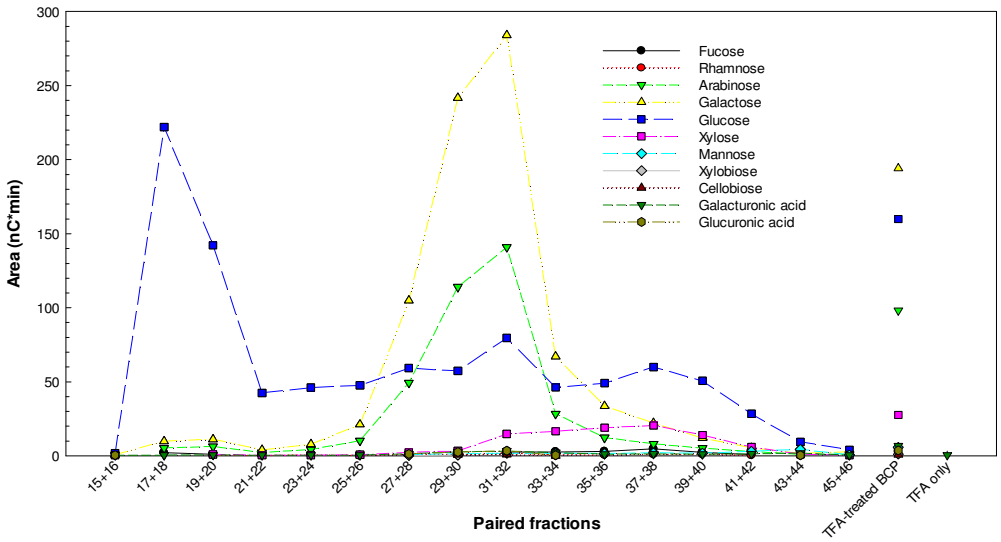


Figure 46. Sugar composition of TFA-hydrolysates of fractions of BCP after Sepharose CL-6B column chromatography.

Paired fractions from CL-6B column in Figure 44 were treated with 2 M TFA at 120ºC for 60 min. After re-dissolving in 1 ml water, 850 µl of the samples were dried in the SpeedVac, re-dissolved in 30 µl water and 16.7% of that were analysed by HPLC.

In conclusion, partially purified XAF was stable to mild acid treatment (Figure 35) but was destroyed after 60 min treatment with severe acid treatment (Figure 34), suggesting that a pyranosyl backbone was responsible for the XAF activity. Thus, some proteins or glycoproteins which have polysaccharide chains of arabinogalactan, xyloglucan or mannan may contribute for the XAF activity.

### 3.3.2.2 Alkaline hydrolysis of the XAF-active fractions

The XAF-active fractions from the CL-6B column in Figure 33 were pooled and treated with 0.47 M NaOH at room temperature, over a time course. After 8 h treatment, it still retained most XAF activity (Figure 47) indicating that XAF was stable to alkaline treatment, suggesting that XAF did not have ester bonds necessary for its activity.

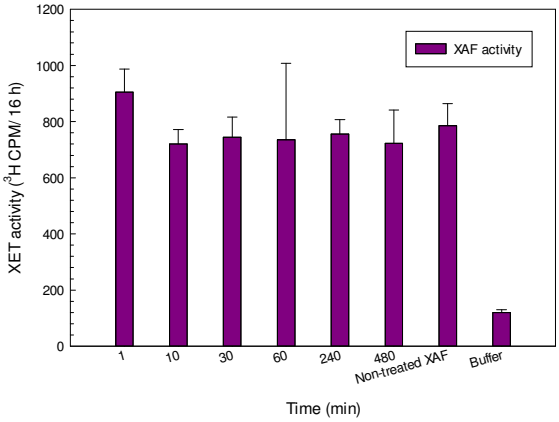


Figure 47. XAF activity of the XAF-active fractions of BCP after being treated with alkaline.

The XAF-active fractions (fractions 24 to 31 from the Sepharose CL-6B column in Figure 33) were pooled, and 250 µl of it was treated with 0.48 M NaOH at room temperature, over a time course. The reactions were stopped by the addition of acetic acid to a final concentration of 0.89 M. The hydrolysates were precipitated with ethanol (which left the sodium acetate in solution), re-dissolved in 0.25 ml NaCl/MES buffer for XAF assay. Non-treated XAF: acetic acid was added to the XAF-active fractions before adding NaOH, buffer: water instead of XAF-active fractions; both were incubated for 480 min. Data show the mean of four determinations ± SE.

### 3.3.2.3 Enzyme digestions

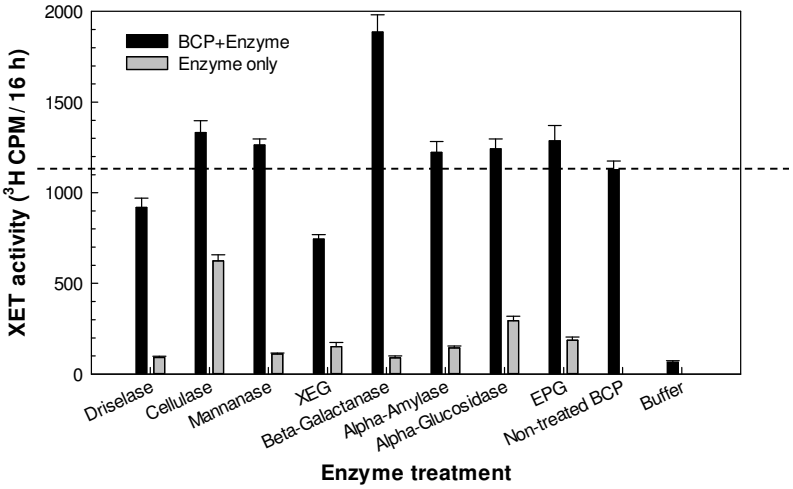


Figure 48. XAF activity of BCP after being treated with different enzymes.

Aliquots of BCP (0.4 mg) were incubated with 300 µl 0.0003% Driselase, 0.017 U/µl cellulase, 0.017 U/µl mannanase, 0.083 mg/ml XEG, 0.0013 U/µl β-galactanase, 0.017 U/µl amylase, 0.017 U/µl α-glucosidase or 0.017 U/µl EPG, all made in PyAW 1:1:98, for 24 h. Water was used in place of BCP for enzyme only, and buffer was used in place of enzyme for non-treated BCP. The reactions were stopped by heating to 120ºC for 1 h and the samples were centrifuged. Supernatants were collected, dried in the SpeedVac, re-dissolved in 200 µl NaCl/MES buffer and assayed XAF activity. Data show the means of six determinations ± SE.

Results in 3.3.2.1.3 revealed the presence of some polysaccharides in BCP that may be responsible for the XAF activity. Thus in this experiment, I treated BCP with a wide range of enzymes capable of cleaving polysaccharides to elucidate whether any of these polysaccharides were responsible for the XAF activity.

Among all enzymes tested, Driselase and XEG partly reduced XAF activity while the other enzymes did not. Curiously, cellulase appeared to have its own XAF activity. Interestingly, treatment with β-galactanase significantly increased the XAF activity of BCP (Figure 48). Further experiments were conducted to yield a better understanding of the effects of each enzyme on the XAF.

#### 3.3.2.3.1 α-Amylase, β-galactanase and α-glucosidase digestion

I treated BCP with α-amylase, β-galactanase and α-glucosidase again, considering not only the XAF activity but also the monosaccharides profile after treatment.

Although α-amylase digested BCP, resulting in several malto-oligosaccharides (Figure 50), it did not destroy the XAF activity of BCP (Figure 49) suggesting that the starch present in BCP did not contribute to the XAF activity.

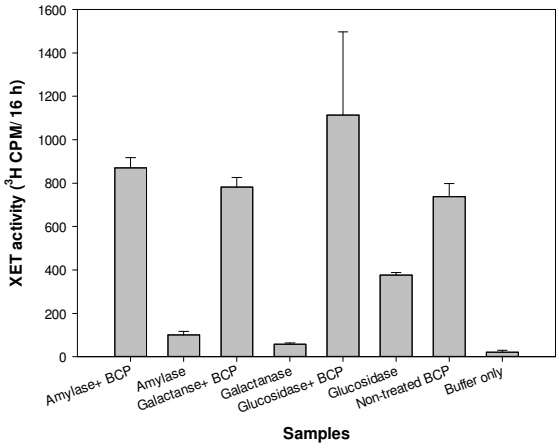


Figure 49. XAF activity of α-amylase, β-galactanase, α-glucosidase digests of BCP.

BCP (0.4 mg) was incubated with 300 µl of 0.0013 U/µl β-galactanase in PyA, pH 5.6 (0.15% (v/v) acetic acid and 0.55% (v/v) pyridine) at 55°C for 4 h; 0.017 U/µl amylase in PyAW 1:1:98, room temperature for 24 h; or 0.017 U/µl α-glucosidase in PyAW 1:1:98, room temperature for 24 h. Non-treated BCP: buffer was used in place of enzyme, data show the average value of BCP in PyAW 1:1:98 and BCP in PyA, pH 5.6. Amylase, galactanase, glucosidase: water was used in place of BCP. The reactions were stopped by heating to 120ºC, 70 min. The solutions were centrifuged and the supernatants were dried in the SpeedVac, re-dried from water, and re-dissolved in NaCl/MES buffer for XAF assay. Data show the means of four determinations ± SE.

β-Galactanase partially digested BCP, resulting in Gal (tentative identification). The products also included several oligosaccharides that co-migrated with cellulose oligosaccharides and xyloglucan oligosaccharides (Figure 50), suggesting that β-galactanase was not working only with its intended activity and that it was contaminated with other activities. However, these activities did not destroy XAF activity of BCP (Figure 49), so their substrates presenting in BCP were not responsible for the XAF activity. A better β-galactanase which could digest β-1,3-1,6-galactan was necessary for studying on the XAF activity of AGPs; unfortunately, there was not any such commercial enzyme available.

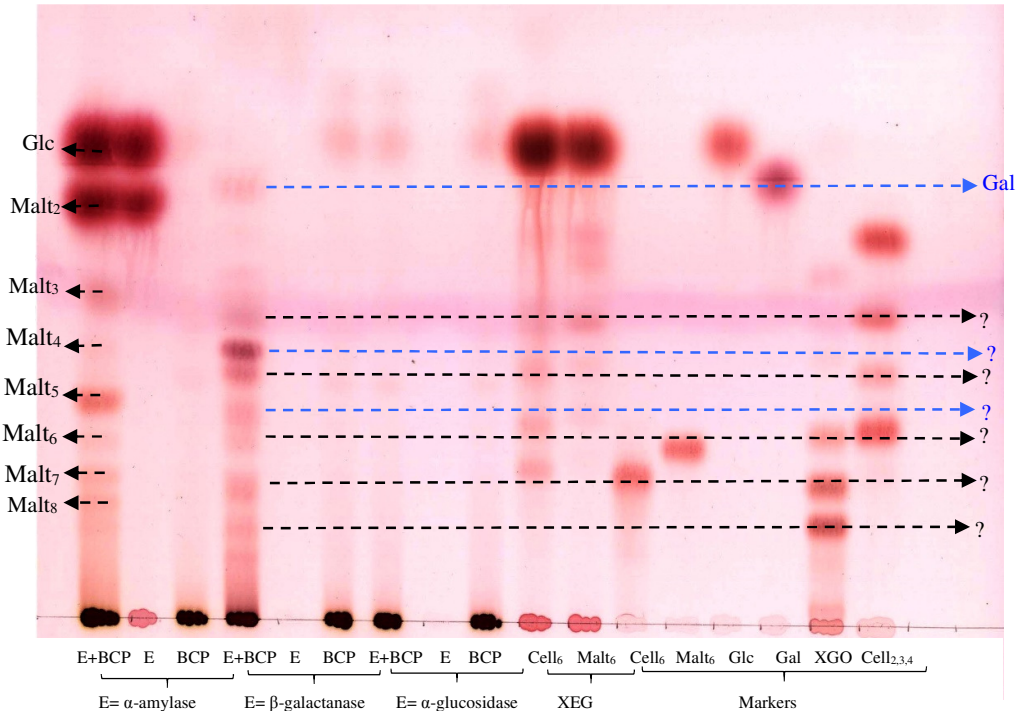


Figure 50. Thin-layer chromatography of α-amylase, β-galactanase and α-glucosidase digests of BCP.

After enzyme treatments (details as in Figure 49), 8.3% of the products were loaded onto a TLC plate. Solvent: BAW 2:1:1, thymol staining. ?: Unknown sugars.

Monosaccharide profiles resulting from α-glucosidase-treated BCP and non-treated BCP were identical, suggesting that this enzyme was inactive in this experiment (Figure 50). Not surprisingly, therefore, the XAF activity of BCP did not change after α-glucosidase treatment (Figure 49). Thus, the experiment on glucosidase needed to be repeated under better conditions.

### 3.3.2.3.2 Cellulase digestion

I treated paired fractions from the CL-6B column in Figure 44 and BCP with cellulase (the one does not digest XyG) and analysed the products by TLC and HPLC. Cellulase digested all fractions from the CL-6B column and BCP, resulting in Glc, an unknown sugar in paired fraction 29+30 and another unknown sugar in paired fraction 43+44 (Figure 50). Although cellulase activity was working under these conditions, it did not reduce either XAF activity of BCP (Figure 48, Figure 52) or paired fractions from CL-6B column (Figure 52). This result suggested that β-glucan and glucomannan did not contribute to XAF activity. Cellulase digested BCP and some paired fractions, yielding Glc (Figure 53) and some XGOs (Figure 51) revealing that the cellulase was contaminated with XEG activity, although I have used the cellulase that supposed to not digest XyG.

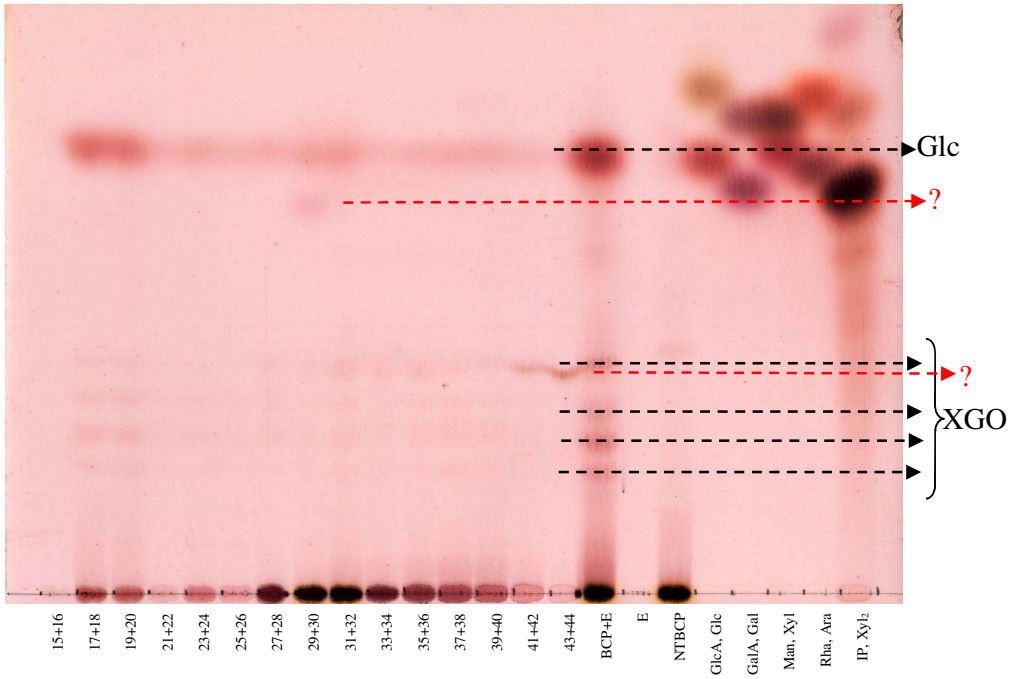


Figure 51. Thin-layer chromatography of cellulase digests of paired fractions from CL-6B column and BCP.

Pairs of fraction from the CL-6B column in Figure 44 (200 µl) were digested with 0.017 U/µl cellulase in PyAW 1:1:98 in a final volume of 300 µl for 24 h at room temperature. Water was used in place of BCP for cellulase only and buffer was used in place of enzyme for non-treated BCP. The reactions were stopped by heating to 120°C for 1 h and the samples were centrifuged. Half of the supernatant (150 µl) was dried in the SpeedVac and re-dissolved in 9 µl water and 33.3% of the sample was loaded onto a TLC plate. Solvent: BAW 2:1:1, thymol staining. E: Cellulase, NTBCP: Non-treated BCP. Red arrow: Unknown sugars. Other details as in Figure 44.

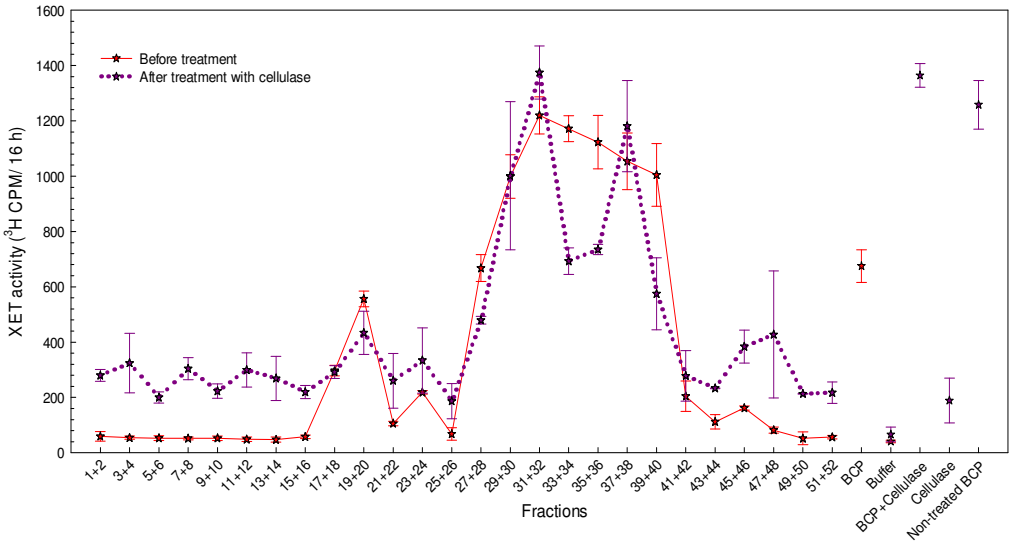


Figure 52. XAF activity of cellulase digests of pair fractions from CL-6B column.

The paired fractions from the CL-6B column in Figure 44 and BCP were treated with cellulase under the same conditions as in Figure 48 (details as in Figure 51). After centrifugation, the other half of the supernatant (150 µl) was dried in the SpeedVac, re-dissolved in 150 µl NaCl/MES buffer for XAF assay. Data show the means of two determinations ± SE. The XAF assay of paired fractions and BCP before treatment with cellulase was done separately and plot on the same graph for the comparison.

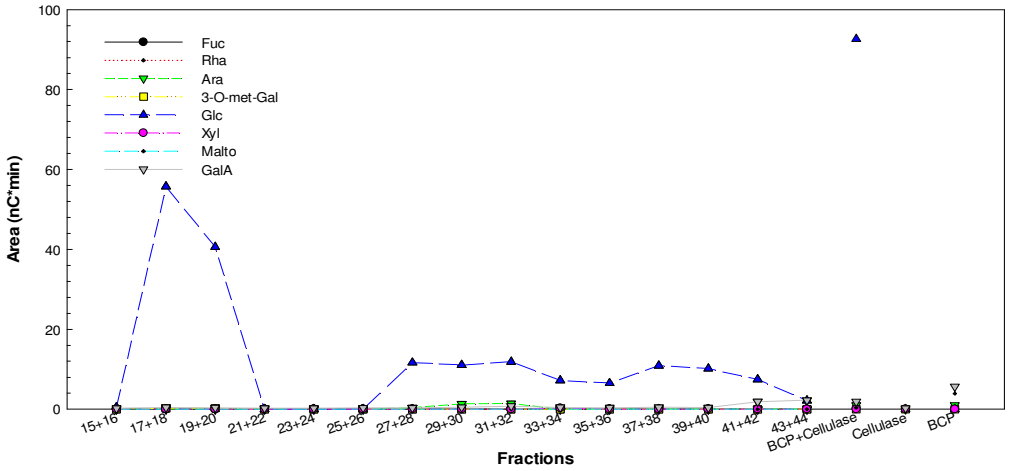


Figure 53. Sugar composition of cellulase digests of BCP and paired fractions from a CL-6B column.

The paired fractions from the CL-6B column in Figure 44 and BCP were treated with cellulase under the same conditions as in Figure 14 (details as in Figure 17). From the half of the supernatant that was re-dissolved in 9 µl water, 55.6% was analysed by HPLC.

#### 3.3.2.3.3 Mannanase, endo-polygalacturonase and α-glucosidase digestion

The result in Figure 48 showed that mannanase, endo-polygalacturonase (EPG) and α-glucosidase did not change the XAF activity of BCP. To make sure that those enzymes were still active but could not digest XAF, I tested mannanase, α-glucosidase and EPG on their specific substrates including manno-hexaose ($Man_6$), malto-hexaose ($Malt_6$), and polygalacturonic acid (PGA), respectively and looked for their specific products on a TLC.

Under the same conditions as in 3.3.2.3, EPG digested PGA, resulting in GalA, GalA2, GalA3 (Figure 54) proving that EPG was active. The TLC pattern of non-treated PGA indicated that PGA was of different degrees of polymerisation and all of them were digested by EPG in this experiment. The fact that it did not reduce XAF activity of BCP (Figure 48) suggested that PGA or pectin was not responsible for XAF activity.

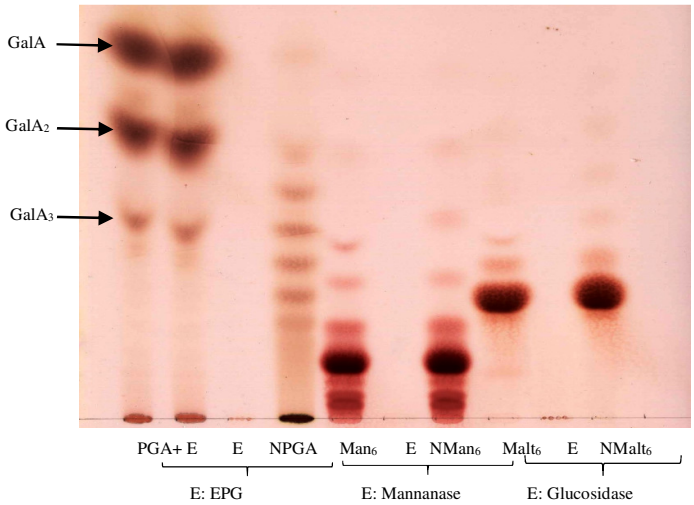


Figure 54. Thin-layer chromatography of EPG, mannanase and α-glucosidase digests of their specific substrates.

PGA, $Man_6$, or $Malt_6$ was dissolved in water as a concentration of 1 mg/ml and 40 µl of each was incubated with 20 µl EPG, mannanase, and α-glucosidase, all 0.05 U/µl in PyAW 1:1:98, respectively at room temperature for 24 h. The final concentration of each enzyme was thus a third during enzyme reaction. The reactions were stopped by heating to 120ºC for 70 min and the reaction mixtures were centrifuged, and the supernatants were dried in the SpeedVac, re-dissolved in 2 µl water and loaded onto a TLC plate. NPGA: non-treated PGA; $Man_6$: $Man_6$ + mannanase, $NMan_6$: non-treated $Man_6$; $Malt_6$: $Malt_6$ + α-glucosidase, $NMalt_6$: Non-treated $Malt_6$. Solvent: BAW 2:1:1, thymol staining. The reaction of PGA and EPG was done twice, the two results are presented.

Both mannanase and α-glucosidase did not digest their specific substrates (Figure 54) suggesting that the reaction conditions were not suitable for their intended activities. Thus, I optimized these conditions in following experiments.

In the experiment in Figure 54, I prepared mannanase and α-glucosidase in PyAW 1:1:98, pH 4.7 and they did not show their activities. Thus, I tested different buffers.

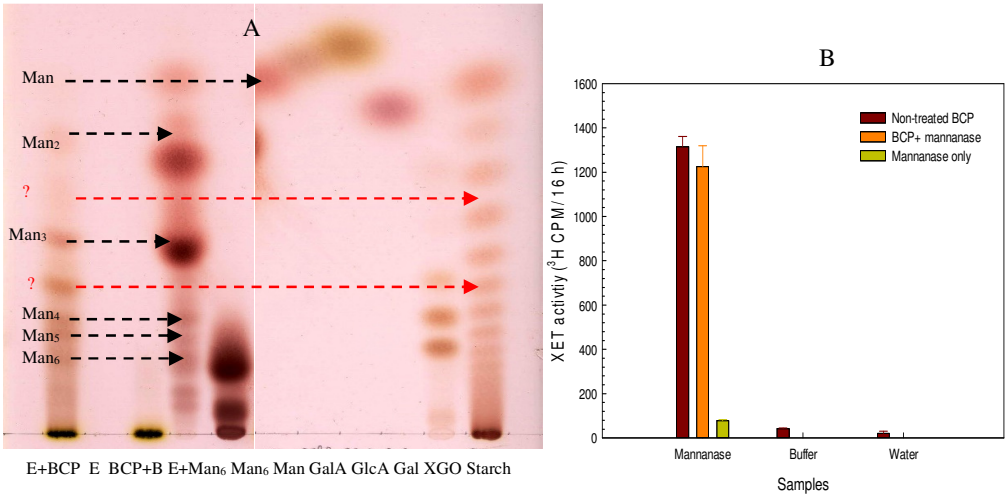


Figure 55. Thin-layer chromatography and XAF activity of mannanase digests of BCP.

A, BCP (0.4 mg) was incubated with 0.017 U/µl mannanase in 50 mM ammonium acetate, pH 8.8 for 24 h in a final volume of 300 µl. The reaction was stopped by the addition of 100 µl formic acid, and the reaction mixtures were centrifuged and half of the supernatant was dried in the SpeedVac, re-dissolved in 4 µl water and 2 µl of it was loaded onto a TLC plate. Solvent: BAW 2:1:1, thymol staining. E: mannanase, B: buffer. Red arrow: Unknown oligosaccharides. B, The other half was dried in the SpeedVac, re-dissolved in 100 µl NaCl/MES for XAF assay. Data show the means of two determinations ± SE.

After testing several buffers (data not show), I discovered that 0.05 M ammonium acetate, pH 8.8 was the most suitable for mannanase activity. Thus, I treated BCP with mannanase prepared in this buffer at a final concentration of 0.0167 U/µl. Under these conditions, mannanase digested $Man_6$ and BCP, resulting in a range of manno-oligosaccharides and Man in case of $Man_6$ (Figure 55A) but did not change the XAF activity of BCP (Figure 55B). This result indicated that mannan was not responsible for XAF activity. The mannanase digests of BCP also contained some unknown oligosaccharides (Figure 55A), probably from glucomannan or galactomannan, which are legitimately digested by mannanase.

I did an extra experiment showing the optimum conditions for α-glucosidase action were the final concentration: 0.0167 U/µl, buffer: 1% lutidin/0.3% acetic acid, pH 6.66 and the incubation time: 48 h (data not show). Under these conditions, α-glucosidase digested $Malt_6$, maltose and BCP, resulting in Glc (Figure 56A). However, it did not destroy XAF activity of BCP (Figure 56B), suggesting that starch and other terminal α-Glc residues did not contribute to XAF activity.

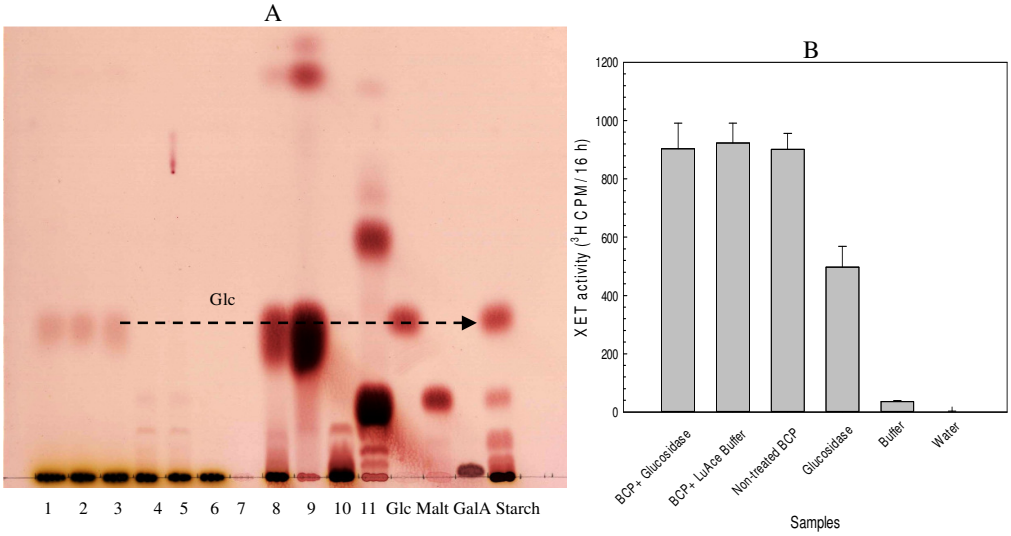


Figure 56. Thin-layer chromatography and XAF activity of α-glucosidase digests of BCP.

A, BCP (0.4 mg) was incubated with 0.017 U/µl α-glucosidase in 1% lutidine/0.3% acetic buffer, pH 6.66 at room temperature for 48 h in a final volume of 300 µl. The reaction was stopped by the addition of 100 µl formic acid, and the reaction mixtures were centrifuged, and a half of the supernatant was dried in the SpeedVac, re-dissolved in 4 µl water and 2 µl of that was loaded onto the TLC plate. Solvent: EPAW 6:3:1:1, thymol staining. 1, 2, 3: BCP+glucosidase, 4, 5: BCP+buffer, 6: Non-treated BCP, 7: glusosidase only, 8: $Malt_6$+glucosidase, 9: Maltose+glucosidase, 10: $Malt_6$+ buffer, 11: Maltose+ buffer. B, The other half was dried in the SpeedVac, re-dried twice from water, and re-dissolved in 150 µl NaCl/MES buffer for XAF assay. Data show the means of four determinations ± SE.

### 3.3.2.3.4 Driselase digestion

Driselase, which is a commercial cell wall degrading enzyme that contains several enzymes such as cellulase, hemicellulose, pectinase… destroyed the XAF activity of BCP as well as the XAF-active fractions (fractions 27 to 40) of BCP from a Sepharose CL-6B column (Figure 57). The products included a major amount of Gal, Ara, and Glc and a trace amount of Man, GalA, and $Xyl_2$ in fractions from 27 to 34; smaller amounts of IP and Glc, Man, GalA and $Xyl_2$ in fractions from 34 to 42; and a major amount of Glc in the void volume (fraction 19 and 20) (Figure 58). Mannose was also

present in the Driselase solution in the same amount as in all Driselase digests suggesting that mannose was not a product of the enzyme reaction.

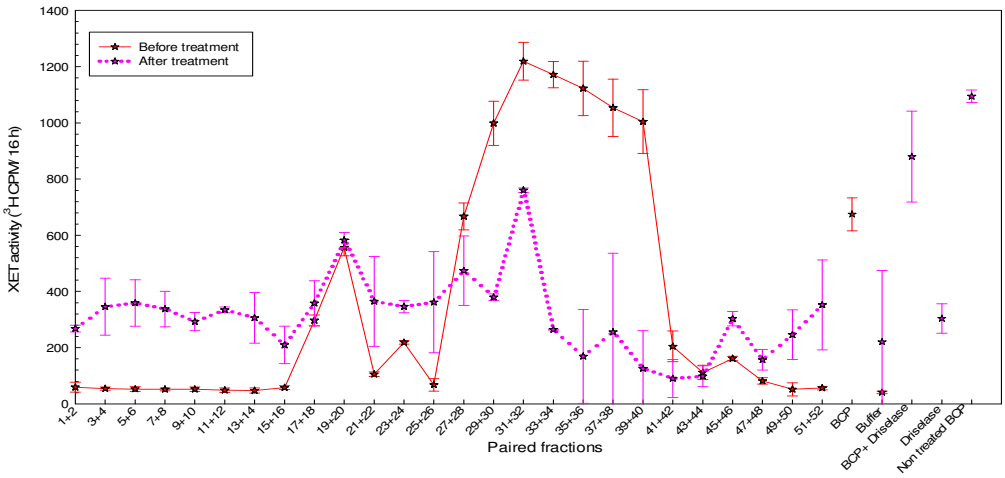


Figure 57. XAF activity of paired fractions of BCP from a Sepharose CL-6B column before and after treatment with 0.0003% Driselase.

Paired fractions (200 µl) from the CL-6B column in Figure 44 and crude BCP (2 mg/ml, 200 µl) were incubated with 0.0003% Driselase in PyAW 1:1:98 for 24 h in a final volume of 300 µl. The reaction was stopped by heating to 120ºC for 1 h and the reaction mixtures were centrifuged. The supernatant (150 µl) was dried in the SpeedVac, re-dried from water, and re-dissolved in 150 µl NaCl/MES buffer for XAF assay. Red line: XAF activity before treatment, pink line: XAF activity after treatment. Data show the means of two determinations ± SE.

Since Driselase is a commercial preparation containing multiple enzymes, it is difficult to predict what specific enzymes were responsible for this loss of the activity. However, the peak of Gal and Ara at the peak of XAF activity suggested that the presence of arabinogalactans was responsible for XAF activity. This result agrees with the HPLC profile of TFA hydrolysate of BCP in Figure 46.

.

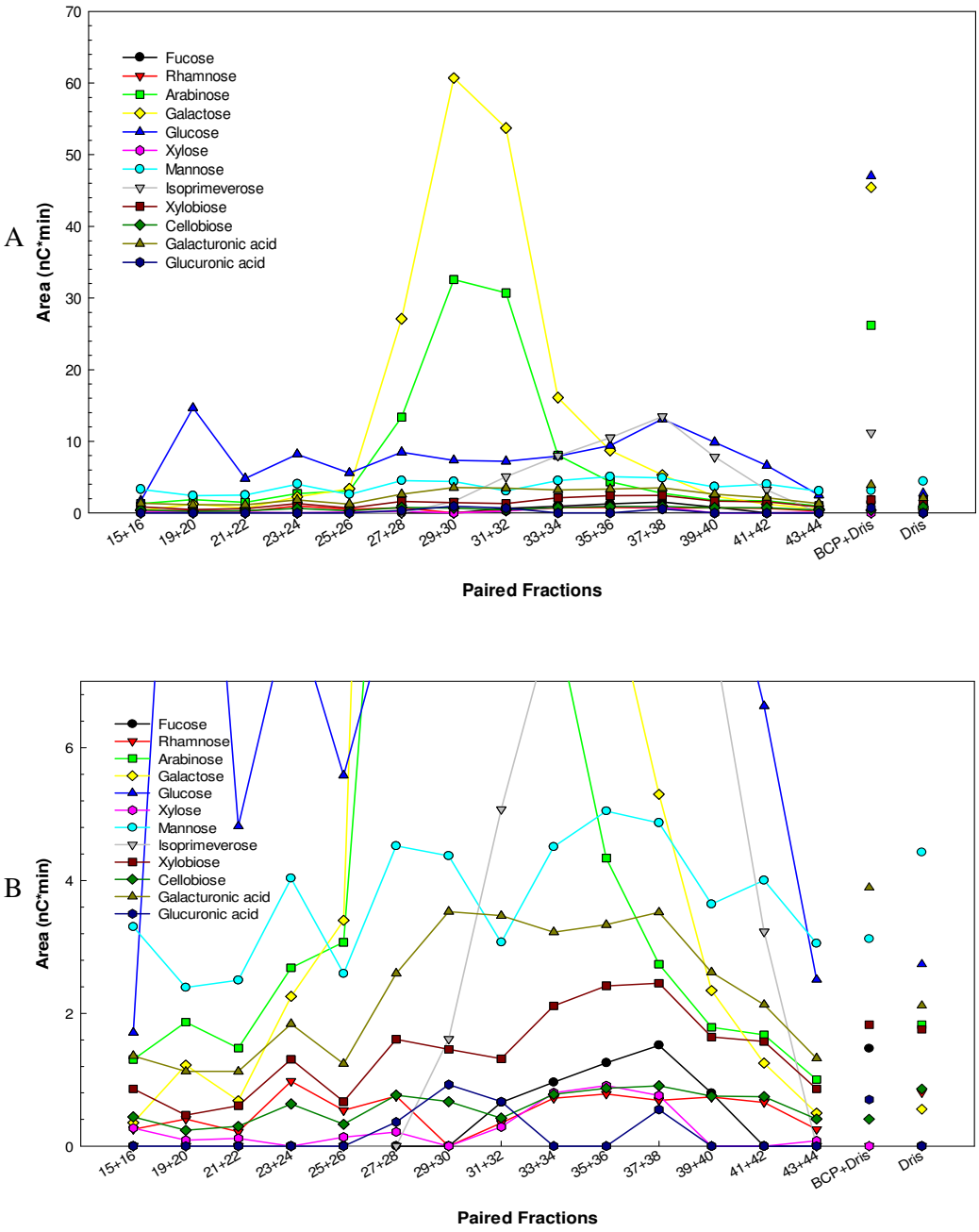


Figure 58. Sugar compositions of Driselase digests of paired fractions of BCP from CL-6B column chromatography.

Paired fractions of BCP (200 µl) after the CL-6B column in Figure 44 and BCP (200 µl) were incubated with 0.17% Driselase in PyAW 1:1:98 for 24 h in a final volume of 300 µl. The reaction was stopped by heating to 120ºC for 1 h and the reaction mixtures were centrifuged. The supernatant (150 µl) was dried in the SpeedVac, re-dried from water, re-dissolved in 9 µl water and 6 µl of that was diluted 6-fold for HPLC analysis. A, 0-70 y-axis; B, 0-7 y-axis.

### 3.3.2.4 Xyloglucan endo-glucanase digestion

In 3.3.2.3, xyloglucan endo-glucanase (XEG) partly destroyed XAF activity of BCP. However, after doing additional experiments, I realised that the concentration of XEG used in that experiment, 0.083 mg/ml, was quite high; thus, its contaminant activity was high enough to attack XAF, even after the XEG had been 'denatured' by boiling . This could be seen even in case of using formic acid to denature XEG (Figure 59).

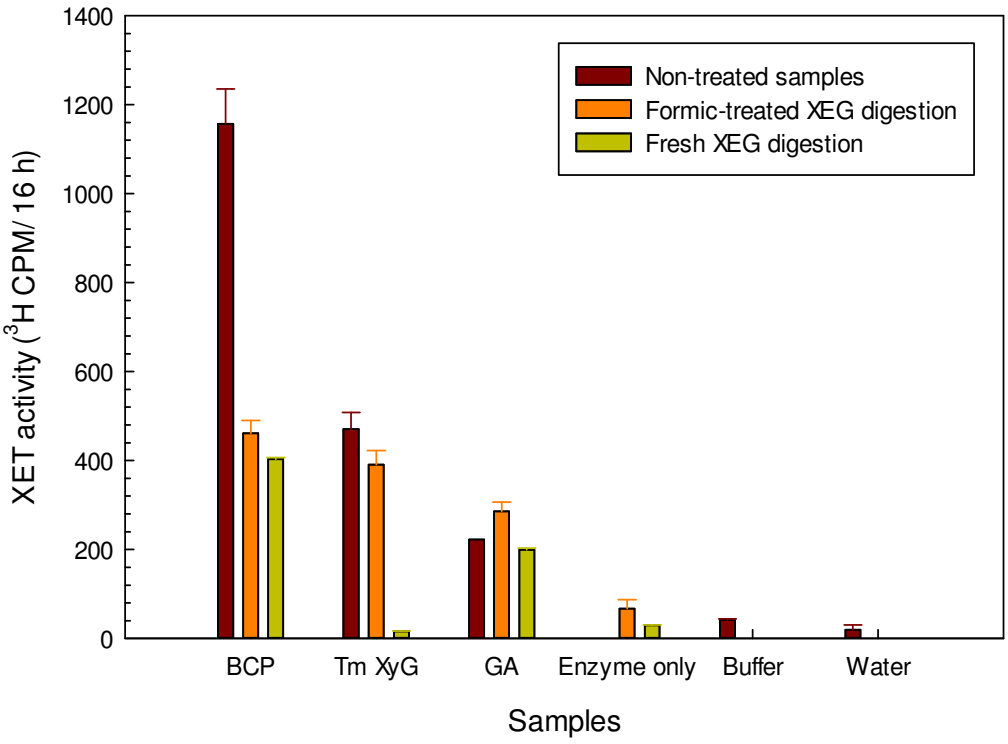


Figure 59. Apparent XAF activity of BCP, Tm XyG and gum arabic before and after treatment with formic-treated XEG or fresh XEG.

XEG at a concentration of 15.6 µg/ml (300µl) was treated with 100 µl formic acid, dried in the SpeedVac, re-dissolved in 400 µl water and divided into four 100-µl aliquots. Each aliquot was dried in the SpeedVac and added to 150 µl BCP, 0.5% Tm XyG, 0.5% gum arabic (GA) or water for 1.5 h. Of that, 75 µl was re-dried in the SpeedVac and re-dissolved in 75 µl NaCl/MES buffer for XAF assay. For non-treated samples, 75 µl of BCP, 0.5% Tm XyG or 0.5% GA was dried in the SpeedVac and re-dissolved in 75 µl NaCl/MES buffer for XAF assay. For the fresh XEG digestion, 75 µl of 15.6 mg/ml XEG was dried in the SpeedVac and 150 µl of BCP, Tm XyG, GA or water was added, left for 1.5 h and the reaction was stopped by the addition of 75 µl formic acid. Of that, 112.5 µl was dried in the SpeedVac and re-dissolved in 75 µl NaCl/MES buffer for XAF assay. Data show the means of two determinations ± SE.

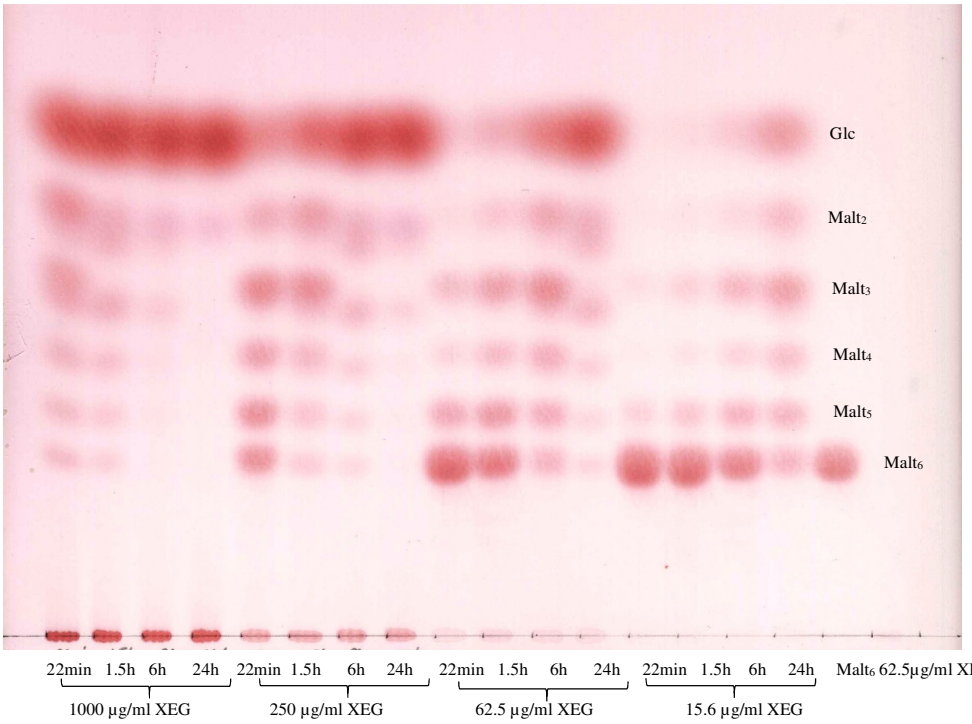


**A/ 1 mg/ml Maltohexaose + XEG, BAW 2:1:1, 15 h**

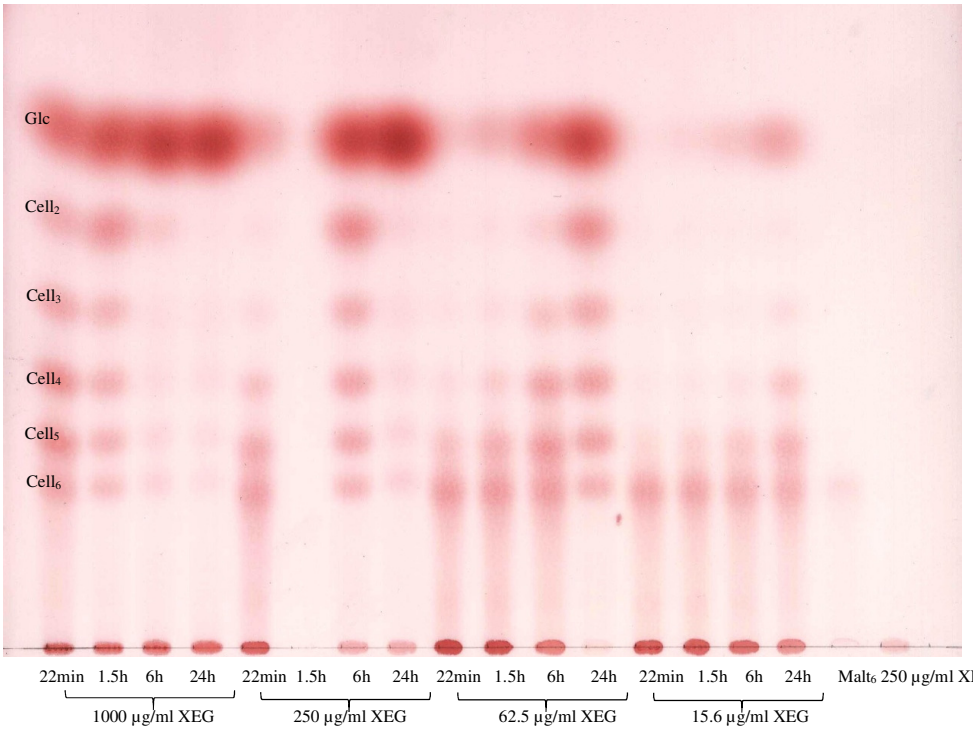


**B/ 1 mg/ml Cellohexaose + XEG, BAW 2:1:1, 15 h**

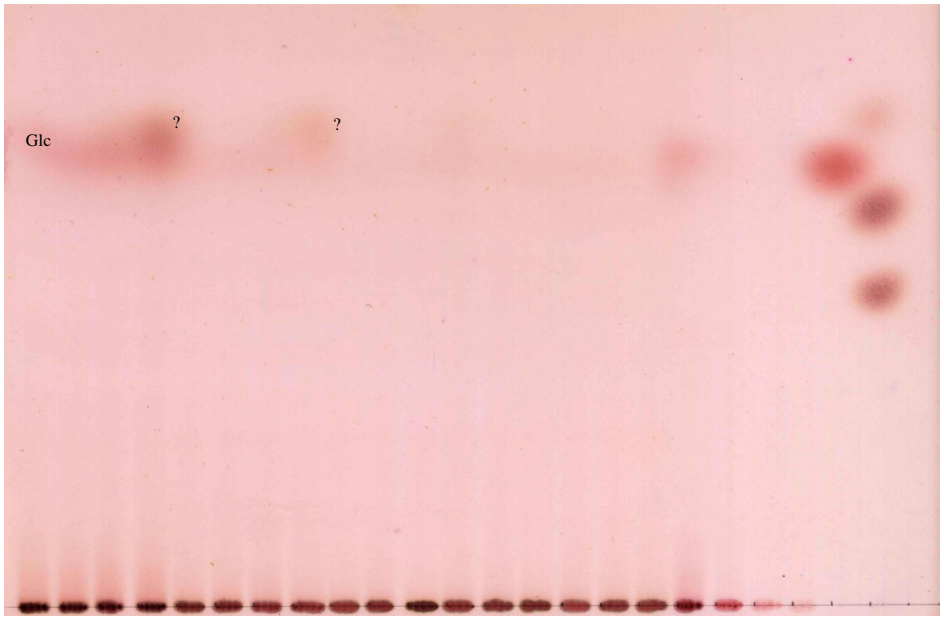


**C/ 1 mg/ml Polygalacturonic acid + XEG, BAW 2: 1:1, 15 h**

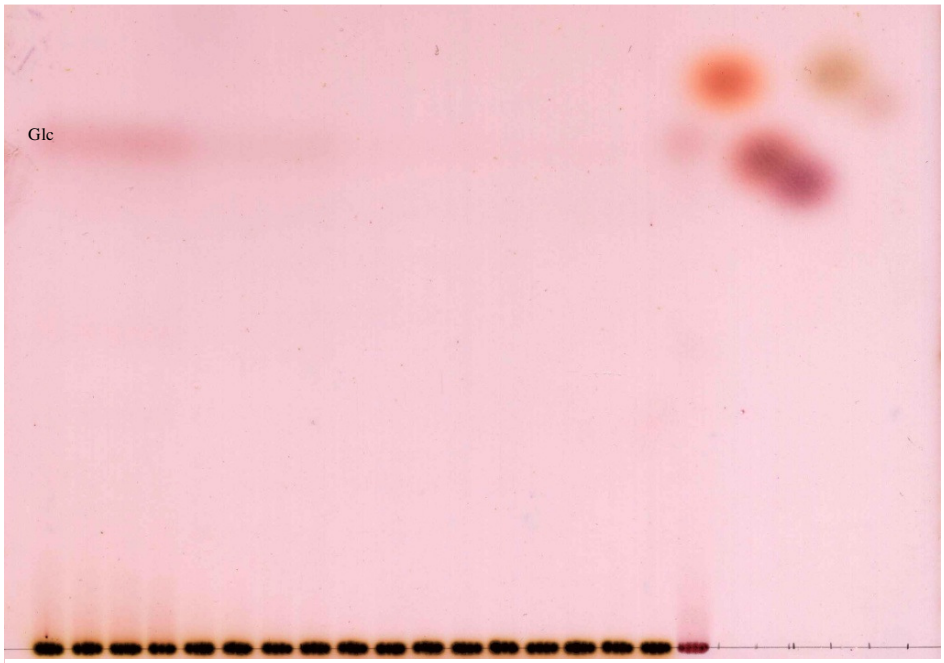


**D/ 1 mg/ml Gum Arabic + XEG, BAW 2:1:1, 15 h**

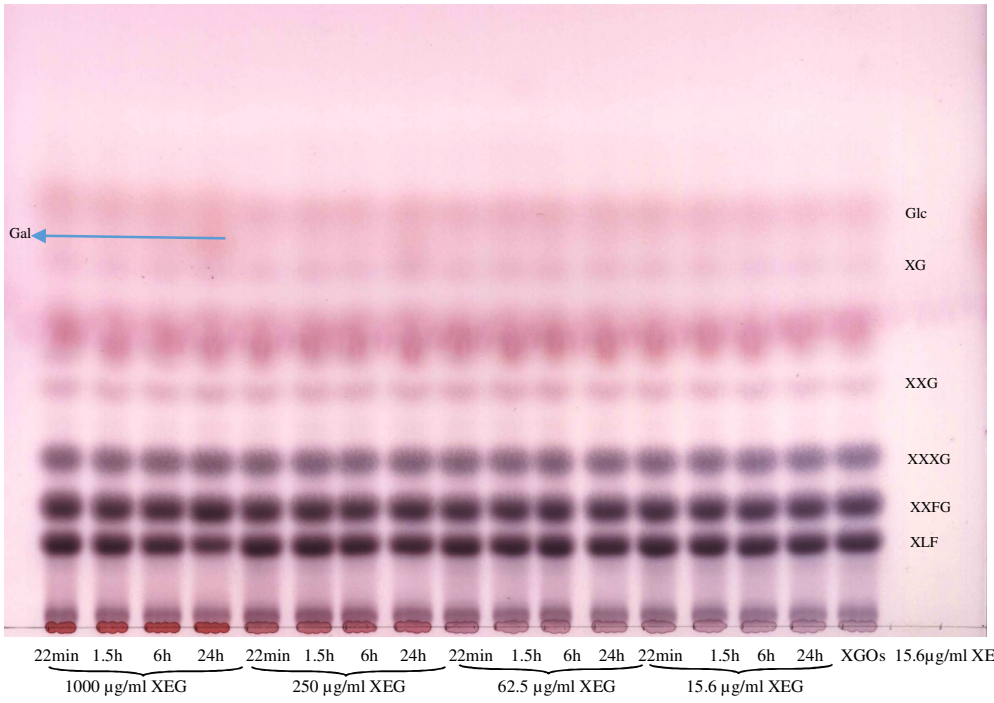


**E/ 1 mg/ml Xyloglucan oligosaccharides + XEG, BAW 2: 1:1, 15 h**

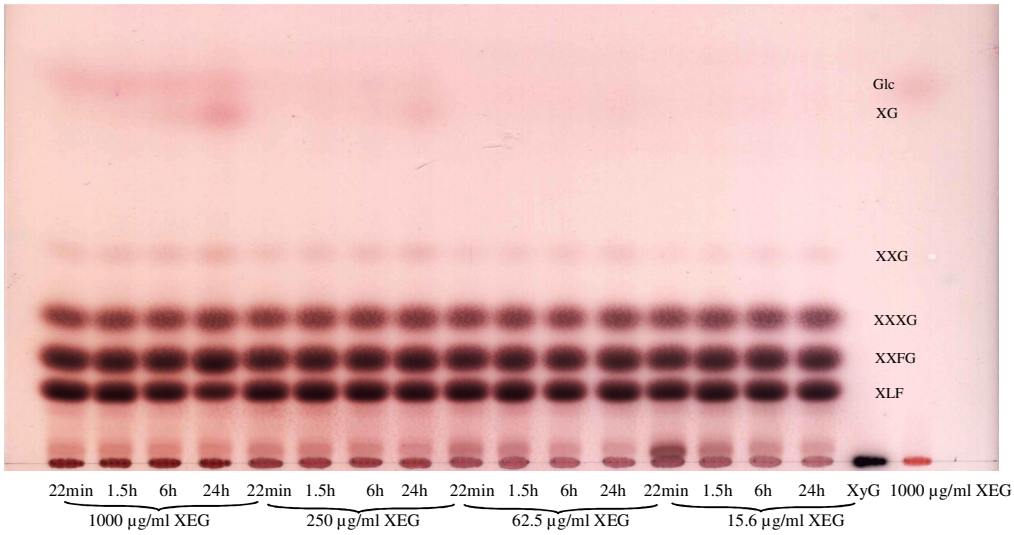


**F/ 1 mg/ml Tamarind Xyloglucan + XEG, BAW 2: 1:1, 15 h**

Figure 60. Thin-layer chromatography of products of XEG on different substrates.

Each potential substrate including malto-hexaose (A), cello-hexaose (B), polygalacturonic acid (C), gum arabic (D), xyloglucan oligosaccharides (E) or tamarind xyloglucan (F) was dissolved at 1 mg/ml in water and 40 µl of each (= 40 µg) was digested with 20 µl XEG at different concentration (1000, 250, 62.5, or 15.6 µg/ml) in PyAW 1:1:98 at room temperature, for different times. The enzyme concentration was a third during the reaction. The reaction was stopped by heating to 120°C for 70 min. The reaction mixture was centrifuged and the supernatant was dried in the SpeedVac, re-dissolved in 2 µl water and loaded onto a TLC plate. Solvent: BAW 2:1:1, thymol staining.

Figure 59 shows that BCP, tamarind xyloglucan (Tm XyG) and gum arabic (GA) had XAF activity and that treatment with fresh XEG destroyed half of the XAF activity of BCP and all XAF activity of Tm XyG but not any of the XAF activity of GA. This result indicated that XEG did not digest the XAF-active component(s) of GA. The formic-treated XEG did not reduce the XAF activity of Tm XyG and GA but reduced about half of the XAF activity of BCP suggesting that the XEG activity was destroyed by formic acid but other contaminant activities still survived and those activities could attack XAF. Therefore, I carried out some experiments to optimise the conditions for XEG digestion so it has maximum digestion of XyG and minimum digestion of everything else.

Different concentrations of XEG were used in a test of its actions on some substrates including XGO, Tm XyG, $Malt_6$, $Cell_6$, PGA and GA at different time. The products were tested by TLC to find out the optimal XEG concentration for its XEG-specific activity.

At a concentration of 333 µg/ml, XEG digested all substrates tested, except for GA (Figure 60D), producing a range of malto-oligosaccharides from $Malt_6$ (Figure 60A), a range of cello-oligosaccharides from $Cell_6$ (Figure 60B), a range of xyloglucan-oligosaccharides from Tm XyG (Figure 60 F), a trace of galactose from XGOs (Figure 60E), and various unknown monomers from PGA (Figure 60C). This result suggested that XEG was not pure, but was contaminated with other enzyme activities such as α-glucosidase, β-glucosidase, amylase… The XEG preparation was also contaminated with Glc, as shown in all TLCs in Figure 60. From this experiment, I concluded the optimal conditions for the XEG activity of XEG were final concentration: 5.2 µg/ml and incubation time: 1.5 h, stopping the reaction by heating to 120°C for 70 min. These conditions were applied for all further XEG digestions.

Under the optimal conditions, XEG slightly destroyed XAF activity of BCP (24% loss) but dramatically reduced XAF activity of paired XAF-active fractions of BCP after a CL-6B column, especially in pairs of fraction 29+30 (reduced by 77%) and 41+42 (reduced by 92%) (Figure 60). The products of these digestions included several xyloglucan oligosaccharides and Glc (Figure 62). This suggested that XyG contributed

to the XAF activity and the column chromatography helped to separate it from XAF, thus it was more accessible for XEG digestion.

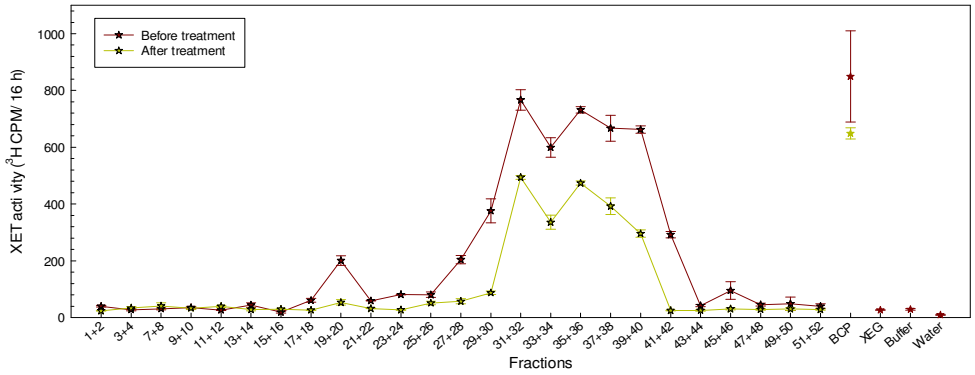


Figure 61. XAF activity of XEG digests of BCP and paired fractions of BCP from a CL-6B column.

BCP (0.4 mg) and XAF-active fractions of BCP from the CL-6B column in Figure 44 (200 µl) were treated with 5.2 µg/ml XEG under the optimum conditions in a final volume of 300 µl. The reaction was stopped by heating to 120°C for 70 min and the reaction mixtures were centrifuged. Half of the supernatant (150 µl) was dried in the SpeedVac, re-dissolved in NaCl/MES buffer for XAF assay. Paired fractions (150 µl) before XEG digestion were also dried in the SpeedVac and re-dissolved in 150 µl NaCl/MES buffer for XAF assay. Data show the means of two determinations ± SE.

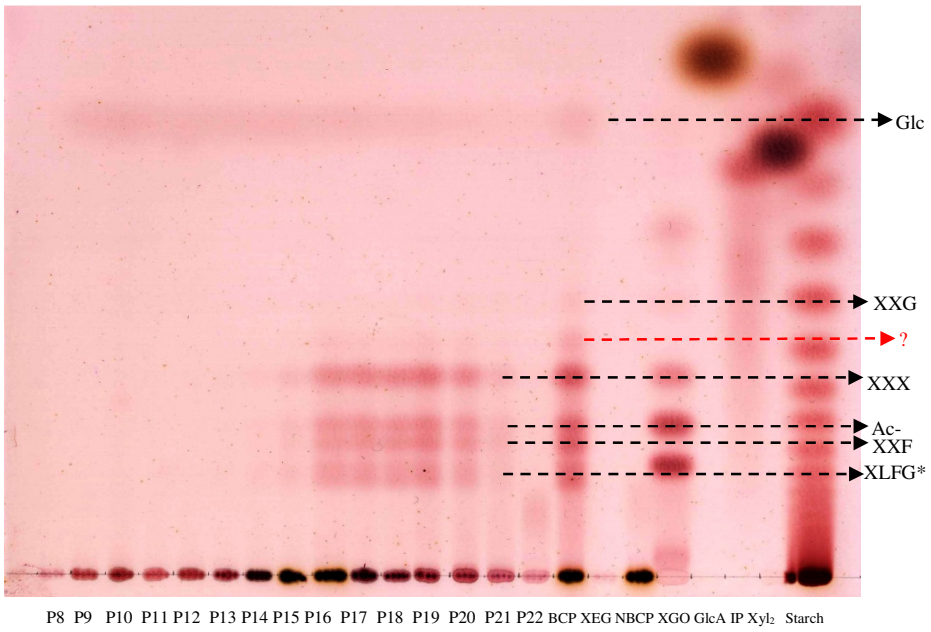


Figure 62. Thin-layer chromatography of XEG digests of BCP and paired fractions of BCP from a CL-6B column.

The other half of the supernatant (see legend to Figure 61)) was dried in the SpeedVac, re-dissolved in 9 µl water and 33.3% of the sample was loaded onto the TLC plate. BCP: BCP treated with XEG, XEG: enzyme only, NBCP: Non-treated BCP, XGO: xyloglucan oligosaccharides. Red arrow: unknown oligosaccharides; * = tentative identifications. Other details as in Figure 60.

### 3.3.2.5 Proteinase K digestion of XAF

The last experiments suggested that XAF may be protein(s) or glycosylation(s). To investigate that, I treated XAF with enzymes that are capable of digesting protein. Proteinase K was chosen because of its broad substrate specificity.

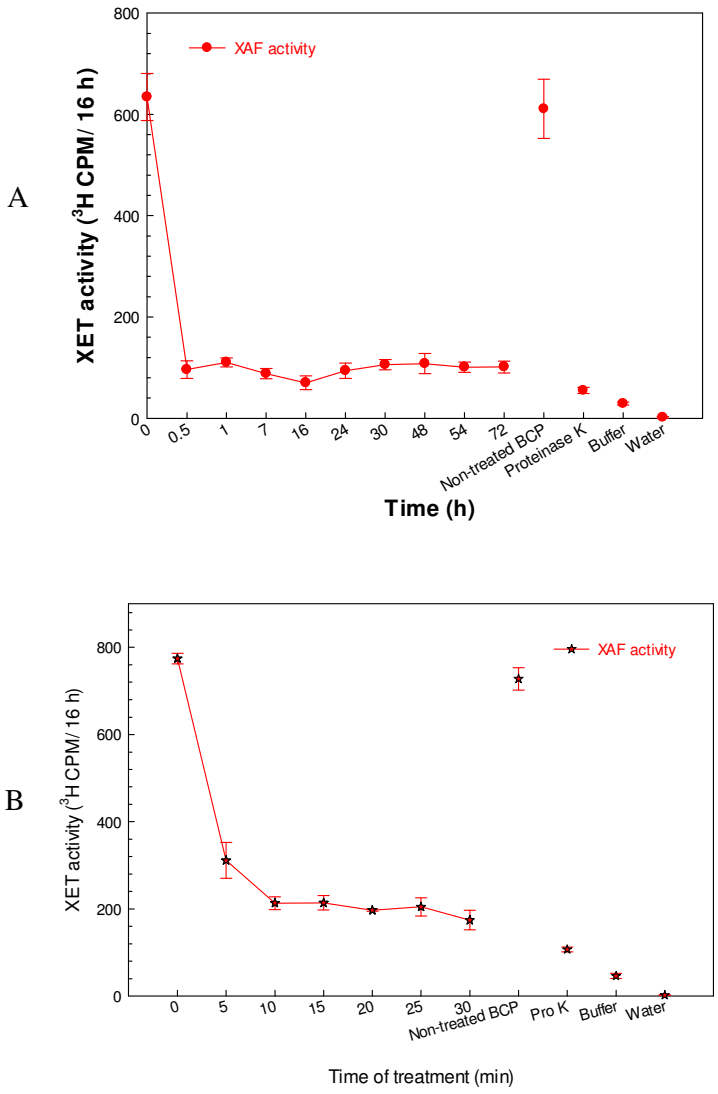


Figure 63. XAF activity of BCP after being treated with proteinase K.

BCP (0.6 mg) was incubated in 600 µl of 100 µg/ml proteinase K in 25 mM ammonium acetate, pH 8.8 at 37ºC, over two time-courses. A, longer time course; B, shorter time course. The reaction was stopped by heating at 107ºC for 10 min and the reaction mixture was centrifuged. After that, 150 µl of the supernatant was dried in the SpeedVac and re-dissolved in 150 µl NaCl/MES buffer for XAF assay. For the sample at 0 h, the enzyme was heated before the addition of BCP. Buffer (25 mM ammonium acetate) was used in place of enzyme in the non-treated BCP. Water was used in place of BCP in the proteinase K sample. 'Buffer' (on *x*-axis): NaCl/MES buffer. Data show the means of four determinations ± SE.

Treatment of BCP with 100 µg/ml proteinase K destroyed most XAF activity after 30 min and the 16% remaining activity did not change after up to 72 h (Figure 63A). To further investigate the action of proteinase K on BCP, I treated BCP with proteinase K under the same conditions with a shorter time-course. Proteinase K destroyed 60% of the XAF activity after just 5 min of treatment and 71% XAF activity after 10 min, then the remaining XAF activity was slightly reduced to 24% after 30 min (Figure 63B). This remaining activity may be due to the lack of proteinase K or the polysaccharide component of XAF which was expected not to be digested by the proteinase K.

Although I did not do any further experiment to see if proteinase K had been inactivated after 30 min, I did an experiment to check if proteinase K did not attack the carbohydrate component of XAF. In order to do that, I precipitated the enzyme products with ethanol, hydrolysed the precipitate with 2 M TFA at 120ºC, and analysed the hydrolysates by TLC. The TLC plate showed that all monosaccharides released by TFA from the polymers of BCP after proteinase K digestion at any time point were identical to those from non-treated BCP (Figure 64), indicating that proteinase K only digested the protein component and did not digest the carbohydrate component of BCP. It could be several polysaccharides as showed elsewhere in the thesis with enzyme digestions. It could also be a part of a glycosylated protein and may cover some of the protein part, thus protecting them from being denatured by boiling or being digested by proteinase K.

On the SDS-PAGE of the proteinase K digestion products, many Coomassie blue-stained bands and silver-stained bands representing the main proteins or glycoproteins disappeared or reduced in amount after a 5-minute treatment (Figure 65).

In conclusion, after 10 min of proteinase K digestion, 71% XAF activity was destroyed corresponding to the disappearance of the main Coomassie-blue stained bands and the change of the major silver-nitrate stained bands on the SDS-PAGE indicating that XAF was proteinase K-sensitive, thus was a protein. The preparation of XAF included boiling and the storage of XAF included routine freezing and thawing, thus, it must be a heat-stable protein, for example a heavily glycosylated glycoprotein.

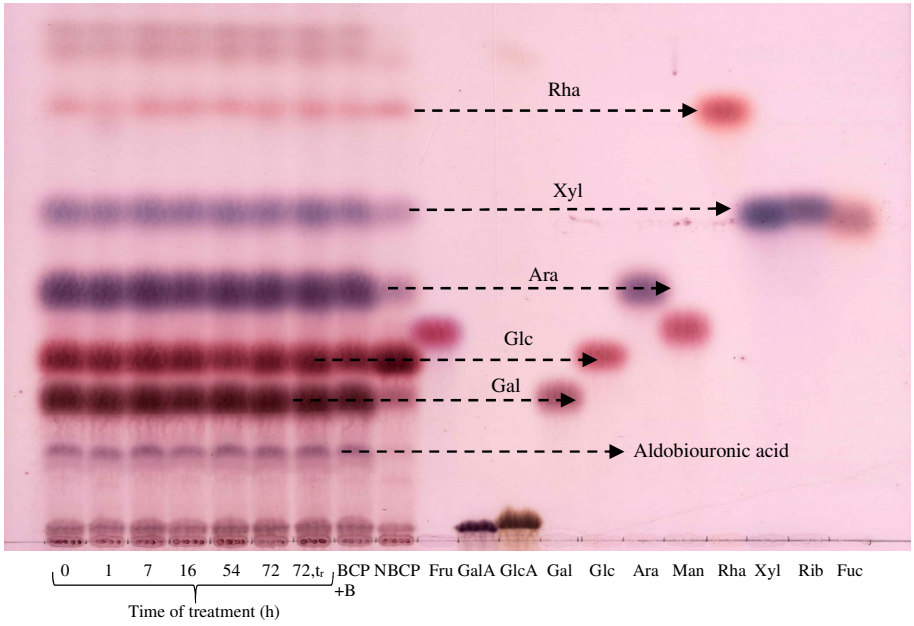


Figure 64. Thin-layer chromatography of TFA-hydrolysates of the BCP/proteinase K digestion products precipitated by ethanol.

Products of the proteinase K digestion in Figure 63A (5 µl) at each time point were mixed with 95 µl water and precipitated with 76% ethanol. The pellet was washed with ethanol, dried in the SpeedVac, and treated with 2 M TFA, 120ºC for 60 min. The TFA-hydrolysate was dried in the SpeedVac, re-dissolved in 3 µl water and loaded onto a TLC plate. Solvent: EPyAW 6:3:1:1, thymol staining. 72h, $t_r$: BCP incubated with proteinase K at room temperature instead of 37°C for control, BCP+B: BCP incubated with 25 mM ammonium acetate in place of enzyme, NBCP: new BCP.

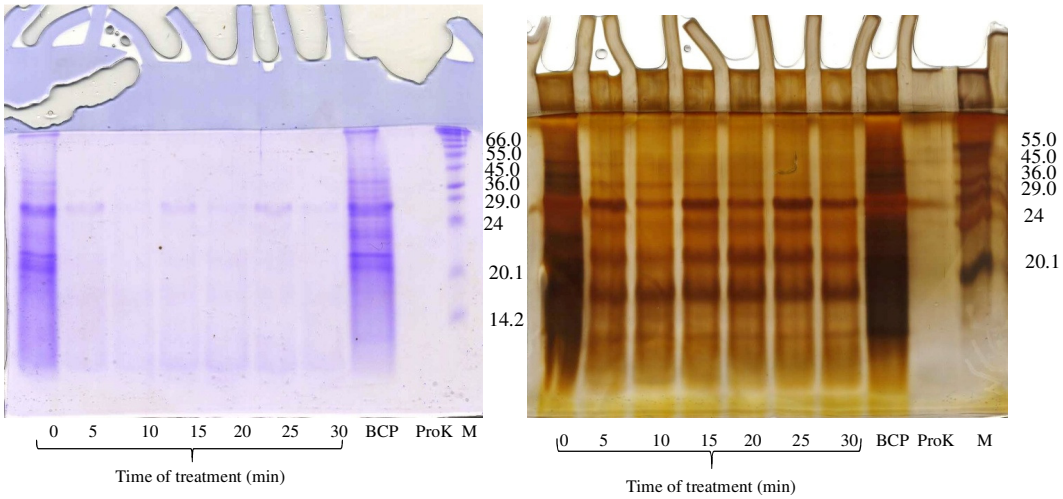


Figure 65. SDS-PAGE of products of the proteinase K digestion of BCP.

Products of the proteinase K digestion in Figure 63B (200 µl) were dried in the SpeedVac, re-dissolved in 12 µl water, and mixed with 3 µl sample loading buffer. Of that, 5 µl was loaded onto 18% acrylamide SDS-gel for electrophoresis, stained with silver nitrate (B); another 10 µl was loaded onto another 18% acrylamide SDS-gel for electrophoresis, stained with Coomassie blue (A). BCP: non-treated BCP, M: protein ladder (in kDa), ProK: proteinase K with water in place of BCP.

### 3.3.2.6 Trypsin digestion of XAF

Another enzyme that can digest proteins is trypsin. Unlike proteinase K, trypsin action is quite specific. It is an endopeptidase that predominantly cleaves proteins at the carboxyl side (or "C-terminal side") of the amino acids lysine and arginine except when either is bound to a C-terminal proline. In order to find out the optimal concentration for trypsin digestion of XAF, I treated BCP with different concentrations of trypsin.

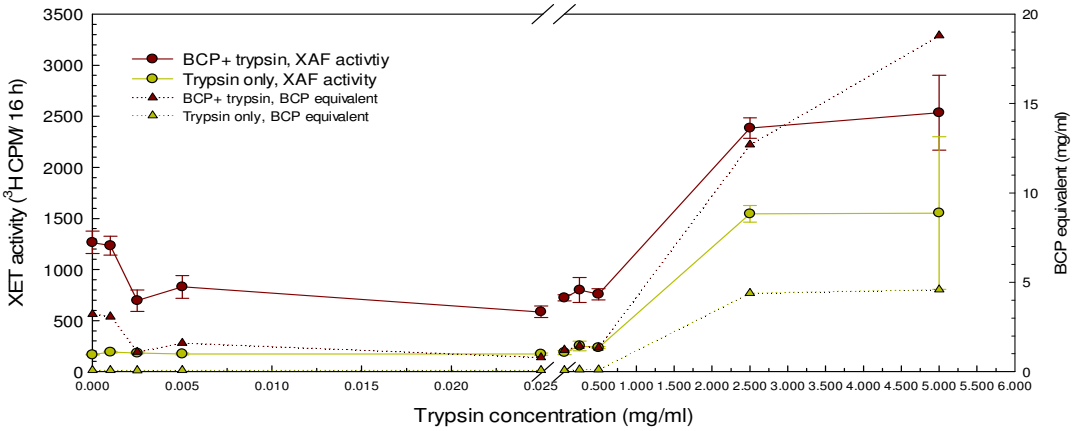


Figure 66. XAF activity and BCP equivalent of trypsin digestion of BCP.

BCP (0.3 mg) was treated with 300 µl of trypsin at different concentrations, from 0.5 µg/ml to 5 mg/ml, in 25 mM ammonium acetate, pH 8.8 at 37ºC for 24 h. The reaction was stopped by heating at 105ºC for 30 min and the reaction mixture was centrifuged. The supernatant (150 µl) was dried in the SpeedVac, and re-dissolved in 75 µl NaCl/MES buffer for XAF assay. Data show the means of four determinations ± SE. The BCP equivalent was calculated from the standard curve in Figure 13.

A high concentration of trypsin (≥ 2.5 mg/ml) had its own XAF activity, equivalent to that of 4.6 mg/ml BCP (Figure 66). Trypsin at any final concentration less than 0.5 mg/ml had no XAF activity. At a concentration of 0.5 mg/ml, trypsin destroyed 40% XAF activity of BCP and this remaining activity did not change when I reduced trypsin concentration to 2.5 µg/ml. When the trypsin concentration was lowered to 1 µg/ml, trypsin did not destroy any XAF activity (Figure 66).

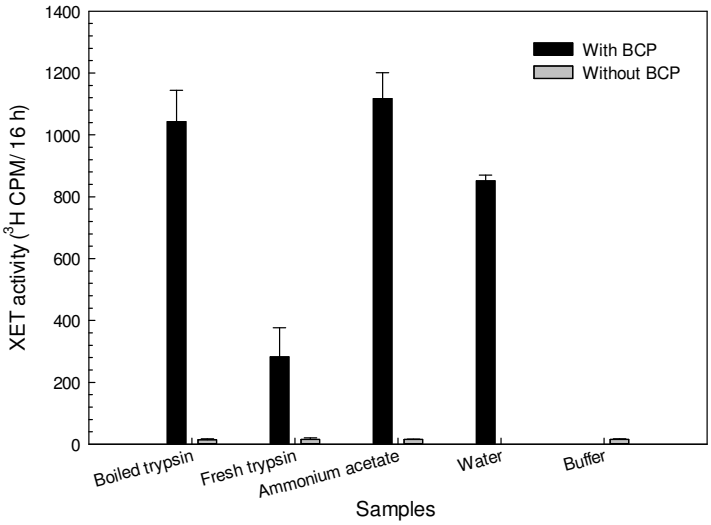


Figure 67. XAF activity of BCP treated with boiled and fresh trypsin.

Trypsin was made at a concentration of 5 µg/ml. Half of it was heated at 105ºC for 30 min and the other half was kept fresh. The fresh or boiled trypsin (300 µl) was incubated with 0.6 mg BCP in a final volume of 600 µl at 37ºC for 24 h. The reaction was stopped by heating at 105ºC for 30 min and the reaction mixture was centrifuged. The supernatant (300 µl) was dried and re-dissolved in 150 µl NaCl/MES buffer for XAF assay. Data show the means of eight determinations ± SE. BCP in ammonium acetate in place of trypsin and BCP in water were used as controls.

To make sure that the boiled trypsin in this procedure was inactive and did not affect XAF activity, I tested the effect of heat-treated trypsin on XAF activity. Boiled trypsin did not reduce XAF activity while the fresh trypsin did, confirming that under the conditions that I had used to denature trypsin after the reaction, trypsin was inactive. The result also confirmed that the ammonium acetate buffer did not affect to the XAF activity, showing that it was an appropriate buffer for the enzyme reaction (Figure 67).

From these results, 2.5 µg/ml of trypsin was the optimal concentration for the action of trypsin on XAF activity, while having negligible XAF activity of its own, and I used this concentration for further analysis. Trypsin destroyed about a half of the XAF activity, indicating that XAF was trypsin-sensitive, thus was protein. The remaining activity could be due to the other parts of XAF that were not digested by trypsin such as a carbohydrate chain. It also could be due to other trypsin-insensitive polymers in BCP; either a polysaccharide or a protein lacking Lys or Arg residue, or having Arg and Lys residues inaccessible to trypsin because these amino acids were covered by other components such as a carbohydrate chain of a glycoprotein.

## 3.4 XAF can be purified by sequential use of ion-exchange column chromatography or native-PAGE with electro-elution

### 3.4.1 Partial purification of XAF by ion-exchange column chromatography

#### 3.4.1.1 Anion-exchange column chromatography

BCP was applied onto a Q-Sepharose column, and the fractions were collected, measured for $A_{280}$ and assayed for carbohydrate and protein concentration. Fractions were pooled into groups of four, precipitated with ethanol and assayed for XAF activity. The pools were treated with TFA, and the products were analysed by HPLC and TLC, or treated with HCl and the products analysed by paper chromatography. The XAF-active pools were loaded onto SDS-PAGE for determining the main protein and polysaccharide bands. These pooled fractions were also tested with Yariv reagent for AGP determination.

From the Q-Sepharose column in Figure 68, I obtained a wide peak of XAF activity (fraction 25 to fraction 44), eluted with 500 mM and 1000 mM acetate ($Na^+$), indicating that the active XAF had a moderate number of negative charges. All XAF-active pools contained a high concentration of carbohydrate and protein (Figure 67) suggesting that XAF was a glycoprotein.

The highest XAF activity was obtained in pooled fractions 29-32 and 41-44. Although having the same XAF activity, these pooled fractions contained different amounts of carbohydrate and protein. Pooled fraction 29-32 contained a large amount of both carbohydrate and protein while pooled fraction 41-44 contained a large amount protein but a small amount of carbohydrate (Figure 68). This result suggested that more than one protein was responsible for XAF activity.

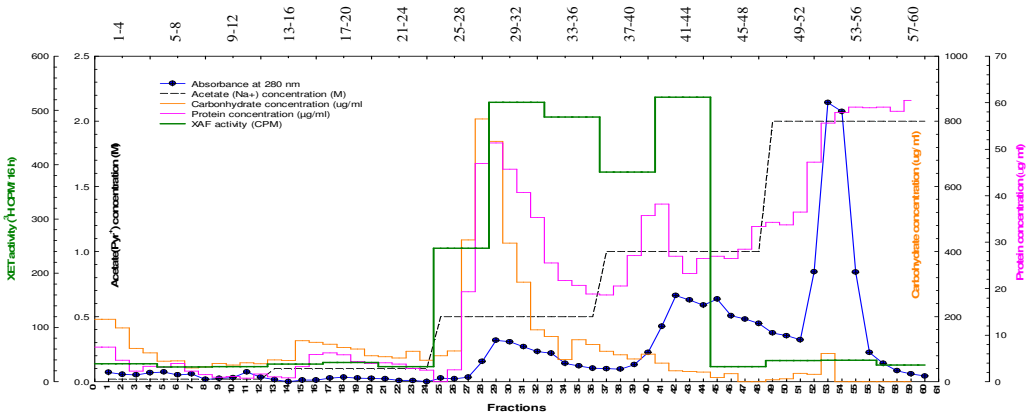


Figure 68. Anion-exchange column chromatography of BCP.

BCP (10 mg) was applied onto a 5-ml bed volume Q-Sepharose column in the acetate form. Of each acetate concentration, pH 4.7, 12 ml was used to elute 1-ml fractions. Fractions were measured for $A_{280}$. Of each fraction, 100 µl was used in a Bradford assay to measure the protein concentration, 40 µl was used in a phenol-sulphuric assay to measure the carbohydrate concentration, and 250 µl of each of pool of four neighbouring fractions were pooled, adjusted to 1 M acetate ($Na^+$), and precipitated with 76% ethanol; the precipitate was washed with 76% ethanol and 96% ethanol, dried in the SpeedVac and re-dissolved in 1 ml water. Of that, 150 µl was dried in the SpeedVac, re-dissolved in 150 µl NaCl/MES buffer for XAF assay. The XAF activity data show the means of four different determinations.

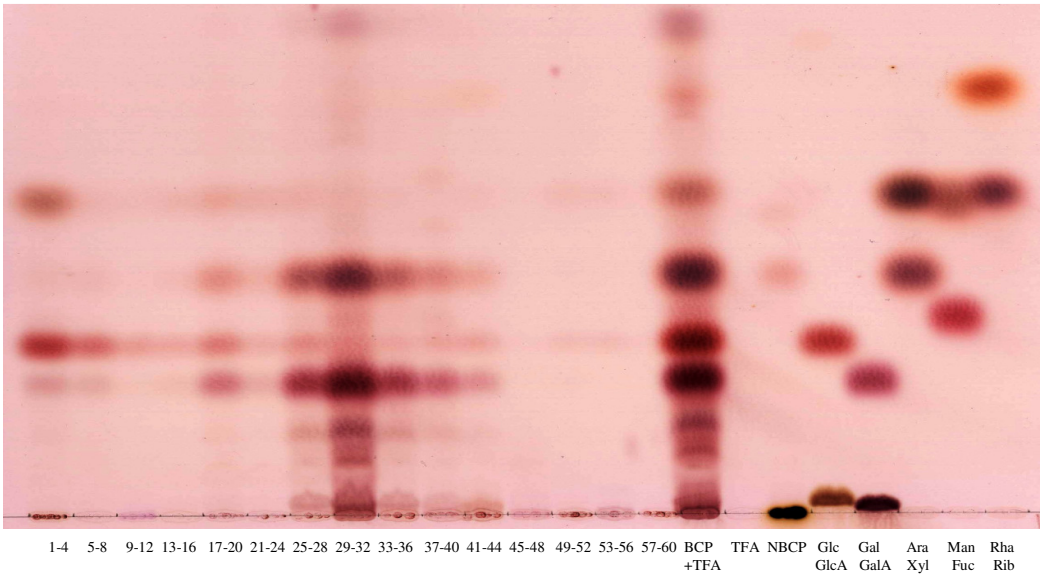


Figure 69. Thin-layer chromatography of TFA-hydrolysates of pooled fractions of BCP from the anion-exchange column chromatography.

After ethanol precipitation, each of pool was re-dissolved in 1 ml water (details an in Figure 68). Of that, 250 µl was hydrolysed with 2 M TFA, centrifuged, dried in the SpeedVac and re-dissolved in water, and 17% of the sample was loaded onto the TLC plate. NBCP: Non-treated BCP. Other details as in Figure 68.

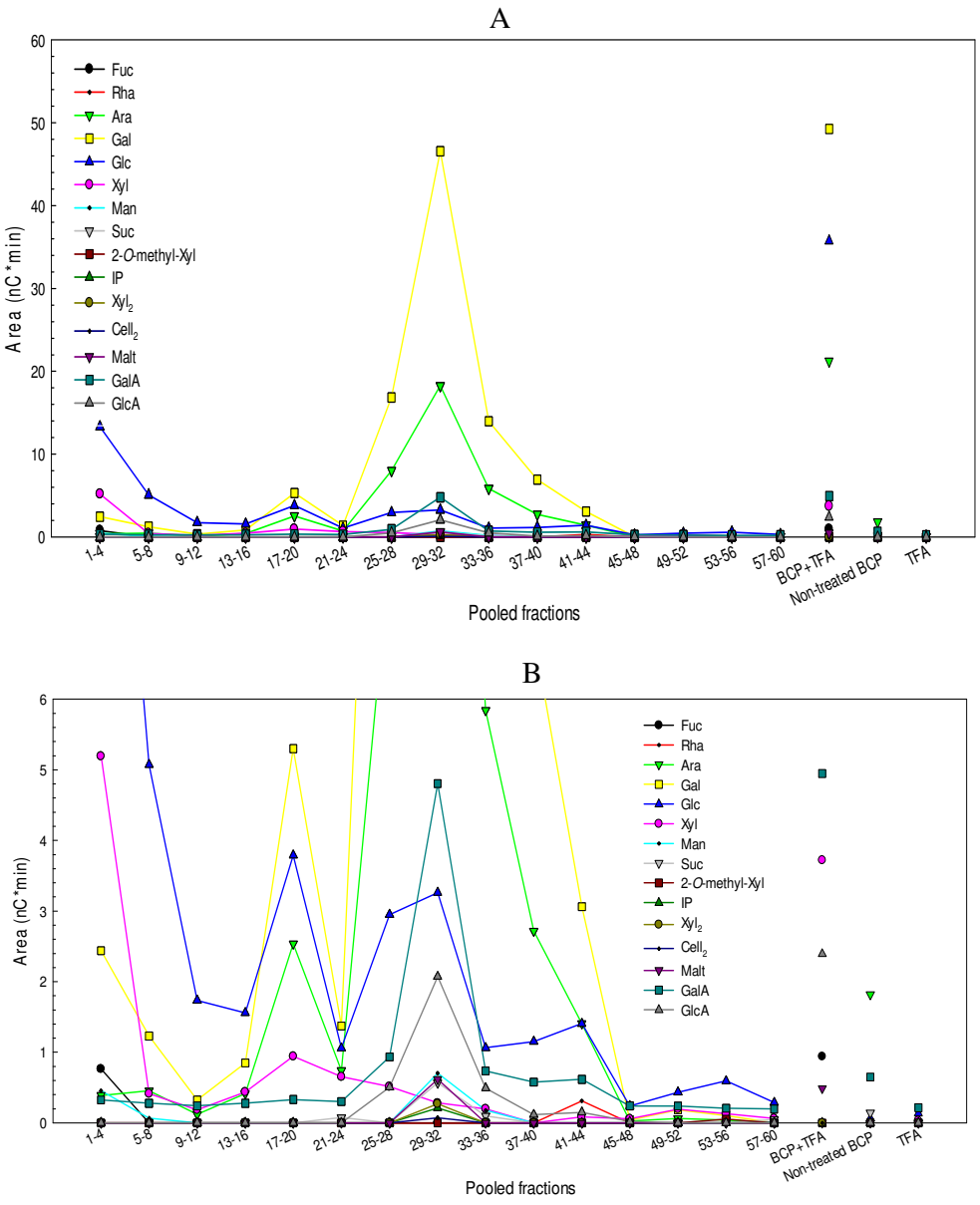


Figure 70. Sugar compositions of TFA-hydrolysates of pooled fractions of BCP from the anion-exchange column chromatography.

After acid hydrolysis (details as in Figure 69), TFA was removed in the SpeedVac and 11.3% of the sample was analysed by HPLC. A, large y scale; B, small y scale.

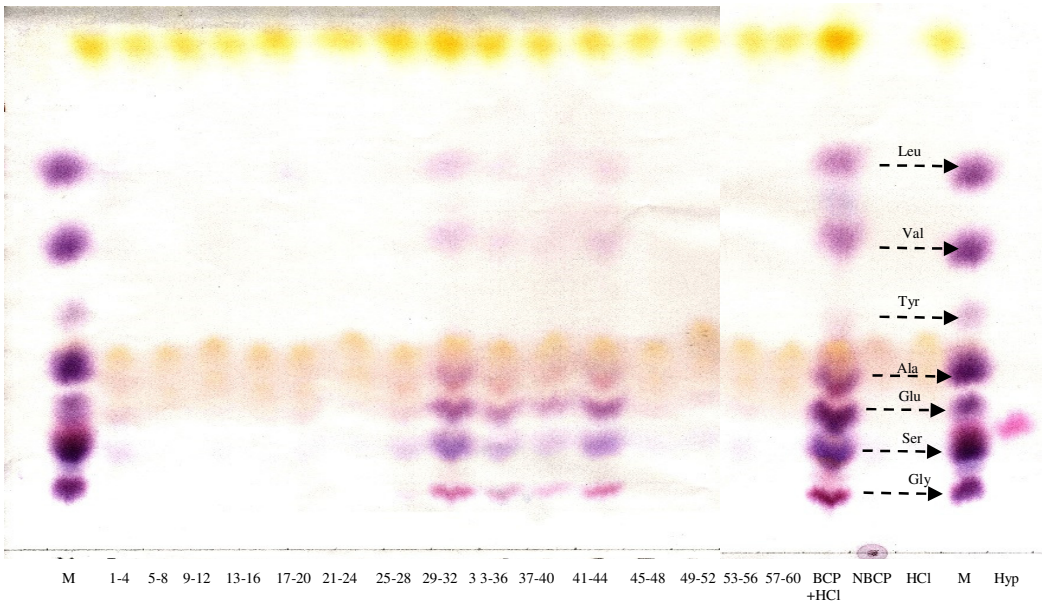


Figure 71. Paper chromatography of HCl-hydrolysates of pooled fractions from the anion-exchange column chromatography.

After the ethanol precipitation (details as in Figure 67), 200 µl of each pool was hydrolysed with 6 M HCl/ 10 mM phenol at 110ºC for 20 h, cooled on ice, dried in the SpeedVac, re-dried from water, and re-dissolved in water; 33.3% of the samples were loaded onto Whatman No.1. Solvent: BAW 12:3:5, 23 h, ninhydrin staining. Each amino acid (5 µg) was used as a marker.

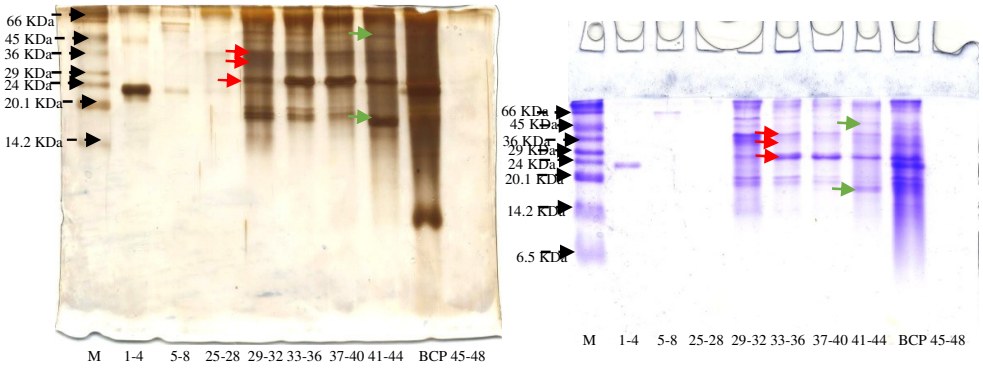


Figure 72. SDS-PAGE of pooled fractions of BCP from the anion-exchange column chromatography.

After the ethanol precipitation (details as in Figure 68), 100 µl of each pooled fraction was dried in the SpeedVac, re-dissolved in 12 µl water and mixed with 3 µl loading sample buffer. Of that, 66.7% of the sample was loaded onto an 18% acrylamide gel, electrophoresed, stained with Coomassie blue (right) and the other 33.3% of the sample was loaded onto another 18% acrylamide gel, electrophoresed, stained with silver nitrate (left). Marker: 30 µl protein ladder was mixed with 7.5 µl loading sample buffer, concentrated to 15 µl, and of that 10 µl was loaded onto the Coomassie blue gel and the other 5 µl was loaded onto the silver nitrate gel.

The HPLC and TLC profiles showed that pool 29-32 contained a major amount of Ara, Gal, GalA, Glc, GlcA, and aldobiouronic acids while pool 41-44 contained a trace of Gal, Ara, Glc, GalA, and Rha (Figure 69, Figure 70). The paper chromatography showed that pools 29-32 and 41-44 had about the same amount of several amino acids, including Gly, Ser, Glu, Ala, Val and Leu/Ile (Figure 71).

On the SDS-PAGE, pool 29-32 had two major bands of approximately 31 and 36 kDa (red arrow) which were faint in other pools, three same bands as pool 33-36 and 37-40 of approximately 19, 20, and 27 kDa (Figure 72). In the reaction with Yariv reagent, this pool showed detectable precipitation, as much as that of crude BCP (Figure 73). These results suggest that there are arabinogalactan-proteins in pool 29-32 that may be responsible for its high XAF activity.

Pool 41-44 contained the three same bands of 27, 31, and 36 kDa and two different bands compared to other pools on both gels (green arrow) at approximately 45 and 17 kDa (Figure 72). In addition, this pool was negative to Yariv reagent (Figure 73) suggesting that these bands were not classical AGPs. The high XAF activity of pool 41-44 may be due to the presence of other proteins. These proteins could be either non-classical AGPs or other glycosylated proteins.

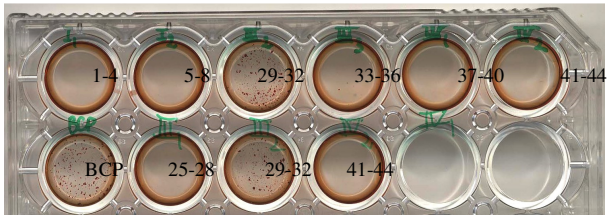


Figure 73. Reaction of Yariv reagent with pooled fractions of BCP from the anion-exchange column chromatography.

After the ethanol precipitation (details as in Figure 68), 20 µl of each pooled fraction or BCP (2 mg/ml) was mixed with 0.04 mg Yariv reagent in a final volume of 40 µl and 20 µl of water added. The plate was photographed 0.5 h after mixing.

In conclusion, after the anion-exchange column chromatography, a wide peak of XAF activity was obtained which had a moderate number of negative charges. This XAF-active peak contained both carbohydrate and protein, and was rich in Ara, Gal, Glc, GalA, GlcA, and Rha as well as Gly, Ser, Glu, Ala, Val and Leu/Ileu residues. These monosaccharides and amino acids were either components of these glycoproteins or of co-eluting polysaccharides or proteins. Some of the XAF-active fractions were

positive with Yariv reagent and some were not. These results indicate the presence of more than one polymer in BCP that are responsible for the XAF activity, some of them are AGPs and some are not. Also, further purification is needed for the determination of XAFs because there were still many proteins and polysaccharides in the XAF-active fractions (Figure 72) that made it not suitable for analyse by mass-spectrometry.

### 3.4.1.2 Cation-exchange column chromatography

BCP was applied onto an SP-Sephadex column and fractions were measured for $A_{280}$ and carbohydrate concentration. Fractions were then dried, and re-dissolved in water. A portion of the solution was re-dissolved in NaCl/MES buffer for XAF activity assay; another portion was dried, re-dissolved in water, hydrolysed with TFA and analysed by TLC or with HCl and analysed by paper chromatography and paper electrophoresis for testing sugars and amino acids composition. A third portion was tested on SDS-PAGE.

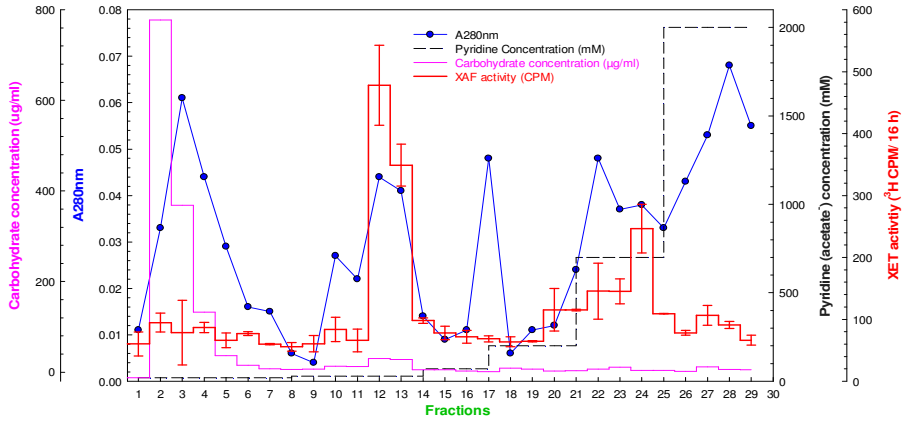


Figure 74. Cation-exchange column chromatography of BCP.

Dried BCP (2 mg) was dissolved in 1 ml 20 mM pyridine (formate), pH 3.0, and applied onto a 20-ml bed volume SP-Sephadex column (in the pyridinium form). Fractions (2 ml) were collected with different concentrations of pyridine adjusted to pH 5.3 with acetic acid and measured for $A_{280}$ (blue line), and 200 µl of each fraction was used in a phenol-sulphuric assay to measure carbohydrate concentration (pink line). Fractions were dried in the SpeedVac, re-dried from water, and re-dissolved in 2 ml water. Of that, 150 µl was dried in the SpeedVac, re-dissolved in 150 µl NaCl/MES buffer for XAF assay; data show the means of two determinations ± SE.

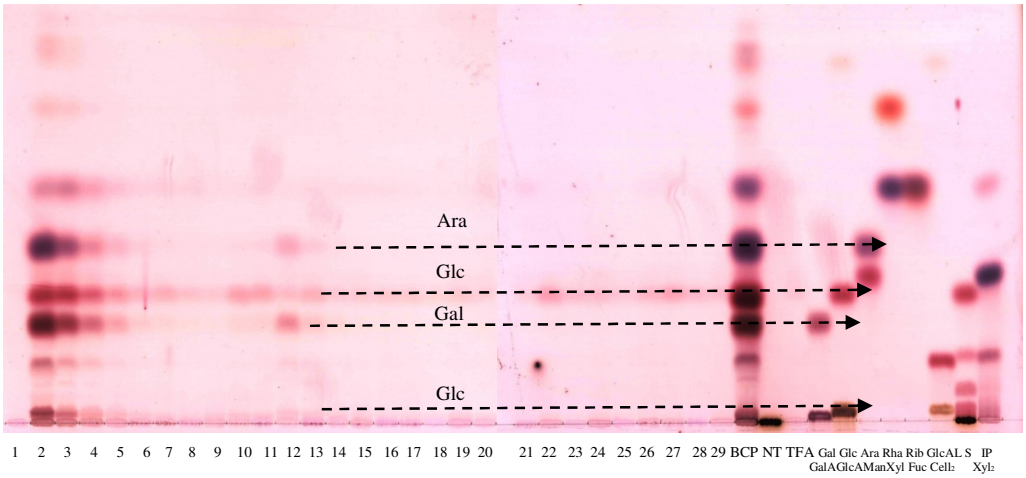


Figure 75. Thin-layer chromatography of TFA-hydrolysates of fractions of BCP from the cation-exchange column.

After the SP-Sephadex column (details as in Figure 74), 50 µl of each fraction in water was hydrolysed with 2 M TFA, dried in the SpeedVac, re-dissolved in 3 µl water, and loaded onto the TLC plate. Solvent: EPyAW 6:3:1:1, thymol staining.

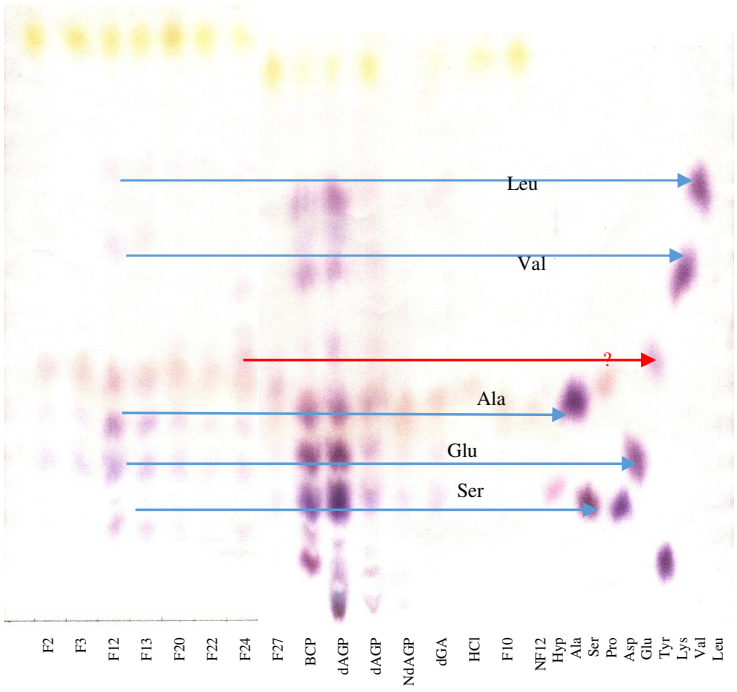


Figure 76. Paper chromatography of HCl-hydrolysates of fractions of BCP from the cation-exchange column.

After the SP-Sephadex column (details as in Figure 74), 200 µl of each fraction in water was hydrolysed with 6 M HCl/ 10 mM phenol at 110ºC for 20 h, dried in the SpeedVac, re-dissolved in 20 µl 1 M $NH_3$. Of that, 5 µl was loaded onto Whatman No.1 for chromatography. Solvent: BAW 12:3:5, 22 h, ninhydrin staining. Each marker was used as 5 µg. BCP, dAGP (dialysed AGP) and dGA (dialysed GA) were all treated with HCl; NdAGP is non-treated dAGP; NF12 is non-treated fraction 12.

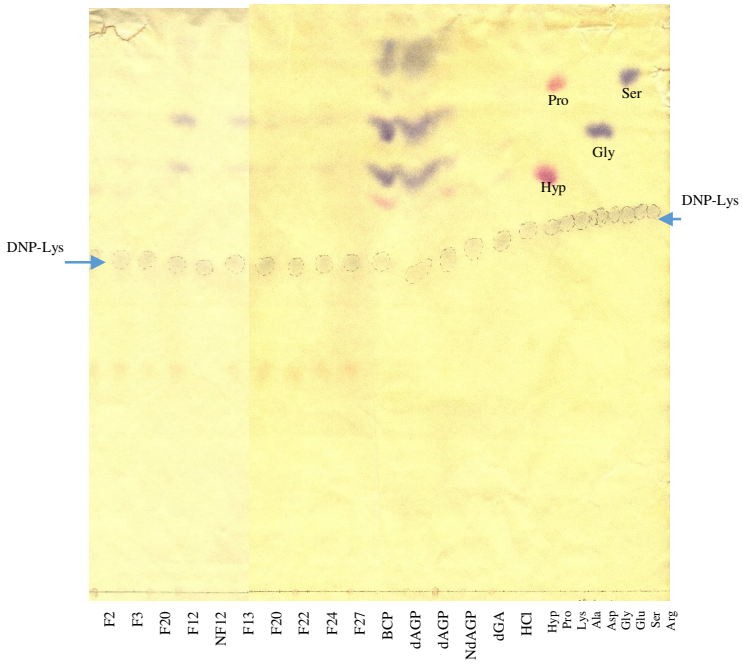


Figure 77. Paper electrophoresis of HCl-hydrolysates of fractions of BCP from the cation-exchange column.

After the SP-Sephadex column, 200 µl of each fraction in water was hydrolysed with HCl; details as in Figure 74. After acid hydrolysis, 10 µl sample was mixed with 5 µl 0.5% DNP-Lys, and loaded onto Whatman No.1 for paper electrophoresis at 3.5 kV, 20 min. Isatin/ninhydrin staining. Each marker (5 µg) was mixed with 5 µl 0.5% DNP-Lys. Other details as in Figure 74.

After the cation-exchange column in Figure 74, I obtained 2 separate peaks of XAF activity. The first peak was in fractions 12 and 13, eluted with 30 mM pyridine suggesting that it had a small number of positive charges. The second peak was in fractions 23 and 24, eluted with 700 mM pyridine suggesting that it had a large number of positive charges. Both peaks contained a very small amount of carbohydrate and a high concentration of protein (Figure 74). Fraction 2, 3, 4 which contained the majority of carbohydrate had no XAF activity.

On the TLC plate, fractions 12 and 13 contained a trace of Ara, Gal, Glc and uronic acid residues while fractions 23 and 24 contained only detectable Glc; however, Glc was found in all fractions after the cation column (Figure 75). On the paper chromatogram, fractions 12 and 13 contained the same amino acids as BCP, including Ser, Glu, Ala, Val, and Leu/Ile while fractions 23 and 24 contained a trace amount of Ser, Glu, Ala, and an unknown amino acid (Figure 76).

Using isatin/ninhydrin, a specific stain to detect Hyp and Pro, after paper electrophoresis, I found that although Hyp and Pro were released in HCl-treated BCP as in non-dialysed AGP, none of the HCl-treated cation-fractions contained detectable Hyp whereas Gly and Ser were detected in fraction 12 (Figure 77).

On the SDS-PAGE, fractions 12 and 13 contained several protein bands with molecular weights of approximately 66, 45, 31, 27, 20 and 19 kDa (Figure 78). All these bands were also found in the XAF-active fractions after the anion-exchange column (Figure 72).

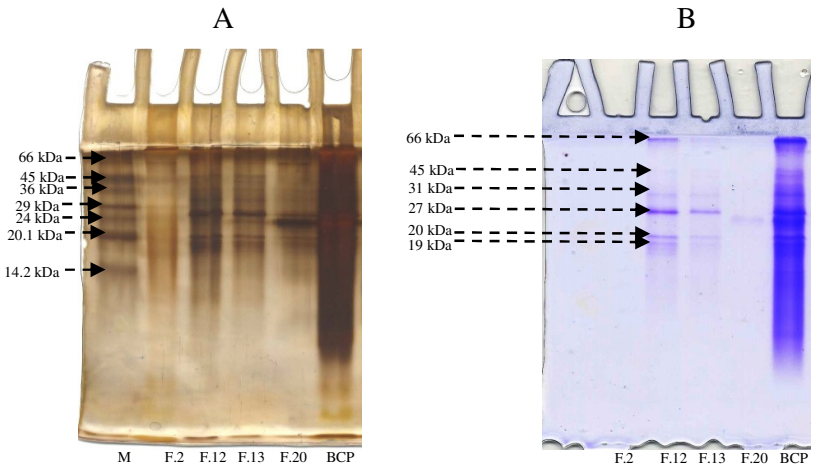


Figure 78. SDS-PAGE of fractions of BCP from the cation-exchange column.

After the SP-Sephadex column (details as in Figure 74), 100 µl of each sample in water was dried in the SpeedVac, re-dissolved in 12 µl water and mixed with 3 µl loading sample buffer. Of that, 10 µl was loaded onto an 18% acrylamide gel, electrophoresed, and stained with Coomassie blue (B) and the other 5 µl was loaded onto another gel, electrophoresed, and stained with silver nitrate (B). M: Protein ladder.

In conclusion, using cation-exchange column chromatography, I obtained two separate narrow peaks of XAF activity; one had a small number of positive charges with high activity and the other had a large number of positive charges with a smaller XAF activity suggesting that XAFs are proteins because there are no known polysaccharides in the plant cell which have a positive charge. The high XAF-activity peak contained a predominance of Ara, Gal, Glc and uronic acid as well as Glu, Ala, Val, Leu/Ile, Gly and Ser. The result continues to support the idea that AGPs were present in BCP and may work as XAF. From the above results, I realised that using a single method could not purify XAF from BCP. Therefore, I tried different combinations of several

methods to improve purification. Two successful combinations were found which are described in sections 3.4.2 and 3.4.3.

### 3.4.2 Purification of XAF by the use of sequential cation- and anion-exchange column chromatography

#### 3.4.2.1 Partial purification of BCP by the use of cation-exchange column chromatography

Firstly, BCP was applied onto a cation-exchange column, which gave two peaks of XAF activity (Figure 79). The first peak was eluted from fractions 12 to 14 with 30 mM pyridine, pH 5.3 which had weakly positive charged group. This peak contained the largest amount of protein and was rich in Ser, Glu, Ala, Val, Leu/Ile, Gly and some unnamed amino acid residues (Figure 81). On the SDS-PAGE, there were few bands of proteins which had the molecular weight of approximately 19, 20 and 27 kDa (Figure 82). This peak also contained a small amount of polysaccharides or glycoproteins, mainly in fraction 12, which contained the main monosaccharides Gal and Ara, a trace of GlcA, GalA, Xyl and an aldobiouronic acid (Figure 80).

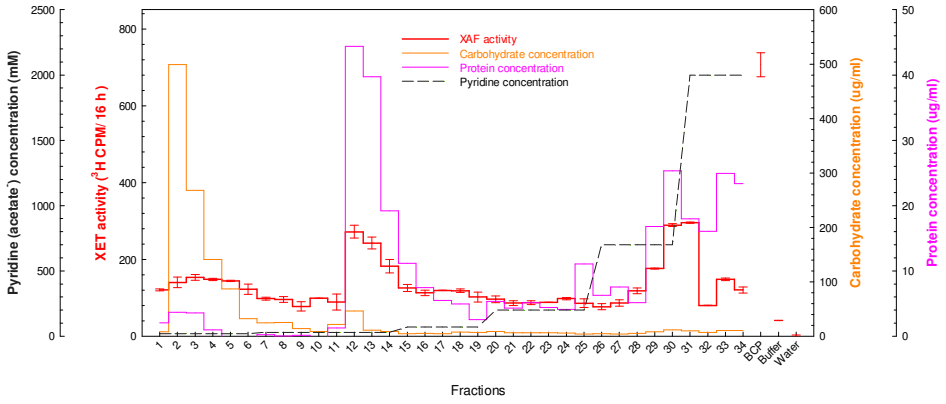


Figure 79. Cation-exchange column chromatography of BCP.

BCP (12 mg) in 20 mM pyridine (formate), pH 3, was loaded onto a 36-ml bed volume column of SP-Sephadex (pyridinium form) and 6-ml fractions were collected. The eluents were different concentrations of pyridine adjusted to pH 5.3 with acetic acid. The fractions were dried in the SpeedVac, re-dried from water and re-dissolved in 6 ml water. Of that solution, 150 µl was dried in the SpeedVac, and re-dissolved in 150 µl NaCl/MES buffer for XAF assay; data show the means of two determinations ± SE (red line). For measuring carbohydrate concentration (orange line), 20 µl of each fractions 2, 3 and 4; 100 µl of each fractions 5 to 12, or 400 µl of each of the other fractions was used in a phenol-sulphuric assay. The protein concentration was measured by Bradford assay in which 300 µl of each fraction was used.

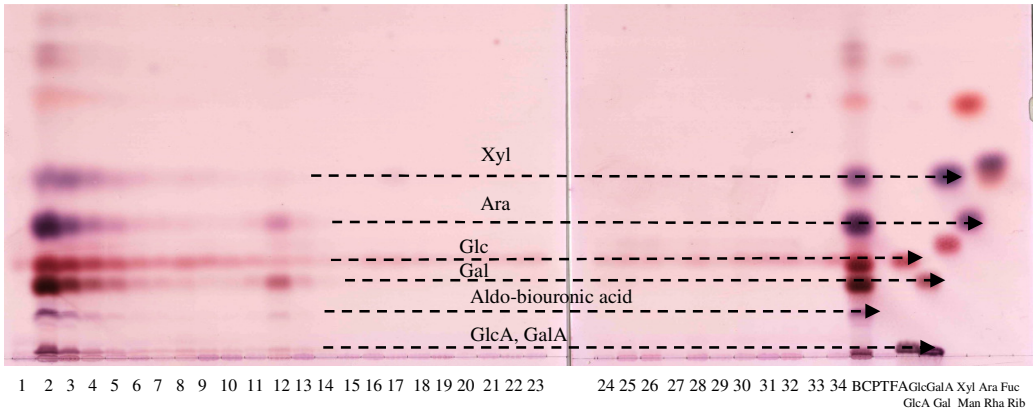


Figure 80. Thin-layer chromatography of TFA-hydrolysates of fractions of BCP after cation-exchange chromatography.

After the SP-Sephadex column in Figure 79, 50 µl of each fraction in water was hydrolysed with 2 M TFA. Acid was removed in the SpeedVac and the sample was re-dissolved in 2 µl water and loaded onto the TLC plate. Solvent: EPyAW 6:3:1:1, thymol staining.

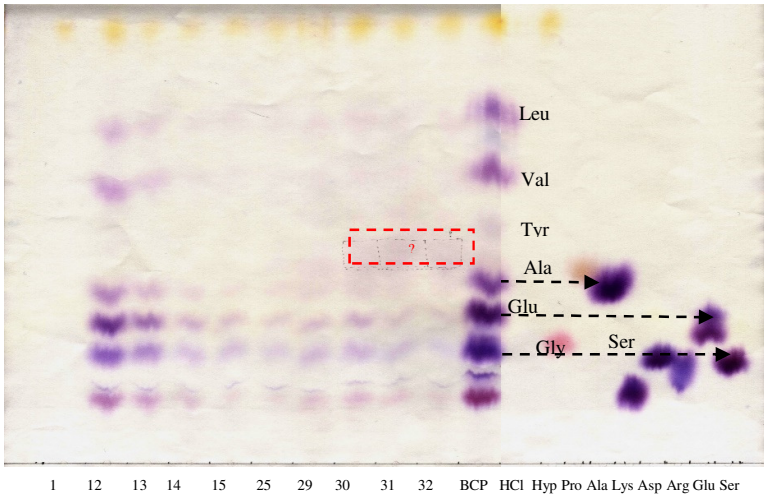


Figure 81. Paper chromatography of HCl-hydrolysates of fractions of BCP after cation-exchange chromatography.

After SP-Sephadex column in Figure 79, 100 µl of each fraction in water was hydrolysed with 6 M HCl/ 10 mM phenol at 110ºC for 20 h, dried in the SpeedVac, re-dissolved in 10 µl 10 mM $NH_3$ and loaded onto a Whatman No.1 to be chromatographed in solvent: BAW 12:3:5, 24 h. Ninhydrin staining.

The second peak was eluted from fraction 29 to 31 with 700-2000 mM pyridine (acetate), pH 5.3, suggesting that it had numerous positively charged groups (Figure 79). This peak had a high protein concentration and same amino acid compositions as in fraction 12 and a trace of unique unknown amino acids (Figure 81). In contrast to the first peak, this peak had a low carbohydrate concentration (Figure 79) which

mainly contained Glc residues; however, Glc was also found in all fractions from the column (Figure 80). On the Coomassie stained gel, this peak had a very faint band of protein with a molecular weight of approximately 24 kDa and on the silver-stained gel, it also had a faint silver-nitrate stained band with a molecular weight less than 6.5 kDa suggesting that the amount of these proteins in BCP are much smaller than those proteins in fractions 12 and 13 (Figure 82).

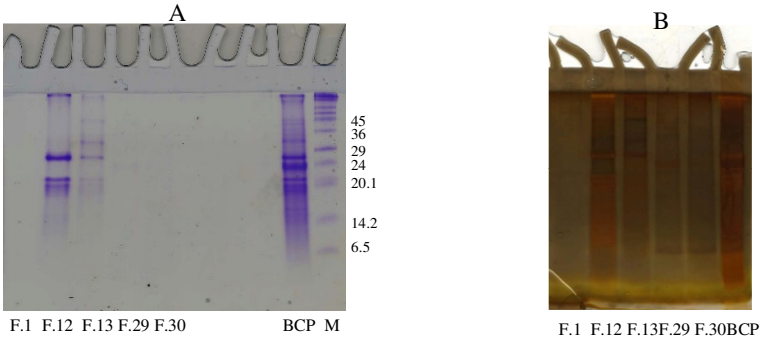


Figure 82. SDS-PAGE of XAF-active fractions of BCP after cation-exchange chromatography.

After SP-Sephadex column in Figure 79, 100 µl of each fraction in water was dried in the SpeedVac, re-dissolved in 12 µl water and mixed with 3 µl loading sample buffer. Of that, 10 µl was loaded onto an 18% acrylamide gel, electrophoresed, and stained with Coomassie blue (A) and 5 µl was loaded onto another 18% acrylamide gel, electrophoresed, and stained with silver nitrate (B).

In conclusion, from the cation-exchange column, I obtained two peaks of XAF activity suggesting that XAF carried positive charges. The cation-exchange chromatography was sufficient to separate a major amount of co-extracted polysaccharides from XAF because most of polysaccharides in plant cells do not possess a positive charge. In addition, the presence of high amount of proteins and carbohydrate in the XAF-active peak suggested that XAF were glycoproteins. The SDS-PAGE showed that the XAF-active peak was not pure and further purification needed to be applied. Fraction 12 from this column was used for further purification. This fraction had a higher amount of protein and carbohydrate as well as XAF activity compared to the other XAF-active fraction.

#### 3.4.2.2 Further purification of fraction 12 from the cation-exchange column by anion-exchange chromatography

Fraction 12 from the cation-exchange column in Figure 79 was passed through an anion-exchange column. Fractions were collected, assayed XAF activity and

hydrolysed with TFA for sugar compositions. After the chromatography, two main peaks of XAF activity were eluted (Figure 83) from fraction 12 which was already known to have a positively charged group, suggesting that XAF also carried negative charges. Proteins in plant cells that also have negatively charged groups are likely to be glycoproteins. The first peak was eluted in fractions 17 to 19 with 0.5 M acetate (pyridinium$^+$) buffer indicating that it had a moderate number of negative charges. This peak contained Gal, Glc and Ara residues (Figure 84), suggesting the presence of an AGP-like proteins. The second peak was eluted from fractions 24 and 25 with 1 M acetate (pyridinium$^+$) buffer revealing that it had a large number of negative charges. This peak had Glc and Gal residues (Figure 84). Fractions 19 and 25 from this column were further analysed by mass-spectrometry.

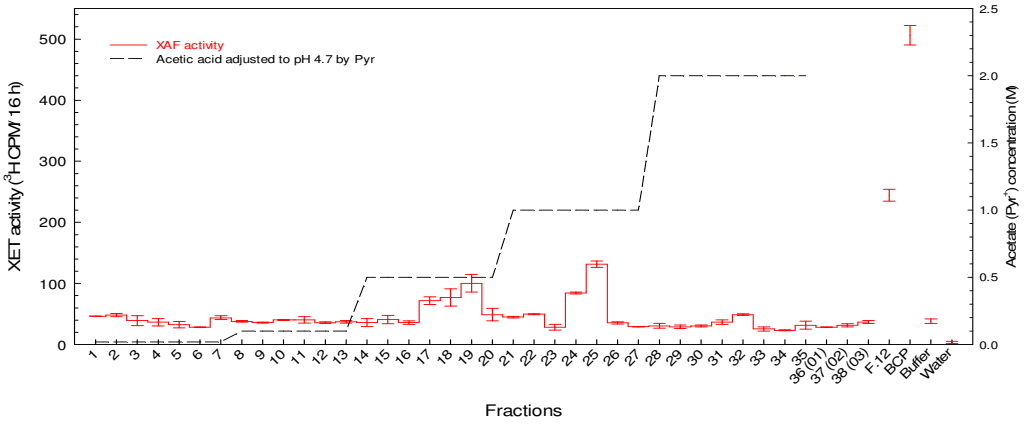


Figure 83. Anion-exchange chromatography of fraction 12 from the cation-exchange column.

After the SP-Sephadex column in Figure 79, 1 ml of fraction 12 was applied onto a 2-ml bed volume Q-Sepharose column (acetate form), and eluted with different concentrations of pyridine adjusted to pH 5.3 with acetic acid. Each fraction was collected as 1 ml, dried in the SpeedVac, re-dried from water and re-dissolved in 1 ml water. Of that, 300 µl was dried in the SpeedVac, re-dissolved in 75 µl NaCl/MES buffer for XAF activity assay; data show the mean of two determinations ± SE.

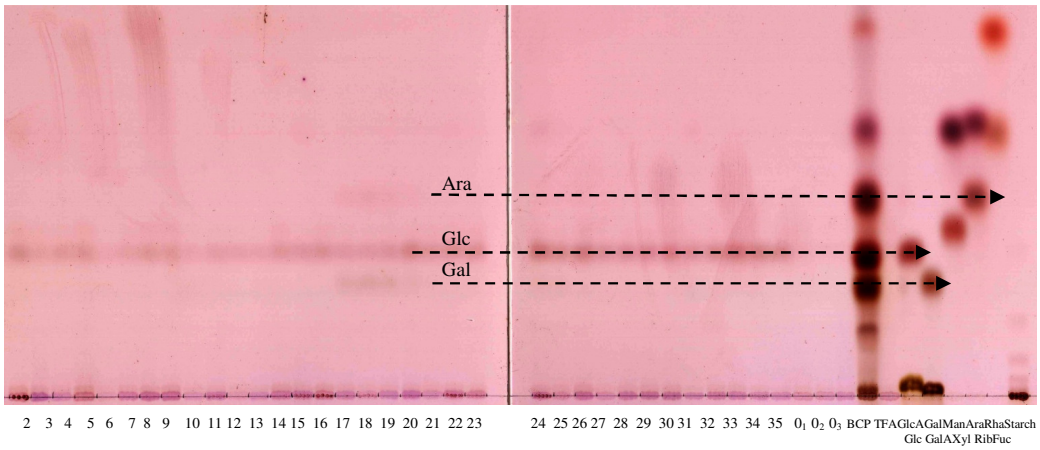


Figure 84. Thin-layer chromatography of TFA-hydrolysates of fractions from anion-exchange column.

After the Q-Sepharose column in Figure 83, 50 µl of each fraction was hydrolysed with 2 M TFA, dried in the SpeedVac, re-dissolved in 2 µl water and loaded onto the TLC plate. Solvent: EPyAW 6:3:1:1, thymol staining. $0_1$, $0_2$, and $0_3$: fractions collected before loading fraction 12 onto the column.

### 3.4.3 Purification of XAF by sequential cation-exchange column chromatography, native-PAGE, and electro-elution

#### 3.4.3.1 Purification of XAF from native gels of BCP by electro-elution

The above column method was successful to purify XAF, although after the cation-exchange column, there were still several bands of (glyco?)proteins on gels (Figure 82). I wanted to know which, if any, of these bands was responsible for the XAF activity. Therefore, I considered another method to purify protein bands from gel. Native-PAGE was a potential method because of its advantage in keeping the un-denatured form of the protein, thus retaining its activity. XAF is expected to be stable under the native-PAGE conditions because it had withstood boiling. Electro-elution from the gel was a suitable method to recover the proteins from the gel. In order to set up the method for this purpose, I firstly tried total BCP, which has very high XAF activity.

After running BCP on a 10% acrylamide native gel, the gel was cut into 1-cm slices, which were put into dialysis tubes together with native running buffer (Tris-glycine, pH 8.5). The dialysis sacs were placed into a normal electrophoresis tank which was filled with the same running buffer and the electrophoresis was allowed to occur for 15 min at 200 volts. This time and voltage was sufficient for all proteins to be mobile out of the gel slices but still inside the sac. The sacs were then dialysed with water to

get rid of Tris-glycine and the solution inside each sac was tested on an analytical gel (Figure 85) and assayed for XAF activity (Figure 86).

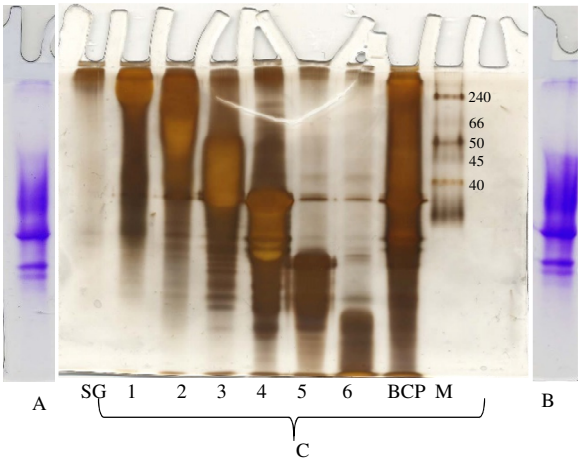


Figure 85. Preparative and analytical native-PAGE of fractions of BCP before and after electro-elution.

BCP was loaded onto a 10% acrylamide native gel. After running, the gel was cut into 1-cm slices and each slice was put into 12000-14000 MWCO dialysis tubing with 5 ml native gel running buffer (Tris-glycine, pH 8.5). The sacs were put into a running electrophoresis tank filled with Tris-glycine pH 8.5 buffer which then ran at 200 volts, 15 min to be eluted. After that, the sacs were dialysed against 5 l of 0.2% chlorobutanol in a 5-l beaker for 18 h (changed to water at 14 h). Each sac was rinsed with water and the solution inside each sac was adjusted to 6 ml. Of that, 2 ml was dried in the SpeedVac, re-dissolved in 9 µl water to be analysed by native-PAGE. A, B: Two edges of the preparative gel, stained with Coomassie blue. C: The analytical gel of fractions after the gel electro-elution, stained with silver nitrate. SG, 1… 6: fraction stacking gel (SG), fraction 1… fraction 6. M: protein marker.

I was successful in separating BCP by this method. After the electro-elution, each gel slice yielded many proteins (Figure 85). All gel slices yielded XAF activity (Figure 86), except the stacking gel (which contained almost nothing) and gel slice 6 which probably contained very low molecular weight peptides.

Therefore, this method was applied for further purification of XAF from the XAF-active fractions after a cation-exchange column.

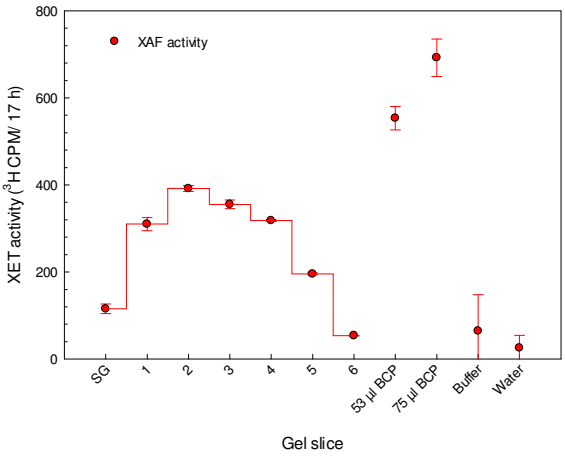


Figure 86. XAF activity of fractions of BCP after native gel electrophoresis and electro-elution.

Details as in Figure 85. After the gel elution, each of 26.7-fold concentrated fraction was assayed for XAF. Data show the mean of two determinations ± SE.

### 3.4.3.2 Purification of XAF by native-PAGE of XAF-active fractions from a cation-exchange column

Firstly, BCP was partially purified by cation-exchange chromatography (Figure 87). Fractions 15 and 30, which had the highest XAF activities from each XAF-active peak, were used to further purify XAF by gel electro-elution (Figure 87).

Fraction 15 was electrophoresed on a 10% acrylamide native gel, and electro-eluted with the method described above. I obtained a peak of XAF activity in gel slice 2 (Figure 89). This peak contained a band of a protein with the molecular weight of approximately 40 kDa (Figure 88A, B). This fraction, putative XAF, was analysed by mass-spectrometry.

Similarly, fraction 30 from the cation-exchange column was preparatively electrophoresed, yielding three fractions with XAF activity, eluted from slices 2, 3 and 6 (Figure 91). Slice 6 did not yield any detectable bands on the analytical gel (Figure 90). Slice 2 showed a faint band of protein on the preparative gel and several bands on the analytical gel (Figure 90). Slice 3 yielded the most abundant protein band from the preparative gel with a molecular weight of approximately 29 kDa and several bands on the analytical gel (Figure 90). These three solutions were further analysed by mass-spectrometry.

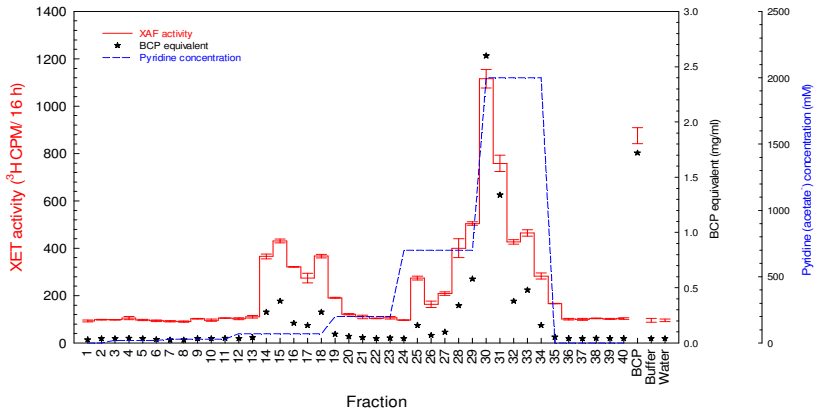


Figure 87. Fractions of BCP after cation-exchange chromatography.

Dried BCP (24 mg) was re-dissolved in 12 ml 20 mM pyridine (formate), pH 3, loaded onto a 48-ml bed volume SP-Sephadex column (pyridinium form), and eluted with different concentrations of pyridine adjusted to pH 5.3 with acetic acid. After elution, 6-ml fractions were dried in the SpeedVac and re-dissolved in 6 ml water. Of that solution, 300 µl was dried and re-dissolved in 150 µl NaCl/MES buffer for XAF assay. Data show the mean of two determinations ± SE.

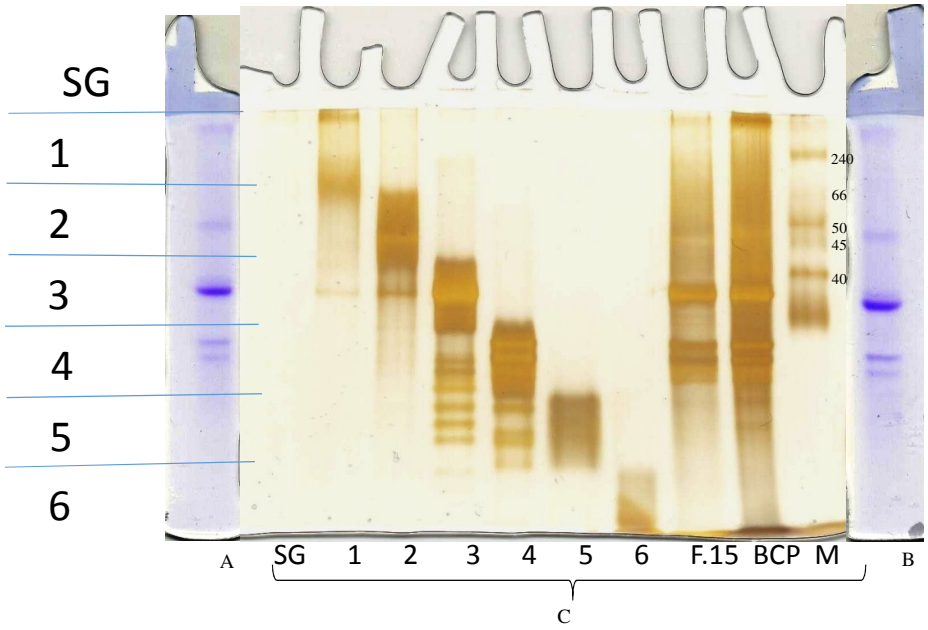


Figure 88. Preparative and analytical native-PAGE of fraction 15 from the cation-exchange chromatography.

Fraction 15 (2 ml) from the column in Figure 87 was electrophoresed on a 10% acrylamide native gel, which was cut into slices, and the slices were put into dialysis sacs and run in an electrophoresis tank, dialysed against water for 18 h. After that, the solution inside each sac was adjusted to 6 ml. Of that, 2 ml was dried in the SpeedVac, re-dissolved in water, mixed with loading sample buffer, run, and stained with silver nitrate. A, B: Two edges of the preparative gel, stained with Coomassie blue. C: The analytical gel, stained with silver nitrate.

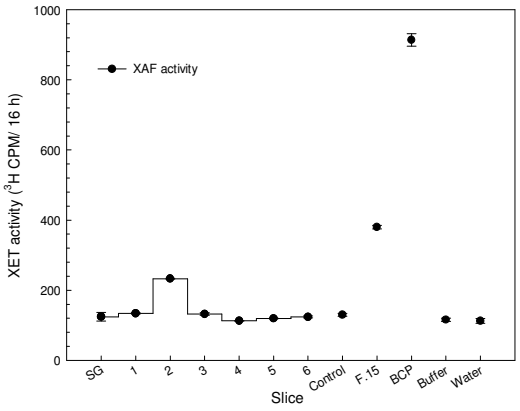


Figure 89. XAF activity of fractions eluted from a native-PAGE of cation-exchange chromatography fraction 15.

After the gel elution (details as in Figure 88), 26.7-fold concentrated fraction inside each sac was assayed for XAF activity. Data show the means of two determinations ± SE. Control: a blank well on a PAGE without loading sample. Fraction 15 (F.15) from the column and BCP (2 mg/ml) were also assayed for XAF activity.

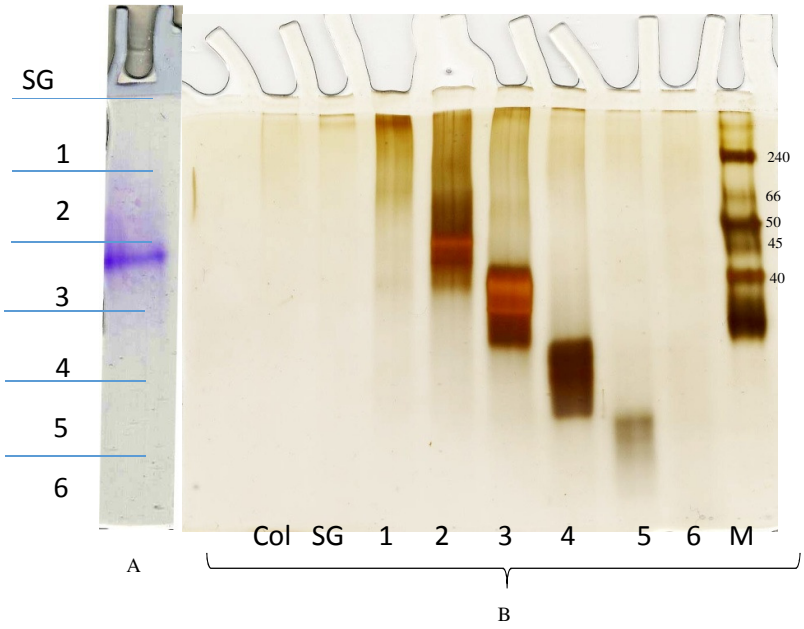


Figure 90. Preparative and analytical native-PAGE of fraction 30 from cation-exchange chromatography.

Fraction 30 (1.8 ml) (Figure 87) was electrophoresed on a 10% acrylamide gel, which was then cut into slices, and the slides were put into dialysis sacs and run in an electrophoresis tank. After that, the solution inside each sac was adjusted to 6 ml. Of that, 2 ml was dried in the SpeedVac, re-dissolved in water, mixed with loading sample buffer, run, and stained with silver nitrate. A, An edge of the preparative gel, stained with Coomassie blue. B: The analytical gel, stained with silver nitrate.

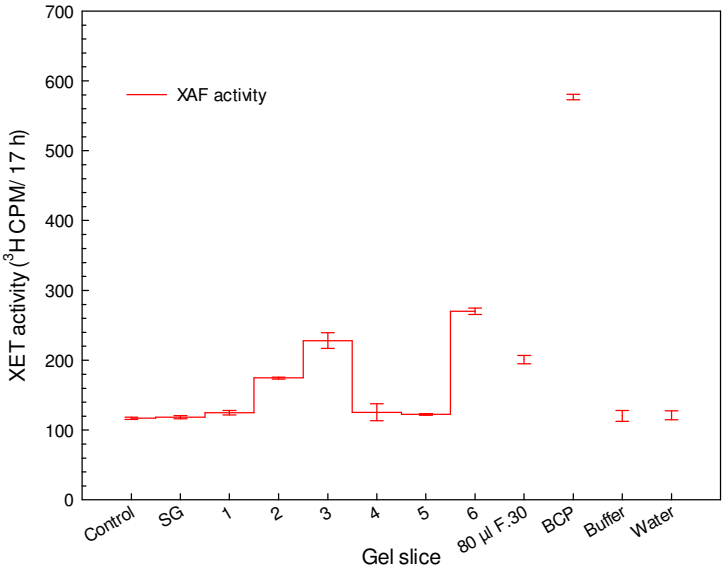


Figure 91. XAF activity of fractions eluted from a native-PAGE of cation-exchange chromatography fraction 30.

After the gel elution (details as in Figure 90, each 26.7-fold concentrated fraction from inside the dialysis sac was assayed for XAF activity. BCP = a control with 2 mg/ml of crude BCP. Data show the means of two determinations ± SE.

## 3.5 BCP and partially purified XAF contained AGP epitopes but purification of AGP from BCP did not enrich in XAF activity

### 3.5.1 Immunological assays of BCP and partially purified XAF with AGP antibodies

Previous experiments showed that BCP and partially purified XAF contained a major amount of Ara, Gal, GalA, GlcA residues, suggesting the presence of arabinogalactan. They also contained some amino acid residues, indicating that glycoproteins such as AGPs were present. Testing with Yariv reagent revealed that BCP and partially purified XAF also gave a positive result for AGPs (Figure 73). Therefore, I used AGP antibodies to investigate which AGP epitopes were present and to study the specific affinity (if any) between XAF-active AGPs and AGP antibodies. BCP and XAF-active fractions (from a cation-exchange column) were assayed with several AGP antibodies, including JIM4, JIM13, JIM16, LM2, and LM14.

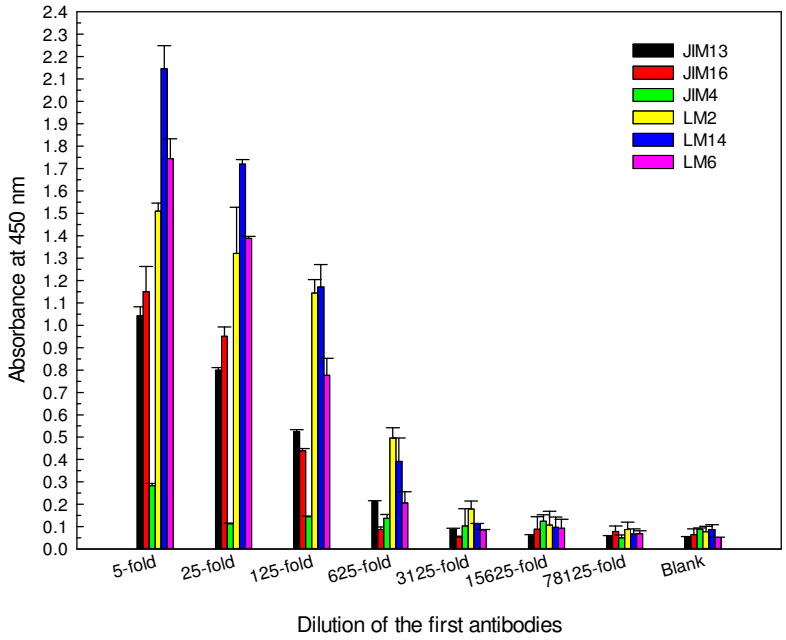


Figure 92. ELISA of BCP with AGP-specific antibodies.

Dried BCP (50 µg) was dissolved in 1 ml 50 mM $Na_2CO_3$, pH 9.6. Of that, 100 µl was mixed with 100 µl of the primary antibody, diluted in BSA in PBS as in the x-axis and the ELISA was carried out as described in section 2.2.15. Briefly, after the incubation with the primary antibody, the second antibody was added for 1.5 h. The horseradish peroxidase substrate was then added, resulting in the development of a blue colour. Colour development was stopped by the addition of sulphuric acid which changed the colour to yellow and optical density is measured spectrophotometrically at 450 nm. Data show the means of two determinations ± SE.

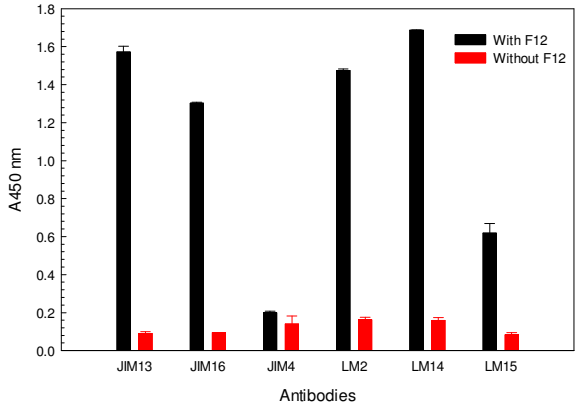


Figure 93. ELISA of fraction 12 of BCP after a cation-exchange chromatography with AGP-specific antibodies.

After the SP-Sephadex column in Figure 79, 1.3 ml of fraction 12 (F.12) was dried in the SpeedVac, re-dissolved in 1.3 ml 50 mM $Na_2CO_3$, pH 9.6 and 100 µl of that was used in an ELISA. The primary antibodies were used as 5-fold dilution and the ELISA was carried out as in Figure 92. Data show the means of two determinations ± SE.

The ELISA showed that BCP was positive with most of the six AGP antibodies tested, up to 625-fold dilution of the antibodies, demonstrating the presence of AGP epitopes. The immunological signals of BCP with all antibodies were clearly dependent on the concentration of the AGP antibodies. BCP had the strongest affinity to LM14, then LM2, JIM16, JIM13, in that order (Figure 92). LM14 recognises AGPs in several species and also binds to larch arabinogalactan (Moller et al., 2008). LM2 recognises AGPs which have a carbohydrate epitope containing β-linked glucuronic acid in several species (Smallwood et al., 1996). The other AGP antibodies are epitope-specific, but recognise as-yet unknown oligosaccharide sequences (Knox et al., 1991). BCP also had affinity to LM6 which was used as a negative control in this experiment (Figure 92). In fact, LM6 may have the ability to bind to AGPs (Prof. J. P. Knox, private communication). LM6 is a high affinity antibody to (1→5)-α-L-arabinosyl residues found in the arabinan components of certain pectic polymers. In immunodot binding assays, LM6 detected 100 ng of purified sugar beet arabinans and was found to be approximately 10-fold more reactive with debranched arabinans suggesting that LM6 does not require a terminal arabinose residue for recognition but can bind to linear (1→5)-*α*-L-linked arabinosyl residues within an extended polymer (Willats et al., 1998). Such structures can be found in some AGPs which contain short arabino-oligosaccharide chains (Ellis et al., 2010). This result suggested that I needed to use a different antibody such as LM15 or LM9 for the negative control. Nevertheless, the fact that BCP did not bind to JIM4 indicated that the ELISA was working fine and that the binding of BCP to other antibodies could be trusted. This result indicated the presence of arabinogalactan-proteins in BCP. AGPs in BCP did not bind to JIM4, suggesting that they had a special structure.

Fraction 12 (F12, from the cation-exchange column), which had the highest XAF activity after cation-exchange chromatography (Figure 79), was also tested with AGP antibodies. There were similar immunological signals of AGP antibodies with F12 compared to those of BCP. F12 was positive with all AGP antibodies tested except JIM4. It had the strongest affinity to LM14, JIM13, LM2 and JIM16, in that order (Figure 93). In this experiment, I used LM15 (an anti-xyloglucan antibody) instead of LM6 as a negative control. F12 also had some affinity to LM15, although the immunological signal between them was 48% of that of JIM16, the lowest

immunological signal obtained between F12 and any of the tested AGP antibodies. This result indicated the presence of AGPs in F12, which agreed with the TLC profile in Figure 80 which showed an abundance of Ara, Gal, GalA and GlcA in F12 and the paper chromatogram in Figure 81 which showed a major amount of Ser, Ala, Glu, Gly, Val and Leu/Ile, thus suggesting the presence of AGPs. It also revealed that there was a small amount of xyloglucan in F12.

To further investigate the contribution of AGPs to the XAF activity, I tested the immunological signals between several XAF-active fractions from another cation-exchange column chromatography and the AGP antibodies (Figure 94).

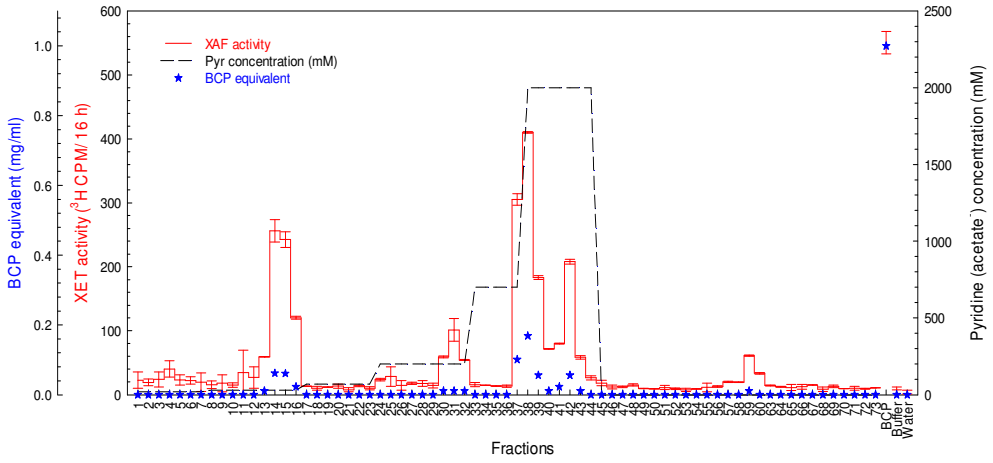


Figure 94. Fractionation of BCP by cation-exchange chromatography prior to ELISA with AGP-specific antibodies.

Dried BCP (20 mg) was dissolved in 10 ml 20 mM pyridine (formate), pH 3.0, and applied onto a 40-ml bed volume SP-Sephadex column (pyridinium form). After elution with different concentrations of pyridine adjusted to pH 5.3 with acetic acid, each fraction was collected as 6 ml, dried in the SpeedVac, re-dried from water and re-dissolved in 4 ml water. Two-fold concentrated fractions were XAF assayed. Data show the mean of two determinations ± SE. BCP equivalent was calculated based on the graphs in Figure 13. Fractions 46 to 56 were eluted with 5 M $NH_3$ and fractions 57 to 73 were eluted with water.

Several XAF-active fractions (F14, 15, 31, 38, 42 and 59) and a fraction with no XAF activity (F3) from the cation-exchange column in Figure 94 were tested with AGP antibodies. LM14, LM2 and JIM16 had the strongest affinities to each fraction tested, in that order, while JIM 13 had affinity to fractions 3, 14 and 15. Again, JIM4 did not show affinity to any of the fractions tested, agreeing with the results from BCP and F12 (Figure 92, Figure 93). LM9, which was used as a negative control in this

experiment, did not have affinity to any of the fractions, except a very low signal with fraction 15 (Figure 95). LM9 recognises the feruloylated (1→4)-β-D-galactan, a structural feature of the pectic polymers of plant species of the Amaranthaceae (formerly termed Chenopodiaceae), which has no known cross-reactivity with other polymers (Prof. J. P. Knox, private communication). LM9 is normally used for the analysis of phenolic substitution of cell wall pectic polymers and of cell wall structure in the Amaranthaceae including sugar beet (*Beta vulgaris* L.) and spinach (*Spinacia oleracea* L.) (Clausen et al., 2004).

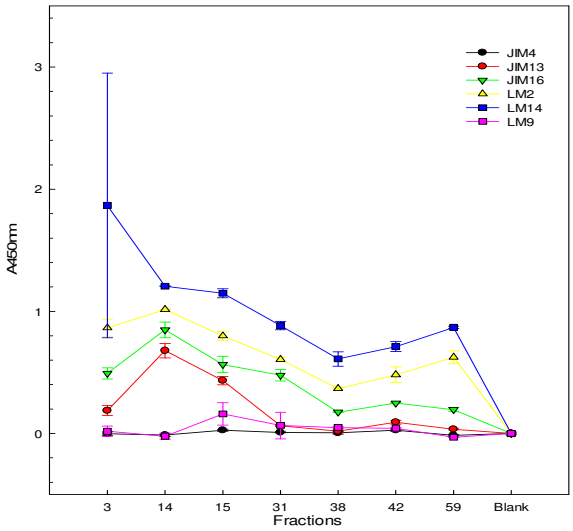


Figure 95. ELISA with AGP antibodies of fractions of BCP after cation-exchange chromatography.

After the SP-Sephadex column in Figure 94, 1.4 ml of each fraction was dried in the SpeedVac, re-dissolved in 1.4 ml 50 mM $Na_2CO_3$, pH 9.6, and 100 µl of that was used in an ELISA. The primary antibodies were used as 5-fold dilution. Data show the means of two determinations ± SE.

Among all fractions tested, fractions 14 and 15 had the highest affinity for all AGP antibodies (Figure 95). Fractions 14 and 15 were the two fractions that had the highest XAF activity in the first XAF-active peak from the cation-exchange column. These two fractions were eluted with low concentration of pyridine (Figure 94), thus contained some polymers which had a small number of positive charge, for example a glycoprotein. These results suggested that the presence of AGPs in these fractions may responsible for the XAF activity.

Fraction 3 had affinity to several AGP antibodies (Figure 95) but did not have any XAF activity (Figure 94) revealing that there were several AGPs in BCP without XAF

activity. A similar explanation could also account for the cases of fractions 31 and 59: although these fractions had a high affinity for most AGP antibodies (Figure 95), they had relatively low XAF activity (Figure 94).

Fraction 38 had the highest XAF activity among all of the fractions from the column (Figure 94); however, it had the lowest immunological signals with all AGP antibodies tested (Figure 95). This suggests that minor polymers rather than the classical AGPs contributed XAF activity.

In conclusion, there was more than one polymer responsible for XAF activity. They were eluted in different fractions from a cation-exchange column. Some of them had a high affinity to AGP-specific antibodies and some of them did not. If only one AGP had been responsible for the XAF activity, I would have expected that the ELISA result would have had the same trend with the XAF activity result. In particular, the affinity with AGP antibodies would have been highest in fraction 38; in fact, it was not. It is possible that in fractions 14 and 15, classical AGP was responsible for the XAF activity while in fraction 38 different proteins or non-classical AGPs were responsible for its high XAF activity.

### 3.5.2 Purification of AGPs from BCP by the use of Yariv reagent did not enrich XAF activity

Yariv reagent is a well-known reagent for determination and purification of AGPs. Since 0.2% Yariv reagent in 1% (0.17 M) NaCl had its own [slight] XAF activity (Figure 97), as seen elsewhere in the thesis it was important to eliminate the salt from the final solution before testing the XAF activity. Two methods were chosen for this purpose: dialysis of the solution containing Yariv-precipitated BCP in NaCl, DMSO and $Na_2S_2O_4$ in 12000-14000 MWCO tubing against water, or passing it through a Bio-Gel P-2 gel-permeation chromatography column.

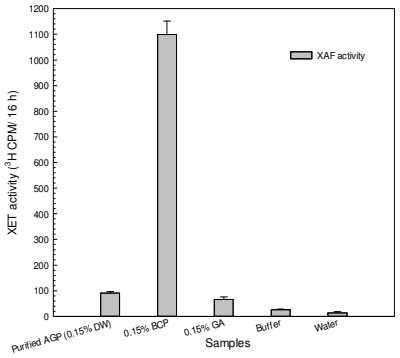


Figure 96. XAF activity of AGP purified from BCP by Yariv reagent followed by dialysis.

Dried BCP (1 mg) was dissolved in 10 ml 1% NaCl and mixed with 0.5 mg β-glucosyl Yariv reagent in a final volume of 20 ml for 24 h at 6°C. The solution was centrifuged and the pellet was collected. The supernatant was re-precipitated, centrifuged and a second pellet was collected. The pellets were pooled, washed 3 times with 50 ml 1% NaCl and 50 ml methanol, and left to dry at room temperature. The pellet was re-dissolved in 5 ml DMSO and minimal solid $Na_2S_2O_4$ with water until pale yellow. This solution was dialysed in 12000-14000 MWCO dialysis tubing against water. The solution inside the sac was freeze-dried; the solids were weighed and re-dissolved in NaCl/MES buffer as a final concentration of 0.15% and assayed for XAF activity. Data show the means of four determinations ± SE. Crude BCP and commercial gum arabic (GA) were also made as 0.15% solutions in NaCl/MES buffer.

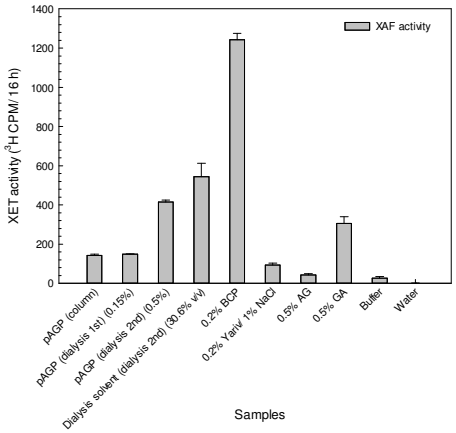


Figure 97. XAF activity of AGP purified by Yariv reagent from BCP followed by gel-permeation chromatography.

Dried BCP (1 mg) was dissolved in 5 ml 1% NaCl and mixed with 0.5 mg β-glucosyl Yariv reagent. The precipitated pellet was washed sequentially with 1% NaCl and 50 ml methanol, and re-dissolved in 5 ml DMSO. Of that, 1 ml was applied onto a 21-ml bed volume Bio-Gel P-2 column, eluting with PyAW 1:1:98, and 1-ml fractions were collected. Factions 10-16, which contained carbohydrate (confirmed by TLC with thymol staining; data not show), were pooled (approximately 6 ml in total), dried in the SpeedVac, re-dried from 200 µl water and re-dissolved in 150 µl NaCl/MES buffer for XAF assay: pAGP (column). Two AGP separately purified by the dialysis method (the first time: pAGP (dialysis 1$^{st}$) 0.15% and the second time: pAGP (dialysed 2$^{nd}$) (0.5%)), and dialysis solvent of the second time of dialysis which then freeze-dried and re-dissolved in NaCl/MES buffer as 30.6% v/v (dialysis solvent (dialyse 2$^{nd}$) 30.6% v/v), crude BCP (0.2% BCP), 0.5% larch arabinogalactan (0.5% AG), 0.5% gum arabic (0.5% GA) were also tested for XAF activity. Data show the means of two determinations ± SE.

With the dialysis method, the purified AGP had 8.3% XAF activity compared to that of BCP and had a slightly higher XAF activity than that of commercial GA at the same concentration (Figure 96). A higher concentration of AGP (0.5%, purified from BCP, and de-salted by dialysis) gave a higher XAF activity; 33.5% that of 0.2% crude BCP and also had a higher XAF activity than that of 0.5% GA (Figure 97). The dialysis solvent also had a high XAF activity suggesting that some purified AGPs escaped from the sac during the dialysis (Figure 97).

The XAF activity of Yariv-precipitated AGP re-dissolved in 1 ml DMSO, de-salted by the column chromatography method, was as same as that of 0.15% AGP de-salted by the dialysis method (Figure 97). Therefore, from 1 mg of dried BCP, the chromatography method gave a higher yield of purified AGP than the dialysis method.

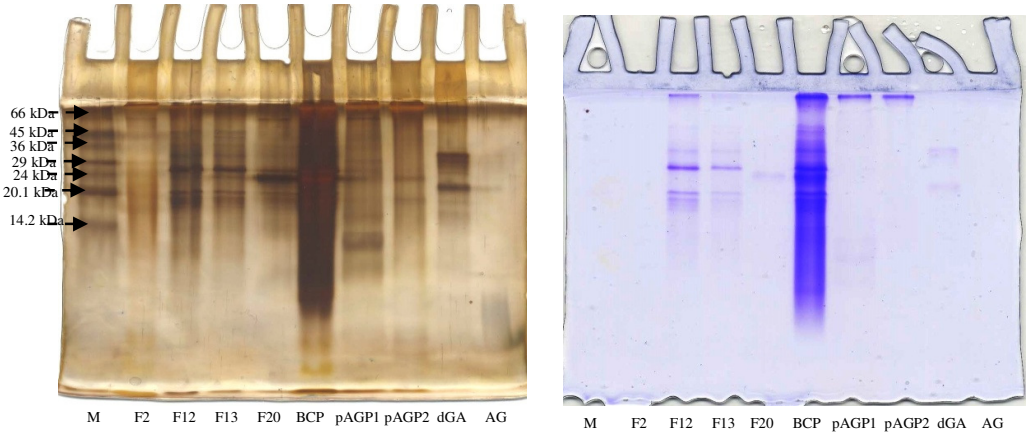


Figure 98. Native-PAGE of fractions of BCP after a cation-exchange column, crude BCP, and purified AGP.

BCP, purified AGP and fractions of BCP from an SP-Sephadex column in Figure 74 (100 µl each) were dried in the SpeedVac, re-dissolved in 12 µl water and mixed with 3 µl sample loading buffer. Of that, 10 µl was loaded onto an 18% acrylamide gel, electrophoresed and stained with Coomassie blue, and another 5 µl was loaded onto another gel, electrophoresed and stained with silver nitrate. M: Markers. F2, 12, 13, 20: Fractions from the cation-exchange column. pAGP1, pAGP2: two separate AGP purified from BCP by Yariv reagent followed by dialysis. dGA: dialysed GA, AG: arabinogalactan from larch wood.

In conclusion, AGP purified from BCP by the use of Yariv reagent had XAF activity. However, the XAF activity of the AGP was lower than that of crude BCP, at the same concentration, regardless of de-salting method, suggesting that the purification of AGP from BCP by Yariv reagent did not enrich the XAF activity. Crude BCP at 0.2% had a much higher XAF activity than that of 0.5% purified AGP or commercial GA or arabinogalactan (Figure 97), indicating that there were other polymers in BCP that

were responsible for the XAF activity besides Yariv-precipitable (classical) AGPs. Crude BCP and the purified AGP showed different bands on the SDS gel (Figure 98) compared with those of a commercial GA, confirming that they contained different AGPs.

## 3.6 Mass-spectrometry analysis results of pure XAF

After being purified by sequential cation- and anion-exchange column chromatography, XAF-active fractions were analysed by mass-spectrometry (MS).

The two XAF-active fractions (19 and 25) from the anion-exchange column in Figure 83 were analysed by MS for potential XAF-active proteins. The results are shown in Table 12 and Table 13.

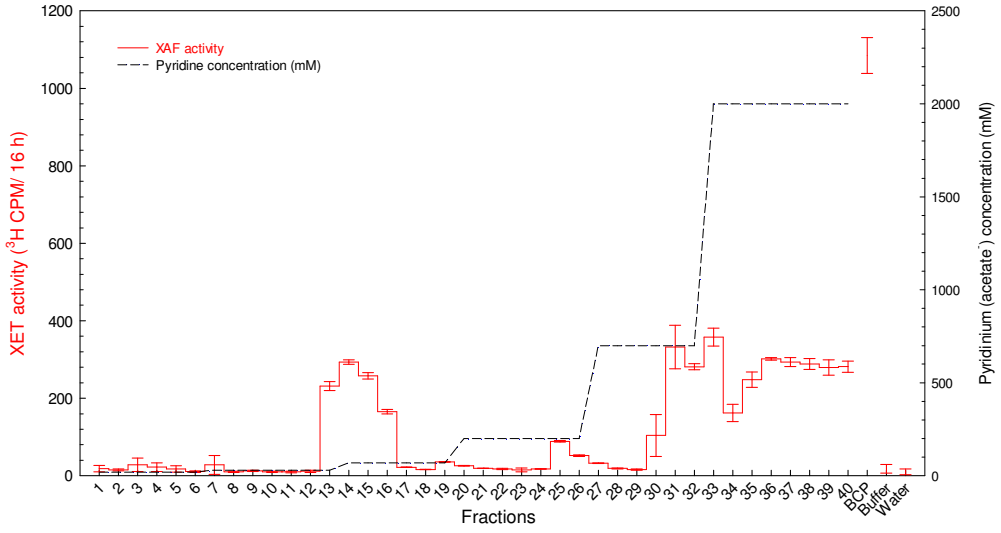


Figure 99. XAF activity of fractions of BCP from a cation-exchange column.

Dried BCP (20 mg) was dissolved in 10 ml 20 mM pyridine (formate), pH 3.0, and applied onto a 40-ml bed volume SP-Sephadex column (pyridinium form). After elution with different concentrations of pyridine adjusted to pH 5.3 with acetic acid, each fraction was collected as 6 ml, dried in the SpeedVac, re-dried from water and re-dissolved in 4 ml water. Two-fold concentrated fractions were XAF assayed. Data show the mean of two determinations ± SE. BCP equivalent was calculated based on the graphs in Figure 13.

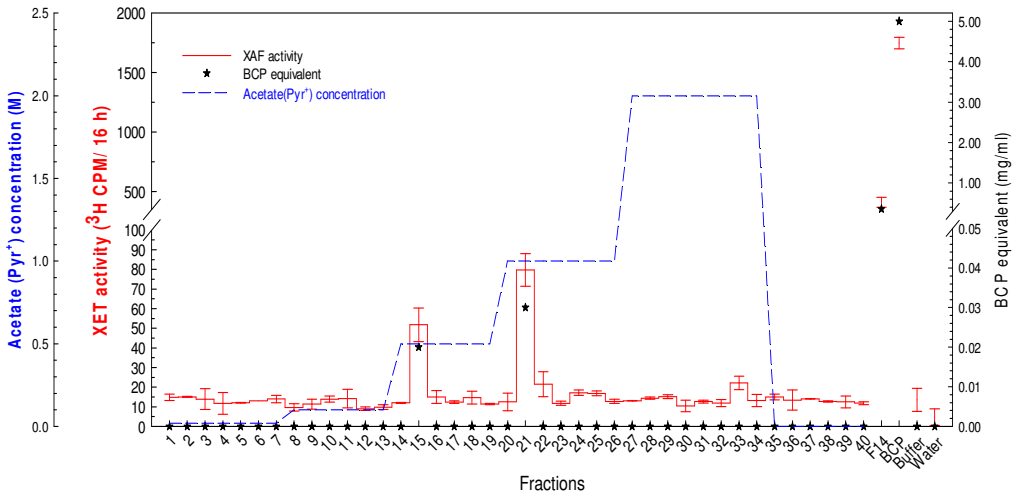


Figure 100. Anion-exchange chromatography of fraction 14 from the cation-exchange column.

Fraction 14 from the SP-Sephadex column in Figure 99 was applied onto a Q-Sepharose column (acetate form); elution was performed as in Figure 83 and fractions were collected, dried in the SpeedVac and re-dissolved in water. Four-fold concentrated fractions were XAF assayed. Two-fold concentrated fraction 14 (F14) (from Figure 99) was also assayed. Data show the mean of two determinations ± SE. BCP equivalent was calculated based on the graphs in Figure 13.

For a repetition, another sequential cation- and anion-exchange column chromatography was also carried out. BCP was applied onto the cation-exchange column in Figure 99 and the fractions were collected as routinely. The fractions were assayed for XAF activity and fraction 14 was used to further purify by anion-exchange column in Figure 100. Fractions were collected and half of each fraction was assayed for XAF activity. Fractions 15 and 21 from the anion-exchange column in Figure 100 which had the highest XAF activity were also analysed by MS, the results are shown in Table 14 and Table 15.

The MS analyses were performed by Ms Lisa Imrie from KPF SynthSys, the University of Edinburgh. In summary, sample's proteins were solubilised in 2 M urea, disulphide bridges were reduced with dithiothreitol (20 mM), blocked with iodoacetamide (50 mM) and digested with trypsin. The resulting peptide mixture was loaded onto a high performance liquid chromatography (HPLC) column coupled to a mass spectrometer to be analysed for identifying its components. The samples were ionised by nano electrospray ionisation (nanoESI). The mass spectrometer was used

in data dependant mode, the five most abundant peptides were selected, isolated and fragmented using collision induced dissociation (CID) to generate MSMS spectra which will be used for identification. The MSMS data were extracted and analysed using a search engine Mascot (Matrix Science) (Perkins et al., 1999) in order to identify the possible peptides from the samples. These search engines matched the tandem mass spectra with peptide sequences from a protein sequence database (in this case, we used the entire NCBI database) and used the identified peptides to infer the protein content of the sample. Data were further analysed by the use of NCBI basic local alignment search tool (BLAST) for the determination of proteins in *Arabidopsis* and *Brassica*. Only proteins which have more than one peptides identified with a threshold score of 20 were considered for further analysis.

Table 12. Mass-spectrometry result of fraction 19 from the column in Figure 83.

| Prot_acc[1] | Protein description[2] | Protein score[3] | Protein mass | Significant different peptides | Peptide sequences |
|---|---|---|---|---|---|
| gi\|15238698\|ref\|NP_197891.1\| | Predicted: Early nodulin-like protein 3 (ENODL3) [*Brassica rapa*]; ENODL13 [*Arabidopsis thaliana*] | 66 | 19926 | 2 | DSVLQVTK |
| | | | | | IPSSPSESLNK |
| gi\|4559346\|gb\|AAD23007.1\| | Predicted: ENODL1 [*Brassica rapa*]; ENODL14 [*Arabidopsis thaliana*] | 59 | 19062 | 3 | VGDFIVFR |
| | | | | | IPPSSSYSFTEWAQK |
| | | | | | DSVLQVTR |
| gi\|18395849\|ref\|NP_565313.1\| | Fasciclin-like arabinogalactan protein 7 (FLA7) [*Brassica rapa*], [*Arabidopsis thaliana*] | 44 | 26886 | 2 | FTDVSGTVR |
| | | | | | VSSSVFSTDPVAVYQVNR |

[1]Protein gi identifier from NCBI database

[2]Protein description from NCBI database

[3]Sum of the Mascot peptide scores

Table 13. Mass-spectrometry result of fraction 25 from the column in Figure 83.

| Prot_acc[1] | Protein description[2] | Protein score[3] | Protein mass | Significant different peptides | Peptide sequences |
|---|---|---|---|---|---|
| gi\|18395849\|ref\|NP_565313.1\| | FLA7 [*Brassica rapa*], [*Arabidopsis thaliana*] | 192 | 26886 | 2 | FTDVSGTVR |
| | | | | | VSSSVFSTDPVAVYQVNR |
| gi\|1154629\|emb\|CAA64428.1\| | Pollen coat protein [*Brassica oleracea*]; Early response to dehydration 14 (ERD14) [*Arabidopsis thaliana*] | 124 | 22425 | 4 | VHISEPVPEVK |
| | | | | | VATEESSTATGEVTDR |
| | | | | | VHISEPVVPEVK |
| | | | | | VTTEESSAEVTDR |
| gi\|38456238\|gb\|AAR21079.1\| | Stress responsive protein [*Brassica oleracea var. acephala*]; Low-temperature-induced protein 65 (LTI65, LTI140) [*Arabidopsis thaliana*] | 237 | 66964 | 6 | LPGDEIFPTR |
| | | | | | HVAPVNEVSNVR |
| | | | | | DAAYEHEAPLYPVR |
| | | | | | ETHHAPLNTPVSLLSGTEDVTTPGGDGLLGGQR |
| | | | | | GLPTETDDHFSPEFSGPK |
| | | | | | TSQPESLTHPGENNVPAPEEIIPSETK |
| gi\|4559346\|gb\|AAD23007.1\| | Predicted: ENODL1 [*Brassica rapa*]; ENODL14 [*Arabidopsis thaliana*] | 49 | 19062 | 4 | VGDFIVFR |
| | | | | | IPPSSSYSFTEWAQK |
| | | | | | DSVLQVTK |
| | | | | | IPSSPSESLNK |
| gi\|15240353\|ref\|NP_200987.1\| | Predicted: calnexin homolog 1-like [*Brassica rapa*]; Calnexin 1 (CNX1) [*Arabidopsis thaliana*] | 32 | 60790 | 3 | ILVDGEEK |
| | | | | | CEAAPGCGEWK |
| | | | | | ANLLSGEDFEPALIPAK |
| gi\|4588474\|gb\|AAD26119.1\|AF108123_1 | Predicted: phosphoinositide phospholipase C2 [*Brassica rapa*]; Phosphoinositide | 32 | 66632 | 2 | EVPSFIER |
| | | | | | ALGDEEVWGR |

| | | | | | |
|---|---|---|---|---|---|
| | phospholipase C2 [*Arabidopsis thaliana*] | | | | |
| gi\|1402947\|emb\|CAA67054.1\| | Calmodulin 1 [*Brassica oleracea*] | 100 | 16879 | 2 | EAFSLFDK |
| | | | | | EADVDGDGQINYDEFVK |
| gi\|89257499\|gb\|ABD64989.1\| | Hypothetical protein 26.t00005 [*Brassica oleracea*] | 68 | 190413 | 2 | SIAIPVGEAAEETNEK |
| | | | | | MESTTELMTEDQEYGK |
| gi\|14190409\|gb\|AAK55685.1\|AF378882_1 | FLA10 [*Brassica rapa*] ; FLA8 [*Arabidopsis thaliana*] | 53 | 42471 | 2 | DAISTLATNGAGK |
| | | | | | GLTVFAPSDEAFK |

Table 14. Mass-spectrometry result of fraction 15 from the anion-exchange column in Figure 100.

| Prot_acc[1] | Protein description[2] | Protein score[3] | Protein mass | Significant different peptides | Peptide sequences |
|---|---|---|---|---|---|
| gi\|38456238\|gb\|AAR21079.1\| | Stress responsive protein [*Brassica oleracea var. viridis*] ; LTI65, LTI140 [*Arabidopsis thaliana*] | 231 | 66964 | 8 | LNLGEEK |
| | | | | | LPGDEIFPTR |
| | | | | | HVAPVNEVSNVR |
| | | | | | DSTDYTGTVPEPSR |
| | | | | | DAAYEHEAPLYPVR |
| | | | | | GLPTETDDHFSPEFSGPK |
| | | | | | GHEFEQAIGSGIGEDNGAGK |
| | | | | | TSQPESLTHPGENNVPAPEEIIPSETK |
| gi\|4559346\|gb\|AAD23007.1\| | Predicted: ENODL1 [*Brassica rapa*]; ENODL14 [*Arabidopsis thaliana*] | 102 | 19062 | 3 | VGDFIVFR |
| | | | | | IPPSSSYSFTEWAQK |
| | | | | | DSVLQVTR |
| | Predicted: lysM domain-containing GPI-anchored | 248 | 44572 | 2 | IPITCSCVDGIR |

| | | | | | |
|---|---|---|---|---|---|
| gi\|297845178\|ref\|XP_002890470.1\| | protein 1-like [*Brassica rapa*], [*Arabidopsis thaliana*] | | | | CPGPQQFAPLLAPPDTVPK |
| gi\|60498645\|dbj\|BAD90706.1\| | Plastid DNA-binding protein [*Brassica napus*] | 120 | 52258 | 2 | GLEETPFIETR |
| | | | | | TVNPASVDVESADTK |
| gi\|90654235\|gb\|ABD95987.1\| | Predicted: dehydrin ERD14-like [*Brassica rapa*]; Dehydrin 14 (ERD14) [*Arabidopsis thaliana*] | 104 | 22033 | 2 | VHISEPVVPEVK |
| | | | | | VTTEESSAEVTDR |
| gi\|238837078\|gb\|AAR15704.3\| | Class III heme peroxidase [*Brassica rapa*]; Peroxidase ATP29a [*Arabidopsis thaliana*] | 41 | 32467 | 2 | GFNVVDDIK |
| | | | | | MGNISPLTGSSGEIR |
| gi\|18395849\|ref\|NP_565313.1\| | FLA7 [*Brassica rapa*], [*Arabidopsis thaliana*] | 80 | 26886 | 1 | VSSSVFSTDPVAVYQVNR |

Table 15. Mass-spectrometry result of fraction 21 from the anion-exchange column in Figure 100.

| prot_acc Protein identifier[1] | Protein description[2] | Protein Score[3] | Protein mass | prot_sequences_sig | Peptide sequences |
|---|---|---|---|---|---|
| gi\|38456238\|gb\|AAR21079.1\| | Stress responsive protein [*Brassica oleracea var. viridis*] ; LTI65, LTI140 [*Arabidopsis thaliana*] | 249 | 66964 | 6 | DDFDSQAEQTR |
| | | | | | DSTDYTGTVPEPSR |
| | | | | | DAAYEHEAPLYPVR |
| | | | | | GLPTETDDHFSPEFSGPK |
| | | | | | TSQPESLTHPGENNVPAPEEIIPSETK |
| | | | | | ETHHAPLNTPVSLLSGTEDVTTPGGDGLLGGQR |
| gi\|18395849\|ref\|NP_565313.1\| | FLA7 [*Brassica rapa*] | 79 | 26886 | 2 | FTDVSGTVR |
| | | | | | VSSSVFSTDPVAVYQVNR |
| gi\|4559346\|gb\|AAD23007.1\| | Predicted: ENODL1 [*Brassica rapa*]; ENODL14 [*Arabidopsis thaliana*] | 66 | 19062 | 3 | VGDFIVFR |
| | | | | | IPPSSSYSFTEWAQK |

| | | | | | |
|---|---|---|---|---|---|
| gi\|1518113\|gb\|AAB49423.1\| | Predicted: methyltransferase-like protein 10 [*Brassica rapa*]; AR401 [*Arabidopsis thaliana*] | 49 | 37291 | | HADAAEALSSANFR |
| gi\|118487683\|gb\|ABK95666.1\| | Predicted: mediator of RNA polymerase II transcription subunit 37f [*Brassica rapa*]; luminal binding protein [*Arabidopsis thaliana*] | 44 | 13550 | 2 | NSLETYVYNMK |
| | | | | | EVEAVCNPIITAVYQR |

Several different proteins co-eluted in the XAF-active fractions (fraction 19 and 15, fraction 25 and 21). This was because I changed the way to prepare samples for MS. After the Q-Sepharose column in Figure 83, the XAF-active fractions were directly applied to MS, and thus were contaminated with many non-plant proteins such as trypsin, keratin and albumin (data not show), probably from hair, finger nail and dust in the laboratory. In order to avoid this contamination, XAF-active fractions from the later Q-Sepharose column (Figure 100) were filtered through a 0.45-µm Minisart filter unit. As a result, contaminating insoluble materials (hair, dust, finger nail) were removed so the contaminating proteins were eliminated but not the proteins of interest because all of them are soluble and thus passed through the 0.45-µm filter. More relevant proteins were therefore detected (Table 14, Table 15).

Interestingly, two proteins appeared in the four fractions including FLA7 and ENODL14. One protein, LTI65, appeared in both fractions from the anion-exchange column (Figure 100). This suggests that FLA7, ENODL14 and LTI65 were abundant proteins which were likely to be responsible for the XAF activity. Looking for their functions on The *Arabidopsis* Information Research (TAIR) website (https://www.arabidopsis.org/), I found possible reasons why those three proteins could have potential abilities to work as an XAF. FLA7 is a non-classical arabinogalactan-protein which is located in the plasma membrane (Borner et al., 2003; Johnson et al., 2003), a position that makes it easy to contact and solubilise XTHs from the cell walls. ENODL14 is also a non-classical AGP, also located in the plasma membrane that has known electron carrier activity (Mashiguchi et al., 2009; Denancé et al., 2014). LTI65 is a stress-responsive protein (Nordin et al., 1993) and was found

abundantly in both fractions (fractions 15 and 21) so it may somehow contribute to the XAF activity.

Therefore, I chose those three proteins to further investigate their functions on the model plant, *Arabidopsis*. *Arabidopsis* mutants defective in those genes were grown and tissues were collected for testing the XAF activity. The results are shown in 3.8.

## 3.7 HF-treatment of pure XAF-active fractions and their mass-spectrometry results

Many results in this study support the idea that XAFs were glycosylated proteins. Thus, a method was considered to specifically attack the carbohydrate part of XAF, to see how they contributed to the XAF activity. BCP and the XAF-active fractions from a cation-exchange column (fractions 16 and 35 in Figure 101) were HF-treated (kindly conducted by Mick Held in Marcia Kieliszewski's laboratory, University of Ohio, USA). HF-treatment is a well-known method (Mort, 1978) for cleaving the carbohydrate parts of *O*-glycosylated proteins, resulting in an intact protein part and monosaccharide fluorides.

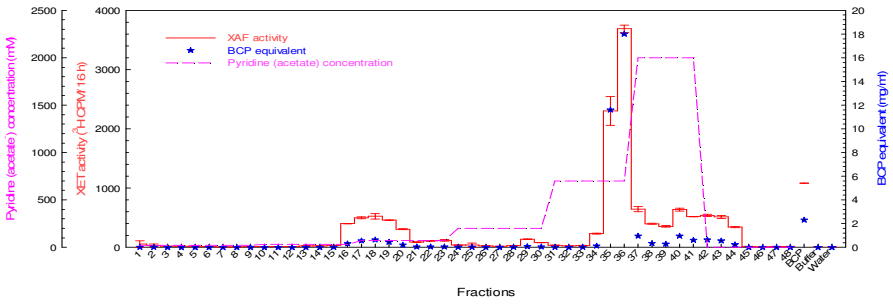


Figure 101. XAF activity of fractions of BCP after cation-exchange chromatography.

Dried BCP (20 mg) was dissolved in 10 ml 20 mM pyridine (formate), pH 3.0, and applied onto a 40-ml bed volume SP-Sephadex column (pyridinium form). After elution with different concentrations of pyridine adjusted to pH 5.3 with acetic acid, each fraction was collected as 6 ml, dried in the SpeedVac, re-dried from water and re-dissolved in 4 ml water. Four-fold concentrated fraction was XAF-assayed. Crude BCP (2 mg/ml) was also XAF assayed. Data show the mean of two determinations ± SE. BCP equivalent was calculated based on the graphs in Figure 13. The XAF assay was repeated with the similar results and one of them is presented here. Fraction 16 and 35 after this column were used for HF-treatment.

The TLC in Figure 102 showed that even before treating with TFA, HF-treated BCP contained several monosaccharides. Thus, I used ethanol to precipitate HF-treated

BCP to obtain the polypeptides and remove the monomers. A non HF-treated BCP was also ethanol precipitated as a control. Both samples had the same XAF activity, approximately 28% that of the original BCP (Figure 103). Some of the activity was lost due to the cleavage of the carbohydrate part from BCP suggesting that the carbohydrate part was responsible for the XAF activity. That XAF-active carbohydrate part could be a polysaccharide or part of glycosylated proteins. The remaining XAF activity was due to proteins which were not attacked by HF.

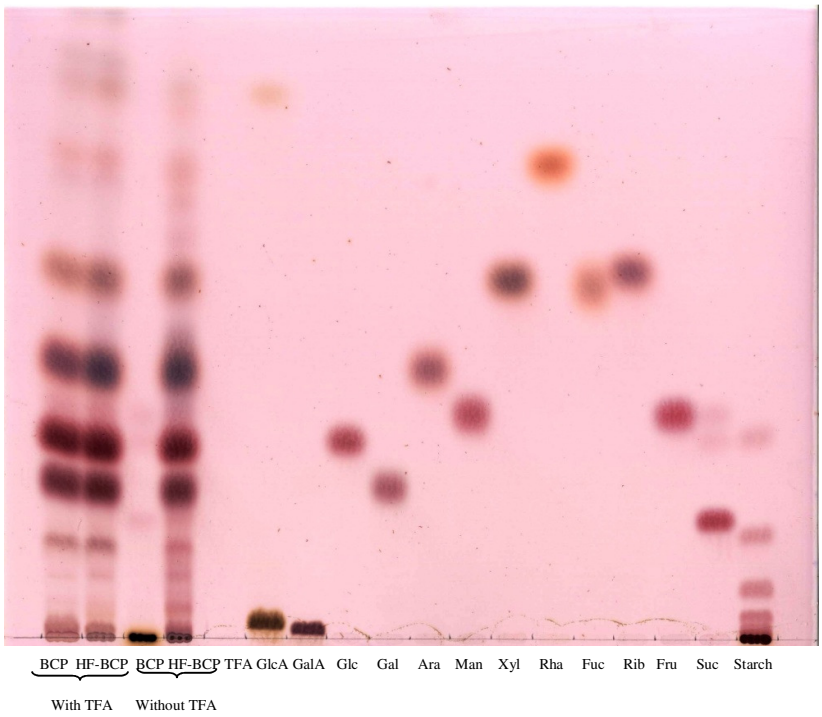


Figure 102. Thin-layer chromatography of TFA-hydrolysates of BCP and HF-treated BCP.

BCP and HF-BCP (BCP treated with HF, then dried to remove HF but without removal of monosaccharides) (0.1 mg) were hydrolysed with 2 M TFA and the dried product was re-dissolved in 2 µl water and subjected to TLC, solvent: EPyAW 6:3:1:1, thymol staining.

Moreover, frozen ethanol-precipitated BCP had the same XAF activity as boiled ethanol-precipitated BCP, while boiled, ethanol-precipitated, HF-treated BCP had less XAF activity than frozen ethanol-precipitated BCP (Figure 104). HF-treatment destroyed the heat-stable characteristic of XAF, which have been already shown to be proteins, thus now suggesting that XAFs are glycosylated proteins. This also indicates that the carbohydrate part was important to protect the XAF activity of the

glycosylated proteins under boiling conditions that I had used throughout this project for preparing BCP.

After treatment with HF, many (glyco)protein bands in BCP disappeared from the native-PAGE pattern. The glycosylated protein bands which were less than 20 kDa in fraction 16 became very faint while all bands in fraction 35 disappeared (Figure 105).

The XAF activity result (Figure 106) showed that after being treated with HF, fraction 16 increased in XAF-activity while fraction 35 lost all of its XAF-activity. Fraction 16 still retained its XAF activity after the carbohydrate part was broken down, suggesting that only the protein part played an important role in its XAF activity. In contrast, fraction 35 lost all of its activity when the carbohydrate part was cleaved, suggesting that the carbohydrate part was much more important than the protein part for its XAF activity (Figure 106). These results indicate that more than one (glyco)protein contributed to XAF activity in the cauliflower extract. This result agrees with the result in section 3.5.1.

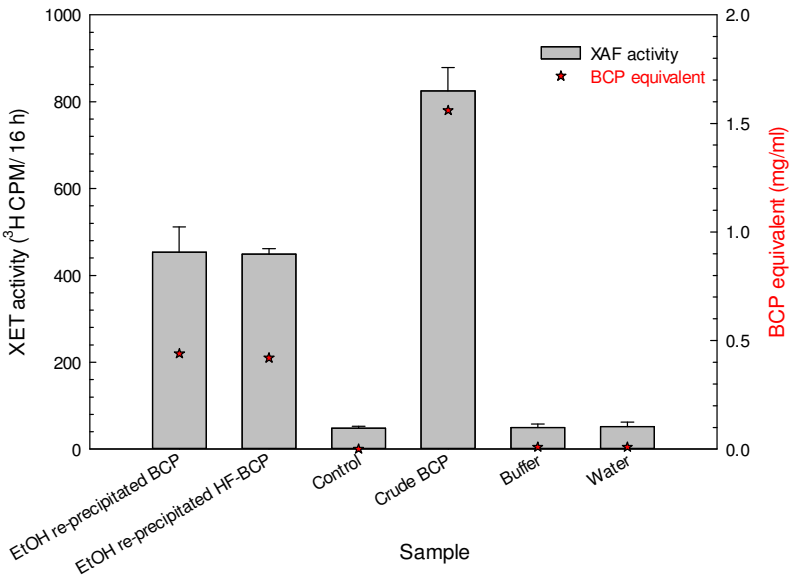


Figure 103. XAF activity of BCP and HF-treated BCP after being re-precipitated by ethanol.

BCP and HF-treated BCP (2 mg each) were dissolved in 1 ml water and precipitated with 69% ethanol. The pellets were washed twice with 96% ethanol and once with 80% ethanol, dried in the SpeedVac, and re-dissolved in 1 ml water. Of that solution, 150 µl was dried in the SpeedVac and re-dissolved in 150 µl NaCl/MES buffer for XAF assay. For the control, 1 ml water was used in place of BCP or HF-treated BCP in the ethanol 'precipitation'. Crude BCP (2 mg/ml) was also XAF-assayed. Data show the means of four determinations ± SE. The experiment was repeated with similar results; one result is presented here.

Mass-spectrometry showed that there was a larger number of detectable proteins in the HF-treated fractions than in the non-treated ones, probably because when the carbohydrate parts were cleaved, the intact protein part became more accessible to trypsin action. Interestingly, in fraction 16, I detected one more peptide for FLA7 (TKVSSSVFSTDPVAVYQVNR) and 2 more peptides for ENODL14 (FKVGDFIVFR, YEAGKDSVLQVTR) that had never been detected before HF-treatment (compare Table 12 and Table 14 with Table 16). This result suggests that FLA7 and ENODL14 were glycosylated proteins which were sensitive to HF-treatment and likely to be an XAF.

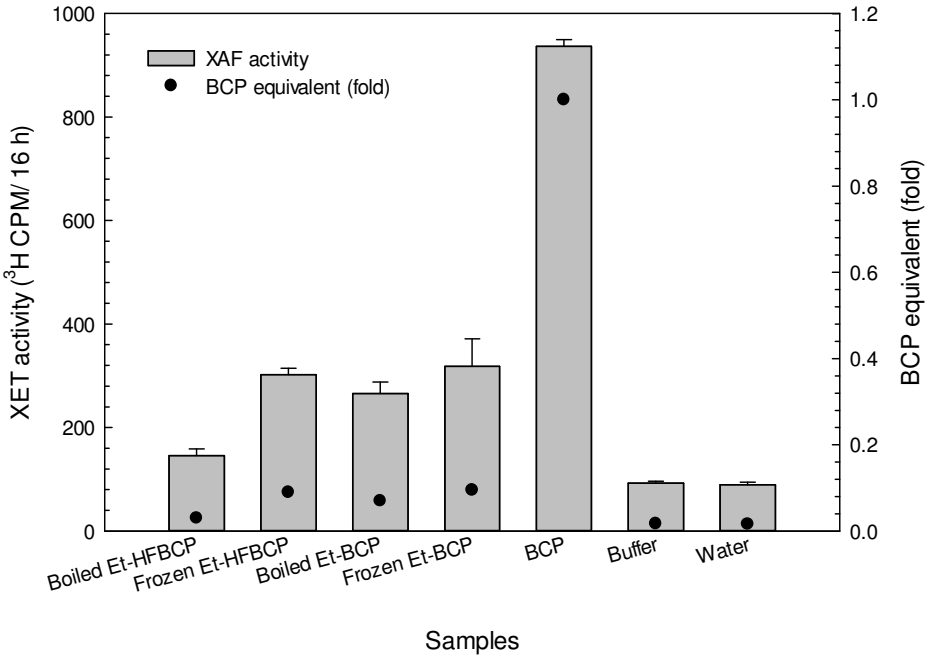


Figure 104. XAF activity of ethanol re-precipitated BCP and HF-treated BCP followed by boiling or freezing.

The ethanol re-precipitated BCP and HF-BCP (Et-BCP and Et-HFBCP, respectively) in Figure 103 were divided into two 150-µl aliquots. One aliquot was boiled for 30 min (Boiled Et-BCP and Boiled Et-HFBCP) and the other was frozen (Frozen Et-BCP and Frozen Et-HFBCP). Both samples were then dried in the SpeedVac and re-dissolved in 150 µl NaCl/MES buffer for XAF assay. Crude BCP (2 mg/ml) was also XAF assayed for comparison. Data show the means of four determinations ± SE.

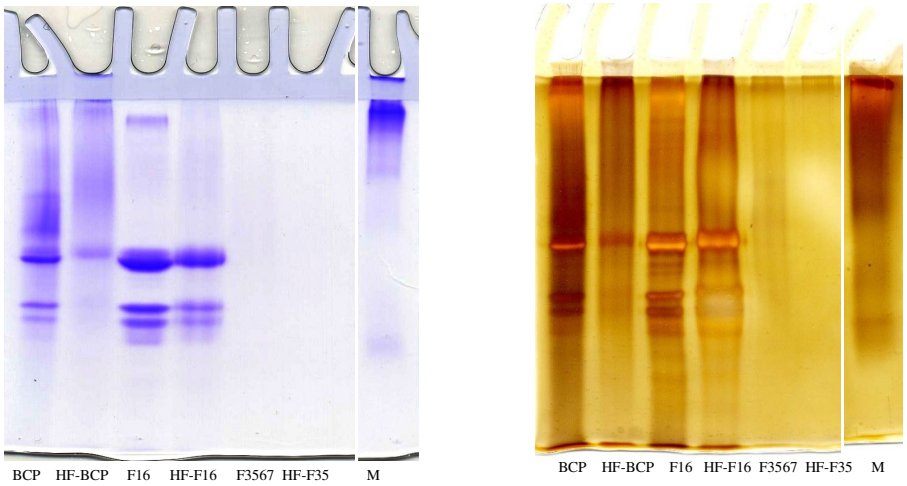


Figure 105. Native-PAGE of cation-exchange fractions of BCP before and after HF-treatment.

After cation-exchange chromatography (details as in Figure 101), 1.5 ml each of fraction 16 (F16) and fraction 35 (F35) were dried and HF-treated (HF-F16 and HF-F35), dried to remove HF but without removal of monosaccharides, and re-dissolved in 1.5 ml water. Of that solution, 100 µl was dried in the SpeedVac and re-dissolved in 9 µl water, mixed with 1 µl loading buffer sample. Of that, I loaded 1 µl onto a 10% acrylamide gel, electrophoresed, and stained with silver nitrate (right-hand gel) and 9 µl onto another gel, electrophoresed, and stained with Coomassie blue (left-hand gel). For controls, non-treated F16 and F3567 (100 µl each) were also tested on the same gel. HF-BCP (HF-treated BCP) or non-treated BCP (BCP) (0.1 mg each) were also tested on the same gel.

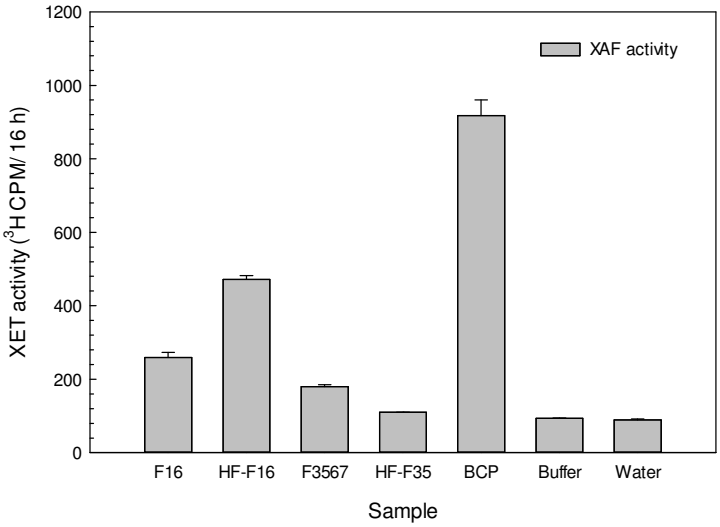


Figure 106. XAF activity of HF-treated BCP and HF-treated XAF-active fractions

After cation-exchange chromatography (details as in Figure 100), 1.5 ml each of fraction 16 (F16) and fraction 35 (F35) were dried and HF-treated (HF-F16 and HF-F35), dried to remove HF but without removal of monosaccharides, and re-dissolved in 1.5 ml water. Of that solution, 75 µl was re-dried in the SpeedVac and re-dissolved in 75 µl NaCl/MES buffer for XAF assay. For a comparison, fraction 16 and a pool of fractions 35, 36 and 37 (F3567) from the same column (75 µl each) were also XAF-assayed. Crude BCP (2 mg/ml) was also assayed for XAF activity. Data show the means of two determinations ± SE.

Table 16. Mass-spectrometry result of fraction 16 after HF-treatment.

Fraction 16 from the cation-exchange chromatography in Figure 100 was HF-treated (details as in Figure 106) and re-dissolved in water. From 1.5 ml solution, 0.5 ml was used for MS.

| Prot_acc[1] | Protein description[2] | Protein score[3] | Protein mass | Significant different peptides | Peptide sequences |
|---|---|---|---|---|---|
| gi\|18395849\|ref\|NP_565313.1\| | FLA7 [*Arabidopsis thaliana*] | 355 | 26886 | 3 | FTDVSGTVR |
| | | | | | VSSSVFSTDPVAVYQVNR |
| | | | | | TKVSSSVFSTDPVAVYQVNR |
| gi\|297845178\|ref\|XP_002890470.1\| | Predicted: lysM domain-containing GPI-anchored protein 2 [*Brassica rapa*]; LysM domain-containing GPI-anchored protein 1 [*Arabidopsis thaliana*] | 194 | 44572 | 2 | IPITCSCVDGIR |
| | | | | | IPITCSCVDGIRK |
| gi\|4559346\|gb\|AAD23007.1\| | Predicted: ENODL1 [*Brassica rapa*]; ENODL14 [*Arabidopsis thaliana*] | 97 | 19062 | 5 | VGDFIVFR |
| | | | | | FKVGDFIVFR |
| | | | | | IPPSSSYSFTEWAQK |
| | | | | | DSVLQVTR |
| | | | | | YEAGKDSVLQVTR |
| gi\|16223\|emb\|CAA78057.1\| | Calmodulin 1 [*Brassica oleracea*]; calmodulin 1 [*Arabidopsis thaliana*] | 73 | 16882 | 2 | ELGTVMR |
| | | | | | VFDKDQNGFISAAELR |
| gi\|297812711\|ref\|XP_002874239.1\| | Predicted: ENODL3 [*Brassica rapa*]; ENODL13 [*Arabidopsis thaliana*] | 61 | 19817 | 2 | FHVGDSLVWK |
| | | | | | YDGEKDSVLQVTK |

Table 17. Mass-spectrometry result of fraction 35 after HF-treatment.

Fraction 35 from the cation-exchange chromatography in Figure 100 was HF-treated (details as in Figure 106) and re-dissolved in water. From 1.5 ml solution, 0.5 ml was used for MS.

| Prot_acc[1] | Protein description[2] | Protein score[3] | Protein mass | Significant different peptides | Peptide sequences |
|---|---|---|---|---|---|
| gi\|38564509\|gb\|AAR23753.1\| | Predicted: dehydrin ERD10-like [*Brassica rapa*]; LTI45 [*Arabidopsis thaliana*] | 616 | 30987 | 16 | GLFDFLGK |
| | | | | | EKFPHGTK |
| | | | | | KGVMEQIR |
| | | | | | GLFDFLGKK |
| | | | | | KGVMEQIREK |
| | | | | | AQVSEPPAFVAK |
| | | | | | IKEKLPGYHAK |
| | | | | | TEDDTPVIATLPVK |
| | | | | | VATTEEPSATTGEVK |
| | | | | | VATTEEPSATTGEVKDR |
| | | | | | EEVKPQETTTLESEFEHK |
| | | | | | KEEVKPQETTTLESEFEHK |
| | | | | | EKFPHGTKTEDDTPVIATLPVK |
| | | | | | LPGHSEKPEDSQVVDTAAAVPVTEK |
| | | | | | TEDDTPVIATLPVKEETVEHPEEK |
| | | | | | EKLPGHSEKPEDSQVVDTAAAVPVTEK |
| gi\|1154629\|emb\|CAA64428.1\| | Pollen coat protein [*Brassica oleracea*]; Cold-regulated 47 [*Arabidopsis thaliana*] | 407 | 22425 | 12 | KHSLLEK |
| | | | | | GLFDFLGK |
| | | | | | KGFMDKLK |
| | | | | | GLFDFLGKK |

| | | | | | |
|---|---|---|---|---|---|
| | | | | | VHISEPVPEVK |
| | | | | | VATEESSTATGEVTDR |
| | | | | | KDETKPEETIDSEFEQK |
| | | | | | NVHEHEAPKVATEESSTATGEVTDR |
| | | | | | IKEKLPGYHPK |
| | | | | | VTTEESSAEVTDR |
| | | | | | KGFMDKIK |
| | | | | | IKEKLPGYHAK |
| gi\|256674064\|gb\|ACV04872.1\| | RecName: Full=Superoxide dismutase [*Brassica oleracea var. capitata*]; Superoxide dismutase [Cu-Zn] [*Arabidopsis thaliana*] | 85 | 15476 | 4 | AVVVHADPDDLGK |
| | | | | | GGHELSLSTGNAGGR |
| | | | | | GVAVLNSSEGVK |
| | | | | | AVVVHADPDDLGKGGHELSLATGNAGGR |
| gi\|15241485\|ref\|NP_196417.1\| | Predicted: Plasmodesmata callose-binding protein 2 [*Brassica rapa*]; Glucan endo-1,3-beta-glucosidase-like protein 3 [*Arabidopsis thaliana*] | 129 | 20400 | 2 | GSCFNPDNVR |
| | | | | | TLDYACGNGADCNPTHPK |
| gi\|295789\|emb\|CAA34456.1\| | Elongation factor 1 alpha [*Brassica oleracea var. viridis*]; Translation elongation factor eEF-1 alpha chain [*Arabidopsis thaliana*] | 91 | 49799 | 3 | QTVAVGVIK |
| | | | | | IGGIGTVPVGR |
| | | | | | MTPTKPMVVETFSEYPPLGR |
| gi\|297830162\|ref\|XP_002882963.1\| | Predicted: methyl-CpG-binding domain-containing protein 11 [*Brassica rapa*]; Methyl-CPG-binding domain-containing protein 11 [*Arabidopsis thaliana*] | 67 | 27736 | 2 | KQLEQYLK |
| | | | | | KTEIVFVAPTGEEISNR |
| gi\|19347816\|gb\|AAL86321.1\| | Predicted: polyadenylate-binding protein 2 [*Brassica rapa*]; Polyadenylate- | 124 | 67131 | 5 | FTNVYVK |
| | | | | | ITSAVVMKDGEGK |

| | | | | | |
|---|---|---|---|---|---|
| | binding protein 2 [*Arabidopsis thaliana*] | | | | GFGFVNFENADDAAR |
| | | | | | SKGFGFVNFENADDAAR |
| | | | | | MIENKPLYVAVAQR |
| gi\|18394229\|ref\|NP_563971.1\| | Predicted: methyl-CpG-binding domain-containing protein 10 [*Brassica rapa*]; Methyl-CPG-binding domain 10 [*Arabidopsis thaliana*] | 47 | 42390 | 2 | LFYPKR |
| | | | | | ATTPTPDKEPLLK |
| gi\|115466912\|ref\|NP_001057055.1\| | Predicted: 20 kDa chaperonin, chloroplastic-like [*Brassica rapa*]; Chaperonin 20 [*Arabidopsis thaliana*] | 36 | 23021 | 2 | YTSLKPLGDR |
| | | | | | TAGGLILTETTK |
| gi\|147742765\|gb\|ABQ50547.1\| | Predicted: keratin, type II cytoskeletal 2 epidermal isoform X2 [*Brassica rapa*]; Eukaryotic translation initiation factor 4B1 [*Arabidopsis thaliana*] | 68 | 25300 | 2 | VSDFPLQSR |
| | | | | | GGIGGGFSSYGGR |
| gi\|18422620\|ref\|NP_568653.1\| | Predicted: 28 kDa heat- and acid-stable phosphoprotein-like [*Brassica rapa*]; Uncharacterized protein [*Arabidopsis thaliana*] | 48 | 18966 | 2 | FSSAADILAGTSAAR |
| | | | | | FSSAADILAGTSAARPR |
| gi\|15225733\|ref\|NP_180832.1\| | Predicted: 26S proteasome non-ATPase regulatory subunit 1 homolog A-like isoform X2 [*Brassica rapa*]; 26S proteasome regulatory subunit [*Arabidopsis thaliana*] | 42 | 109365 | 2 | LAPSGFVLLK |
| | | | | | LPTAVLSTSVK |
| gi\|89257548\|gb\|ABD65038.1\| | Nuclear RNA binding protein, putative [*Brassica oleracea*]; Hyaluronan / mRNA binding domain-containing protein [*Arabidopsis thaliana*] | 42 | 35931 | 3 | KTNNEEIFIK |
| | | | | | VFESMQQLSSK |
| | | | | | VFESMQQLSNKK |
| gi\|297837237\|ref\|XP_002886500.1\| | Predicted: uncharacterized GPI-anchored protein At1g61900 [*Brassica rapa*]; ESTs gb\|AA728658 and gb\|N95943 come from this gene [*Arabidopsis thaliana*] | 41 | 47662 | 2 | VCPLVFPHMR |
| | | | | | HCLSDLEQILVGK |
| gi\|4115918\|gb\|AAD03429.1\| | Predicted: nascent polypeptide-associated complex subunit alpha-like protein 4 [*Brassica rapa*]; Nascent polypeptide- | 37 | 25580 | 2 | LGMKPVTDVSR |
| | | | | | NVLFVISKPDVFK |

| | | | | | |
|---|---|---|---|---|---|
| | associated complex subunit alpha-like protein 4 [*Arabidopsis thaliana*] | | | | |

## 3.8 XAF activity extractable from mutants of *Arabidopsis*

Homozygous mutant *Arabidopsis* plants (confirmed by genotyping) were RNA extracted and the transcription products were tested on an agarose gel (Figure 107, Figure 108). The boiled *Arabidopsis* preparation (BAP; equivalent to the BCP used in the remainder of the thesis) was extracted and tested for XAF activity (Figure 109).

Several organs of the mutant plants had significant changes in XAF activity compared with wild type plants. Among three mutants of the gene *FLA7*, only *fla7.3* had a different XAF activity compared with the wild type. More specifically, almost half the XAF activity in the flowers and seeds of the mutant disappeared while XAF activity in the leaves increased (Figure 109). Although *FLA7* RNA accumulation in *fla7.1* and *fla7.2* was reduced (Figure 107), the XAF activity in those mutant plants did not reduce, possibly because the effect of the inserted T-DNAs were only knock-down, not knock-out. Besides that, *FLA7* belongs to a big *FLA*- multigene family (Johnson et al., 2003). It is probable that when one *FLA* gene is mutated, the others can take over its role and their activities are complementary.

A mutant in the *ENODL14* gene also showed reductions in the XAF activity in the stems and the flowers and seeds (Figure 109). The RNA accumulation of *enodl14* also showed a knock-down, but not knock-out effect (Figure 107, Figure 108), thus the XAF activity did not change in other organs. The *ENODL14* belongs to a large early nodulin like family which consists of 22 genes in *Arabidopsis thaliana* and 41 genes in *Brassica rapa*. Nodulin-like gene are usually expressed in all *Arabidopsis* organs (Mashiguchi et al., 2009). XAF activity did not change and there was no mutant phenotype in *enodl14*, maybe due to functional redundancy.

Of the two (LTI65 and LTI140) low temperature-induced genes tested, only the *lti65* mutant showed a reduction in XAF activity in flowers and seeds (Figure 109). *LTI65* was the only gene having a knock-out effect from the insertion mutation: this gene did not express at all in mutant *Arabidopsis* (Figure 107 and Figure 108). Although there was a knock-out effect on LTI65, there was no phenotype observed probably due to

the functional redundancy. For example, LTI140, one of the homologues of LTI65 may take over its role in *lti65*.

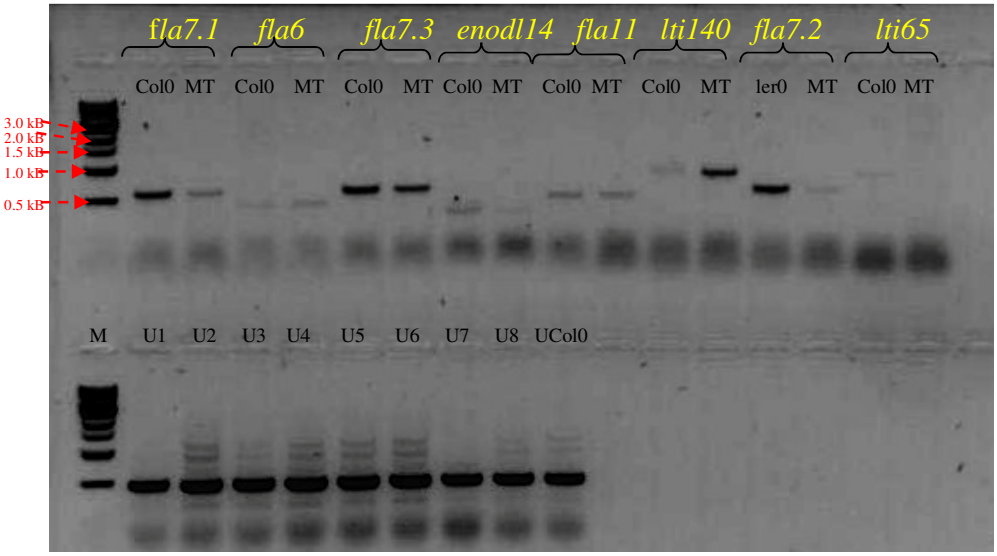


Figure 107. RT-PCR products of homozygous mutants of *Arabidopsis* (1st run, 25 cycles PCR).

mRNA extracted from *Arabidopsis* mutants and Col0. Col0: mRNA from Col0; ler0: mRNA from ler0, MT: mRNA from mutants of *Arabidopsis*; M: 1 kB DNA ladder. U1: ubiquitin in *fla7.1*, U2: ubiquitin in *fla6*, U3: ubiquitin in *fla7.3,* U4: ubiquitin in *enodl14,* U5: ubiquitin in *fla11,* U6*:* ubiquitin in *lti140,* U7*:* ubiquitin in *fla7.2, U*8: ubiquitin in *lti65*, and UCol0: ubiquitin in Col0, used as positive controls. The PCR was done in 25 cycles.

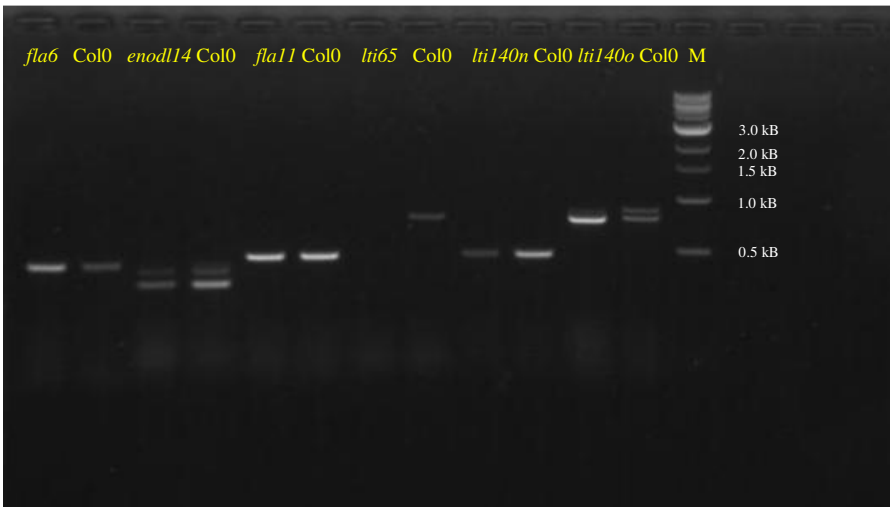


Figure 108. RT-PCR products of homozygous mutants of *Arabidopsis* (2nd run, 30 cycles PCR).

mRNA extracted from *Arabidopsis* mutants and Col0. lti140n: PCR product of lti140 with new primers which are more specific than the old primers for this mutant, lti140o: old primers which are not specific for this mutant. M: 1 kB DNA ladder.

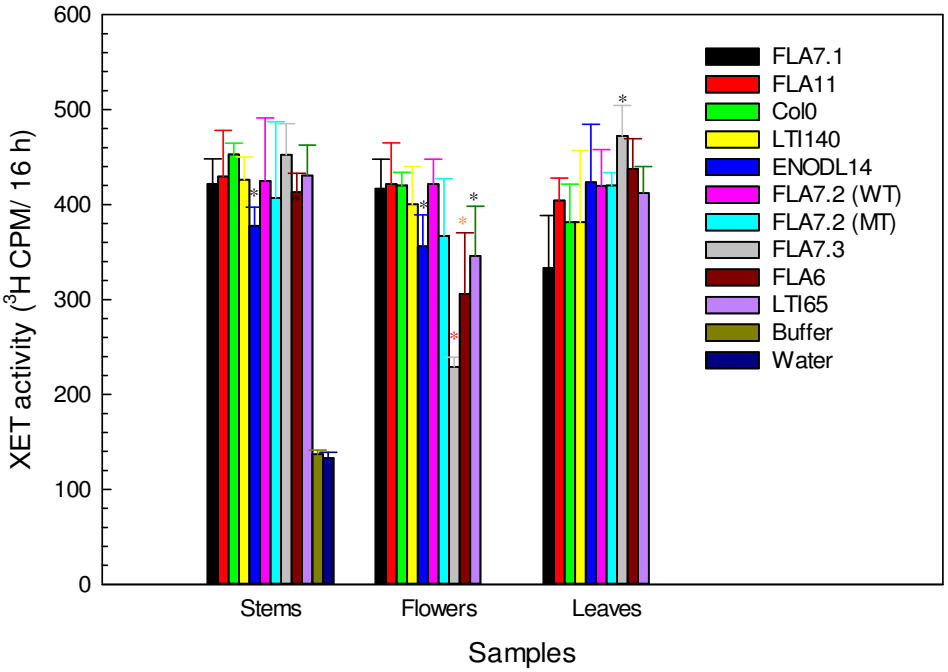


Figure 109. XAF activity of BAP from mutant *Arabidopsis* plants.

BAP from various organs of *Arabidopsis* mutants and wild-types, at a concentration of 0.5 mg/ml, were assayed for XAF activity as routinely. All of the mutants are in a Col0 background so the XAF activity in Col0 should be used as the valid comparator, except *fla7.2* which has the Landsberg-erecta (ler) background, thus the FLA7.2 (WT) should be used to compare the FLA7.2 (MT). The asterisk (*) indicates results which are statistically significant different from the relevant wild-type: '*': $p \leq 0.05$, '*': $p \leq 0.01$, '*': $p \leq 0.001$. The statistic were analysed with ANOVA on R. Data show the means of two assays of each of four different samples extracted independently ± SE.

These results suggest that FLA7, ENOL14 and LTI65 were all contributing to the XAF activity in *Arabidopsis* flowers and seeds while (of the proteins tested) only ENODL14 was contributing to the XAF activity in *Arabidopsis* stems. The results suggest that multiple proteins are responsible for the XAF activity in plants and that different XAF-determining genes were expressed in different organs of *Arabidopsis* for the XAF activity.

# 4 DISCUSSION

## 4.1 A novel method for testing the solubilisation of XET *in vivo*

Since being discovered in early 1900 (Baydoun and Fry, 1989; Fry et al., 1992; Nishitani and Tominga, 1992; Farcaš et al., 1992; Okazawa et al., 1993), XET activity has been of interest because of its ability to modify xyloglucan. Xyloglucan is one of the main polysaccharides contributing to the structure of the PCW by hydrogen-bonding to, and probably tethering, cellulose microfibrils (Fry, 1989; Hayashi et al., 1994). XET is responsible for cutting and re-joining of xyloglucan, causing the transient matrix cleavage without hydrolysis, thus providing a molecular mechanism for controlled, turgor-driven wall expansion (Rose et al., 2002). XET activity may be involved in both wall-loosening, thus facilitating cell expansion, and wall-tightening, thus suppressing cell expansion depending on the molecular size, location and age of the participating xyloglucan chains (Thompson and Fry, 2001; Maris et al., 2009). XET is one of the enzymes whose reactions involving structural wall polysaccharides can be tracked *in vivo* (Fry, 2004). Although there have been many researches on determination of XTHs and analysis of XET and XEH activity, as well as its roles in plant cells, little is known about how this enzyme action is regulated *in vivo*, which is very important for plant cell growth control.

XTHs are glycoproteins located in the cell walls; XTHs contribute 1.2% of total apoplastic proteins in Azuki hypocotyls (Nishitani and Tominaga, 1992; Takeda et al., 2002). Since the optimal pH for the XET-catalysed transglycosylation is 5.8 (Nishitani and Tominaga, 1992), the apoplastic with its typical pH between 5 and 6 is the ideal place where XET can exhibit its maximal action (Campbell and Braam, 1999; Rose et al., 2002). Therefore, the solubilisation of the enzyme may be important for its action *in vivo* and there may be the presence of endogenous factors at the cell wall-membrane interface that have the ability to solubilise XTHs. Such endogenous factor is of interest because it may act as a regulator of XET action *in vivo*. Moreover, in a previous work, Sharples and Fry (unpublished work) find that after 2 h incubation in the glass borosilicate tubes, insect-expressed XTH24 lost its XET activity. This loss is probably due to the binding of the enzyme to the tube surfaces and can be prevented by the adding of NaCl, $CaCl_2$ and this effect is more remarkable with the adding of BCP

(boiled cauliflower preparation: cauliflower florets were homogenised in water, boiled, centrifuged and the supernatant was ethanol precipitated, then the pellet was freeze-dried and re-dissolved in water). This observation continue support the idea that the solubilisation of XTHs is important for the activation of XET activity.

In this study, such endogenous factors that may modulate XET action have been investigated and a new method has been successfully optimised (based on Sharples and Fry (unpublished work)) to study the solubilisation of XET activity *in vivo*. In this method, *Arabidopsis* cells were frozen and thawed to disrupt the plasma membrane and all soluble materials were washed away with water, leaving water-insoluble components such as starch, lipid, chromatin and the intact cell wall with its firmly bound proteins. The washed-*Arabidopsis* cells was incubated with putative XET-activating factors (XAFs), either salts, polysaccharides or BCP. The solubilised XET activity was analysed in an assay (Fry et al., 1992) where tamarind xyloglucan as a donor substrate and [$^3$H]XXXGol as a acceptor substrate were provided and the radioactive products were measured. Although I did not test whether other parts of the cell were present, there were no radioactive products detected without BCP and NaCl, proving that the *Arabidopsis* cells had been carefully washed and there was almost no water-soluble XET activity in the cells before treatment. Thus, any water-soluble XET activity observed in the radioactive reaction after the incubation of the cells with XAF is due to the solubilisation or activation of the wall-XTHs.

Sharples and Fry (unpublished work) distinguished whether BCP released or activated bound XTH24 from a reaction vessel. They allowed XTH24 to bind to borosilicate glass tubes and any unbound enzyme was washed from the tube and replaced with an assay mixture in the presence or absence of BCP. Half the contents of the original tube were then transferred to a new tube and the reaction was allowed to proceed. The result showed that both tubes maintained a linear $^3$H incorporation rate suggesting that BCP releases the bound enzyme from their binding sites on a glass surface. Therefore, XAF promotes XET activity assumably by solubilising XTH from their binding sites in the cell wall but not by activating them.

This method was facilitated by the use of 96-well PCR plates allowing me to deal with a large number of samples (hundreds) in small volumes (66 µl) at the same time. The

dry weight of *Arabidopsis* cells used in an assay had a strong effect on the solubilisation of XET activity by 2 mg/ml BCP, and the optimum dry cell weight of *Arabidopsis* for testing XAF activity was concluded to be from 15.2 to 18.3 µg. The time of the incubation of BCP and *Arabidopsis* cells was also important and the optimal time for the incubation of BCP and the cells was 30 min, according to my experience. If the incubation time is longer, there will be too much XTHs solubilised from the cell wall so the XET activity will not be on a linear rate, thus it will be difficult to relate the solubilised activity with the amount of BCP. When the incubation time was more than 1 h, Sharples and Fry (unpublished work) observed a decrease in solubilised XET activity, probably due to the re-binding of enzymes to the cell or the tube walls. On the other hand, if the time of incubation is shorter, the solubilised XET activity is not high enough to be detectable. With this method, I am able to test the solubilisation of *Arabidopsis* XET-active XTHs *in vivo* by any putative XAF, salts or detergent with a high repetitive ability and a small error bar. This method can be used to look for an endogenous factor which can solubilise XET activity, thus regulating XET action *in vivo*.

## 4.2 BCP has an XAF effect similar to that of salt on promoting XTH solubilisation although it contains a very low concentration of salt

Inorganic salts had the ability to promote, more specifically, to solubilise XET activity from washed *Arabidopsis* cells and this effect was salt concentration-dependent. NaCl at the maximum concentration tested, which was 0.338 M, increased extractable XET activity by up to 1400-fold while 0.03 M $CaCl_2$, caused an increment in XET activity of up to 90-fold. Lower concentration of salts that had XAF effect were 50 mM NaCl, which caused 25-fold promotion, and 2.5 mM $CaCl_2$, which caused 10-fold promotion of solubilised XET activity. The result agreed with Takeda and Fry (2004), who showed that extracted cauliflower floret enzyme has high XET activity, but that this was largely lost after partial purification and de-salting. The lost XET activity of de-salted cauliflower extracts, due to the lack of low-$M_r$ substances, could be restored (up to 40-fold) by 300 mM $Na^+$, $K^+$, and $NH_4^+$ and lower concentration of $Ca^{2+}$, $Mg^{2+}$, $Al^{3+}$, and $La^{3+}$. In my experiment, NaCl had a linear promotion effect up to a concentration of 100 mM while that of $CaCl_2$ was only 15 mM. At the optimum concentration, 60

mM (ionic strength: μ=150 mM), $CaCl_2$ promoted XET activity up to 100-fold. To cause this fold-promotion effect, the required concentration of NaCl was approximately 85 mM (μ=85 mM). When $CaCl_2$ concentration was higher than 60 mM, the XET activity solubilised was reduced. This result is correspondent with Takeda and Fry (2004) that at a high concentration, the multivalent cations inhibited XET activity. There was no optimum concentration of NaCl observed in my study because the fold-effect of NaCl was continuing to go up even when its concentration reached 338 mM. Although I did not test effect of NaCl at a concentration higher than 338 mM, it is showed by Thiyagarajah et al. (1996) that NaCl has little inhibitory effect on XET activity, even at concentrations at high at 2000 mM. Moreover, Takeda and Fry (2004) demonstrated that the nature of the anion, for example, $Cl^-$, $NO_3^-$, $SO_4^{2-}$ in contrast, had relatively little effect on restoration of the XET activity. These results suggested that inorganic salts can act as XAF *in vivo*. However, the effect of each salt on the solubilisation of XTH was not simply due to the ionic strength.

Salts have been demonstrated to affect to cell wall enzyme action *in vivo*. Goldberg et al. (1992) showed that the cation content of isolated walls affects their susceptibility to pectin methylesterase. The de-esterification rate of *Citrus* pectin by isolated cell walls was strongly enhanced by the addition of any of NaCl, KCl, $CaCl_2$, $MgCl_2$, at a concentration of from 8 to 167 mM, though not with 167 mM $MnCl_2$. It was evident that cations can interact not only with the enzyme molecules but perhaps also with the pectic substrate, and possibly even with the products generated by the de-esterification. Tomato endo-polygalacturonase (PG) action is strongly influenced by the cations present ($Na^+$, $K^+$ or $Ca^{2+}$) and the pH. Activities of both isoforms (PG1 and PG2) of the enzyme are strongly enhanced by NaC1. At pH 4.5, pectin release from the cell walls of mature-green cv Ailsa Craig tomato fruit increased linearly with increasing KCl to 100 mM (Chun and Huber, 1998). Recently, Yang et al. (2011) showed that XET action of *Arabidopsis* XTHs measured by a cytochemical assay was greatly reduced after 30 min of treatment with 50 μM Al and further decreased after 24 h of treatment, thus causing an inhibition in root elongation by about 40%. They suggests that Al targets hemicellulose easily and inhibits XET action, which will be the key process responsible for Al-induced root growth inhibition in *Arabidopsis*.

BCP itself caused an increment in solubilised XET activity of up to120-fold when its concentration was increased to 1.82 mg/ml even though at this concentration, its ionic strength was only 9 mM NaCl-equivalent, much smaller than the optimum ionic strength of $CaCl_2$ which caused a 100-fold promotion. At this concentration, NaCl had almost no XET-promotion effect. This conclusion totally agreed with Takeda and Fry (2004) that XAF was much more effective than would have been predicted from its conductivity in comparison with NaCl. Moreover, when I de-salted BCP in dialysis tubing with MWCO 3500 or 12000-14000, the XAF activity was lost by approximately the same amount (63-65%), suggesting that the lost activity was not simply due to the loss of inorganic salts. These results lead to the conclusion that there are other factors in BCP, rather than salts, that can solubilise XET from the cell walls. In addition, the ionic environment of an XTH molecule *in vivo* will include not only low-$M_r$ apoplastic salts but also charged polysaccharides and glycoproteins which may act as endogenous modulators of XET activity.

It was also clear from my results that there was a synergistic effect between NaCl (but not $CaCl_2$) and BCP in solubilising XET activity from *Arabidopsis* cells. Together with the data from the effect of NaCl and $CaCl_2$ on the solubilisation of *Arabidopsis* XTHs, I suspected that the effect of $Ca^{2+}$ is not simply an ionic effect. There may be a unique relationship between XAF and $Ca^{2+}$. Such a relationship is documented between classical AGPs and $Ca^{2+}$ (Lamport and Várnai, 2012). Using rapid ultrafiltration assays and mass-spectrometry analysis, they verified that typical AGPs contain 30 sites that bind $Ca^{2+}$ tightly and stoichiometrically at pH 5, and hence are a substantial source of cytosolic $Ca^{2+}$. They also proposed that AGPs are an essential component of the global $Ca^{2+}$ signalling process in plant. XAF, which may be a fasciclin-like arabinogalactan-protein 7 (FLA7) as shown elsewhere in the thesis, may bind to $Ca^{2+}$ and this binding may somehow contribute to promotion effect of $Ca^{2+}$ and XAF on the XET activity.

BSA, a neutral protein, could not solubilise XET activity from *Arabidopsis* cells by itself, thus is not XAF-active; however, it could stabilise the *Arabidopsis* XET activity already solubilised by BCP, $CaCl_2$ or NaCl, presumably by preventing XTHs from binding to the tube walls or being denatured. A similar effect was also observed with Triton X-100 (a surfactant) and a high concentration of NaCl. XAF may also have the same ability because in the present of BCP, the effect of BSA was not observed.

I hypothesise that cauliflower XAF had effects similar to those of $Ca^{2+}$ and $Na^{+}$, solubilising XET activity by releasing XTHs from their binding sites in the cell wall. XAF also had an effect similar to that of BSA, preventing solubilised XTHs from re-binding to the cells or tube walls or being de-natured. Probably, this effect is because cauliflower XAF has a specific affinity, targeting XTH–wall bonds without having any general ionic effect so releasing them from cell wall.

## 4.3 XAF is a heavily-glycosylated proteins and its physical and chemical properties importantly contribute to its ability to solubilise XET

XAF was prepared by extracting cauliflower florets or a wide range of other plant organs in cold water, boiling for 1 h and filtering to de-nature and remove proteins, then precipitating in ethanol to get rid of low molecular weight compounds. Thus XAF could be water-soluble polysaccharides, heat-stable proteins, or RNA. At a concentration of 1.82 mg/ml and a pH of 5.5, its conductivity was equivalent to approximately 9 mM NaCl indicating that XAF was weakly ionic.

Cold alkali could not destroy XAF activity, suggesting that XAF does not have an ester group, for examples, methyl esters, acetyl esters or feruloyl esters, which are sometimes found decorating hemicellulose or pectin (Fry, 2000), that is essential for its activity.

XAF can be purified by both cation- and anion-exchange column chromatography indicating that it contains both negatively and positively charged parts, for example a protein or glycoprotein. Treatment with proteinase K destroyed only 70% of the XAF activity of BCP even after 72 h of incubation. This suggests that a protein contributes to the structure of XAF, but that in addition XAF possesses an additional domain which is either not a protein or is protected from hydrolysis by proteinase K. The proteinase K treatment also suggests that there may be multiple different XAFs; some of them are proteins, thus are completely destroyed by proteinase K and the other are non-proteins, for example, polysaccharides, thus are completely resistant to proteinase K. On treatment with anhydrous HF, which cleaves glycosidic but not peptide bonds (Mort and Lamport, 1977), XAF lost 70% its activity, suggesting that polysaccharides and/or the carbohydrate part of glycoproteins contribute to XAF activity. The simplest

explanation is that XAF is a glycosylated protein, with both the carbohydrate and the polypeptide moieties being required for maximal XAF activity.

The heat-stable property of XAF may be due to the carbohydrate part of it which could stabilise the protein part during the boiling because HF-treatment destroyed the heat-stable characteristic of XAF. Solubility in boiling water is a common feature of glycosylated proteins, for example, AGPs (Sharples and Fry, unpublished). Several arabinogalactan-peptides isolated in 1 h-boiled 80% ethanol are documented in barley and rice flour (Van den Bulck et al., 2005). It also may have helped to maintain the XAF activity during the freezing and thawing process which I used during my study.

Further purification of XAF from the ion-exchange column reduced XAF activity. Perhaps, when I fractionated XAF using the ionic-exchange column, its conformation was changed so the purification did not increase XAF activity. The carbohydrate part and the polypeptides part can give to XAF an ionic characteristic, as was mentioned before, that helps to solubilise XTHs from their binding sites on the cell wall. There is also a possibility of a co-operative effect of different compounds present in XAF.

## 4.4 Non-classical arabinogalactan-proteins such as fasciclin-like arabinogalactan-protein (FLA) and early nodulin-like protein may be XAFs

Mild acid treatment could not destroy XAF activity indicating that glycofuranosyl-based carbohydrate is not responsible for the XAF activity. More severe hot acid treatment reduced XAF activity in a time-dependent manner. Under acid conditions used, both the glycopyranosyl-based carbohydrate part and the polypeptide part of a (glyco)protein can both be hydrolysed. Moreover, the XAF activity was completely destroyed after 32 min treatment with 2 M TFA at 100°C correspondent with the releasing of Gal from BCP (Figure 34, Figure 36) suggesting that a galactopyranosyl-based carbohydrate is essential for the XAF activity. That carbohydrate may be backbone of a polysaccharide or sidechains of a glycoprotein, for example, the (1→3, 1→6)-β-galactan chain in the arabinogalactan chain of AGPs (Bacic et al., 1987; Ellis et al., 2010). XAF partially purified by the anion-exchange column was positive with Yariv reagent but XAF-active fraction from any further purification, for example

cation-exchange column, did not show precipitate with Yariv. In agreement with this observation, purification of XAF by Yariv reagent precipitation did not enrich the XAF activity: the XAF activity of AGP purified by Yariv reagent was lower than that of crude BCP at the same concentration. Possibly, the amount of the XAF-active AGP after several purifications was not high enough to be precipitated by Yariv or XAF is a non-classical AGP which does not exhibit Yariv reactivity (Showalter, 2001; Kitazawa et al., 2013; Ellis et al., 2010). For example, NaPRP4, a clone from *Nicotiana alata* which has a 96% similarity in nucleotides compared to TTS, an AGP from tobacco stylar transmitting tissue and their encoded proteins are 96% similar in amino acids, has been recently classified as a non-classical AGP. However, NaPRP4 protein is not precipitated with Yariv reagent (Sommer-Knudsen et al., 1996; Showalter, 2001). Another explanation is the procedure that I have used to purify AGPs from BCP is not sufficient, thus a different method should be applied for a better purification. Nevertheless, acid hydrolysates of partially purified XAF contained mainly Ara, Gal, Glc, uronic acids as well as Ser, Ala, Gly, Leu/Ile, Val and Glu. Among polysaccharides tested, gum arabic, a commercial AGP, had the highest XAF activity which much higher than the others. These results lead me to the conclusion that XAF is a non-classical AGP, a class of plant cell surface proteoglycans.

The two main amino acids of classical AGPs that classified them into the Pro/Hyp-rich glycoproteins, which are Pro and Hyp, unfortunately, could not be seen on the paper chromatogram in my study. Hyp and Pro spots were quite faint (pink or orange) compared to the dark purple of the other amino acids. Thus Hyp maybe overlapped with the nearby Ser, Gly and Glu while Pro was overlapped with a brown spot that occurred in the HCl-hydrolysate of all fractions. To overcome that, I used paper electrophoresis and isatin/ninhydrin which was expected to visualise only Pro, Hyp, Gly and Ser spots. With this method, I was able to find those four amino acids in BCP but only Gly and Ser in the purified XAF from a cation-exchange column. Perhaps the Pro and Hyp quantities in XAF were not high enough to be detected by either method that I have used, suggesting that XAF is a non-classical AGP. This was supported by the mass-spectrometry.

Mass-spectrometry analysis of XAF-active peak fractions purified by both methods, ion-exchange column chromatography and native-PAGE with electro elution, showed

with high confidence the presence of fasciclin-like arabinogalactan-protein 7 (FLA7) (Figure 110) and early-nodulin like protein 14 (ENODL14) (Figure 111). They are both chimeric AGPs and are sensitive to HF-treatment (Mort and Lamport, 1977). After HF-treatment, one more peptide for FLA7 (TKVSSSVFSTDPVAVYQVNR) and 2 more peptides for ENODL14 (FKVGDFIVFR, YEAGKDSVLQVTR) that had never been detected before HF-treatment were detected, probably because HF-treatment cleaves the carbohydrate parts of the glycoproteins, thus helped the intact protein parts became more accessible to trypsin action. These results suggests that FLA7 and ENODL14 may be XAFs.

1 MAKMQLSIFI AVVALIVCSA SAKTASPPAP VLPPTPAPAP APENVNLTEL

51 LSVAGPFHTF LDYLLSTGVI ETFQNQANNT EEGITIFVPK DDAFKAQKNP

101 PLSNLTKDQL KQLVLFHALP HYYSLSEFKN LSQSGPVSTF AGGQYSLKFT

151 DVSGTVRIDS LWTRTKVSSS VFSTDPVAVY QVNRVLLPEA IFGTDVPPMP

201 APAPAPIVSA PSDSPSVADS EGASSPKSSH KNSGQKLLLA PISMVISGLV

251 ALFL

Figure 110. FLA7 amino acid sequence (McMillan et al., 2010).

1 MFLSASMASS SLHVAIFSLI FLFSLAAANE VTVGGKSGDW KIPPSSSYSF

51 TEWAQKARFK VGDFIVFRYE SGKDSVLEVT KEAYNSCNTT NPLANYTDGE

101 TKVKLDRSGP FYFISGANGH CEKGQKLSLV VISPRHSVIS PAPSPVEFED

151 GPALAPAPIS GSVRLGGCYV VLGLVLGLCA WF

Figure 111. ENODL14 amino acid sequence (Mashiguchi et al., 2009).

Showalter et al. (2010) developed BIO OHIO software program that identifies and classifies 85 AGPs, including 22 classical AGPs, three Lys-rich classical AGPs, 16 AG peptides, 21 chimeric FLAs, 17 chimeric PAGs, and six other chimeric AGPs. Classical AGPs can be identified by their biased amino acid compositions of greater than 50% Pro (P), Ala (A), Ser (S), and Thr (T); described as '>50% PAST' (Showalter et al., 2010). According to that, the two AGPs found in my study are both non-classical AGPs. FLA7 has its amino acid compositions of 9.8% Pro, 10.2% Ala, 11.0% Ser, 6.3% Thr, 10.2% Leu and 9.1% Val (thus 37.3 % PAST). Likewise, the amino acid

composition of ENODL14 is 3.8% Pro, 8.8% Ala, 12.6% Ser, 3.3% Thr, 8.8% Gly, 8.8% Val and 7.7% Leu (thus 28.5% PAST).

Partially purified XAF from a cation-exchange column had affinity to most of AGP antibodies tested including JIM13, JIM16, LM2 and LM14, except JIM4. Although most of the anti-AGP monoclonal antibodies that have been used widely for the investigation of the developmental regulation of AGPs recognise carbohydrate epitopes, the precise structures of these epitopes have not been determined (Knox, 1995, Nothnagel et al., 2000). Despite the effort of scientists, there was no clear evidence for the involvement of terminal arabinofuranosides, nor of the galactan backbone, in the recognition of the glycan structure of AGPs by any of the antibodies. There has been only an acidic trisaccharide, isolated from a partial acid hydrolysate of gum karaya which has the structure: GlcAβ(1→3)GalAα (1→2)Rha, determined by a combination of FAB-MS, GC-MS and NMR spectroscopy, demonstrated to be the most effective inhibitor of the binding of the monoclonal antibodies MAC207, JIM4 and JIM13 to exudate gum antigens (Yates et al., 1996). Recently, Kitazawa et al. (2013) concludes that β-1,3-galactooligosaccharides longer than β-1,3-galactoheptaose exhibits significant precipitation with Yariv in a radial diffusion assay on agar and that a pull-down assay using oligosaccharides cross links to hydrazine beads detects interactions between β-1,3-galactooligosaccharides longer than β-1,3-galactopentaose with Yariv reagent, suggesting the importance of the β-1,3-galactan main chains to the reaction with Yariv reagent. The fact that the putative XAF binds to JIM13 and the other AGP antibodies but not JIM4 suggests that XAF-active AGP has a special structure that has no affinity to JIM4 and is different from the classical AGPs.

One of the most challenging issues in the study of AGPs is the isolation and purification of individual AGPs because of the great heterogeneity of AGP structures and the complex structure of the cell wall where AGPs may strongly bond to the wall polysaccharides (Tan et al., 2012). As a consequence, most studies on AGPs have been on a family of molecules and often in the presence of contaminating polymers. Here I report two methods used for purification and characterisation of non-classical AGPs from cauliflower florets, using both traditional chromatographic and molecular and genetic biology techniques. The sequential use of cation-exchange column

chromatography and anion-exchange column chromatography or native-PAGE electro-elution allowed me to obtain materials pure enough for the mass-spectrometry analysis. After that, I was able to study mutants in several single genes of AGP-like proteins, in particular FLA7 and ENODL14, to discover their biological roles in the plant. As they had been purified based on their ability to promote XET activity in the plant, by solubilising XTH from the cell wall, I expected that the mutants in these genes would have less XAF activity in plant organs and may have a phenotype.

Although no phenotype was observed, several organs of the mutant plants had significant changes in XAF activity compared with wild-type *Arabidopsis*. For example, half the XAF activity in the flowers and seeds of the *fla7.3* mutant disappeared while XAF activity in the leaves increased. RT-PCR showed that the effect of T-DNA insertion on *fla7* was only a knock-down, not a knock-out, therefore, it was not simple to have a definite result. One explanation is that maybe other genes of the *FLA* family take over the role of *fla7* when it is mutated and enhance the XAF activity, for examples, *FLA6* or *FLA11* in the same group A. *Enodl14* mutants also showed reductions in the XAF activity in the stems and the flowers and seeds. Again, T-DNA insertion also caused a knock-down but not knock-out on *enodl14*, thus, there was no phenotype occurred. *AtENODL14* and *AtENODL15* have been shown to be highly homologous in the *AtENODL* family at the protein level, and both are expressed in whole seedlings, roots, and flowers. Moreover, *AtENDOL*-13, -14, -15 have been suggested to have functional redundancy. Indeed, the expression patterns of *AtENODL13* and *AtENODL14* (61% identity) are very similar to *AtENODL15*. They all belongs to neighbouring branches in the phylogenetic tree and all have a putative C-terminal GPI anchor additional signals and putative AG glycomodules (Mashiguchi et al., 2009). Therefore, when *enodl14* is mutated, the other *enodl*, more likely, *enodl13* and *endol15* may compensate its role. This work needs to be followed with extended experiments before a solid conclusion can be made; for example, using double and triple mutants in place of single mutants or suppression the genes by RNAi or overexpression of the targeted genes. Nevertheless, it is the first work has been suggested a role of chimeric AGPs for the promotion of XET activity *in vivo* in plants.

## 4.5 The possible ability of FLA7 and ENODL14 to solubilise XET activity in the cell wall suggests a role of AGPs in plant cell growth control

AGPs, ubiquitous cell surface proteoglycans in both land plants and algae, are found predominantly in the plasma membrane, cell wall and extracellular secretions (e.g. stigma surface and wound exudates) (Ellis et al., 2010). Several AGPs are secreted into the medium by cultured *Arabidopsis* cells (Darjania et al., 2002). Most AGPs are attached to the outer leaflet of the plasma membrane via a GPI membrane anchor (Ellis et al., 2010; Tan et al., 2012). This location is ideal for AGPs to have a role in controlling plant growth and development. In fact, it has been widely proposed that AGPs play essential roles in cell expansion, cell proliferation, somatic embryo development, cell and tissue differentiation in roots, flowers and embryos (Willats and Knox, 1996; Tan et al., 2012). Despite intense researches to unravel AGP functions, their molecular mechanism(s) of action remain elusive.

Most of our knowledge on the role of AGPs has come broadly indirectly from the use of Yariv reagent and AGP antibodies in tissue culture and in planta (Seifert and Roberts, 2007; Ellis et al., 2010). For examples, the addition of Yariv reagent to rose cell cultures inhibits cell growth (Serpe and Nothnagel, 1994). The interaction of Yariv reagent with AGPs in the load-bearing cell layers inhibits root elongation in *Arabidopsis* as well as cell elongation of carrot suspension-cultured cells that had been induced to elongate rather than proliferate. Yariv-reactive AGPs may therefore be involved in expansion per se and/or in the directional control of expansion necessary for elongation (Willats and Knox, 1996). Treatment *Arabidopsis* suspension cell cultures with Yariv reagent decreased cell viability, increased cell wall apposition and cytoplasmic vesiculation, and induced callose deposition (Guan and Nothnagel, 2004). The authors hypothesise a role of surface AGPs in triggering a wound-like response. Addition of JIM13 antibody to the medium of sugar beet protoplasts inhibited proliferation but did not affect short-term viability suggested a role of AGPs in cell wall formation and growth under *in vitro* conditions (Butowt et al., 1999).

My results suggest a role of non-classical AGPs in the control of cell expansion. In my study, AGP-like molecules have been shown to relate to the solubilisation of XTH, an enzyme involved in both assembling and re-structuring of the wall's inner, load-

bearing stratum — from its binding sites in the cell wall as well as preventing it re-binding to the cell. Single mutants defective in these AGP-like genes resulted in a decrease or increase in the XAF activity in different *Arabidopsis* organs. Numerous investigations have demonstrated that expression of AGPs is developmentally regulated in both space (different organs or tissues produce different AGPs) and time (one tissue or organ produces different AGPs at different developmental times) (Majewska-Sawka and Nothnagel, 2000).

FLA7 is a fasciclin-like arabinogalactan-protein (FLA), a subclass of AGPs that have, in addition to predicted AGP-like glycosylated regions, putative cell adhesion domains known as fasciclin domains, thus, is a chimeric AGP (Johnson et al., 2003). Proteins containing fasciclin domains, from a broad spectrum of organisms including animals, have been shown to function as adhesion molecules. Monoclonal antibodies raised against algal-CAM, a fasciclin-like adhesion protein, prevent appropriate cell–cell contacts in the four-cell *Volvox carteri* embryo (Huber and Sumper, 1994). FLAs have the ability to participating protein–protein interactions with cell wall or plasma membrane-associated ligands via their fasciclin-like domains, shown in other eukaryotic systems for example *Drosophila melanogaster* and *Homo sapiens* to facilitate cell adhesion (Johnson et al., 2003; Tan et al., 2012). FLA7 is among the FLAs, together with FLA1, 8, and 10 which were demonstrated to be sensitive to phospholipase C cleavage from the plasma membrane (Borner et al., 2003), and to be thus GPI-anchored. GPI-anchored proteins in mammalian and yeast cells are involved in cell–cell signalling by interacting with other proteins (Ellis et al., 2010). My hypothesis is that the fasciclin domain and/or the GPI-anchor is involved in the binding of FLA7 with XTHs, solubilising them from the cell wall, thus promoting their XET activity. How they bind to each other was not covered in my study and remains to be elucidated. The fact that NaCl can solubilise many cell wall enzyme activities such as β-glucosidase, phosphatase, peroxidase and XET, while FLA7 can only solubilise XET, shows that the interaction between XTH and FLA7 is not simply ionic and is unique, giving it a potential role in plant cell growth control. The interaction between FLA and XTH aids progress towards understanding some fundamental mechanisms in plant biology.

Indeed, the function of FLAs in cell wall integrity, cell expansion and cell elongation- some of physiological aspects of plant growth- that are widely known to be closely related to XET activity (Nishitani and Matsuda, 1982; Fry et al., 1992) have been documented. *AtFLA4/SOS5* is isolated in a screen for *Arabidopsis* salt-hypersensitive mutants. Under salt stress, the root tips of *fla4* mutants swell and root growth is arrested, caused by abnormal expansion of epidermal, cortical and endodermal cells. The cell walls are thinner in the *fla4* mutant, and those between neighbouring epidermal and cortical cells in *fla4* roots appear less organized. On the medium without salt, the root-swelling phenotype was also observed for *fla4* roots growing on an agar surface or when the root tip grew at the interface between the agar medium and the petri dish but not for the root grew inside the agar suggesting that the *fla4* cell wall was weakened because external physical constraints could prevent or limit root swelling (Shi et al., 2003). Johnson et al. (2003) proposed that the fasciclin domains of FLA4 are involved in ionic interactions, most likely with other FLAs, such that they form a network at either the plasma membrane, or in the cell wall that controls the rate of cell expansion. Possibly, an interaction between FLA and XTHs, as mentioning in my study, occurs and thus, control the cell expansion in *fla4*.

A cotton *FLA*, *GhAGP4* has been showed to have a role in cotton fibre initiation and elongation. In transgenic plants with an RNA interfering (RNAi) construct according to the sequence of *GhAGP4*, a significant reduction in *AGP4* mRNA level and an inhibition of fibre initiation and fibre elongation is occurred. As for the mature fibres of transgenic cotton, the fibre length became significantly shorter and the fibre quality become worse. Also, the cytoskeleton network and the cellulose deposition were affected in the mutant (Li et al., 2010). One hypothesis is, according to my study, maybe the interaction between AGP4 and XTH was affected in the mutant, causing a reduction in XET activity, thus changing the xyloglucan moieties that tethering and hydro-bonding to the cellulose microfibril, resulting in the inhibition of fibre elongation.

FLAs 11 and 12 have also been implicated in contributing to plant stem strength and elasticity by affecting cell wall integrity. Gene-function analyses revealed that *Arabidopsis* T-DNA knockout double mutant *fla11 fla12* stems had altered stem biomechanics with reduced tensile strength and a reduced tensile modulus of elasticity,

as well as altered cell-wall architecture and composition, with increased cellulose microfibril angle and reduced arabinose, galactose and cellulose content (MacMillan et al., 2010). These results suggest that FLAs contributes to plant stem strength by affecting cellulose deposition, and to the stem modulus of elasticity by affecting the integrity of the cell-wall matrix. The change in the integrity of the cell wall matrix maybe due to the reducing of XET action that was hypothesised to be regulated by FLA in my study.

Early nodulin-like proteins (ENODLs) are chimeric AGPs related to the phytocyanin family. Although they show similarities with other phytocyanins, they lack the necessary amino acid residues for copper binding. One study characterised the *ENODL* genes constituting 22 members of the *ENODL* family in *Arabidopsis thaliana* and predicted that most of them are GPI-anchored. There have been few reports on the *ENODL* family and their function in plants (Mashiguchi et al., 2009). In an attempt to determine the biological role of *ENODL*, 26 homozygous T-DNA insertion lines of 15 *ENODL* genes were analysed. Unfortunately, no novel role was reported, probably because of functional redundancy. Nevertheless, the specific expression of many *AtENODL* genes in reproductive tissues suggests that *ENODLs* might work as signalling molecules, because they are relatively small GPI-anchored glycoproteins (Mashiguchi et al., 2009). The function of most of the nodulin-like proteins studied to date deals with the transport of various solutes throughout plant development, for examples, *Arabidopsis* and rice *MtN3* orthologs function as glucose, sucrose or fructose transporters; *Arabidopsis AtUMAMIT18/AtSIAR1* (siliques are red 1) was reported to act as a bidirectional amino acid transporter, and *AtENODL9* may transport carbohydrate (Denancé et al., 2014). In this study, I report that ENODL14 may solubilise, and thus 'transport', XTHs from their binding sites in the cell wall, thus helping to promote XET activity in *Arabidopsis*. The *enodl14* mutant in the *Arabidopsis* Col0 background shows a significant reduction of XAF activity in the stems and flowers and seeds samples, but not in leaves. However, there are still few questions on this remain to be answered: How does ENODL14 interact with XTHs? Are there any other proteins, such as stress responsive proteins or FLAs, involve in this interaction?

# 5 FUTURE WORK

In my study, a limitation on the characterisation of the arabinogalactan part of XAF occurred because of the lack of an available commercial enzyme specific for cleavage of the type II AG chain. If there is any application of such enzyme, the effect of it on XAF activity will be clearer and more targeted. Alternatively an NMR analysis on the carbohydrate part of XAF could be a suitable replacement. Testing the effect of XAF in the presence and/ or absence of AGP antibodies is also an alternative method to test whether the effect of XAF on the solubilisation of XTH is inhibited by any of the antibodies. ELISA with AGP antibodies can also be used to quantitatively analyse XAF in plants.

The use of *Arabidopsis* mutants defective in *FLA7*, *ENODL14*, *LTI65* and *LTI140* did not give any noticeable phenotype. This is perhaps due to functional redundancy. It has been shown that the expression patterns of *AtENODL13* and *AtENODL14* are very similar to that of *AtENODL15*. Therefore, double or triple mutants would be better to look for a phenotype. Such mutants can be *fla7 fla6*, *fla7 fla11*, *fla6 fla7 fla11*, *fla7 enodl14*, *endol14 enodl15/ enodl13*. Overexpression or RNAi suppression of each gene is also a good method to generate a phenotype.

Also, *ENODL14*, *LTI65* or *LTI140* might be involved in plant development only under altered conditions including stress or pathogen response. It would be worth expressing each gene under some stress conditions (such as cold or salt stress) to look for a phenotype. Another strategy would be to explore the effects of these mutations of hypocotyl elongation in the dark.

If I had had more time, I would have studied the interaction between ENODL14 and/or FLA7 and XTHs. To do that, it would be necessary to have those (glyco)proteins in pure form, which could be achieved by either purification of XAF based on its affinity to XTHs or cloning the appropriate *Arabidopsis* gene and expression in a suitable heterologous system. *Pichia* systems have been successfully used in our laboratory for the expression of a hetero-trans-β-glucanase (HTG) (Simmons et al., 2015) and thus could have been applied in my study. The main consideration is that AGP-like proteins are typically heavily-glycosylated proteins in which the carbohydrate parts comprises up to 90%. Therefore, the expression of AGP-like genes in any other organisms rather

than plants may cause lacking or mistaken glycosylation. If that is the case then expression in tobacco would be another approach. If the pure form of FLA7 or ENODL14 can be obtained, I would be able to test its XAF activity in my system and a wide range of treatment or techniques, for example mass-spectrometry, gel electrophoresis, column chromatography could be used to elucidate the interaction between it and XTH, giving us an understanding of the regulation of XET action as well as plant cell growth *in vivo*. An assay on the time-dependent aspect of the interaction between solubilised XTH and the enzyme substrates in the presence or absence of XAF may be useful to look for a chemical reaction between XAF and XTH. It would be worth using sulphorodamine-labelled XXXGol instead of [$^{3}$H]XXXGol in order to visualise the action of XAF on XTH *in vitro* as well as to quantitatively analyse the solubilisation of XTH by XAF.

# 6 REFERENCES


Albenne C, Canut H, Hoffman L, Jamet E (2014) Plant cell wall proteins: a large body of data, but what about runaways? Proteomes 2: 224-242.

Alberts B, Johnson A, Lewis J, Raff M, Roberts K, Walter P (2002) Molecular biology of the cell 4th edition. New York: Garland Science.

Bacic A, Churms S C, Stephen A M, Cohen P B, Fincher G B (1987) Fine structure of the arabinogalactan-protein from *Lolium multiflorum*. Carbohydrate Research 162: 85-93.

Baumann M J, Eklöf J M, Michel G, Kallas Å M, Teeri T T, Czjzek M, Brumer H (2007) Structural evidence for the evolution of xyloglucanase activity from xyloglucan endo-transglycosylases: biological implications for cell wall metabolism. The Plant Cell 19: 1947-1963.

Baydoun E A-H, Fry S C (1989) *In vivo* degradation and extracellular polymer-binding of xyloglucan nonasaccharide, a naturally-occurring anti-auxin. Journal of Plant Physiology 134: 453-459.

Bellincampi D, Cervone F, Lionetti V (2014) Plant cell wall dynamics and wall-related susceptibility in plant-pathogen interactions. Frontiers in Plant Science 5: 1-8.

Berg J M, Tymoczko J L, Stryer L (2002) Biochemistry 5th edition. New York: W H Freeman.

Borner G H H, Lilley K S, Stevens T J, Dupree P (2003) Identification of glycosylphosphatidylinositol-anchored proteins in *Arabidopsis*. A proteomic and genomic analysis. Plant Physiology 132: 568-577.

Bourquin V, Nishikubo N, Abe H, Brumer H, Denman S, Eklund M, Christiernin M, Teeri T T, Sundberg B, Mellerowicz E (2002) Xyloglucan endotransglycosylases have a function during the formation of secondary cell walls of vascular tissue. The Plant Cell 14: 3073-3088.

Boyer J S, Cavalieri A J, Schulze E D (1985) Control the rate of cell enlargement: excision, wall relaxation, and growth-induced water potentials. Planta 163: 527-543.

Braam J (1992) Regulated expression of the calmodulin-related TCH genes in cultured *Arabidopsis* cells: induction by calcium and heat shock. Proceedings of National Academy of Sciences 89: 3213-3216.

Brownlee C (2002) Role of the extracellular matrix in cell-cell signalling: paracrine paradigms. Current Opinion in Plant Biology 5: 396-401.

Brummell D A, Bird C R, Schuch W, Bennett A B (1997a) An endo-1,4-beta-glucanase expressed at high levels in rapidly expanding tissues. Plant Molecular Biology 33: 87-95.

Brummell D A, Harpster M H, Civello P M, Palys J M, Bennett A B, Dunsmuir P (1999b) Modification of expansin protein abundance in tomato fruit alters softening and cell wall polymer metabolism. The Plant Cell 11: 2203-2216.

Buckeridge M S, dos Santos H P, Tiné M A S (2000) Mobilisation of storage cell wall polysaccharides in seeds. Plant Physiology and Biochemistry 38: 141-156.

Buckeridge M S (2010) Seed cell wall storage polysaccharides: models to understand cell wall biosynthesis and degradation. Plant Physiology 154: 1017-1023.

Butowt R, Niklas A, Rodriguez-Garcia MI, Majewska-Sawka A (1999). Involvement of JIM13- and JIM8-responsive carbohydrate epitopes in early stages of cell wall formation. Journal of Plant Research 112: 107–116.

Caffall K H, Mohnen D (2009) The structure, function, and biosynthesis of plant cell wall pectic polysaccharides. Carbohydrate Research 344: 1879-1900.

Carpita N C, Gibeaut D M (1993) Structural models of primary cell walls in flowering plants: consistency of molecular structure with the physical properties of the walls during growth. The Plant Journal 3: 1-30.

Carpita N C, Defernez M, Findlay K, Wells B, Shoue D A, Catchpole G, Wilson R H, McCann M C (2001a) Cell wall architecture of the elongating maize coleoptile. Plant Physiology 127: 551-565.

Carpita N, Tierney M, Campbell M (2001b) Molecular biology of the plant cell wall: searching for the genes that define structure, architecture and dyamics. Plant Cell Walls: 1-5.

Cassab G I (1998) Plant cell wall proteins. Annual Review of Plant Physiology and Plant Molecular Biology 49: 281-309.

Cavalier D M, Lerouxel O, Neumetzler L, Yamauchi K, Reinecke A, Freshour G, Zabotina O A, Hahn M G, Burget I, Pauly M, Raikhel N V, Keegstra K (2008) Disrupting two *Arabidopsis thaliana* xylosyltransferase genes results in plants deficient in xyloglucan, a major primary cell wall component. The Plant Cell 20: 1519-1537.

Cimen H, Han M-J, Yang Y, Tong Q, Koc H, Koc E C (2010) Regulation of succinate dehydrogenase activity by SIRT3 in mammalian mitochondria. Biochemistry 49: 304-311.

Clarke A E, Anderson R L, Stone B A (1979) Form and function of arabinogalactans and arabinogalactan-proteins. Phytochemistry 18: 521-540.

Chun J-P, Huber D J (1998) Polygalacturonase-mediated solubilisation and depolymerisation of pectic polymers in tomato fruit cell walls. Plant physiology 117: 1293-1299.

Cocuron J-C, Lerouxel O, Drakakaki G, Alonso A P, Liepman A H, Keegstra K, Raikhel N, Wilkerson C G (2007) A gene from the cellulose synthase-like C family encodes a β-1,4 glucan synthase. Plant Biology 104: 8550-8555.

Coenen G J, Bakx E J, Verhoef R P, Schols H A, Voragen A G J (2007) Identification of the connecting linkage between homo- or xylogalacturonan and rhamnogalacturonan type I. Carbohydrate Polymers 70: 224-235.

Cooper G M (2000) The cell. A molecular approach 2nd edition. Sunderland (MA): Sinauer Associates.

Correia M A S, Mazumder K, Brás J L A, Firbank S J, Zhu Y, Lewis R J, York W S, Fontes C M G A, Gilbert H J (2011) Structure and function of an arabinoxylan-specific xylanase. The Journal of Biological Chemistry 286: 22510- 22520.

Cosgrove D J (1985) Cell wall yield properties of growing tissue. Evaluation by *in vivo* stress relaxation. Plant Physiology 78: 347-356.

Cosgrove D J (1986) Biophysical control of plant cell growth. Plant Physiology 37: 377-405.

Cosgrove D J (1987) Wall relaxation and the driving forces for cell expansive growth. Plant Physiology 84: 561-564.

Cosgrove D J (1993) Wall extensibility: its nature, measurement and relationship to plant cell growth. New Physiologist 124: 1-23.

Cosgrove D J, Li L C, Cho H-T, Hoffmann-Benning A, Moore R C, Blecker D (2002) The growing world of expansins. Plant Cell Physiology 43: 1436-1444.

Cosgrove D J (2005) Growth of the plant cell wall. Nature Review Molecular Cell Biology 6: 850-861.

Cosgrove D J, Jarvis M C (2012) Comparative structure and biomechanics of plant primary and secondary cell walls. Frontiers in Plant Sciences 3: 204.

Darjania L, Ichise N, Ichikawa S, Okamoto T, Okuyama H, Thompson Jr G A (2002) Dynamic turnover of arabinogalactan-proteins in cultured *Arabidopsis* cells. Plant Physiology and Biochemistry 40: 69-79.

Darvill A G, McNeil M, Albersheim P (1978) Structure of plant cell walls. WIII. A new pectic polysaccharide. Plant Physiology 62: 418-422.

Denancé N, Szurek B, Noël L D (2014) Emerging function of nodulin-like proteins in non-nodulating plant species. Plant and Cell Physiology 0: 1-6.

Ding L, Zhu J K (1997) A role for arabinogalactan-proteins in root epidermal cell expansion. Planta 203: 289-294.

Dolan L, Linstead P, Roberts K (1997) Developmental regulation of pectic polysaccharides in the root meristem of *Arabidopsis*. Journal of Experimental Botany 48: 713-720.

Doubnerova V, Ryslava H (2013) Enzyme regulation during plant stress. Biochemistry and Analytical Biochemistry.

Edelmann H G, Fry S C (1992) Factors that affect the extraction of xyloglucan from the primary cell walls of suspension-cultured rose cells. Carbohydrate Research 228: 423-431.

Ellis M, Egelund, Schultz C, Bacic A (2010) Arabinogalactan-proteins: key regulators at the cell surface? Plant Physiology 153: 403-419.

Eklöf J M, Brumer H (2010) The XTHs gene family: an update on enzyme structure, function, and phylogeny in xyloglucan remodelling. Plant Physiology 153: 456-466.

Fanutti C, Gidley M J, Reid J S G (1993) Action of a pure xyloglucan endo-transglycosylase (formerly called Xyloglucan-specific endo-(1→4)-β-D-

glucanase) from the cotyledons of germinated nasturtium seeds. Plant Journal 3: 691-700.

Farkaš V, Sulová Z, Stratilova E, Hanna R, Maclachlan G (1992) Cleavage of xyloglucan by nasturtium seed xyloglucanase and transglycosylation to xyloglucan subunit oligosaccharides. Archives of Biochemistry and Biophysics 298: 365-370.

Fenwick K M, Apperley D C, Cosgrove D J, Jarvis M C (1999) Polymer mobility in cell walls of cucumber hypocotyls. Phytochemistry 51: 17-22.

Franková L, Fry S C (2012) Trans-α-xylosidase, a widespread enzyme activity in plants, introduces (1→4)-α-D-xylobiose side-chains into xyloglucan structures. Phytochemistry 78: 29-43.

Fry S C (1982) Phenolic components of the primary cell wall feruloylated disaccharides of D-galactose and L-arabinose from spinach polysaccharide. Biochemical Journal 203: 493-504.

Fry S C (1989) The structure and functions of xyloglucan. Journal of Experimental Botany 40: 1-11.

Fry S C, Smith R C, Renwick K F, Martin D J, Hodge S K, and Matthews K J (1992) Xyloglucan endotransglycosylase, a new wall-loosening enzyme activity from plants. Biochemical Journal 282: 821-828.

Fry S C, York W S, Albersheim P, Darvill A, Hayashi T, Joseleau J-P, Kato Y, Lorences E P, Maclachlan G A, McNeil M, Mort A J, Reid J S G, Seitz H U, Selvendran R R, Voragen A G J, White A R (1993) An unambiguous nomenclature for xyloglucan-derived oligosaccharides. Physiologia Plantarum 89: 1-3.

Fry S C (1994) Oligosaccharins as plant growth regulators. Biochemical Society Symposium 60: 5-14.

Fry S C (1998) Oxidative scission of plant cell wall polysaccharides by ascorbate-induced hydroxyl radicals. Biochemical Journal 332: 507-515.

Fry S C (2000) 'The growing plant cell wall: Chemical and metabolic analysis'. Reprint edition, the Blackburn Press, Caldwell, New Jersey. Pp xviii + 333.

Fry S C (2001) Plant cell walls. Encyclopedia of Life Sciences 1-11.

Fry S C (2004) Primary cell wall metabolism: tracking the careers of wall polymers in living plant cells. New Phytologist 161: 641-675.

Fry S C, Nesselrode B H, Miller J G, Mewburn B R (2008) Mixed-linkage (1→3, 1→4)-β-D-glucan is major hemicellulose of *Equisetum* (horsetail) cell walls. New Phytologist 179: 104-115.

Gao M, Kieliszewski M J, Lamport D T A, Showalter A M (1999) Isolation, characterization and immunolocalisation of a novel, modular tomato arabinogalactan-protein corresponding to the *LeAGP-1* gene. Plant Journal 18: 43-55.

Gibeaut D M, Pauly M, Bacic A, Fincher G B (2005) Changes in cell wall polysaccharides in developing barley (*Hordeum vulgare*) coleoptiles. Planta 221: 729-738.

Gilbert H J, Stalbrand H, Brumer H (2008) How the walls come crumbling down: recent structural biochemistry of plant polysaccharide degradation. Current Opinion in Plant Biology 11: 338-348.

Gille S, de Souza A, Xiong G, Benz M, Cheng K, Schultink A, Reca I-B, Pauly M (2011) *O*-Acetylation of *Arabidopsis* hemicellulose xyloglucan requires AXY4 or AXYL4, proteins with a TBL and DUF231 domain. The Plant Cell 23: 4041-4053.

Gilkes N R, Hall M A (1977) The hormonal control of cell wall turnover in *Pisum sativum* L. New Phytologist 78: 1-15.

Glazebrook J (2005) Contrasting mechanisms of defence against biotrophic and necrotrophic pathogens. Annual Review of Phytopathology 43: 205-227.

Golgberg R, Pierron M, Durand L, Mutaftschiev S (1992) *In vitro* and *in situ* properties of cell wall pectinmethylesterases from mung bean hypocotyls. Journal of Experimental Botany 43: 41-46.

Guan Y, Nothnagel E A (2004) Binding of arabinogalactan-proteins by Yariv phenylglycoside triggers wound-like responses in *Arabidopsis* cell cultures. Plant physiology 135: 1346-1366.

Hamant O, Traas J (2010) The mechanics behind plant development. New Phytologist 185: 369-385.

Harrison E P, McQueen-Mason S J, Manning K (2001) Expression of six expansin genes in relation to extension activity in developing strawberry fruit. Journal of Experimental Botany 52: 1437-1446.

Hayashi T (1989) Xyloglucans in the primary cell wall. Annual Review of Plant Physiology and Plant Molecular Biology 40: 139-168.

Hayashi T, Takeda T, Ogawa K, Mitsuishi Y (1994) Effects of the degree of polymerization on the binding of xyloglucan to cellulose. Plant Cell Physiology 35: 893-899.

Heldt H-W, Piechulla B, Heldt F (2011) Plant Biochemistry 4th edition. Amsterdam: Academic Press.

Henrissat B (1991) A classification of glycosyl hydrolases based on amino acid sequence similarities. The Biochemical Journal 280: 309-316.

Hetherington P R, Fry S C (1993) Xyloglucan endotransglycosylase activity in carrot cell suspensions during cell elongation and somatic embryogenesis. Plant Physiology 103: 987-992.

Hoffman M, Jia Z, Pena M J, Cash M, Harper A, Blackburn A R, II, Darvill A, York W S (2005) Structural analysis of xyloglucan in the primary cell walls of plants in the subclass *Asteridae*. Carbohydrate Research 340: 1826-1840.

Hoson T, Masuda Y, Sone Y, Misaki A (1991) Xyloglucan antibodies inhibit auxin-induced elongation and cell wall loosening of azuki bean epicotyls but not of oat coleoptiles. Plant Physiology 96: 551-557.

Ito M, Kodama H, Komamine A, Watanabe A (1998) Expression of extensin genes is dependent on the stage of the cell cycle and cell proliferation in suspension-cultured *Catharanthus roseus* cells. Plant Molecular Biology 36: 343-351.

Ibatullin F M, Banasiak A, Baumann M J, Greffe L, Takahashi J, Mellerowicz E Jm Brumer H (2009) A real-time fluorogenic assay for the visualisation of glycosidie hydrolase activity in planta. Plant Physiology 151: 1741-1750.

Jamet E, Canut H, Boudart G, Pont-Lezica R F (2006) Cell wall proteins: a new insight through proteomics. Trends in Plant Science 11: 33-39.

Jia Z, Cash M, Darvill A G, York W S (2005) NMR characteristic of endogenously *O*-acetylated oligosaccharides isolated from tomato (*Lycopersicon esculentum*) xyloglucan. Carbohydrate Research 340: 1818-1825.

Jiang W, Wang S, Xiao M, Lin Y, Zhou L, Lei Q, Xiong Y, Guan K-L, Zhao S (2011) Acetylation regulates gluconeogenesis by promoting PEPCK1 degradation via recruiting the UBR5 ubiquitin ligase. Molecular Cell 43: 33-44.

Jones J D G, Dang J L (2006) The plant immune system. Nature 444: 323-329.

Johnson K L, Jones B J, Bacic A, Schultz C J (2003) The fasciclin-like arabinogalactan-proteins of *Arabidopsis*. A multigene family of putative cell adhesion molecules. Plant Physiology 133: 1911-1925.

Keegstra K, Talmadge K W, Bauer W D, Albersheim P (1973) The structure of plant cell walls: III. A model of the walls of suspension-cultured sycamore cells based on the interconnection of the macromolecular components. Plant Physiology 51: 188-197.

Keegstra K (2010) Plant cell walls. Plant Physiology 154: 483-486.

Keller B (1993) Structural cell wall proteins. Plant physiology 101: 1127-1130.

Kiefer L L, York W S, Darvill A G, Albersheim P (1989) Xyloglucan isolated from suspension-cultured sycamore cell walls is *O*-acetylated. Phytochemistry 28: 2105-2107.

Kimura S, Laosinchai W, Itoh T, Cui X, Linder C R, Brown R M J (1999) Immunogold labelling of rosette terminal cellulose-synthesising complexes in the vascular plant *Vigna angularis*. The Plant Cell 11: 2075- 2085.

Kollist H, Moldau H, Oksanen E, Vapaavuori E (2008) Ascorbate transport from the apoplast to the symplast in intact leaves. Physiologia Plantarum 113: 377-383.

Knox J P, Day S, Roberts K (1989) A set of surface glycoproteins forms an early marker of cell position, but not cell type, in the root apical meristem of *Daucus carota* L.. Development 106: 47-56.

Knox J P, Linstead P J, Peart J, Cooper C, Roberts K (1991) Developmentally regulated epitopes of cell surface arabinogalactan-proteins and their relation to root tissue pattern formation. The Plant Journal 1: 317-326.

Knox J P (1995) The extracellular matrix in higher plants. 4. Developmentally regulated proteoglycans and glycoproteins of the plant cell surface. Federation of American Societies for Experimental Biology Journal 9: 1004-1012.

Labavitch J M, Ray P M (1974) Turnover of cell wall polysaccharides in elongating pea stem segments. Plant Physiology 53: 669-673.

Labavitch J M, Ray P M (1978) Structure of hemicellulosic polysaccharides of *Avena sativa* coleoptile cell walls 17: 933-937.

Lamport D T A, Kieliszewski M J, Chen Y, Cannon M C (2011) Role of the extensin superfamily in primary cell wall architecture. Plant Physiology 156: 11-19.

Lee D, Polisensky D H, Braam J (2005) Genome-wide identification of touch- and darkness-regulated *Arabidopsis* genes: a focus on *calmodulin-like* and *XTH* genes. New Phytologist 165: 429-444.

Levy S, Maclachlan G, Staehelin L A (1997) Xyloglucan sidechains modulate binding to cellulose during *in vitro* binding assays as predicted by conformational dynamics simulations. The Plant Journal 11: 373-386.

Li Y, Darley C P, Ongaro V, Fleming A, Schipper O, Baldauf S L, McQueen-Mason S J (2002) Plant expansins are complex multigene family with an ancient evolutionary origin. Plant Physiology 128: 854-864.

Li Y, Liu D, Zhang X, Wang L, Zhu L, Tan J, Deng F (2010) Suppression of GhAGP4 gene expression repressed the initiation and elongation of cotton fibre. Plant Cell Reports 29: 193-202.

Libertini E, Li Y, McQueen-Mason S J (2004) Phylogenetic analysis of the plant *endo-β-1,4-glucanase* gene family. Journal of Molecular Evolution 58: 506- 515.

Liu C, Meldy M C (2007) A nonclassical arabinogalactan-protein gene highly expressed in vascular tissues, *AGP31*, is transcriptionally repressed by methyl jasmonic acid in *Arabidopsis*. Plant Physiology 145: 863-874.

Liu Y-B, Lu S-M, Zhang J-F, Liu S, and Lu Y-T (2007) A xyloglucan endotransglucosylase/hydrolase involves in growth of primary root and alters the deposition of cellulose in *Arabidopsis.* Planta 226: 1547-1560.

Lockhart J A (1965) An analysis of irreversible plant cell elongation. Journal of Theoretical Biology 8: 264-275.

Lorimer G H, Badger M R, Andrews T J (1976) The activation of ribulose-1,5-bisphosphate carboxylase by carbon dioxide and magnesium ions. Equilibria, kinetic, a suggested mechanism, and physiological implications. Biochemistry 15: 529-536.

Llop-Tous I, Dominguez-Puigjaner E, Palomer X, Vendrell M (1999) Characterisation of two divergent endo-β-1,4-glucanase cDNA clones highly expressed in the nonclimacteric strawberry fruit. Plant Physiology 119: 1415-1421.

Lv L, Li D, Zhao D, Lin R, Chu Y, Zhang H, Zha Z, Liu Y, Li Z, Xu Y, Wang G, Huang Y, Xiong Y, Guan K-L, Lei Q-Y (2011) Acetylation targets the M2 isoform of pyruvate kinase for degradation through chaperone-mediated autophagy and promotes tumor growth. Molecular Cell 42: 719-730.

MacMillan C P, Mansfield S D, Stachurski Z H, Evans R, Southerton S G (2010) Fasciclin-like arabinogalactan-proteins: specialisation for stem biomechanics and cell wall architecture in *Arabidopsis* and *Eucalyptus*. The plant journal 62: 689-703.

Madson M, Dunand C, Li X, Verma R, Vanzin G F, Caplan J, Shoue D A, Carpita N C, Reiter W-D (2003) The *MUR3* gene of *Arabidopsis* encodes a xyloglucan galactosyltransferase that is evolutionarily related to animal exostosins. The Plant Cell 15: 1662-1670.

Majewska-Sawka A, Nothnagel E A (2000) The multiple roles of arabinogalactan-proteins in plant development. Plant Physiology 122: 3-10.

Maloney V J, Samuels A L, Mansfield S D (2012) The endo-1,4-β-glucanase Korrigan exhibits functional conservation between gymnosperms and angiosperms and is required for proper cell wall formation in gymnosperms. New Phytologist 193: 1076-1087.

Maris A, Suslov D, Fry S C, Verbelen J-P, Vissenberg K (2009) Enzymic characterization of two recombinant xyloglucan endotransglucosylase/hydrolase (XTHS) proteins of *Arabidopsis* and their effect on root growth and cell wall extension. Journal of Experimental Botany 60: 3959-3972.

Maris A, Kaewthai N, Eklof J M, Miller J G, Brumer H, Fry S C, Verbelen J P, Vissenberg K (2011) Differences in enzymic properties of five recombinant xyloglucan endotransglucosylase/ hydrolase (XTHs) proteins of *Arabidopsis thaliana*. Journal of Experimental Botany 62: 261-271.

Mashiguchi K, Asami T, Suzuki Y (2009) Genome-wide identification, structure and expression studies, and mutant collection of 22 early nodulin-like proteins genes in *Arabidopsis*. Bioscience and Biotechnology and Biochemistry 73: 2452-2459.

Matsui A, Yokoyama R, Seki M, Ito T, Shinozaki K, Takahashi T, Komeda Y, Nishitani K (2005) *AtXTH27* plays an essential role in cell wall modification during the development of treachery elements. The Plant Journal 42: 525-534.

Matsumoto T, Sakai F, Hayashi T (1997) A xyloglucan specific endo-1,4-β-glucanase isolated from auxin-treated pea stems. Plant Physiology 114: 661-667.

McCann M C, Wells B, Roberts K (1990) Direct visualization of cross-links in the primary plant cell wall. Journal of Cell Science 96: 323-334.

McCann M C, Bush M, Milioni D, Sado P, Stacey N J, Catchpole G, Defernez M, Carpita N C, Hofte H, Ulvskov P, Wilson R H, Roberts K (2001) Approaches to understanding the functional architecture of the plant cell wall. Phytochemistry 57: 811-821.

McQueen-Mason S J, Durachko S J, Cosgrove D J (1992) Two endogenous proteins that induce cell wall extension in plants. The Plant Cell 4: 1425-1433.

McQueen-Mason S J and Cosgrove D J (1995) Expansin mode of action on cell walls. Analysis of wall hydrolysis, stress relaxation, and binding. Plant Physiology 107: 87-100.

Mellerowicz E J, Sundberg B (2008) Wood cell walls: biosynthesis, development dynamics and their implications for wood properties. Current Opinion in Plant Biology 11: 293-300.

Mewalal R, Mizrachi E, Mansfield S D, Myburg A A (2014) Cell wall-related proteins of unknown function: missing links in plant cell wall development. Plant Cell Physiology 55: 1031-1043.

Miller A R (1986) Oxidation of cell wall polysaccharides by hydrogen peroxide: a potential mechanism for cell wall breakdown in plants. Biochemical and Biophysical Research Communications 141: 238-244.

Mitsuda N, Iwase A, Yanomoto H, Yoshida M, Seki M, Shinozaki K, Ohme-Takagi M (2007) NAC transcription factors, NST1 and NST3, are key regulators of formation of secondary walls in woody tissues of *Arabidopsis*. The Plant Cell 19: 270-280.

Mohnen D (2008) Pectin structure and biosynthesis. Current Opinion in Plant Biology 11: 266-277.

Molhoj M, Pagant S, Höfte H (2002) Towards understanding the role of membrane-bound endo-beta-1,4-glucanases in cellulose biosynthesis. Plant Cell Physiology 43: 1399-1406.

Moller I, Marcus S E, Haeger A, Verhertbruggen Y, Verhoef R, Schols H, Ulvskov P, Mikkelsen J D, Knox J P, Willats W (2008) High-throughput screening of monoclonal antibodies against plant cell wall glycans by hierarchical clustering of their carbohydrate microarray binding profiles. Glycoconjugate Journal 25: 37-48.

Mort A J, Lamport D T A (1977) Anhydrous hydrogen fluoride deglycosylates glycoproteins. Analytical Biochemistry 82: 289-309.

Mueller S C, Brown R M Jr (1980) Evidence for an intramembrane component associated with a cellulose microfibril-synthesising complex in higher plants. Journal of Cell Biology 84: 315- 326.

Nakamura A, Furuta H, Maeda H, Takao T, Nagamatsu Y (2002) Structural studies by stepwise enzymatic degradation of the main backbone of soybean soluble polysaccharides consisting of galacturonan and rhamnogalacturonan. Bioscience, Biotechnology, and Biochemistry 66: 1301-1313.

Narváez-Vásquez J, Pearce G, Ryan C A (2005) The plant cell wall matrix harbours a precursor of defence signalling peptides. Proceedings of the National Academy of Sciences of the United States of America 102: 12974-12977.

Nebenfürh A, Gallagher L A, Dunahay T G, Frohlick J A, Mazurkiewicz A M, Meehl J B, Staehelin L A (1999) Stop-and-go movements of plant Golgi stacks are mediated by the acto-myosin system. Plant Physiology 121: 1127-1141.

Nicol F, His I, Jauneau A, Vernhettes S, Canut H, Höfte H (1998) A plasma membrane-bound putative endo-1,4-β-D-glucanase is required for normal wall assembly and cell elongation in *Arabidopsis*. The EMBO Journal 17: 5563-5576.

Nishitani K, Masuda Y (1982) Acid pH-induced structural changes in cell wall xyloglucan in *Vigna angularis* epicotyl segments. Plant Science Letter 28: 87-94.

Nishitani K, Tominaga R (1992) Endo-xyloglucan transferase, a novel class of glycosyltransferase that catalyses transfer of a segment of xyloglucan molecule to another xyloglucan molecule. The Journal of Biological Chemistry 267: 21058-21064.

Nordin K, Vahala T, Palva E T (1993) Differential express of two related, low-temperature-induced genes in *Arabidopsis thaliana* (L.) Heynh. Plant Molecular Biology 21: 641-653.

Nothnagel E A (1997) Proteoglycans and related components in plant cells. International Review of Cytology 174: 195-291.

Nothnagel E A, Bacic A, Clarke A E (2000) Cell and developmental biology of arabinogalactan-proteins. Springer Science+Business Media New York. Xiii+295.

Okazawa K, Sato Y, Nakagawa T, Asada K, Kato I, Tomita E, Nishitani K (1993) Molecular cloning and cDNA sequencing of endoxyloglucan transferase, a novel class of glycosyltransferase that mediates molecular grafting between matrix polysaccharides in plant cell walls. Journal of Biological Chemistry 268: 25364–25368.

Osato Y, Yokoyama R, Nishitani K (2006) A principal role for *AtXTH18* in *Arabidopsis thaliana* root growth: a functional analysis using RNAi plants. Journal of Plant Research 119: 153-162.

Park Y W, Tominaga R, Sugiyama J, Furuta Y, Tanimoto E, Samejima M, Sakai F, Hayashi T (2003) Enhancement of growth by expression of poplar cellulase in *Arabidopsis thaliana*. The Plant Journal 33: 1099-1106.

Park Y W, Baba K, Furuta Y, Iida I, Sameshima K, Arai M, Hayashi T (2004) Enhancement of growth and cellulose accumulation by overexpression of xyloglucanase in poplar. Federation of European Biochemical Societies Letters 564: 183-187.

Passioura J B, Fry S C (1992) Turgor and cell expansion: beyond the Lockhart equation. Journal of Plant Physiology 19: 565-576.

Pauly M, Albersheim P, Darvill A, York W S (1999a) Molecular domains of the cellulose/ xyloglucan network in the cell wall of higher plants. The Plant Journal 20: 629–639.

Pauly M, Andersen L N, Kauppinen S, Kofod L V, York W S, Albersheim P, Darvill A (1999b) A xyloglucan-specific endo-β-1,4-glucanase from *Aspergillus aculeatus*: expression cloning in yeast, purification and characterisation of the recombinant enzyme. Glycobiology 9: 93-100.

Peña m J, Kong Y, York W S, O'Neil M A (2012) A galacturonic acid-containing xyloglucan is involved in *Arabidopsis* root hair tip growth. The Plant Cell 24: 4511-4524.

Peng L, Kawagoe Y, Hogan P, Delmer D (2002) Sitosterol-beta-glucoside as primer for cellulose synthesis in plants. Science 295: 147-150.

Pennell R (1998) Cell walls: structures and signals. Current Opinion in Plant Biology 1: 504-510.

Perkins D N, Pappin D J C, Creasy D M, Cottrell J S (1999) Probability-based protein identification by searching sequenc databases using mass spectrometry data. Electrophoresis 20: 3551-3567.

Persson S, Caffall K H, Freshour G, Hilley M T, Bauer S, Poindexter p, Hahn M G, Mohnen D, Somerville C (2007) The *Arabidopsis irregular xylem 8* mutant is deficient in glucuronoxylan and homogalacturonan, which are essential for secondary cell wall integrity. Plant Cell 19: 237-255.

Popper Z A, Fry S C (2003) Primary cell wall composition of bryophytes and charophytes. Annals of Botany 91: 1-12.

Popper Z A, Fry S C (2004) Primary cell wall composition of pteridophytes and spermatophytes. New Phytologist 164: 165-174.

Popper Z A (2008) Evolution and diversity of green plant cell walls. Current Opinion in Plant Biology 11: 286-292.

Popper Z A, Fry S C (2008) Xyloglucan–pectin linkages are formed intra-protoplasmically, contribute to wall-assembly, and remain stable in the cell wall. Planta 227: 781-794.

Popper Z A, Tuohy M G (2010) Beyond the green: understanding the evolutionary puzzle of plant and algal cell walls. Plant Physiology 153: 373-383.

Redgwell R J, Fry S C (1993) Xyloglucan endotransglycosylase activity increases during kiwifruit (*Actinidia deliciosa*) ripening. Plant Physiology 103: 1399-1406.

Reid J S G (1985) Cell wall storage carbohydrates in seeds: biochemistry of the seen “gum” and “hemicellulose”. Advances in Botanical Research 11: 125-155.

Rose J K C, Bennett A B (1999) Cooperative disassembly of the cellulose-xyloglucan network of plant cell walls: parallels between cell expansion and fruit ripening. Trends in Plant Science 4: 176-183.

Rose J K, Braam J, Fry S C, Nishitani K (2002) The XTHs family of enzymes involved in xyloglucan endotransglucosylation and endohydrolysis: Current perspectives and a new unifying nomenclature. Plant Cell Physiology 43: 1421-1435.

Rose J K (2009) Annual plant reviews, volume 8, the plant cell wall. Wiley-Blackwell. Pp 400.

Sampedro J, Cosgrove D J (2005) The expansin superfamily. Genome Biology 6: 242.

Saxena I M, Brown R M Jr (2005) Cellulose biosynthesis: current view and evolving concepts. Annals of Botany 96: 9-21.

Scheller H V, Ulvskov P (2010) Hemicelluloses. Annual Review of Plant Biology 61: 263-289.

Schopfer P, Plachy C, Frahry G (2001) Release of reactive oxygen intermediates (superoxide radicals, hydrogen peroxide, and hydroxyl radicals) and peroxidase in germinating radish seeds controlled by light, gibberellin, and abscisic acid. Plant Physiology 125: 1591-1602.

Schopfer P (2001) Hydroxyl radical-induced cell-wall loosening *in vitro* and *in vivo*: implications for the control of elongation growth. The Plant Journal 28: 679-688.

Schuchmann M N, Von Sonntag C (1978) The effect of oxygen on the OH-radical-induced scission of the glycosidic linkage of cellobiose. International Journal of Radiation Biology 34: 397-400.

Schultink A, Cheng K, Park Y B, Cosgrove D J, Pauly M (2013) The identification of two arabinosyltransferases from tomato reveals functional equivalency of xyloglucan side chain substituents. Plant Physiology 163: 86-94.

Schultink A, Liu L, Zhu L, Pauly M (2014) Structural diversity and function of xyloglucan sidechain substituents. Plants 3: 526-542.

Schultz C, Gilson P, Oxley D, Youl J, Bacic A (1998) GPI-anchors on arabinogalactan-proteins: implications for signalling in plants. Trends Plant Science 3: 426-431.

Schultz C J, Johnson K L, Currie G, Bacic A (2000) The classical arabinogalactan-protein family of *Arabidopsis*. The Plant Cell 12: 1751-1767.

Schultz C J, Rumsewicz M P, Johnson K l, Jones B J, Gaspar Y M, Bacic A (2002) Using genomic resources to guide research directions. The arabinogalactan-protein gene family as a test case. Plant Physiology 129: 1448-1463.

Seifert G J, Barber C, Wells B, Dolan L, Roberts K (2002) Galactose biosynthesis in *Arabidopsis*: genetic evidence for substrate channeling from UDP-D-Galactose into cell wall polymers. Current Biology 12: 1840-1845.

Seifert G J, Roberts K (2007) The biology of arabinogalactan-proteins. Annual Review of Plant Biology 58: 137-161.

Serpe M D, Nothnagel E A (1994) Effects of Yariv phenylglycosides on *Rosa* cell suspensions: evidence for the involvement of arabinogalactan-proteins in cell proliferation. Planta 193: 542-550.

Shani Z, Dekel M, Tsabary G, Shoseyov (1997) Cloning and characterization of elongation specific endo-1,4-β-glucanase (cel1) from *Arabidopsis thaliana*. Plant Molecular Biology 34: 837-842.

Shi D, Morizono H, Yu X, Tong L, Allewell N M, Tuchman M (2001) Human ornithine transcarbamylase: crystallographic insights into substrate recognition and conformational changes. Biochemical Journal 354: 501-509.

Shi H, Kim Y, Guo Y, Stevenson B, Zhu J K (2003) The *Arabidopsis SOS5* locus encodes a putative cell surface adhesion protein and is required for normal cell expansion. Plant cell 15: 19-32.

Showalter A M (1993) Structure and function of plant cell wall proteins. Plant Cell 5: 9-23.

Showalter A M (2001) Arabinogalactan-proteins: structure, expression and function. Cellular and Molecular Life Sciences 58: 1399-1417.

Showalter A M, Keppler B, Lichtenberg J, Gu D, Welch L R (2010) A bioinformatics approach to the identification, classification, and analysis of hydroxyproline-rich glycoproteins. American Society of Plant Biologists 153: 485-513.

Simmons T J, Mohler K E, Holland C, Goubet F, Franková L, Houston D R, Hudson A D, Meulewaeter F, Fry S C (2015) Hetero-trans-β-glucanase, an enzyme unique to Equisetum plants, functionalises cellulose. The Plant Journal 83: 753-769.

Somerville C (2006) Cellulose synthesis in higher plants. Annual Review Cell Development Biology 22: 53-78.

Sommer-Knudsen J, Clarke A E, Bacic A (1996) A galactose-rich, cell-wall glycoprotein from styles of Nicotiana alata. The Plant Journal 9: 71-83.

Souza A D, Xiong G, Benz M, Cheng K, Schultink A, Reca I-B, Pauly M (2011) *O*-acetylation of *Arabidopsis* hemicellulose xyloglucan requires AXY4 or AXY4L, proteins with a TBL and DUF231 domain. The Plant Cell 23: 4041-4053.

Smallwood M, Yates E A, Willats W G T, Martin H, Knox J P (1996) Immunochemical comparison of membrane-associated and secreted arabinogalactan-proteins in rice and carrot. Planta 198: 452-459.

Smith R C, Fry S C (1991) Endotransglycosylation of xyloglucans in plant cell suspension cultures. Biochemical Journal 279: 529-535.

Tabuchi A, Mori H, Kamisaka S, Hoson T (2001) A new type of endo-xyloglucan transferase devoted to xyloglucan hydrolysis in the cell wall of azuki bean epicotyls. Plant Cell Physiology 42: 154-161.

Tan L, Showalter A M, Egelund J, Hermandez-Sanchez A, Doblin M S, Bacic A (2012) Arabinogalactan-proteins and the research challenges for these enigmatic plant cell surface proteoglycans. Frontiers in Plant Science 3: 140.

Takeda T, Mitsuishi Y, Sakai F, Hayashi T (1996) Xyloglucan endotransglycosylation in suspension-cultured poplar cells. Bioscience Biotechnology and Biochemistry 60: 1950-1955.

Takeda T, Furuta Y, Awano T, Mizuno K, Mitsuishi Y, Hayashi T (2002) Suppression and acceleration of cell elongation by integration of xyloglucans in pea stem segments. Proceedings of the National Academy of sciences of the United States of America 99: 9055-9060.

Takeda T, Fry S C (2004) Control of xyloglucan endotransglucosylase activity by salts and anionic polymers. Planta 219: 722-732.

Takeda T, Miller J G, Fry S C (2008) Anionic derivatives of xyloglucan function as acceptor but not donor substrates for xyloglucan endotransglucosylase activity. Planta 227: 893-905.

Taylor G, Davies W J (1986) Yield turgor of growing leaves of *Betula* and *Acer*. New Phytologist 104: 347-353.

Thiyagarajah M, Fry S C, Yeo A R (1996) *In vitro* salt tolerance of cell wall enzymes from halophytes and glycophytes. Journal of Experimental Botany 47: 1717-1724.

Thompson J E, Fry S C (2001) Restructuring of wall-bound xyloglucan by transglycosylation in living plant cells. The Plant Journal 26: 23-34.

Thompson D S (2005) How do cell walls regulate plant growth? Journal of Experimental Botany 56: 2275-2285.

Tomos D, Pritchard J (1994) Biophysical and biochemical control of cell expansion in roots and leaves. Journal of Experimental Botany 45: 1721-1731.

Tuomivaara S T, Yaoi K, O'Neil M A, York W S (2015) Generation and structural validation of library of diverse xyloglucan-derived oligosaccharides, including an update on xyloglucan nomenclature. Carbohydrate Research 402: 56-66.

Urbanowicz B R, Bennett A B, Campillo E D, Catalá C, Hayashi T, Henrissat B, Höfte H, McQueen-Mason S J, Patterson S E, Shoseyov O, Teeri T T, Rose J K C (2007) Structural organisation and a standardised nomenclature for plant endo-1,4-β-glucanases (cellulase) or glycosyl hydrolase family 9. Plant Physiology 144: 1693-1696.

Van den Bulck K, Swennen K, Loosveld A A-M, Courtin C M, Brijs K, Proost P, Van Damme J, Van Campenhout S, Mort A, Delcour J A (2005) Isolation of cereal arabinogalactan-pectides and structural comparison of their carbohydrate and peptide moieties. Journal of Cereal Science 41: 59-67.

Van Sandt V S T, Guisez Y, Verbelen J-P, Vissenberg K (2006) Analysis of a xyloglucan endotransglycosylase/hydrolase (XTH) from the lycopodiophyte *Selaginella kraussiana* suggests that XTH sequence characteristics and function are highly conserved during the evolution of vascular. Journal of Experimental Botany 57: 2909-2922.

Van Sandt V S T, Suslov D, Verbelen J-P, Vissenberg K (2007) Xyloglucan endotransglucosylase activity loosens a plant cell wall. Annals of Botany 100: 1467-1473.

Vanacker H, Harbinson J, Ruisch J, Carver T L W, Foyer C H (1998) Antioxidant defences of the apoplast. Protoplasma 205: 129-140.

Vanzin G F, Madson M, Carpita N C, Raikhel N V, Keegstra K, Reiter W D (2002). The *mur2* mutant of *Arabidopsis thaliana* lacks fucosylated xyloglucan because of a lesion in fucosyltransferase *AtFUT1*. Proceedings of the National Academy of Sciences of the United States of America 99: 3340-3345.

Verhertbruggen Y, Marcus S E, Chen J, Knox J P (2013). Cell wall pectic arabinans influence the mechanical properties of *Arabidopsis thaliana* inflorescence stems and their response to mechanical stress. Plant and Cell Physiology 54:1278-1288.

Vissenberg K, Martinez-Vilchez I M, Verbelen J-P, Miller J G, Fry S C (2000) *In vivo* colocalisation of xyloglucan endotransglucosylase activity and its donor substrate in the elongation zone of *Arabidopsis* roots. The Plant Cell 12: 1229-1237.

Volkenburgh E V, Cleland R E (1986) Wall yield threshold and effective turgor in growing bean leaves. Planta 167: 37-43.

Voragen A G J, Coenen G-J, Verhoef R P, Schols H A (2009) Pectin, a versatile polysaccharide present in plant cell walls. Structural Chemistry 20: 263-275.

Vorwerk S, Somerwille S, Somerville C (2004) The role of plant cell wall polysaccharide composition in disease resistance. Trends in Plant Science 9: 203-209.

Vuttipongchaikij S, Brocklehurst D, Steele-King C, Ashford D A, Gomez L D, McQueen-Mason S J (2012). *Arabidopsis GT34* family contains five xyloglucan α-1,6-xylosyltransferases. New Phytologist 195: 585-595.

Wagstaff C, Clarkson G J J, Zhang F Z, Rothwell S D, Fry S C, Taylor G, Dixon M S (2010) Modification of cell wall properties in lettuce improves shelf life. Journal of Experimental Botany 61: 1239-1248.

Westgate M E, Boyer J S (1985) Osmotic adjustment and the inhibition of leaf, root, stem and silk growth at low water potentials in maize. Planta 164: 540-549.

Williats W G T, Knox J P (1996) A role from arabinogalactan-proteins in plant cell expansion: evidence from studies on the interaction of β-glucosyl Yariv reagent with seedlings of *Arabidopsis thaliana*. The Plant Journal 9: 919-925.

Xiong Y, Guan K-L (2012) Mechanistic insights into the regulation of metabolic enzymes by acetylation. Journal of Cell Biology 198: 155-164.

Xu W, Purugganan M M, Polisensky D H, Antosiewicz D M, Fry S C, Braam J (1995). *Arabidopsis* TCH4, regulated by hormones and the environment, encodes a xyloglucan endotransglycosylase. The Plant Cell 7: 1555-1567.

Yariv J, Lis H, Katchalski E (1967) Precipitation of arabic acid and some seed polysaccharides by glycosylphenylazo dyes. Biochemistry Journal 105: 1c-2c.

Yates E A, Valdor J-F, Haslam S M, Morris H R, Dell A, Mackie W, Knox J P (1996) Characterisation of carbohydrate structural features recognised by anti-arabinogalactan-protein monoclonal antibodies. Glycobiology 6: 131-139.

Yokoyama R, Nishitani K (2001) A comprehensive expression analysis of all members of a gene family encoding cell-wall enzymes allowed us to predict *cis*-regulatory regions involved in cell-wall construction in specific organs of *Arabidopsis*. Plant Cell Physiology 46: 192-200.

Yokoyama R, Rose J K C, Nishitani K (2004) A surprising diversity and abundance of xyloglucan endotransglucosylase/ hydrolase in rice. Classification and expression analysis. Plant Physiology 134: 1088-1099.

York W S, Darvill A G, Neil M Mc, Albersheim P (1985) 3-deoxy-D-manno-2-octulosonic acid (Kdo) is a component of rhamnogalacturonan II, a pectin polysaccharide in the primary cell wall of plants. Carbohydrate Research 138: 109-126.

York W S, O'Neill M A (2008) Biochemical control of xylan biosynthesis- which end is up? Current Opinion in Plant Biology 11: 258- 265.

Yu L, Sun J, Li L (2013) *PtrCel9A6*, an endo-1,4-glucanase, is required for cell wall formation during xylem differentiation in *Populus*. Molecular Plant 6: 1904-1917.

Zhang G F, Staehelin L A (1992) Functional compartmentation of the Golgi apparatus of plant cells. Immunocytochemical analysis of high-pressure frozen-

and freeze-substituted sycamore maple suspension culture cells. Plant Physiology 99: 1070-1083.

Zhong R, Ye Z-H (2014) Secondary cell walls: biosynthesis, patterned deposition and transcriptional regulation. Plant and Cell Physiology 56: 195-214.

Zhu J-K, Shi J, Singh U, Wyatt S E, Bressan R A, Hasegawa P M, Carpita N C (1993) Enrichment of vitronectin- and fibronectin-like proteins in NaCl-adapted plant cells and evidence for their involvement in plasma membrane-cell wall adhesion. The Plant Journal 3: 637-646.

Zuo J, Niu Q-W, Nishizawa N, Wu Y, Kost B, Chua N-H (2000) *Korrigan*, an *Arabidopsis* endo-1,4-β-glucanase, localises to the cell plate by polarised targeting and is essential for cytokinesis. The Plant Cell 12: 1137-1152.